

**Characterisation and expression of Receptor-like
Cytoplasmic Kinases in *Medicago truncatula* during
Rhizobial and Arbuscular Mycorrhizal symbioses**

Kirsty J. Jackson

A thesis submitted to the University of East Anglia for the degree of Masters of
Philosophy

John Innes Centre

April 2015

Copyright © 2015 K. J. Jackson. This copy of the thesis has been supplied on condition that anyone who consults it is understood to recognise that its copyright rests with the author and that use of any information derived there from must be in accordance with current UK Copyright Law. In addition, any quotation or extract must include full attribution.

Table of Contents

Table of Contents	2
Publications	4
Abstract	5
Acknowledgements.....	6
List of Figures	7
List of Tables	9
List of abbreviations.....	10
Chapter 1: Introduction	12
1.1 Legume Endosymbiosis	13
1.1.1 The Common Symbiosis Pathway and symbiotic gene expression	13
1.1.2 Early stages of Rhizobial and AMF colonisation of Legume roots.....	15
1.1.2.1 Rhizobial infection and Infection thread formation.....	15
1.1.2.2 AMF infection and PPA formation.....	16
1.1.3 Nodule development in Legumes	17
1.1.4 Arbuscule development and genetic regulation in root cortical cells	18
1.2 Similarities between symbiosis and pathogenesis of plants.....	21
1.3 Plant Receptor-like Kinases	22
1.3.1 The brassinosteroid signalling pathway	24
1.3.2 The flagellin defence signalling pathway	27
1.3.3 Comparison of the CSP with BR and flg22 signalling.....	28
Chapter 2: Materials and methods	29
2.1. Plant material	29
2.1.1 Seed preparation.....	29
2.2 Bacterial and Yeast strains.....	30
2.3 Growth Media.....	31
2.4 <i>Agrobacterium</i> transformation, growth and plant transformation.....	31
2.4.1 <i>Agrobacterium rhizogenes</i> 'Hairy root' transformation of <i>M. truncatula</i>	31
2.4.2 <i>Agrobacterium tumefaciens</i> transformation of <i>Nicotiana benthamiana</i>	32
2.5 Image capture and microscopy.....	32
2.6 DNA amplification, purification and sequencing.....	32
2.6.1 Standard Polymerase Chain Reaction (PCR).....	32
2.6.2 Restriction Digest	33
2.6.3 Sequencing	33
2.7 qRT-PCR	33
2.8 Cloning.....	34
2.8.1 Gateway® Cloning, Invitrogen	34
2.8.2 TOPO® Cloning, Life technologies	34
2.8.3 Golden Gate Cloning.....	34
2.9 Nodulation Phenotyping	35
2.9.1 Histochemical staining procedure	35

2.10 Mycorrhizal Phenotyping	35
2.10.1 Growth media and inoculation	35
2.10.2 Mycorrhizal staining and scoring.....	36
2.11 Gene silencing – RNA interference.....	36
2.11.1 Constructs	36
2.11.2 Transformation of RNAi constructs	36
2.11.3 Rhizobial Inoculation and scoring	37
2.12 Gene expression analysis	37
2.12.1 <i>In silico</i> gene expression analysis (MtGEA).....	37
2.12.2 Promoter-GUS analysis	37
2.13 Phylogenetic Analysis	38
2.14 Protein Analysis.....	38
2.14.1 <i>In silico</i> protein analysis	38
2.14.2 Protein localisation constructs	38
2.14.3 Yeast 2-Hybrid	39
2.15 Co-Immunoprecipitation	39
2.15.1 Protein Extraction.....	39
2.15.2 Western Blot.....	40
Chapter 3: Characterisation and expression of <i>Receptor-Like Cytoplasmic Kinase 1 and 2</i>	41
3.1 Introduction	41
3.2 Identification of Mutants for <i>RLCK1</i> and <i>RLCK2</i>	43
3.3 Nodulation phenotypes of <i>rlck1</i> and <i>rlck2</i>	45
3.3.1 Rhizobial Infection.....	45
3.3.2 Nodule formation.....	48
3.4 Mycorrhizal phenotyping of <i>rlck1</i> and <i>rlck2</i>	52
3.5 Expression of <i>RLCK1</i> and <i>RLCK2</i>	56
3.5.1 Expression of <i>RLCK1</i> and <i>RLCK2</i> by Microarray	56
3.5.2 Symbiotically enhanced expression of <i>RLCK1</i> and <i>RLCK2</i>	61
3.6 Phylogenetic analysis of <i>RLCK1</i> and <i>RLCK2</i> proteins.....	65
3.7 Discussion.....	67
Chapter 4: Double Knockdown of <i>RLCK1</i> and <i>RLCK2</i>	69
4.1 Introduction	69
4.2 Strategy 1: RNAi double knockdown	70
4.3 Strategy 2: <i>RLCK2</i> knockdown in the <i>RLCK1-2</i> mutant.....	74
4.4 Discussion.....	76
Chapter 5: Work towards identification of interacting partners of <i>RLCK1</i> and <i>RLCK2</i> Proteins	77
5.1 Introduction	77
5.2 <i>In silico</i> analysis of <i>RLCK1</i> and <i>RLCK2</i> proteins	79
5.3 Preliminary Yeast 2-Hybrid Analysis.....	80

5.4 Protein localisation	81
5.5 Construction of Golden Gate constructs for future protein interaction studies.....	81
5.6 Discussion.....	86
Chapter 6: Identification of a mycorrhizal phenotype in <i>M. truncatula</i> <i>Tnt1</i> insertion line NF5270.....	88
6.1 Introduction	88
6.2 Identification of the <i>RLCK3</i> mutant and Characterization of its Nodulation and Mycorrhizal Phenotypes	88
6.2.1 Preliminary Nodulation and Mycorrhizal phenotypes of <i>rlck3-1</i>	90
6.2.2 Segregation population of <i>rlck3-1</i>	92
6.3 <i>scooby</i> mycorrhizal phenotype	94
6.4 Discussion.....	96
Chapter 7: Discussion.....	99
<i>scooby</i> is a novel mycorrhizal mutant in <i>M. truncatula</i>	99
Two Receptor-like kinases required for nodulation and mycorrhization	100
<i>RLCK2</i> is a novel symbiotic gene	100
<i>RLCK1/SPK1</i> is required for correct mycorrhizal development as well as nodulation in <i>M.</i> <i>truncatula</i>	101
<i>RLCK1</i> and <i>RLCK2</i> are partially redundant during symbiosis.....	101
Possible roles of <i>RLCK1/RLCK2</i> in symbiosis.....	103
Part of the NF signalling cascade	103
Differentiating between Pathogen and Symbiosis	105
Regulation of developmental processes by ROS	106
Future Work	108
Conclusion	108
Appendix I.....	110
Primers	110
RNAi Plasmid Maps	113
Golden Gate constructs.....	115
Golden Gate Plasmid Maps.....	117
References	157

Publications

Jeremy D. Murray, Donna R. Cousins, Kirsty J. Jackson, Chengwu Liu (2013).

Signaling at the Root Surface: The Role of Cutin Monomers in Mycorrhization. *Molecular Plant*, 6 (5); 1381-1383.

Abstract

Legume plants have evolved the ability to form a mutualistic symbiosis with nitrogen-fixing bacteria known as rhizobia. Studies using mutant *Medicago truncatula* and *Lotus japonicus* have identified many genes that are necessary for this mutualism. Some of these genes have also been shown to be necessary for symbiosis with arbuscular mycorrhiza fungi (AMF). These common genes make up part of a signalling pathway known as the common symbiosis pathway (CSP) which serves to prepare the plant for the entry of the symbiont into the root. Although the core members of this signalling pathway are known there are still large gaps, and many of the genes involved in the infection process haven't yet been identified. Using the *Medicago* Gene Expression Atlas (MtGEA) and in-house gene expression data three family *Receptor-like Cytoplasmic Kinase (RLCK)* genes were identified in *M. truncatula* which were differentially regulated during rhizobial and AMF colonisation. Analysis of *Tnt1* insertion mutants for the one of these genes, named *RLCK3* due to similarity to the rice gene family RLCK-OS3, revealed an apparently novel mycorrhizal phenotype with stunted arbuscule development. However, segregation analysis showed the phenotype was not linked to *RLCK3*; as such the locus was named *SCOOBY*. The other genes identified were similar to the rice gene family RLCK-XV and so named *RLCK1* and *RLCK2*. Both *RLCK1* and *RLCK2* encode soluble RD kinases with high homology to each other. Promoter-GUS analysis showed *RLCK1* and *RLCK2* expression associated with entry and accommodation of the symbionts. *rlck1* and *rlck2* mutants had a low level of arbuscultation and misshaped arbuscules. *rlck1* was hyperinfected by rhizobia and had a significant reduction in nodule number. RNAi knockdown of *rlck1/rlck2* had a significantly reduced nodule number compared to the empty vector control. *RLCK1* and *RLCK2* possibly have partially redundant or synergistic roles during rhizobial and arbuscular mycorrhizal symbioses.

Acknowledgements

Firstly I would like to thank my supervisor Jeremy Murray for taking me on as a PhD student whilst he himself was getting used to his new role as a project leader. We may not always agree but he is always there when you need to talk. I would especially like to thank Myriam Charpentier for all the time and effort she gave to me in support of my lab work and for the initial data that got my project started. I would also like to thank Giles Oldroyd and Cyril Zipfel for their guidance during my PhD. I would also like to thank Kate Conway of the Graduate studies office for her supportive chats at the hard times during the four years.

I would like to thank the members of the Murray, Oldroyd and Downie labs who have been present during my four years. It was like working in one large supportive lab group with everyone being there for each other. In particular I would like to thank Ben Miller, Syliva Singh, Jian Feng, Tatiana Vernie, Enrico Coen and Chengwu Liu for passing lab skills and knowledge on to me. I would like to thank Guru Vighnesh Radhakrishnan for all of his help with the phylogenetics. I would like to thank Sonali Roy, who has travelled through the PhD process with me, for keeping me sane on all of those late nights in the lab and for being my personal curry approver. I want to thank Donna Cousins, Andy Breakspear and Leonie Luginbuehl for fun times in the lab, the tea breaks and for being my friends. Out of all of my friends in the lab I want to thank Sarah Shailes the most. She has been there for me no matter what she was personally going through and kept me together at times when I didn't believe in myself. There will never be enough time to pay her back in kind.

I couldn't have done this PhD without the support of my family. I hope that I have done them proud, even if their eyes do glaze over when I try and explain science to them! I want to thank my Mum for only ever being as far away as the other end of the phone and my Nan for the support and care she gives to the entire family. I want to thank my Dad for the constant reassurance that there was "no pressure" on me. Lastly, and definitely not the least, I want to thank my Husband, Brian John Abbs. He has been my rock and always has my best interests at heart. I really could not have done this without him.

List of Figures

Figure 1.1.3.1. The Zones of an indeterminate nodule	18
Figure 1.1.4.1. Stages of arbuscule development.	20
Figure 1.3.1. BR and flagellin signalling pathways	26
Figure 3.2.1. Allele identification for <i>RLCK1</i>	43
Figure 3.2.2. Allele identification for <i>RLCK2</i>	44
Figure 3.3.1.1. The number of infection events per plant in the <i>rlck</i> mutants and WT.....	45
Figure 3.3.1.2. Differences between <i>rlck1</i> and WT (R108) infection threads.	46
Figure 3.3.1.3. Differences between <i>rlck2</i> and WT (R108 and A17) infection threads.	47
Figure 3.3.2.1. Nodulation in WT and <i>rlck</i> mutants.....	49
Figure 3.3.2.2. Nodule sections of <i>rlck1</i> mutants and R108 WT at different developmental stages.....	50
Figure 3.3.2.3 Nodule sections of <i>rlck2</i> mutants and WT (R108 and A17).....	51
Figure 3.4.1. AMF (<i>R. irregularis</i>) colonisation is reduced in <i>rlck</i> mutants.	53
Figure 3.4.2. AMF colonisation phenotypes of <i>rlck1</i> mutants and WT (R108).	54
Figure 3.4.3. AMF colonisation phenotypes of <i>rlck2</i> mutants and WT plants.....	55
Figure 3.5.1.1. Medicago Gene Expression Atlas (MtGEA) data for <i>RLCK1</i>	57
Figure 3.5.1.2. Unpublished Medicago Gene Expression Atlas data for <i>RLCK1</i>	58
Figure 3.5.1.3 Medicago Gene Expression Atlas (MtGEA) data for <i>RLCK2</i>	59
Figure 3.5.1.4. Unpublished Medicago Gene Expression Atlas data for <i>RLCK2</i>	60
Figure 3.5.2.1. pMtRLCK1:GUS expression during rhizobial symbiosis.	62
Figure 3.5.2.2. pRLCK1:GUS expression during mycorrhizal symbiosis.	63
Figure 3.5.2.3. pRLCK2:GUS expression during rhizobial and mycorrhizal symbioses. ..	64
Figure 3.6.1. Phylogenetic tree for RLCK1 and RLCK2 proteins.	65
Figure 4.2.1. Clustal Omega alignment of <i>RLCK1</i> and <i>RLCK2</i> CDS with 5' and 3' UTR. 72	
Figure 4.2.2. pK7GW WG2D(II)R <i>RLCK1</i> RNAi nodule number and fold change of expression of <i>RLCK1</i> and <i>RLCK2</i> relative to empty vector controls.	73
Figure 4.3.1. pK7GW WG2D(II)R <i>RLCK2</i> RNAi nodule number and relative expression of <i>RLCK2</i> in <i>RLCK2</i> -specific knockdown roots.	75
Figure 5.3.1. Yeast 2-Hybrid assay for RLCK1 and RLCK2 protein interactions.....	80
Figure 5.5.1. Expression of Proteins in <i>N. benthamiana</i> from the Golden Gate constructs.	85
Figure 6.2.1. Medicago Gene Expression Atlas data for <i>RLCK3</i>	89
Figure 6.2.2. Identification of <i>RLCK3 Tnt1</i> insertion mutants in line NF5270.	90
Figure 6.2.3. Preliminary nodulation and AMF colonisation phenotypes of <i>rlck3-1</i>	91
Figure 6.2.4. AMF colonisation of progeny for different genotypic classes from the 14_NF5270 segregating population for <i>rlck3-1</i>	93

Figure 6.3.1. AMF colonisation of NF5270 <i>Tnt1</i> lines	94
Figure 6.3.2. Mycorrhizal phenotypes of <i>scooby</i> and WT (R108).	95
Figure 6.4.1. <i>Tnt1</i> insertion line NF5270	97
Figure A1. pK7GW WG2D(II)R RLCK1 RNAi – RNAi vector designed on <i>RLCK1</i>	113
Figure A2. pK7GW WG2D(II)R RLCK2 RNAi – RNAi vector designed on the 5' UTR region of <i>RLCK2</i>	114
Figure A3. EC67001 plasmid map	117
Figure A4. EC67002 plasmid map	118
Figure A5. EC67003 plasmid map	119
Figure A6. EC67004 plasmid map	120
Figure A7. EC67005 plasmid map	121
Figure A8. EC67006 plasmid map	122
Figure A9. EC67007 plasmid map	123
Figure A10. EC67008 plasmid map	124
Figure A11. EC67009 plasmid map	125
Figure A11. EC67009 plasmid map	126
Figure A13. EC67011 plasmid map	127
Figure A14. EC67012 plasmid map	128
Figure A15. EC67013 plasmid map	129
Figure A16. EC67014 plasmid map	130
Figure A17. EC67015 plasmid map	131
Figure A18. EC67016 plasmid map	132
Figure A19. EC67017 plasmid map	133
Figure A20. EC67018 plasmid map	134
Figure A21. EC67019 plasmid map	135
Figure A22. EC67020 plasmid map	136
Figure A23. EC67021 plasmid map	137
Figure A23. EC67021 plasmid map	138
Figure A25. EC67030 plasmid map	139
Figure A26. EC67031 plasmid map	140
Figure A27. EC67032 plasmid map	141
Figure A28. EC67033 plasmid map	142
Figure A29. EC67034 plasmid map	143
Figure A30. EC67035 plasmid map	144
Figure A31. EC67036 plasmid map	145
Figure A32. EC67037 plasmid map	146

Figure A33. EC67038 plasmid map	147
Figure A34. EC67039 plasmid map	148
Figure A35. EC67040 plasmid map	149
Figure A36. EC67041 plasmid map	150
Figure A37. EC67042 plasmid map	151
Figure A38. EC67043 plasmid map	152
Figure A39. EC67044 plasmid map	153
Figure A40. EC67045 plasmid map	154
Figure A41. EC67046 plasmid map	155
Figure A42. EC67047 plasmid map	156

List of Tables

Table 2.1.1. Plant material.....	29
Table 2.2.1. Bacterial and yeast strains.....	30
Table 2.3.1. Media used for plant, bacterial and yeast growth.	31
Table 5.2.1. Positions of predicted protein domains in RLCK1 and RLCK2.	79
Table 5.5.1. A list of Golden Gate constructs and the proteins they express.	82
Table 5.5.2. Expected protein sizes for the proteins expressed by the Golden Gate constructs.	83
Table A1. List of PCR primers for cloning or genotyping	110
Table A2. List of primers for qPCR.....	111
Table A3. List of sequencing primers	112
Table A4. List of Level 0 Golden gate modules	115
Table A5. List of Level 1 Golden Gate modules	115
Table A6. List of Level 2 Golden Gate constructs.....	116

List of abbreviations

AMF	Arbuscular Mycorrhiza Fungi
ATP	Adenosine Tri-Phosphate
BR	Brassinosteroid
CSP	Common Symbiosis Pathway
dsRNA	Double Stranded RNA
DWA	Distilled Water Agar
EMS	Ethyl methanesulfonate
ENSA	Engineering Nitrogen Symbiosis for Africa
EV	Empty Vector
FST	Flanking Sequence Tag
GFP	Green Fluorescent Protein
hpRNA	Hairpin RNA
LCO	Lipo-chitooligosaccharide
LRR	Leucine-Rich Repeat
LTR	Long Terminal Repeats
LysM	Lysin-motif
IT	Infection Thread
MAMP	Microbe-Associated Molecular Pattern
MAP	Mitogen-activated Protein
MtGEA	Medicago Gene Expression Atlas
mRNA	Messenger RNA
miRNA	MicroRNA
NBT	Nitro Blue Tetrazolium
NF	Nod Factor
PAM	Periarbuscular membrane
PAMP	Pathogen-Associated Molecular Pattern
PAS	Periarbuscular space
PCR	Polymerase Chain Reaction

PIT	Preinfection Thread
PPA	Prepenetraton Apparatus
PTI	PAMP-triggered Immunity
qRT-PCR	Quantitative Reverse Transcription PCR
RD	Arginine-aspartate
RKN	Root Knot Nematode
RLK	Receptor-Like Kinase
RLCK	Receptor-Like Cytoplasmic Kinase
RNAi	RNA interference
RNS	Root Nodule Symbiosis
ROS	Reactive Oxygen Species
RTK	Receptor Tyrosine Kinases
sRNA	Silencing RNA
siRNA	Short Interfering RNA
TGAC	The Genome Analysis Centre
TSL	The Sainsbury Laboratory
WGA	Wheat Germ Agglutinin
WGD	Whole Genome Duplication
WT	Wildtype

Chapter 1: Introduction

The sessile nature of plant life can make the necessary issue of finding nutrition and water a challenge. Plants can only make use of nutrients that are within the rhizosphere, which are sometimes obtained through the uptake of water such as mineral ions like potassium (K^+) and ammonia (NH_3) (Taiz and Zeiger, 1998). However, if the nutrients the plant requires are not within the rhizosphere, or not in such an accessible form, then the plant employs different strategies to obtain the nutrients it requires. One method which the plant uses is extended root growth, either through the lengthening of the tap root or increased branching, to increase the size of the rhizosphere. Plants also exude organic acids into the soil in order to free nutrients which are otherwise bound in salts; Phosphorous (P) is rarely found in a free (ionic) state in soil, tending to be in a salt on the surface of rocks and stones (Taiz and Zeiger, 1998). Despite all the strategies that plants have evolved to cope with these problems on their own, plants can still find themselves in environments where they are not able to find adequate nutrition or water. This is when beneficial symbiosis, or mutualism, becomes advantageous for the plant (Taiz and Zeiger, 1998).

The earliest evidence of a mutualistic symbiosis by a plant with a fungus is a fossil from the Rhynie Chert containing examples of the plant-mycorrhiza symbiosis from ~450 million years ago (mya) (Remy *et al.*, 1994). It is thought that the symbiosis with mycorrhizal fungi was important in the colonisation of land by plants (Harrison, 2005). The first land plants did not have an extensive root system like higher plants. Ancient sea-dwelling plants did not need an extensive root system as the nutrients were dissolved in the water which was all around them. They did have a small root like structure (rhizoid) but this was more for anchorage than nutrient acquisition (Jones and Dolan, 2012). Early diverging lineages of plants, such as the hornworts and liverworts, are restricted to watery areas of land. The mycorrhizal fungi would have acted like a surrogate root system to the early land plants as they do to hornworts and liverworts today (Parniske, 2008). In exchange for providing water and nutrients for the plants, the mycorrhizal fungi receive a supply of carbon in the form of sugars made by the plant during photosynthesis. This symbiosis is present in ~70-90 % of modern day plants (Peterson *et al.*, 2004; Parniske, 2008). It is believed that root nodule symbiosis (RNS), a symbiosis between plants in the Eurosid I clade, including Fabales, Fagales, Cucurbitales and Rosales, and Gram-negative soil bacteria collectively known as rhizobia, evolved from the earlier mycorrhizal fungi-plant symbiosis ~60 mya (Kistner and Parniske, 2002). It is believed that a Whole Genome Duplication (WGD) event at ~58 mya might have led to the recruitment of genes involved in the mycorrhizal symbiosis into the emerging symbiosis with nitrogen fixing bacteria (Parniske, 2000; Cannon *et al.*, 2006; Parniske, 2008; Young *et al.*, 2011).

1.1 Legume Endosymbiosis

Legumes (Fabaceae) are able to form symbioses with both arbuscular mycorrhizal fungi (AMF) and rhizobia within their root cortical cells. Model legumes *Medicago truncatula* (Medicago) and *Lotus japonicus* (Lotus), as well as other legumes such as *Glycine max* (soybean) and *Pisum sativum* (pea) and non-nodulating plants such as *Oryza sativa* (rice) and *Petunia hybrida* (petunia), have been used to investigate these root symbioses in more detail. Unless otherwise stated gene names used will be from *M. truncatula* with *L. japonicus* following in square brackets.

Before the symbionts come into physical contact they communicate via a chemical dialogue through the rhizosphere. Plants exude flavonoid or strigalactone signals, attracting symbionts towards the plant roots where the rhizobia attach to the growing root hair and the AMF form hyphopodia, a specialised, lobed hypha that attaches the fungus to the root surface (Firmin *et al.*, 1986; Redmond *et al.*, 1986; Besserer *et al.*, 2006; Peck *et al.*, 2006). The symbionts exude lipo-chitooligosaccharides, Nod Factors (NF) or Myc Factors (myc-LCOs), which are perceived by the plants and alerts them of a nearby symbiotic partner (Denarie *et al.*, 1996; Maillet *et al.*, 2011). AMF also exude tetra- and pentameric chitin oligomers (COs) that act as symbiosis signalling compounds (Genre *et al.*, 2013). NFs are perceived at the root epidermis by the LysM Receptor-like Kinases (LysM-RLKs) NFP [NFR5] and LYK3 [NFR1] (Limpens *et al.*, 2003; Madsen *et al.*, 2003; Radutoiu *et al.*, 2003; Radutoiu *et al.*, 2007). The Myc Factor receptor has not yet been identified. There is some evidence that a LysM receptor might be required for Myc Factor perception; Op den Camp *et al.* (2011) showed that a knockdown of the MtNFP orthologue in the non-legume *Parasponia abndersonii* (*PaNFP*) inhibited colonisation of roots by both AMF and rhizobia. Perception of these symbiont signals initiates a signalling cascade within the epidermal cell that results in the expression of symbiotic specific genes.

1.1.1 The Common Symbiosis Pathway and symbiotic gene expression

Genetic studies in *M. truncatula* and *L. japonicus* have identified a set of genes that are required for both RNS and arbuscular mycorrhization that are downstream of the NF receptors in the signalling cascade. A leucine-rich repeat-RLK *Does Not Make Infections* (*DMI*) 2 [SYMRK] (Endre *et al.*, 2002; Stracke *et al.*, 2002), a nuclear envelope-localised cation channel *DMI*1 [POLLUX] (Ané *et al.*, 2004; Imaizumi-Anraku *et al.*, 2005; Charpentier *et al.*, 2008; Capoen *et al.*, 2011), a calcium and calmodulin dependent kinase *DMI*3 [CCaMK] and *Interacting protein of DMI3* (*IPD3*) [CYCLOPS] (Catoira *et al.*, 2000; Lévy *et al.*, 2004; Mitra *et al.*, 2004; Messinese *et al.*, 2007; Horváth *et al.*, 2011)

are the core components of the common symbiosis pathway (CSP) with homologues being identified in both *M. truncatula* and *L. japonicus*. In *L. japonicus* nucleoporins *NUP85*, *NUP133* and *NENA* (Kanamori *et al.*, 2006; Saito *et al.*, 2007; Groth *et al.*, 2010), and cation channel *CASTOR* (Imaizumi-Anraku *et al.*, 2005) have been shown to be part of the CSP, however their orthologues in *M. truncatula* have not yet been identified.

The CSP transfers the signal received at the cell surface to the nucleus to initiate calcium oscillations known as calcium spiking (Ehrhardt *et al.*, 1996; Sieberer *et al.*, 2009; Maillet *et al.*, 2011). NF, Myc-LCOs and Myc-COs elicit distinct calcium spiking patterns (Denarie *et al.*, 1996; Maillet *et al.*, 2011; Genre *et al.*, 2013). *DMI2*, *DMI1* [POLLUX], *CASTOR* and the nucleoporins have all been shown to be required for spiking (Wais *et al.*, 2000; Kanamori *et al.*, 2006; Saito *et al.*, 2007; Charpentier *et al.*, 2008; Groth *et al.*, 2010). It is widely believed that *DMI3* [CCaMK] decodes the calcium spiking (Miller *et al.*, 2013). *dmi3* and *ccamk* mutants retain calcium spiking but are not able to form symbioses (Wais *et al.*, 2000). Gain-of-function mutations in *DMI3* (*dmi3*^{*}/*ccamk*^{*}) are capable of producing nodule structures in the absence of rhizobia (Gleason *et al.*, 2006; Tirichine *et al.*, 2007) and results in the expression of mycorrhizal specific markers in the absence of AMF (Takeda *et al.*, 2012). Recent evidence from Singh *et al.* (2014) show that CYCLOPS is able to activate nodule organogenesis independently from the CSP when serines 50 and 154 are replaced with aspartic acids (CYCLOPS-DD) adding to the evidence that IPD3/CYCLOPS may work with *DMI3* in the decoding of the calcium spiking.

Several transcription factors act downstream of the CSP. *Nodule inception (NIN)*, *ERF required for nodulation 1 and 2 (ERN1/ERN2)*, and *Nodulation signalling pathway 1 and 2 (NSP1/NSP2)* have been shown to be required for nodulation (Oldroyd and Long, 2003; Kaló *et al.*, 2005; Smit *et al.*, 2005; Heckmann *et al.*, 2006; Andriankaja *et al.*, 2007; Middleton *et al.*, 2007). *NSP1* and *NSP2* have been shown to form a DNA binding complex that is able to bind to the promoter of symbiosis reporter gene *Early Nodulin 11 (ENOD11)* (Hirsch *et al.*, 2009). *Required for Arbuscular Mycorrhization 1 (RAM1)* has been shown to be required for mycorrhization and *RAM1* has been shown to interact with *NSP2* (Gobbato *et al.*, 2012). There is also some evidence that *NSP1* and *NSP2* may have a role in strigolactone synthesis (Liu *et al.*, 2011). This may explain the mycorrhizal phenotype seen in the *nsp2* mutant (Maillet *et al.*, 2011).

There are a number of genes that have been shown to be required for both RNS and mycorrhization that have not been shown to be part of the CSP and as such are known as common symbiosis genes. It is possible that *3-hydroxy-3-methylglutaryl*

coenzyme A reductase 1 (HMGR1) is a part of the CSP but as yet is not confirmed. There is some evidence that HMGR1 interacts with DMI2 and RNAi knockdown of *HMGR1* expression causes inhibition of RNS and calcium spiking (Kevei *et al.*, 2007) and unpublished evidence from the Ané Lab (presented on a poster at Plant Biology 2011, Minneapolis, Minnesota) suggests that *HMGR1* is also required for colonisation by, and calcium spiking in response to, AMF (Jayaraman, 2011). However, no stable mutant data for *HMGR1* have been published to date. *Vapyrin*, a gene encoding an N-terminal VAMP-associated protein (VAP)/major sperm protein (MSP) domain with a C-terminal ankyrin-repeat domain, appears to be involved in infection stages of both RNS and mycorrhizal symbiosis and acts downstream of the CSP (Feddermann *et al.*, 2010; Pumplin *et al.*, 2010; Murray *et al.*, 2011). It is likely that other components of the CSP exist.

1.1.2 Early stages of Rhizobial and AMF colonisation of Legume roots

For RNS, the perception of NF initiates two spatially and temporally co-ordinated developmental processes, one which allows the entry of the rhizobia into the plant root (infection), and the other creation of the nodule that will house the endosymbiotic nitrogen-fixing bacteria (nodule organogenesis) (Murray, 2011; Oldroyd *et al.*, 2011). For mycorrhization, colonisation of the root by AMF can be separated into three stages; precontact, intraradical development, and arbuscule development (Gutjahr and Parniske, 2013). Although the plant does not make specialist organs for AMF colonisation it has been shown that perception of diffusible signals from the germinating AMF spores by the plant stimulates lateral root formation, increasing the root area available for AMF colonisation (Oláh *et al.*, 2005; Maillet *et al.*, 2011; Gutjahr and Paszkowski, 2013). Although the infection of the root by rhizobia and AMF are morphologically distinct they bear striking similarities at the subcellular level (Kistner and Parniske, 2002).

1.1.2.1 Rhizobial infection and Infection thread formation

On the perception of NF legume root hairs switch from symmetrical polar growth to growth towards the source of the NF, sometimes including root hair swelling and branching (Esseling *et al.*, 2003). The growing root hair cell curls around attached NF-producing rhizobium trapping it within an infection pocket (Geurts and Bisseling, 2002). The rhizobia within the infection pocket divide to form a microcolony or infection focus. The nucleus of the curling root hair cell moves up to the infection focus and the cytoskeleton aligns along the shaft of the hair forming a bridge through the cytoplasm (Fournier *et al.*, 2008) .

An invagination of the plant cell wall and plasma membrane occurs at the infection focus growing inwardly through the root hair cell, following the migrating nucleus along the cytoplasmic bridge down towards the base of the cell creating the infection thread (IT). An

influx of calcium ions seen at the root hair tip which is accompanied by the generation of reactive oxygen species (ROS) is associated with the change of polar growth at the infection foci from an outward to an inward growth (Miwa *et al.*, 2006; Murray, 2011; Oldroyd *et al.*, 2011). The IT is a tube filled with a glycoprotein matrix, which is still technically external to the root hair cell, through the root hair along which the rhizobia grow and divide (Brewin, 1998). As the IT reaches the base of the root hair cell, the nucleus in the outer cortical cell directly below the progressing thread moves to the upper plasma membrane and guides the formation of the preinfection thread (PIT) (Van Brussel *et al.*, 1992; Timmers *et al.*, 1999; Niwa *et al.*, 2001) which is very similar to what occurs in the root hair during infection. The formation of PITs and ITs continue in this way, ramifying and guiding the bacteria through the cell layers of the root, until it reaches the inner cortical cells comprising the nodule where the bacteria are released and begin to fix nitrogen (Timmers *et al.*, 1999). Several mutants have been identified that are impaired in IT formation, creating arrested, lumpy or misshaped ITs, including *lyk3*, *vapyrin*, *ern1*, *ern2*, a remorin *symrem1*, *lumpy infections (lin)*, and the knockdown mutants of flotillins *flot2* and *flot4* (Kuppusamy *et al.*, 2004; Andriankaja *et al.*, 2007; Middleton *et al.*, 2007; Smit *et al.*, 2007; Haney and Long, 2010; Lefebvre *et al.*, 2010; Murray *et al.*, 2011; Tóth *et al.*, 2012).

1.1.2.2 AMF infection and PPA formation

AMF enter the plant root via atrichoblasts rather than root hair cells; despite this difference the changes within the epidermal cells that allow symbiont entry are very similar. Upon perception of mycorrhizal specific diffusible signals, myc-LCOs and hyphopodia formation on the root surface, the epidermal cell undergoes differential gene expression and cytoskeletal changes (Genre *et al.*, 2005). The nucleus moves first to the top of the cell directly beneath the fungal hyphopodia, then moves down through the plant cell forming the pre-penetration apparatus (PPA) a tunnel of cytoskeleton and endoplasmic reticulum (similar to the PIT) through which the AMF hyphae can grow (Genre *et al.*, 2005). The PPA guides the invagination of the plant cell wall creating a tube, like the rhizobial IT but larger, through which the AMF penetrate (Genre *et al.*, 2005). As in rhizobial infection, this process is controlled by the plant and the AMF remains technically external to the plant cell. Once through the epidermal cell the hyphae either travels through the cell directly below the epidermal cell, which has already formed a PPA, or can travel intercellularly until it reaches the root inner cortex, but the AMF must pass intracellularly through at least one plant cell before it is able to form arbuscules (Demchenko *et al.*, 2004).

1.1.3 Nodule development in Legumes

Whilst the root hairs at the epidermis are forming ITs to allow the entry of the rhizobial symbiont into the root, the nodule has already started to develop in the root cortex (Oldroyd and Downie, 2008). There are two types of legume root nodule: determinate, as seen on *L. japonicus* root, and indeterminate, as seen on *M. truncatula* roots. Determinate root nodules develop from the outer cortical cells, grow to a predetermined size and are normally round in shape. Indeterminate root nodules develop from the inner cortical cells and maintain an apical meristem causing them to be more elongated in shape (Sprent, 2001). I shall be referring to indeterminate root nodules unless otherwise stated.

To develop the nodule organ the cortical cells directly below the developing infection thread divide (Oldroyd and Downie, 2008). As the proliferation of cortical cells continues they eventually break through the epidermis causing the characteristic outgrowth, or bump, of the nodule primordia. The growing infection thread ramifies through the nodule primordia distributing the rhizobia across the nodule. When the rhizobia reach the cortical cells they are taken up via a process very similar to endocytosis, such that each bacterial cell is surrounded by a plant derived membrane known as the peribacteroid membrane (Udvardi and Day, 1997). At this stage the rhizobia irreversibly differentiate into bacteroids that are completely dependent on the plant (Mergaert *et al.*, 2006). Plant derived leghaemoglobin binds to oxygen to support respiration of the bacteroids and protect the nitrogenase allowing the bacteroids to fix nitrogen and giving the nodule its pink colour (Appleby, 1984; Starker *et al.*, 2006).

Mature indeterminate nodules contain five zones that progress from the nodule tip to the base (fig. 1.1.3.1) (Vasse *et al.*, 1990; Foucher and Kondorosi, 2000; Timmers *et al.*, 2000). Zone I is the meristem of the nodule. These cells continue to divide and elongate the nodule. Cells that remain in Zone I are never colonised by rhizobia. Zone II is the infection zone. The rhizobia continue to colonise this zone throughout the life of the nodule through ramifying infection threads which can be clearly seen on root nodule sections. Zone III is the nitrogen fixation zone where the cells are packed full of bacteroids. Zone IV is the senescent zone where the bacteria and leghaemoglobin are degraded, often a green-ish yellow in colour. In some nodules a zone between II and III, called the interzone (IZ) or Zone II-III, can be seen where cells undergo many symbiotic specific cell changes (Vasse *et al.*, 1990; Foucher and Kondorosi, 2000). Timmers *et al.* (2000) showed that Zone V comprises a saprophytic zone at the very base of the nodule. Cells start their life in Zone I and progress into Zone V as the nodule grows and matures, Zones III to V may not be seen in young developing nodules.

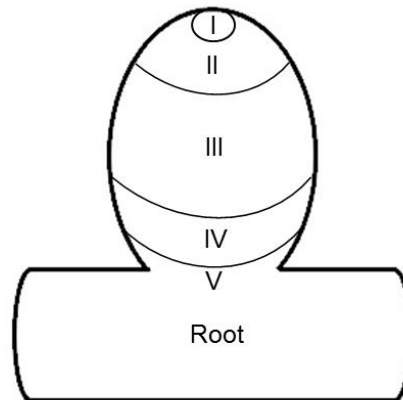


Figure 1.1.3.1. The Zones of an indeterminate nodule

A diagram to demonstrate the zones observed during indeterminate nodule development. Zone I is the nodule meristem. Zone II is the infection zone. Zone III is the fixation zone. Zone IV is the senescence zone. Zone V is the saprophytic zone.

1.1.4 Arbuscule development and genetic regulation in root cortical cells

AMF form arbuscules in the inner cortical cells of the plant root. Arbuscules are highly branched, tree-like structures that are the site of nutrient exchange between the AMF and the plant. The arbuscules are the defining structures of, and give their name to, the AMF. The arbuscule is surrounded by a plant derived membrane called the periarbuscular membrane (PAM), which is continuous with the plasma membrane, and an interfacial glycoprotein-rich matrix known as the periarbuscular space (PAS) made up of AMF and plant cell wall material (Parniske, 2008; Balestrini and Bonfante, 2014). The PAM contains nutrient transporters such as the phosphate transporter MtPT4 (Javot *et al.*, 2007; Yang *et al.*, 2012).

The formation of an arbuscule in a plant inner cortical cell can be genetically divided into 5 stages: 1) PPA formation or pre-arbuscule stage, 2) fungal entry/arbuscule trunk formation, 3) birdsfoot stage, 4) hyphal branching/mature arbuscule and 5) arbuscule collapse/senescence (fig.1.1.4.1) (Gutjahr and Parniske, 2013). The first stage of arbusculation is very similar to the PPA formation in epidermal cells prior to hyphal entry into the plant root. Laser capture microdissection shows that cortical cells ahead of the advancing intraradical mycorrhizal hyphae have differential gene expression compared to cortical cells on non-mycorrhized plants, showing these cells are preparing to receive the AMF (Gomez *et al.*, 2009; Hogekamp *et al.*, 2011; Gaude *et al.*, 2012). The

CSP mutants do not complete stage one of arbuscule formation, although a gain-of-function DMI3 (CCaMK) mutant can induce the gene expression patterns seen in stage one (Takeda *et al.*, 2012). In stage 2, the fungal hypha enters the cell forming the unbranched arbuscule trunk. Mutants such as *vapyrin* in *Medicago* or *penetration and arbuscule morphogenesis1 (pam1)* in petunia occasionally show the formation of arbuscule trunks but do not progress to the birdsfoot stage of arbuscule development (Reddy D. M. R *et al.*, 2007; Feddermann *et al.*, 2010; Murray *et al.*, 2011).

The third stage of arbuscule development initiates the hyphal branching. This stage is referred to as the birdsfoot stage due to the resemblance of the hyphae to the toes on a bird's foot (Gutjahr and Parniske, 2013). Mutants in two half-ABC transporter genes in *Medicago*, *Stunted arbuscule (str and str2)*, progress only to the birds foot stage of arbusculation (Zhang *et al.*, 2010b). The *Medicago* mutant of *Required for Arbuscular Mycorrhization (RAM) 2* occasionally forms birdsfoot arbuscules when the AMF does get through to the cortex (Wang *et al.*, 2012). In addition, overexpression of KP1106 (protease inhibitor), knockdown of *SCP1 (serine carboxypeptidase 1)* or *ERF1 (Ethylene response factor 1)* all result in the birdsfoot type arbuscules in *Medicago* inner cortical cells (Devers *et al.*, 2013; Rech *et al.*, 2013). Stage four of arbuscule development is the ramification of the AMF hyphae to form the highly branched, tree-like mature arbuscules. Live cell imaging in rice (*Oryza sativa*) determined the average life span of an arbuscule was on average 2 to 3 days but could be as little as one day (Kobae and Hata, 2010). MtPT4 and its rice homologue OsPT11 have been shown to be required for the maintenance of the mature arbuscules in mutant studies when nutrients other than phosphate were readily available (Javot *et al.*, 2007; Yang *et al.*, 2012). However, the *pt4* phenotype was suppressed when *Medicago* plants were nitrogen starved, yet not when starved of sulphate (Javot *et al.*, 2011), suggesting a complex system of regulation for arbuscule maintenance that is dependent on nitrogen and phosphate availability.

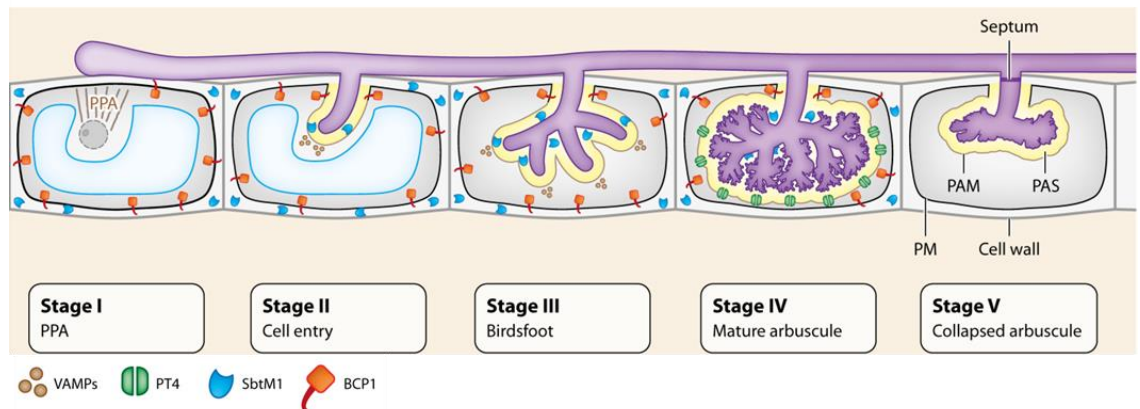


Figure 1.1.4.1. Stages of arbuscule development.

A diagram to demonstrate the stages of arbuscule development. Stage I is PPA development. Stage II is the entry of the hyphae into the cell. Stage III is the birdsfoot stage showing a few larger hyphal ramifications. Stage IV is the hyphal branching/mature arbuscule. Stage V is the collapsed/senescing arbuscule.

Figure adapted from Gutjahr and Parniske (2013). *Annual Review of Cell and Developmental Biology*. 29: 593-617.

1.2 Similarities between symbiosis and pathogenesis of plants

There have been many reviews highlighting the similarities between the mutualisms of rhizobia and AMF, and the pathogenesis by fungi, oomycetes and nematodes with plants (Ausubel and Bisseling, 1999; Parniske, 2000; Kogel *et al.*, 2006; Paszkowski, 2006; Rey and Schornack, 2013). Mutualism and pathogenesis are very different in terms of cost and gain for the plant, but they can also be seen as a sliding scale of biotrophism, with mutualism at one end and plant pathogens at the other with lots of examples in between. For example, Kiers *et al.* (2011) demonstrated that two *Glomus* species and *Rhizophagus irregularis* (*nee. G. intraradices*) acquire differential amounts of carbon from the plant as well as differing in the amount of phosphorus they give in exchange. In fact *G. aggregatum* had almost double the carbon cost per phosphorus molecule than *R. irregularis* (Kiers *et al.*, 2011), it could then be argued that *G. aggregatum* is less mutualistic and more parasitic than *R. irregularis* to the host plant *M. truncatula*. Another example of the blurred lines between friend and foe is the fungal endophyte *Epichl e festucae* and its host ryegrass *Lolium perenne*. A mutation in the NoxA gene in *E. festucae* is enough to switch it to a pathogen that causes great damage to *L. perenne* (Tanaka *et al.*, 2006).

Many aspects of plant colonisation by beneficial symbionts are similar to those seen in plant-pathogen interactions. For example, the Root Knot Nematode (RKN) *Meloidogyne incognita* causes root hair deformation and nuclear movement similar to that seen with NF application and successful cortical colonisation by RKN is dependent on the CSP member *DMI2* (Weerasinghe *et al.*, 2005). Damiani *et al.* (2012) showed an overlap in gene expression in response to rhizobia in Zone II and RKN Giant Cells both of which are responsible for the accommodation of the microbe. *NFP*, a gene regarded as specific to Nod Factor perception, has been shown to play a role in resistance of *M. truncatula* to *Aphanomyces euteiches*, a pathogenic root oomycete (Rey *et al.*, 2013). Chitin oligomers, which are thought to play a positive role in AMF colonisation of the root (Genre *et al.*, 2013) also activate plant defence through the chitin receptor CERK1 in *A. thaliana* and rice (Petutschnig *et al.*, 2010; Shimizu *et al.*, 2010). However, as *A. thaliana* does not form a mutualistic relationship with AMF, plants that have co-evolved with AMF and/or rhizobia presumably have evolved a way of distinguishing the chitin signals through the mixture of chitin oligomers or a suite of receptors that modulate the response, for instance *M. truncatula* has a greatly expanded set of LysM RLKs (Arrighi *et al.*, 2006; Petutschnig *et al.*, 2010; Genre *et al.*, 2013; Rey and Schornack, 2013). It has also been shown through *M. truncatula* mutant *ram2* that cutin C16 monomers are required for the formation of both AMF hyphopodia and oomycete appresoria on the root surface (Wang *et al.*, 2012).

The nuclear movement and cytoskeletal rearrangements seen during AMF infection can also be seen during oomycete and fungal infection, with the nucleus moving directly beneath the contact site. If the plant is resistant to the oomycete, the plant locally thickens the cell wall before the nucleus moves away. If the oomycete continues to invade the cell the association of the nucleus with the haustorium persists until hypersensitive cell death occurs. In susceptible cells, the nucleus does not move toward the oomycete (Guest, 1984; Guest, 1986; Freytag *et al.*, 1994; Daniel and Guest, 2005). During fungal pathogenic infection the nucleus moves to the site of infection in both resistant and susceptible cells. If the fungus successfully enters the cell the nucleus moves away again, and cell death occurs if the plant is resistant. If the fungus is not able to penetrate the nucleus remains at the contact site (Heath *et al.*, 1997). The receptor-like MLO has been shown to interfere with the polarisation of the actin cytoskeleton during infection (Opalski *et al.*, 2005). Interestingly, the barley *mlo* mutant is more resistant to the biotrophic fungal pathogen *Blumeria graminis* in leaves but is also less able to form arbuscules in the roots (Ruiz-Lozano *et al.*, 1999; Bhat *et al.*, 2005; Opalski *et al.*, 2005).

1.3 Plant Receptor-like Kinases

The ability to perceive and respond to information at the cell surface via receptors at the cell surface is a basic property for all living organisms (Stone and Walker, 1995). The ability to transfer that signal to the nucleus requires a signalling cascade through the cytoplasm. The phosphorylation and de-phosphorylation of proteins have been shown to play a central role in signal transduction from the cell surface (Stone and Walker, 1995). Protein kinases catalyse the transfer of the terminal phosphate group from ATP to the side chains of serine, threonine, tyrosine or histidine in a protein (Grebe and Stock, 1999; Alberts, 2002). De-phosphorylation is achieved through the action of protein phosphatases (Alberts, 2002). Approximately 1-3% of a eukaryotic genome is predicted to encode protein kinases, suggesting that they are important in many cellular processes (Stone and Walker, 1995).

In plants, the largest kinase superfamily is the receptor-like kinases (RLKs) (Shiu and Bleecker, 2001a), the first being discovered in *Zea mays* (Maize) by Walker and Zhang (1990). Generally plant RLKs are made up of a signal sequence, an external amino-terminal domain with a transmembrane region and an internal carboxy-terminal kinase domain, similar to the structure of animal receptor tyrosine kinases (RTKs), although the majority of plant RLKs are serine/threonine kinases (Walker, 1994; Shiu and Bleecker, 2001a; Shiu and Bleecker, 2001b; Shiu and Bleecker, 2003). In *A. thaliana* a predicted 610 genes belong to the RLK super family, making up approximately 2.5% of

the protein-coding genes within the genome (Shiu and Bleecker, 2001a). Nearly twice the number of RLKs of *A. thaliana* has been predicted in the rice (*O. indica*) genome (Shiu and Bleecker, 2003; Shiu *et al.*, 2004). Based on their extracellular domains there are 16 families of RLK: C-type Lectin, Crinkly4-like, CrRLK1-like, DUF26, Extensin, Legume Lectin, LRK10-like, Leucine-rich repeat (LRR), Lysin-motif (LysM), URK I, PERK-like, RKF3-like, S-Domain, Thaumatin, WAK-like and receptor-like cytoplasmic kinases (RLCKs) (Shiu and Bleecker, 2001a).

RLCKs are different from most of the RLKs as they lack the external receptor domain, and are similar in structure to the animal non-receptor tyrosine kinases (Shiu and Bleecker, 2001b; Shiu and Bleecker, 2003). Approximately 25% of plant RLKs are RLCKs and can be divided into 19 to 23 subfamilies, with rice having 4 more subfamilies than *A. thaliana* (Shiu *et al.*, 2004). RLCKs can also be organised into different types of kinase; more than 70% of rice RLCKs having only a kinase domain, but the other 30% contain domains that are normally found in the extracellular domains of RLKs such as LRRs, Lectin, DUF, U box and LysM as well as PPR, ECH, USP, UBQ, SPERM and JACALIN (Vij *et al.*, 2008).

RD kinases have an arginine adjacent to an aspartate in the active site of the kinase which can interact with a tyrosine, serine or threonine further down the active site when the aspartate is in a non-phosphorylated. In this inactive state the protein is folded by the amino acid interaction with the active site hidden inside the fold. When the aspartate is phosphorylated the interaction with the tyrosine, serine or threonine is broken and the protein is able to unfold opening up the active site of the kinase. In this activated state RD kinases are then able to phosphorylate other proteins. Therefore RD need to be activated by another kinases before they can function. RLKs can be broadly classified into two groups: The first controlling plant growth and development, such as CLAVATA1 (meristem control) (Clark *et al.*, 1997) and the second involved in plant-microbe interactions, both mutualistic and pathogenic, such as FLS2 (flagellin perception) (Gómez-Gómez and Boller, 2000) and SYMRK (symbiont perception) (Stracke *et al.*, 2002). Typically the RLKs that recognise pathogenic signals are non-RD kinases, but those involved in the recognition of a broad range of pathogens are often RD kinases. In contrast, most RLKs involved in developmental processes are often of the RD class of kinases. However, many non-RD RLKs associate with cytoplasmic RD kinases for signal transduction (Schwessinger and Ronald, 2012). The signalling pathways of plant growth via brassinosteroid signalling and plant defence through the FLS2 have been well studied in *A. thaliana*. Both of these signalling pathways (fig. 1.3.1) contain RLKs at the cell

surface and RLCKs, both RD and non-RD, and share similarities with the CSP, providing useful examples to compare with plant symbiosis signalling.

1.3.1 The brassinosteroid signalling pathway

Brassinosteroid (BR) is a plant hormone that regulates plant growth. Plants that cannot sense BR are dwarfed in height. The BR signalling pathway, characterised through mutant studies in *A. thaliana* and rice, is a signalling cascade from perception of BR at the cell surface through to regulation of gene expression (Kim and Wang, 2010). An RD, LRR-RLK, BRI1 (*BR insensitive 1*) is able to bind BR extracellularly which causes autoactivation of the internal kinase domain (Rusinova *et al.*, 2004; Wang *et al.*, 2005b). BRI1 is found in the plasma membrane in homodimeric receptor complexes or in a heterodimer with another LRR-RLK BAK1 (*BRI1-Associated receptor kinase 1*) (Li *et al.*, 2002; Nam and Li, 2002; Rusinova *et al.*, 2004; Wang *et al.*, 2005b). The addition of BR was found to increase the levels of homo- and heterodimerisation of BRI1 (Wang *et al.*, 2005a; Wang *et al.*, 2008).

BRI1 kinase inhibitor protein (BKI1) is able to inhibit BRI1 by associating with the kinase domain of BRI1 in the absence of BR (Wang and Chory, 2006). When BR binds to BRI1, BKI1 is phosphorylated and dissociates from BRI1 and the plasma membrane enabling access to BRI1 for BAK1 (Wang and Chory, 2006). Modified BKI with an N-terminal myristoylation site stays associated with BRI1 even with BR application and causes the same dwarfed phenotype as the *bri1* mutants (Wang and Chory, 2006). BR signalling kinases (BSKs), RLCKs of the RLCK-XII subfamily, also interact with BRI1 at the plasma membrane. BSKs are phosphorylated upon BR treatment and then dissociate from the membrane (Tang *et al.*, 2008). Overexpression of the BSKs was able to rescue the strong *bri1* phenotype (Tang *et al.*, 2008), suggesting that these RLCKs are the next step in the signal cascade after the membrane bound RLKs.

BIN2 (Brassinosteroid insensitive 2) is a Gibberellin Signalling Kinase (GSK)-like protein that was identified as part of the BR signalling pathway through a semi-dominant mutation *bin2* that displayed a dwarf phenotype like *bri1* (Li *et al.*, 2001). Therefore BIN2 plays a negative role on BR signalling. BIN2 phosphorylates the transcription factors BZR1 (*Brassinole resistant 1*) and BZR2/BES1 (*bri1-EMS suppressor 1*) (He *et al.*, 2002; He *et al.*, 2005) leading to their interaction with 14-3-3 proteins and ultimately proteasomal degradation (Yin *et al.*, 2002; Yin *et al.*, 2005; Vert and Chory, 2006; Gampala *et al.*, 2007). The phosphorylation and association with 14-3-3 proteins stop BZR1 and BZR2 from entering the nucleus where they act (Vert and Chory, 2006; Gampala *et al.*, 2007). BZR1 and BZR2 are dephosphorylated under treatment with BR (He *et al.*, 2002). Wang

et al. (2011) showed that phosphorylated BIK1 is able to bind 14-3-3 proteins and competes with BZR2 for the interaction. It is possible that this acts as another layer of BZR activation upon BR perception by BRI1.

BIN2 is dephosphorylated upon BR treatment by phosphatase BSU1. The dephosphorylated BIN2 is then subject to proteasomal degradation (Mora-García *et al.*, 2004; Kim *et al.*, 2009). Over expression of BSU1 is able to rescue the *bri1* phenotype whilst knockdown of BSU1 causes a severe dwarf phenotype (Mora-García *et al.*, 2004). BSU1 is located mostly in the nucleus but also at the plasma membrane in the absence of BR (Mora-García *et al.*, 2004; Kim *et al.*, 2009). It has been shown that BSU1 interacts with the BSKs at the plasma membrane (Kim *et al.*, 2009). Recently *constitutive differential growth 1 (CDG1)*, an RLCK VII-subfamily member, has been shown to interact with BRI1 and BSU1 suggesting multiple levels of BSU1 regulation (Muto *et al.*, 2004; Kim *et al.*, 2011). The BR signalling pathway is believed to be one of the more completely understood plant signalling pathways and has been used as the basis of understanding other plant signalling pathways (fig. 1.3.1).

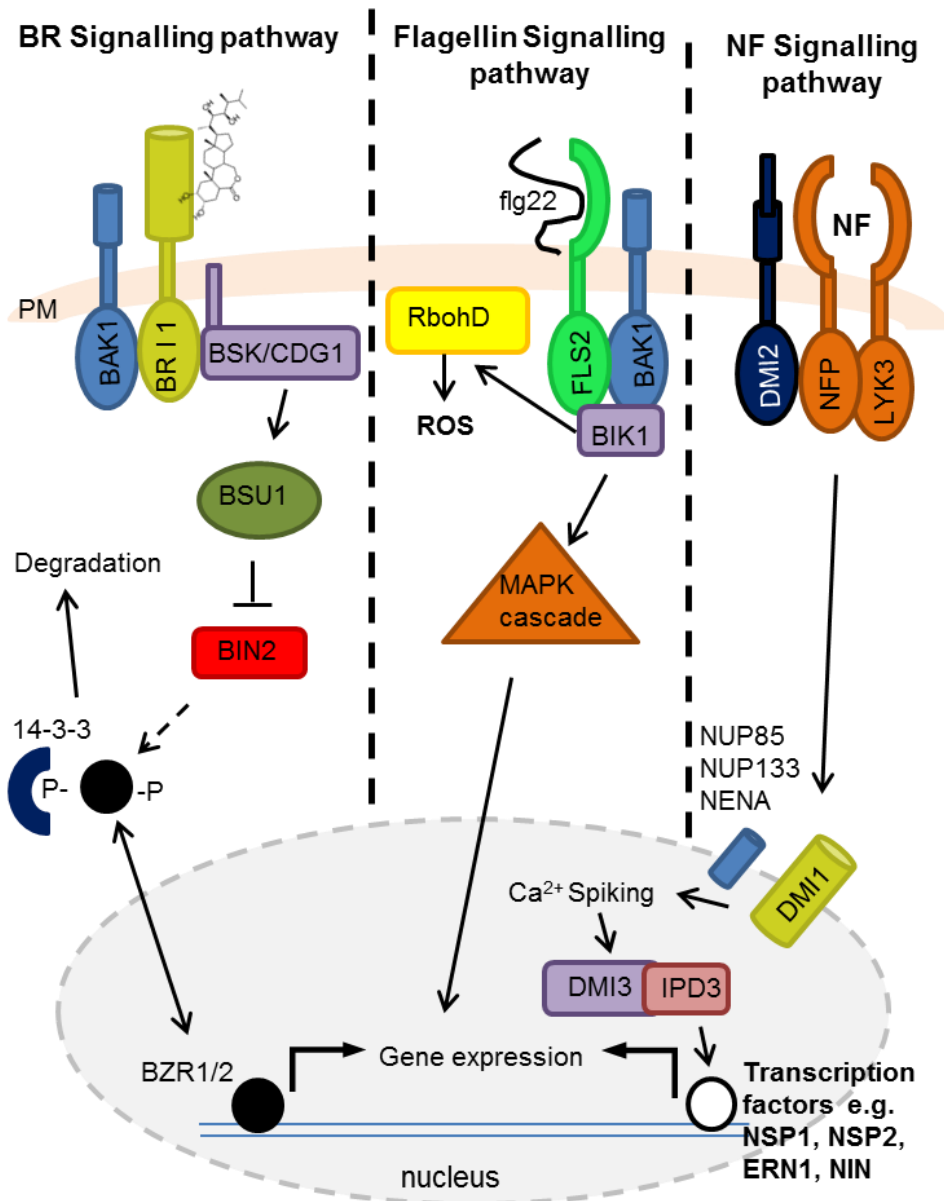


Figure 1.3.1. BR and flagellin signalling pathways

A schematic showing the BR (left), flagellin (middle) and nodulation (right) signalling pathways upon activation by BR, flg22 or NF. Complexes of BAK1 with either BR11 or FLS2 at the plasma membrane (PM) activate RLCKs BSKs/CDG1 or BIK1. In the absence of BR, BIN2 phosphorylates BZR1/2 which is targeted for degradation by interacting with protein 14-3-3. In flagellin signalling, BIK1 interacts with RbohD producing a ROS burst. MAP kinases carry the flagellin triggered signal through the cytoplasm. Perception of NF is at the cell surface by a receptor complex possibly consisting of NFP, LYK3 and DMI2. Activation of DMI1 at the nuclear membrane lead to calcium spiking in the nucleus which is decoded by the DMI3/IPD3 complex and activates symbiosis specific transcription factors. All 3 pathways lead to regulation of gene expression.

1.3.2 The flagellin defence signalling pathway

Plant pathogen recognition is controlled on several levels by RLKs both at the plasma membrane and in the cytoplasm. Pathogens are recognised by molecules that are essential to the life of the pathogen known as microbe-associated molecular patterns (MAMPs) or pathogen-associated molecular patterns (PAMPs) such as bacterial flagellin (Felix *et al.*, 1999), as well as the broader danger-associated molecular patterns (DAMPs) that can be found on more than one type of pathogen such as chitin or peptidoglycan. These patterns trigger defence signalling cascades and gene expression regulation involved in PAMP-triggered immunity (PTI) (Jones and Dangl, 2006; Schwessinger and Ronald, 2012).

The flagellin signalling pathway has been well studied however it is currently not as complete as the BR signalling pathway. The LRR-RLK FLS2 is able to recognise flagellin peptides including flg22, flg15 (in tomato) and a 28-amino acid region in the C-terminal end of the protein flgII-28, as well as full length flagellin (Gómez-Gómez and Boller, 2000; Bauer *et al.*, 2001; Zipfel *et al.*, 2004; Robatzek *et al.*, 2007; Takai *et al.*, 2008; Cai *et al.*, 2011). FLS2 forms a receptor complex at the plasma membrane with BAK1 and the RLCK Botrytis-induced kinase 1 (BIK1) (Veronese *et al.*, 2006; Chinchilla *et al.*, 2007; Lu *et al.*, 2010; Zhang *et al.*, 2010a; Roux *et al.*, 2011; Schwessinger *et al.*, 2011). BIK1 is a PBS-like, RD kinase of the RLCK-VII subfamily (Zhang *et al.*, 2010a). BIK1 and PBL1 (also an RLCK-VII member) have both been shown to be required for full immune responses to *Pseudomonas syringae* and could act partially redundantly in the signalling pathway (Zhang *et al.*, 2010a). flg22 application decreases the association between BIK1 and FLS2, suggesting that BIK1 dissociates from the complex upon activation (Zhang *et al.*, 2010a). Evidence from Lu *et al.* (2010) and Schulze *et al.* (2010) suggests that rapid transphosphorylation occurs between FLS2, BAK1 and BIK1 upon flg22 perception. Mitogen-activated protein (MAP) kinases have been shown to act downstream of the FLS2 receptor complex (Nühse *et al.*, 2000; Asai *et al.*, 2002; Suarez-Rodriguez *et al.*, 2007). However, it is not yet known how they are linked to the receptors (fig.1.3.1).

Recent research by Li *et al.* (2014) has shown that an NADPH oxidase RbohD interacts with BIK1 and FLS2 and is activated upon flg22 perception. PTI has been shown to initiate a transient influx of calcium ions into the cytosol followed by a transient burst of ROS leading to the closure of stomata and callose deposition to strengthen the cell wall (Blume *et al.*, 2000; Lecourieux *et al.*, 2002; Nühse *et al.*, 2007; Zhang *et al.*, 2007). This research has given some insight into the mechanism controlling pathogen-activated ROS generation. There has been increasing evidence of cross-talk between the BR and flg22

signalling pathways. For example, BIK1 has been shown to interact with BRI1 and the BSKs with FLS2 (Lin *et al.*, 2013; Shi *et al.*, 2013b). Brassinosteroids are known to inhibit the FLS2 signalling pathway and flg22 inhibits plant growth (Bethke *et al.*, 2009; Albrecht *et al.*, 2012). It is possible that the activity of RLCKs could holistically modulate the activity of signalling pathways within the cell (Laluk *et al.*, 2011).

1.3.3 Comparison of the CSP with BR and flg22 signalling

Parallels can be drawn between these two signalling pathways and the signalling cascade downstream of the symbiosis RLKs. In the BR and flagellin signalling pathways RLCKs transfer the signal from receptor complexes at the cell surface onto downstream signalling components that ultimately leads to transcriptional changes. It is likely that the receptors NFP, LYK3, and DMI2 may sit in complexes at the plasma membrane along with cytoplasmic components such as a remorin (SYMREM1) and an E3 ubiquitin ligase (PUB1) (Lefebvre *et al.*, 2010; Mbengue *et al.*, 2010; Tóth *et al.*, 2012). It is possible that MAP kinases perform signal transduction from the receptors to the nucleus (Chen *et al.*, 2012). It is also conceivable that RLCKs may act as the next step in the signal relay between the RLKs and the MAP kinases. In symbiosis there are known transient influxes of calcium and ROS in response to NF and during nodule development (Miwa *et al.*, 2006; Pauly *et al.*, 2006). It is possible that currently unknown RLCKs may interact with NFP, LYK3 or DMI2 to regulate the ROS machinery as BIK1 does in flg22 signalling (Peleg-Grossman *et al.*, 2012; Li *et al.*, 2014). RLCKs may also play a role in parallel to the CSP, co-ordinating developmental and defence signalling pathways during symbiosis (Peleg-Grossman *et al.*, 2012).

In this study, three *RLCK* genes were selected using the Medicago Gene Atlas (MtGEA) and in-house microarray data. These genes were investigated for their roles in both RNS and mycorrhizal symbiosis through mutant studies and RNAi. Resources for RLCK protein interaction were also made.

Chapter 2: Materials and methods

2.1. Plant material

Medicago truncatula lines used are listed in table 2.1.1. Homozygous *Tnt1* mutants were identified in the lab by PCR. A homozygous EMS mutant was identified by sequencing of PCR products. See appendix I for primers. *Nicotiana benthamiana* plants were cultivated by Horticultural services and used for infiltration from 3 weeks post sowing.

Line	Background	Description	Mutation	Source
R108	R108	Wild type	WT	Hoffmann <i>et al.</i> (1997)
A17	A17	Wild type	WT	Van den Bosch and Stacy (2003)
NF12390 (<i>rlck1-1</i>)	R108	<i>Tnt1</i> insertion at position 447 (genomic) in <i>RLCK1/SPK1</i>	<i>Tnt1</i>	Samuel Roberts Noble Foundation, USA
NF10796 (<i>rlck1-2</i>)	R108	<i>Tnt1</i> insertion at position 621 (genomic) in <i>RLCK1/SPK1</i>	<i>Tnt1</i>	Samuel Roberts Noble Foundation, USA
NF11296 (<i>rlck1-3</i>)	R108	<i>Tnt1</i> insertion at position 878 (genomic) in <i>RLCK1/SPK1</i>	<i>Tnt1</i>	Samuel Roberts Noble Foundation, USA
NF9810 (<i>rlck2-1</i>)	R108	<i>Tnt1</i> insertion at position 1342 (genomic) in <i>RLCK2</i>	<i>Tnt1</i>	Samuel Roberts Noble Foundation, USA
NF7569 (<i>rlck2-2</i>)	A17	Single base pair mutation C to T at position 1523 (genomic) of <i>RLCK2</i>	EMS mutagenesis	RevGenUK, Norwich, UK
NF5270 (<i>rlck3-1/Scooby</i>)	R108	<i>Tnt1</i> insertion line. Scooby phenotype.	<i>Tnt1</i>	Samuel Roberts Noble Foundation, USA

Table 2.1.1. Plant material.

2.1.1 Seed preparation

Mature seed pods were collected by hand from dry *M. truncatula* plants. They were then placed at 37°C for 4-7 days to dry further. Pods were then opened using wooden blocks covered in corrugated rubber to access the seeds. For germination, seeds were scarified using sand paper. The seeds were then treated with 12.5% bleach for 2 minutes and then a series of five 2 minute washes with dH₂O, until all the bleach was no longer present – tested using indicator blue tissue. Seeds were then immersed in water to imbibe for at least 1 hour before plating out onto Distilled Water Agar (DWA) plates and inverting. Seeds were placed into the dark at 4°C for 3 days for stratification or 7 to 14 days for vernalisation.

2.2 Bacterial and Yeast strains

All bacterial strains used are in table 2.2.1.

Strain	Resistance	Species	Description
DH5 α	-	<i>Escherichia coli</i>	<i>E. coli</i> strain for plasmid amplification
DB3.1	-	<i>E. coli</i>	<i>E. coli</i> strain resistant to the <i>ccdB</i> cassette
AR1193	Rif & Carb	<i>Agrobacterium rhizogenes</i>	For transformation of <i>M. truncatula</i> roots
GV3101	Rif & Gen	<i>Agrobacterium tumefaciens</i>	For transformation of <i>N. benthamiana</i>
AH109	-	<i>Saccharomyces cerevisiae</i>	For yeast 2-hybrid analysis
Sm1021	Tet	<i>Sinorhizobium meliloti</i>	Rhizobial symbiont of <i>M. truncatula</i>

Table 2.2.1. Bacterial and yeast strains.

2.3 Growth Media

The composition of the media used for plant, bacterial and yeast growth are given in table 2.3.1.

Media	Composition for 1L
Rhizobium complete medium (TY)	5 g Difco tryptone, 3 g Difco yeast extract, 1.325 g CaCl ₂ (containing 15 g agar for solid growth medium).
Lennox (L)	10 g tryptone, 5 g yeast extract, 5 g NaCl, 1 g D-Glucose (containing 10 g agar for solid growth medium).
SOC	20 g tryptone, 5 g yeast extract, 0.58 g NaCl, 0.19 g KCl, 2.03 g MgCl ₂ , 2.46 g MgSO ₄ 7H ₂ O, 3.6 g D-Glucose.
Distilled Water Agar (DWA)	1.5 % w/v Bacto agar, pH 5.7 (adjusted with KOH)
Fahraeus plant medium (FP)	0.1 g CaCl ₂ 2H ₂ O, 0.12 g MgSO ₄ , 0.01g KHPO ₄ , 0.150 g NaHPO ₄ .12H ₂ O, 5 mg ferric citrate, 2.86 g H ₃ BO ₃ , 2.03 g MnSO ₄ , 0.22 g ZnSO ₄ .7H ₂ O, 0.08 g CuSO ₄ .5H ₂ O, 0.08 g H ₂ MoO ₄ .4H ₂ O, pH 6.3-6.7. For solid medium 0.5% (w/v) LabM No. 1 agar was added.
Modified FP	FP medium containing 0.5 mM NH ₄ NO ₃
SD⁺-LW	1.9g Yeast Nitrogen Base without Ammonium Sulphate and Amino Acids, 5g (NH ₄)SO ₄ , 20g D-Glucose, 20g Formedium agar, 380mg Leucine, 76mg Tryptophan. pH 5.8
SD⁺-AHLW	1.9g Yeast Nitrogen Base without Ammonium Sulphate and Amino Acids, 5g (NH ₄)SO ₄ , 20g D-Glucose, 20g Formedium agar, 380mg Leucine, 76mg Tryptophan, 76mg Alanine, 76mg Histidine. pH 5.8
Medicago mix (compost)	6:6:1 Mix of Levington F2 compost, John Innes No. 2 compost and 4 mm grit.
50:50 mix Terragreen:Sand	1:1 mix of terragreen (Oil-dry UK Ltd, UK) and sharp sand (BB Minerals, UK)

Table 2.3.1. Media used for plant, bacterial and yeast growth.

2.4 *Agrobacterium* transformation, growth and plant transformation

2.4.1 *Agrobacterium rhizogenes* 'Hairy root' transformation of *M. truncatula*

Agrobacterium rhizogenes strain AR1193 was transformed with constructs via electroporation at 200Ω and 2.5V. The *A. rhizogenes* was then shaken at 28°C for 1 hour with SOC medium. The *Agrobacterium* was plated onto selection plates and left for 3 days at 28°C to grow. Colonies were then grown overnight in liquid culture at 28°C with antibiotic selection and shaking, 600μl were plated out onto selection and left to grown for 3 days on antibiotic selection LB plates to form a thick layer of *A. rhizogenes*. The

transformed *rhizogenes* was then used to inoculate 1 day old A17 seedlings. 3mm of root tip were removed from the seedlings using a scalpel, then the seedling dipped into the *A. rhizogenes* and placed onto square Modified FP (ModFP) plates, poured at a slant and covered in a sterile filter paper. The bottom half of the plates were then covered in black plastic to block out the light and placed in growth chambers at 20°C/15°C day/night temperature with 16 hour days. After 1 week the seedlings were transferred to fresh ModFP plates and the non-transformed roots, identified by fluorescence microscopy, were removed.

2.4.2 *Agrobacterium tumefaciens* transformation of *Nicotiana benthamiana*

Agrobacterium tumefaciens strain GV3101 was transformed with constructs via electroporation at 200Ω and 2.5V. The *A. tumefaciens* was then shaken at 28°C for 1 hour with SOC medium and plated onto antibiotic selection plates and grown for 3 days at 28°C. A colony was grown overnight in liquid culture at 28°C with shaking and antibiotic selection. The liquid culture was spun down and the supernatant removed. The bacteria were resuspended in dH₂O. The *A. tumefaciens* was infiltrated into the leaf by pressure infiltration using a 1ml syringe. dH₂O was used as a mock treatment.

2.5 Image capture and microscopy

Light microscopy was performed on either a Nikon Eclipse E800 with a Pixera Pro 600ES camera or a Zeiss Axiophot with a Retiga-2000R Fast 1394 Color camera, QImaging. Fluorescence microscopy was performed on a Zeiss Axiophot with a Retiga-2000R Fast 1394 Color camera, QImaging, or a Leica MZFLIII Fluorescence stereoscope. Confocal microscopy was performed on a Zeiss 780 LSM. Scale bars were added to the images either using the QCapture Pro software (QImaging) or the Image J software.

2.6 DNA amplification, purification and sequencing

All DNA extraction was carried out using a Qiagen DNeasy Plant Kit by Richard Goram, Norwich. All plasmid extraction was carried out using Qiagen Mini-prep spin columns as per manufacturer's instructions.

2.6.1 Standard Polymerase Chain Reaction (PCR)

GoTaq® Green Master Mix (Promega) was used as the standard Taq polymerase for genotyping and colony PCR following the manufacturer's instructions for a 25µl reaction volume using cycling parameters 95°C 30s (10 minutes if for colony PCR), [94°C 30s, T_m-3°C 30s, 72°C 30s/kb]x28 - 35, 72°C 2- 10 minutes. Phusion High-Fidelity Taq polymerase (New England Biolabs Ltd) was used for cloning PCRs following manufacturer's instructions for a 20µl or 50µl reaction volume using cycling parameters

98°C 30s, [98°C 10s, Tm°C 20s, 72°C 1min/kb]x35, 72°C 2- 10 minutes. All PCRs were cooled to 10°C after cycling and stored at 4°C or chilled on ice if to be used directly. All PCR amplifications were performed using a G-Storm GS1 thermal cycler (Gene Technologies Ltd). See appendix I for primers.

2.6.2 Restriction Digest

Purified plasmids were digested using restriction enzymes. Digests were performed as per the manufacturer's instructions (Life Technologies or New England Biolabs), using 1U of enzyme to a 10µl or 20µl reaction with an incubation time of 1 hour at 37°C.

2.6.3 Sequencing

DNA sequencing was carried out by performing the BigDye® reaction with either purified PCR product or plasmid according to manufacturer's protocol and then completed by The Genome Analysis Centre (TGAC), Norwich or Eurofins (MWG Operon), UK. Purified plasmid of Golden Gate constructs was sent for Next Generation Sequencing by IMGM Laboratory, Germany.

2.7 qRT-PCR

Root material was ground on liquid nitrogen using a pestle and mortar and RNA was extracted using a QIAGEN® RNeasy mini kit. The RLT buffer was pre-warmed to 50°C and the elution volume was reduced to 30µl. RNA was then treated with Turbo DNase (Life Technologies™) to remove the DNA. The quality of the RNA was tested on a 1% Agarose gel containing ethidium bromide and the quantity was tested on a NanoDrop (Thermo Fisher Scientific). cDNA was synthesised using SuperScript®II Reverse Transcriptase (Life Technologies™). The input RNA was normalised to the lowest sample with a lower threshold of 400ng/ total RNA.

qRT-PCR was carried out on a CFX96 Touch™ c1000 thermal cycler (Bio-Rad) using SYBR™ Green JumpStart Taq ReadyMix (without MgCl₂) in a 96 well plate. Each well contained the following: 2.6µl MgCl₂; 5µl SYBR Green, 2µl diluted cDNA, 1.6µl each 20µM primers to give a total of 10µl. The primer efficiencies were calculated using a serial dilution of control cDNA. The following parameters: 95°C 30s, [94°C 30s, 60°C 30s, 72°C 30s]x49. Melt curve 65°C to 95°C in 0.5°C increments in 5s.

The efficiency of all primer pairs was calculated using a dilution series and linear regression of the resulting Ct data points. *Ubiquitin*, *EF1α* and *TIP41*-like protein were determined to be the most stable references. Normalized relative quantities were calculated using the qBase model (Hellemans *et al.*, 2007), which allows for multiple housekeeping genes and primer specific efficiencies. Values based on 3 technical reps

per sample. The expression was then calculated relative to the control. Standard error was calculated as relative standard error to the control. See Appendix I for primers.

2.8 Cloning

2.8.1 Gateway® Cloning, Invitrogen

The desired gene or promoter region was amplified via PCR using Phusion High Fidelity Polymerase, New England Biolabs. The primers were designed to contain the attB site required for the Gateway® BP, for recombination of the PCR fragment into pDONR207 (Karimi *et al.*, 2002). The donor plasmid was then propagated in *E.coli* strain DH5 α and correct colonies were identified by PCR. A Gateway® LR reaction facilitates recombination from the donor vector to the destination vector. The destination plasmid was then propagated in *E.coli* strain DH5 α and potentially correct colonies were identified by PCR and verified by sequencing.

2.8.2 TOPO® Cloning, Life technologies

The desired gene or promoter region was amplified via PCR using Phusion High-fidelity Polymerase, New England Biolabs. The primers were designed to contain a CACC 5' extension compatible with TOPO® cloning, Life Technologies. The PCR fragments were cloned into pENTR-D entry vector following the TOPO manual; the only difference was the incubation at room temperature of the vector, the insert and the clonase was overnight rather than the recommended 5 to 30 minutes. The inserts in the pENTR-D entry vector were then transferred to the compatible Gateway® vector using the LR reaction as described above.

2.8.3 Golden Gate Cloning

Golden Gate cloning was carried out as described in Engler *et al.* (2008) and Weber *et al.* (2011), using compatible sites with the Engineering Nitrogen Symbiosis for Africa (ENSA) project, see below (Oldroyd, communications). Level 0 modules were synthesised by Life Technologies GeneArt® Gene Synthesis. Level 1 modules and level 2 constructs were assembled in the lab. Level 0 modules and Level 1 End linkers are Spec resistant. All Level 1 modules, except the End linkers, are Amp resistant. Level 2 constructs are Kanamycin resistant. After assembly each level was propagated in *E.coli* strain DH5 α . Level 1 modules were checked by colony PCR before being sequenced. Level 2 constructs were checked by restriction digest before being sent for next generation sequencing.

2.9 Nodulation Phenotyping

Medicago truncatula seeds were germinated on DWA and then planted in a 50:50 mix terragreen and sand. Plants were left to grow in the mix for one week before inoculation. *Sinorhizobia meliloti* 1021 *LacZ* was grown overnight in 10ml TY plus Tetracycline to an OD600 absorbance between 0.2 and 0.5. The rhizobia were diluted to an OD600 absorbance between 0.05 and 0.001 with water. 2ml of this diluted rhizobia was pipetted at the base of each plant. After 21 days the plants were removed from the soil, washed and the numbers of white and pink nodules per plant were counted.

2.9.1 Histochemical staining procedure

Root material was submerged in 2.5% glutaraldehyde and placed under a vacuum for 15 minutes. The glutaraldehyde was removed and fresh glutaraldehyde was added before leaving at room temperature for a minimum of 1 hour. The fixed material was then washed with Z buffer with one 5 minute wash followed by a 1 hour wash. Fresh *LacZ* staining solution was made according to the following: 1mM 5-bromo-4-chloro-3-indolyl- β -D-galactopyranoside (X-gal) or 5-bromo-6-chloro-3-indolyl- β -D-galactopyranoside (Magenta-gal); 0.1M sodium phosphate; 10mM Potassium chloride; 1mM Magnesium Sulphate; 5mM Potassium Ferricyanide; 5mM Potassium Ferrocyanide. 30 to 40 μ m longitudinal sections of the nodule were made on a Vibratome.

2.10 Mycorrhizal Phenotyping

2.10.1 Growth media and inoculation

Several sources of AMF inoculum were used in the course of this study. Seedlings were planted directly into one of the following inoculums.

Chive inoculum: *Rhizophagus irregularis* was grown in a 50:50 mix with chive plants. Inoculum was made by chopping up the root mass and soil containing *R. irregularis*. A 50:50 mix of terragreen and sand was made and then mixed with the chive root inoculum at a ratio of 1:20 inoculum : sand mix.

PlantWorks inoculum: A commercial inoculum was obtained from PlantWorks, UK, and mixed with the 50:50 sand mix at a ratio of 1:10 inoculum : sand mix.

Symplanta inoculum: Another commercial inoculum was obtained from Symplanta, Munich, 10,000 spores/ml of *Rhizophagus irregularis* (syn: *Glomus irregulare*) SYMPLANTA-001 research grade. For a more concentrated inoculum, 750 spores/plant was use. For a less concentrated inoculum, 500 spores/plant was used.

For mutant colonisation assays extra R108 WT plants were included in each experiment and level of WT colonisation was checked weekly from 5 weeks post-inoculation until a minimum level of colonisation of 50% was achieved. Once sufficient WT colonisation was achieved all plants were then ready for staining and scoring.

2.10.2 Mycorrhizal staining and scoring

Root material was first washed in fresh 10% KOH at 95°C for 15 minutes, then rinsed in water before being transferred to a 95°C ink and acetic acid solution (5% ink, 5% acetic acid) for 6 minutes. The roots were then left in water over night to de-stain. Colonisation of the root by AMF was scored using the grid method as described by Giovannetti and Mosse (1980)

Alternatively, the AMF was stained using WGA-AlexaFluor549. Roots were placed in 50% ethanol overnight before being transferred to 20%KOH for 2-3 days at room temperature. Roots were rinsed with dH₂O and submerged in 0.1M HCl for 1-2 hours. After another rinse with dH₂O, and again with phosphate buffered saline (PBS) solution, the roots were submerged in PBS/WGA-AF549 (final concentration of 0.2µg/ml) and kept in the dark at room temperature overnight.

2.11 Gene silencing – RNA interference

2.11.1 Constructs

The double knockdown construct was obtained from Myriam Charpentier. It was designed against the *RLCK1* CDS and subsequently shown to knockdown both *RLCK1* and *RLCK2*. The vector used was pK7GW|WG2D(II)R modified from pK7GW|WG2D(II) (Karimi *et al.*, 2002; Capoen *et al.*, 2011).

The *RLCK2* knockdown construct was designed against the *RLCK2* 5' UTR region. It covers 161bp upstream of the start codon. It was cloned into pENTR-D TOPO entry vector using the CACC overhang on the forward primer. It was then cloned into the destination vector pK7GW|WG2D(II)R using GATEWAY® LR reaction, Invitrogen. See Appendix I for sequencing primers.

2.11.2 Transformation of RNAi constructs

A. *rhizogenes* transformation was carried out as described in 2.4.1. Two weeks after the plate transfer, the plants were then transferred to sterilised 50:50 mix in small greenhouse boxes (Sigma) to keep the humidity high. The lid was slowly removed over several days to reduce the humidity without shocking the plants.

2.11.3 Rhizobial Inoculation and scoring

After one week in the pots the plants were inoculated with Sm1021 as described above for nodulation phenotyping. Plants were checked for nodules at 21dpi. Only transformed roots displaying the dsRED transformation marker were included in the count. The transformed roots were then removed from the plants, frozen using liquid nitrogen and stored at -80°C for qRT-PCR.

2.12 Gene expression analysis

2.12.1 *In silico* gene expression analysis (MtGEA)

In silico gene expression analysis was carried out using the Medicago Gene Expression Atlas (MtGEA) Database (Benedito *et al.*, 2008; He *et al.*, 2009), Samuel Roberts Nobel Foundation. Probesets were identified using the BLAST function using the CDS sequence.

2.12.2 Promoter-GUS analysis

RLCK1 promoter:*GUS* construct (pRLCK1:*GUS*) was obtained from Nicolas Pauly, INRA France (Andrio *et al.*, 2013). The *RLCK2* promoter:*GUS* (pRLCK2:*GUS*) construct was made by cloning the 2328bp region upstream of the *RLCK2* start codon into pDONR207. The promoter region was amplified by PCR and confirmed by sequencing. The primers contained overhangs compatible for the Gateway® BP reaction. An LR reaction was then performed to clone the promoter region into the pKGWFS2 promoter:*GUS* vector. The *Lotus japonicus Ubiquitin1 (LjUB1)* promoter:*GUS* construct was used as a positive control for the staining. See Appendix I for primers.

Plants were transformed with the constructs using *A. rhizogenes* transformation. Plants were inoculated with either *LacZ* containing Sm1021 and checked at 4, 7, 14d and 21dpi or *R. irregularis* (chive inoculum) and checked at 5, 10 and 20dpi.

GUS staining solution was freshly made according to the following: 2mM 5-bromo-4-chloro-3-indolyl- β -glucuronic acid (X-GlcA); 10mM Na-EDTA; 1mM potassium ferricyanide; 0.1 M sodium phosphate; 0.1% V/V Triton X-100.

The plant roots were immersed in the *GUS* staining solution and incubated at 37°C and removed when the level of staining seemed appropriate – approximately 5 hours. The *GUS* stained roots were then either counterstained with a Wheat Germ Agglutinin (WGA) Alexa Fluor® 594 dye (Life Technologies) for AMF colonisation or fixed and counterstained with magenta-gal for rhizobial colonisation.

2.13 Phylogenetic Analysis

The protein sequences of MtRLCK1 and MtRLCK2 were used as queries for BLASTP searches against the predicted protein sequence databases of the genomes of *Amborella trichopoda*, *Arabidopsis lyrata*, *A. thaliana*, *Brachypodium distachyon*, *Brassica rapa*, *Chlamydomonas reinhardtii*, *Glycine max*, *L. japonicus*, *M. truncatula*, *N. benthamiana*, *Oryza brachyantha*, *Oryza glaberrima*, *Oryza indica*, *O. sativa*, *Panicum virgatum*, *Phaseolus vulgaris*, *Physcomitrella patens*, *Populus trichocarpa*, *Selaginella moellendorffii*, *Setaria italica*, *Solanum lycopersicum*, *Solanum tuberosum*, *Sorghum bicolor*, *Triticum aestivum*, *Vitis vinifera* and *Zea mays* using Geneious. The top 50 blast hits for each of these genomes were taken forward and aligned with the queries using ClustalW with the default parameters. The resultant alignment was used to construct trees using the Neighbour-joining tree algorithm implemented in Geneious with 1000 bootstrap replicates and default values for the other parameters. From the resulting tree, the RLCK1 and RLCK2 branches were extracted and the proteins were realigned as described above to give the final tree.

2.14 Protein Analysis

2.14.1 *In silico* protein analysis

Proteins were analysed *in silico* using InterProScan4 (Hunter *et al.*, 2012) and the ExPASy Bioinformatics Portal (Artimo *et al.*, 2012) in 2011. In 2014 proteins were analysed *in silico* using InterProScan5 (Jones *et al.*, 2014) and the Calmodulin target database (<http://calcium.uhnres.utoronto.ca/ctdb/ctdb/home.html>).

2.14.2 Protein localisation constructs

Protein localisation constructs were created by PCR fusion of RLCK1 and RLCK2 to mCherry using successive PCR to splice PCR products together. The first PCR (PCR1) amplified *RLCK1* and *RLCK2* CDS with overhanging attB site at the 5' end and complementary sequence to mCherry at the 3' end. mCherry was also amplified with a 5' overhang that was complementary to *RLCK1* or *RLCK2* CDS and 3' attB. The second PCR (PCR2) takes place in two steps. Step a combines the products from PCR1 as the complementary overhangs act as primers for the polymerase to create the fused product. Step b has the addition of 5' and 3' primers for the full length fused product *RLCK1:mCherry* or *RLCK2:mCherry*. See appendix I for primers.

PCR1: Composition: 0.05U Phusion Taq, 1x GC buffer, 1µM dNTP, 0.25µM Forward Primer, 0.25µM Reverse Primer, 50-100ng Template DNA. Cycling parameters: 98°C 30s, [98°C 10s, 55°C 20s, 72°C 2m]x35, 72°C 4m.

PCR2a: Composition: 0.05U Phusion Taq, 1x GC buffer, 0.8 μ M dNTP, 50-100ng Gene CDS, 50-100ng mCherry CDS. Cycling parameters: 98°C 30s, [98°C 10s, 50°C 20s, 72°C 2m30s]x10, 72°C 5m.

PCR2b: Add to PCR2a reaction tubes: 0.1 μ M Forward Primer and 0.1 μ M Reverse Primer. Cycling parameters: 98°C 30s, [98°C 10s, 60°C 20s, 72°C 5m]x28, 72°C 10m.

The fused fragments were cloned into pDONR207 by a BP reaction. They were then put into the pUB-GW-GFP via an LR reaction (Maekawa *et al.*, 2008). Constructs were checked by sequencing, see appendix I for primers. Constructs were transformed into *N. benthamiana* leaves by *A. tumefaciens* infiltration and localisation was checked in leaf discs using a confocal microscope at 1, 2 and 3dpi.

2.14.3 Yeast 2-Hybrid

RLCK1 and *RLCK2* CDS were amplified using Phusion High-Fidelity Taq polymerase and cloned into pENTR-D using TOPO® cloning. The CDS was then transferred by LR reaction into pGADT7 and pGBKT7 Gateway® vectors for expression of *RLCK1* and *RLCK2* proteins as bait and prey respectively. AH109 yeast strain was transformed using the lithium acetate method (Daniel Gietz and Woods, 2002). The yeast was grown at 28°C for 3 days on SD⁺ agar minus leucine and tryptophan (SD⁺-LW) or SD⁺ agar minus alanine, histidine, leucine, and tryptophan (SD⁺-AHLW) for interaction selection.

2.15 Co-Immunoprecipitation

Cloning was performed using the Golden Gate system to make Level 2 constructs encoding myc-tagged *RLCK1* or *RLCK2* and GFP-tagged MtNFP, MtLYK3, MtHMGR1 and MtDMI2. See Appendix I for construct details and plasmid maps. Constructs were transformed into *N. benthamiana* leaves by *A. tumefaciens* infiltration.

2.15.1 Protein Extraction

Leaf discs were taken at 1, 2 and 3dpi, frozen in liquid nitrogen and stored in a -80°C freezer. Samples were ground either using a pestle and mortar chilled using liquid nitrogen, or a tissue lyser using 3mm tungsten carbide beads (Qiagen). The protein was extracted by one of two methods, the first added warm buffer (65°C) to the ground sample [100mM Tris-HCl pH 7.4, 150mM NaCl, 5mM EDTA, 10mM DTT 5% SDS, 4M Urea + Roche protease inhibitor cocktail], incubated at 90°C for 10 minutes, centrifuge maximum speed for 2 minutes, collect supernatant and mix with SDS sample buffer. The second method was as described by (Waadt *et al.*, 2008). Protein extract produced by either method was mixed with SDS sample buffer 4x Laemmli sample buffer (Bio-Rad), heated

at 90°C for 5 minutes, loaded into a 10x SDS-PAGE Gel and ran at 150V for 1 hour 25 minutes.

2.15.2 Western Blot

Proteins were transferred to the membrane at 100V for ~1 hour. The membrane was blocked using 5% milk in TBS-T [10mM Tris-HCl pH7.4, 150mM NaCl, 0.1% Tween 20] for 1 hour. The membrane was washed in TBS-T and incubated overnight at 4°C with the primary antibody. The membrane was washed in TBS-T before incubation with the secondary antibody for 1 hour at room temperature. The membrane was washed in TBS-T 3 times for 10 minutes before treating with enhanced chemiluminescence (ECL) solution and exposing to an X-ray film for times between 30 seconds and 30 minutes. Total protein levels loaded were determined by Coomassie staining of protein gels or by Ponceau staining of the membranes used in the blot.

Chapter 3: Characterisation and expression of *Receptor-Like Cytoplasmic Kinase 1 and 2*

3.1 Introduction

Medicago truncatula (alongside *Lotus japonicus* and *Glycine max*) is one of the model plants used to study the legume symbioses with rhizobia and AMF. Transformation of *Medicago* by floral dip transformation as previously performed in *Arabidopsis* is not possible on a large scale (Bechtold and Pelletier, 1998). T-DNA mutagenesis is not suitable for generating a large mutant collection due to the relative difficulty in transforming *M. truncatula* compared to *Arabidopsis*. D'Erfurth *et al.* (2003) used the long terminal repeats (LTR) retrotransposon *Tnt1* from tobacco (*Nicotiana tabacum*) (Grandbastien *et al.*, 1989) to transform the *M. truncatula* R108 ecotype. They showed that during regeneration from tissue culture the *Tnt1* retrotransposon transposes at a higher frequency into transcriptionally active euchromatin than non-coding euchromatin regions and that they are stable during the life cycle of the plant. The retrotransposon can also be re-activated by tissue culture to generate more mutations. The *Tnt1* retrotransposon uses a “copy and paste” system leaving the transposon in the original position whilst a copy of the transposon is inserted somewhere else in the genome, usually far away from the original. *Tnt1* is 5.3 kb long and creates a 5 bp duplication at each end upon insertion. Each *Tnt1* line is estimated to contain between 6 and 59 new insertions (Tadege *et al.*, 2008). This means that in the case of reverse genetic studies, within a single line there can be many insertions additional to the one in the gene of interest. Hemizygous insertions that arise in the initial generation (R0) segregate in subsequent generations (R1, R2 etc.) and so can be randomly lost or fixed as homozygous as the material is advanced, resulting in genotypically distinct sibling lines at later generations.

At the Samuel Roberts Noble Foundation a *Tnt1* insertion mutant collection has been generated that in 2011 was estimated to cover 85% of the *M. truncatula* genome (D'Erfurth *et al.*, 2003; Tadege *et al.*, 2005; Tadege *et al.*, 2008; Cheng *et al.*, 2011). A Flanking Sequence Tag (FST) database, which was generated by TAIL-PCR showing the sequences surrounding *Tnt1* insertions in each line, can be BLAST searched using the genomic sequence of a gene of interest to find useful *Tnt1* lines. The *Tnt1* collection can also be reverse screened via PCR using gene-specific primers if an FST cannot be found. In this way, this collection can be used to identify mutant lines segregating for a desired mutation.

Another extremely useful resource open to the *Medicago* research community is the Medicago Gene Expression Atlas (MtGEA). It is compiled by the Samuel Roberts Noble Foundation and collates data from Affymetrix Medicago Gene Chip® experiments for *M. truncatula* under a variety of biological and chemical conditions (Benedito *et al.*, 2008; He *et al.*, 2009; Hogekamp *et al.*, 2011; Czaja *et al.*, 2012; Gaude *et al.*, 2012; Seabra *et al.*, 2012). Based on interesting expression profiles that show gene expression during, and induced by, the presence of symbiotic partners, and a high sequence homology to each other (76 % at the nucleotide level and 69 % at the amino acid level), two kinase genes were selected for investigation. Based on their lack of transmembrane domains and close homology to a member of the Rice Receptor-like cytoplasmic Kinase Family XV (Jung *et al.*, 2010) these genes were named *Receptor-like Cytoplasmic Kinase 1 (RLCK1)* and *RLCK2*.

RLCKs have been shown to interact with membrane bound receptor kinases and phosphorylate downstream signalling components in the PAMP-triggered immunity and brassinosteroid signalling pathways (Tang *et al.*, 2008; Kim *et al.*, 2009; Lu *et al.*, 2010; Zhang *et al.*, 2010a; Shi *et al.*, 2013a). There are several RLKs required for symbiosis and currently for the symbiosis signalling pathways we do not know how the signal travels from the plasma membrane to the nuclear envelope to activate DMI1. It is possible that RLCKs are part of the signal relay.

During the course of this study, Damiani *et al.* (2012) published that in *M. truncatula* expression of *RLCK1* was in nodule zones I and II as part of their study into the similarities between the development of a nodule and a pathogenic nematode gall. Andrio *et al.* (2013) later identified *RLCK1* as part of their transcriptome analysis investigating the role of reactive oxygen species (ROS) in nodulation, naming it *MtSpk1 (Symbiotic Protein Kinase 1)*. They showed that *RLCK1* was upregulated both in response to NF and hydrogen peroxide treatment. Using promoter-GUS analysis they showed that *RLCK1* was expressed throughout rhizobial infection, early nodule development and in the nodule infection zone (Zone II) confirming the earlier study (Damiani *et al.*, 2012). Andrio *et al.* (2013) used an artificial micro-RNA (amiRNA) to reduce the gene expression of *RLCK1* to an average of 40% of the control expression and was able to see a significant reduction of 2 nodules/plant on the knock-down plant roots. They also had a preliminary look at the expression of known symbiotic genes in the amiRNA roots and saw a reduction in the expression of transcription factors *MtNIN* and *NF-YC1* (formerly *MtHap2.1*). However, Andrio *et al.* (2013) did not have any stable mutants for *RLCK1* and RNAi silencing can be subject to off-target gene silencing. I discuss the limitations of RNAi in more detail in Chapter 4. They also did not look at *RLCK2* which has a 76% nucleotide sequence

homology with *RLCK1*. Here I show that my work on the RLCKs is complimentary to and expands upon the work already published using stable mutants to characterise the mutant phenotypes.

3.2 Identification of Mutants for *RLCK1* and *RLCK2*

Using the tools available on the Medicago Insertion Database FSTs were identified for insertions in the second intron (447 bp genomic), third exon (621 bp genomic) and third intron (878 bp genomic) of *RLCK1* in *Tnt1* insertion lines NF12390 (*rlck1-1*), NF10796 (*rlck1-2*) and NF11296 (*rlck1-3*) respectively. R1 generation seeds were obtained from the Samuel Roberts Noble Foundation and homozygote mutants for each insertion were identified using gene specific primers #1 and #3 and primers #1 and #10 for *Tnt1* identification (see appendix I) (fig. 3.2.1a). *rlck1-3* produced a very low number of viable seed and so was not studied further. The expression of *RLCK1* in the *rlck1-1* and *rlck1-2* alleles was tested using semi-quantitative PCR on cDNA generated from 21dpi nodulated root tissue (fig. 3.2.1b). *RLCK1* expression was detected in *rlck1-1* but not in *rlck1-2* at 28 cycles. The amplified cDNA band for *RLCK1* in *rlck1-1* was sequenced and was not different from WT (R108). This allele was not used for further investigation.

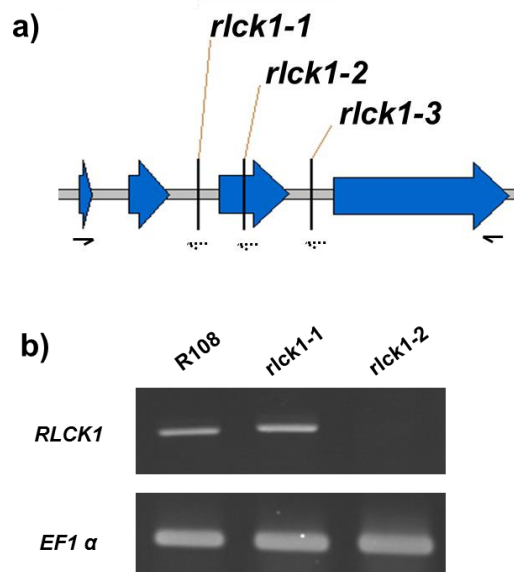


Figure 3.2.1. Allele identification for *RLCK1*.

(a) *RLCK1* comprises of 4 exons (blue) and 3 introns. *Tnt1* insertion alleles at nucleotides 447 (*rlck1-1*), 621 (*rlck1-2*), 878 (*rlck1-3*) of the genomic sequence. Gene specific (solid arrows) and *Tnt1* specific (dashed arrows) primer positions shown beneath the gene structure. (b) Semi-quantitative RT-PCR of *RLCK1* and *EF1α* (positive control) in 21 dpi nodulated root. *RLCK1* band is 1122bp. *EF1α* is a 100 bp fragment. 28 cycles.

For *RLCK2*, an FST was identified in the fourth exon (1342 bp genomic) in line NF5270 and the allele was designated *rlck2-1*. Homozygous mutants for *rlck2-1* were identified by PCR using the gene-specific primers #4 and 6 and primers #4 and #10 for the *Tnt1* identification (See Appendix I). A second allele, designated *rlck2-2*, was identified by TILLING (RevGen UK, Norwich). The mutation is a C to T change at base pair 1407 (genomic) causing a Q to STOP change at amino acid 269, creating a premature stop codon at the protein level (fig. 3.2.2). *RLCK2* expression was tested using semi-quantitative PCR on cDNA generated from 21dpi nodulated root tissue (fig. 3.2.2b). Some *rlck2-1* individuals had some detectable expression at 28 cycles, but the band detected contained a 147bp deletion (478-625) within the cDNA which was confirmed by sequencing of the cDNA. This could occur by the splicing out of the *Tnt1* transcript from the *rlck2-1* mRNA removing some of the *RLCK2* sequence in the process. The resulting protein from the mis-spliced mRNA would have a missense amino acid sequence resulting in a missing RD domain and a premature stop codon that would remove the majority of the kinase domain. *rlck2-2* still has detectable levels of *RLCK2* expression at 28 cycles, however the C to T mutation was confirmed by sequencing at base pair 805 in the cDNA. *rlck2-1* is in the R108 background and *rlck2-2* is in the A7 background.

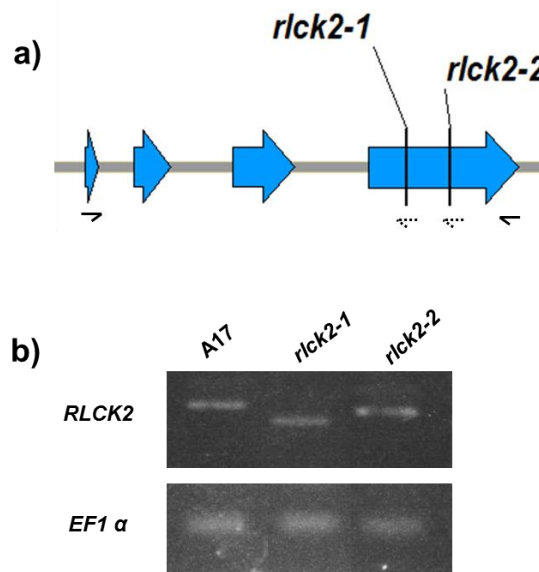


Figure 3.2.2. Allele identification for *RLCK2*.

(a) *RLCK2* comprises of 4 exons (blue) and 3 introns. *rlck2-1* is an exonic *Tnt1* insertion at 1342 bp (genomic). *rlck2-2* is a single base pair mutation at 1407 bp (genomic) causing a premature stop codon. Gene specific (solid arrows) and *Tnt1* specific (dashed arrows) primer positions shown beneath the gene structure. (b) Semi-quantitative RT-PCR for *RLCK2* and *EF1α* in A17 and *rlck2* mutants in 21 dpi nodulated root. *rlck2-1* bands (963 bp) are 147 bp smaller than WT (1110 bp). *rlck2-2* has a full length cDNA and WT expression but contains a premature stop codon. *EF1α* is a 100 bp fragment. 28 cycles.

3.3 Nodulation phenotypes of *rlck1* and *rlck2*

3.3.1 Rhizobial Infection

To score the numbers of infection events *rlck1* and *rlck2* mutant seedlings alongside WT R108 and A17 were inoculated with *LacZ*-expressing Sm1021. Plants were scored for the number of microcolonies, infection threads (ITs) and nodule primordia at 6 dpi. *rlck1-2* was found to have a significantly higher number of microcolonies than WT (R108) ($p=0.029$ and $p=1.59 \times 10^{-6}$ respectively) (fig. 3.3.1.1). The infection threads in the *rlck1-2* mutants sometimes appeared to be thicker than WT (fig. 3.3.1.2a,c,e) but progressed to the nodule primordia as normal (fig. 3.3.1.2f).

The *rlck 2-1* mutant is not significantly different from WT (R108) for any of the infection events (fig. 3.3.1.1) and the infection threads and nodule primordia look normal (fig. 3.3.1.3a). However, *rlck2-2* had significantly fewer infection events at all stages compared to WT (A17) – microcolonies ($p=3.53 \times 10^{-5}$), ITs ($p=2.19 \times 10^{-6}$) and fewer nodule primordia ($p=7.38 \times 10^{-7}$) (fig. 3.3.1.1). The root hairs on the *rlck2-2* mutant appeared shorter and infection threads (where viewed) appeared thicker and misshapen compared to WT (A17) (fig. 3.3.1.3b).

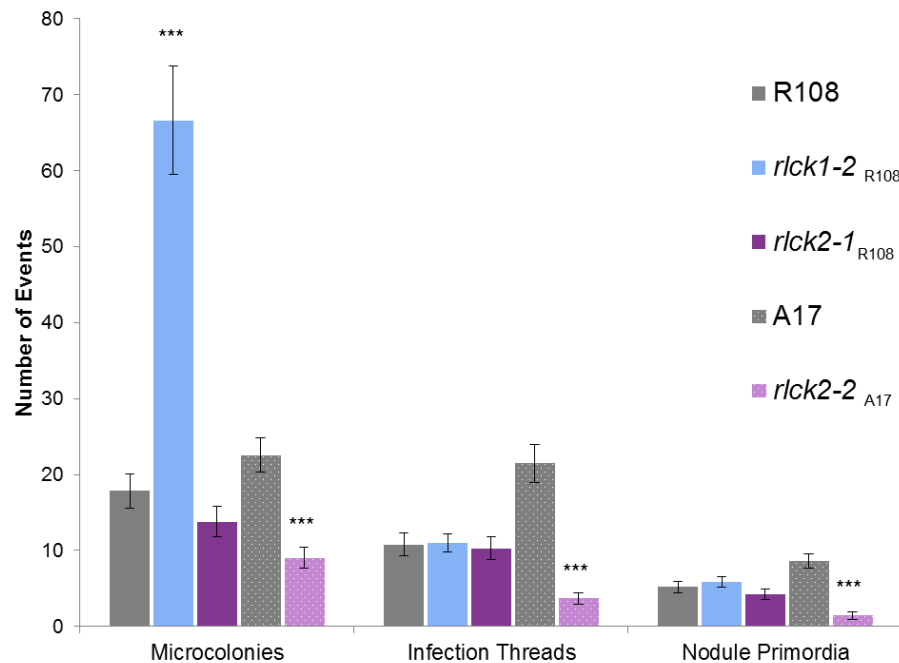


Figure 3.3.1.1. The number of infection events per plant in the *rlck* mutants and WT. Plants were harvested at 6dpi Infections were visualised by *LacZ*-expressing *S. meliloti* 1021 (Sm1021). The subscript next to each allele refers to the background of the allele. A 2-tailed t-test was used to compare means between each allele and their respective control. The data is an average of 16 to 20 individual plants with the bars representing standard error. * $p < 0.05$ *** $p < 0.001$

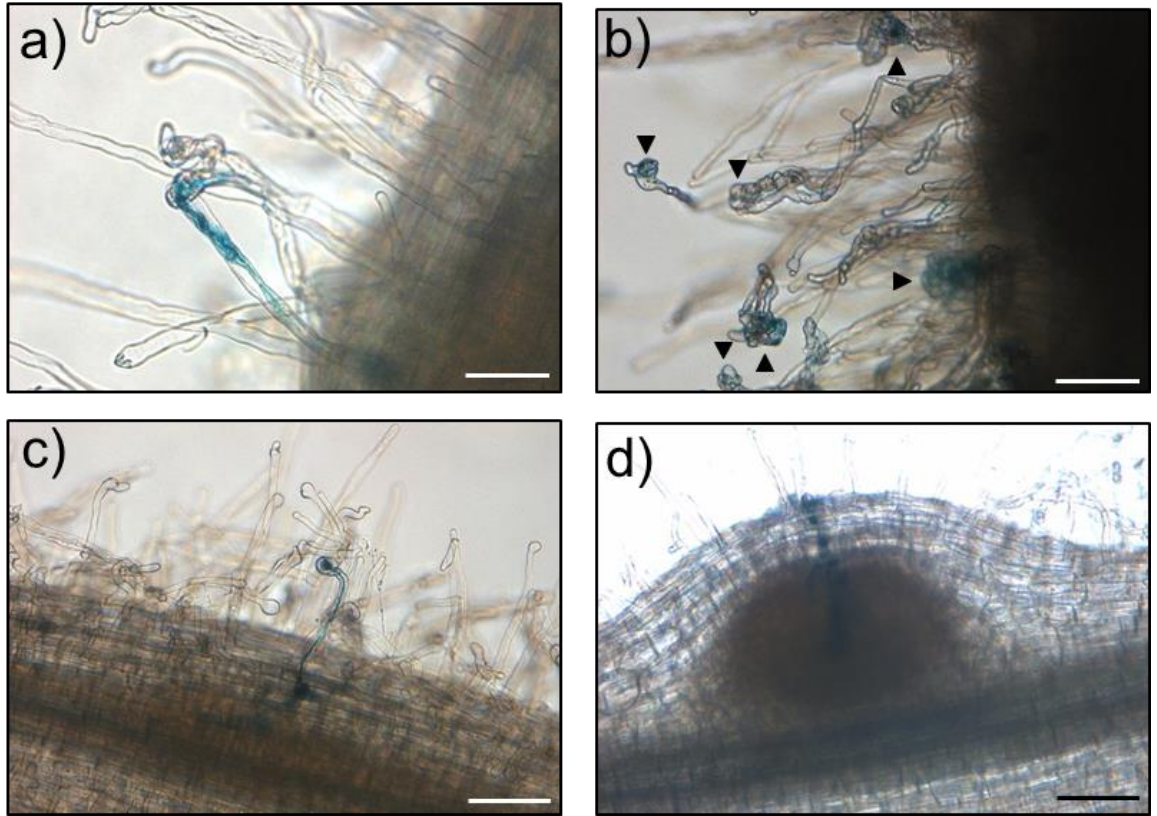


Figure 3.3.1.2. Differences between *rlc1* and WT (R108) infection threads.

The infection threads in *rlc1-2* (a) appear thicker and less regular in shape than WT (c). The *rlc1-2* mutants are also hyper-infected, infection threads are indicated by arrowheads (b) compared to WT (R108) (c). Infection threads in the *rlc1-2* mutants are able to progress to the nodule primordia (d). Infections were visualised by using *LacZ*-expressing *S. meliloti* 1021. Scale bars in (a) is 50 μ m, all other scale bars are 100 μ m. Images taken at 6 dpi.

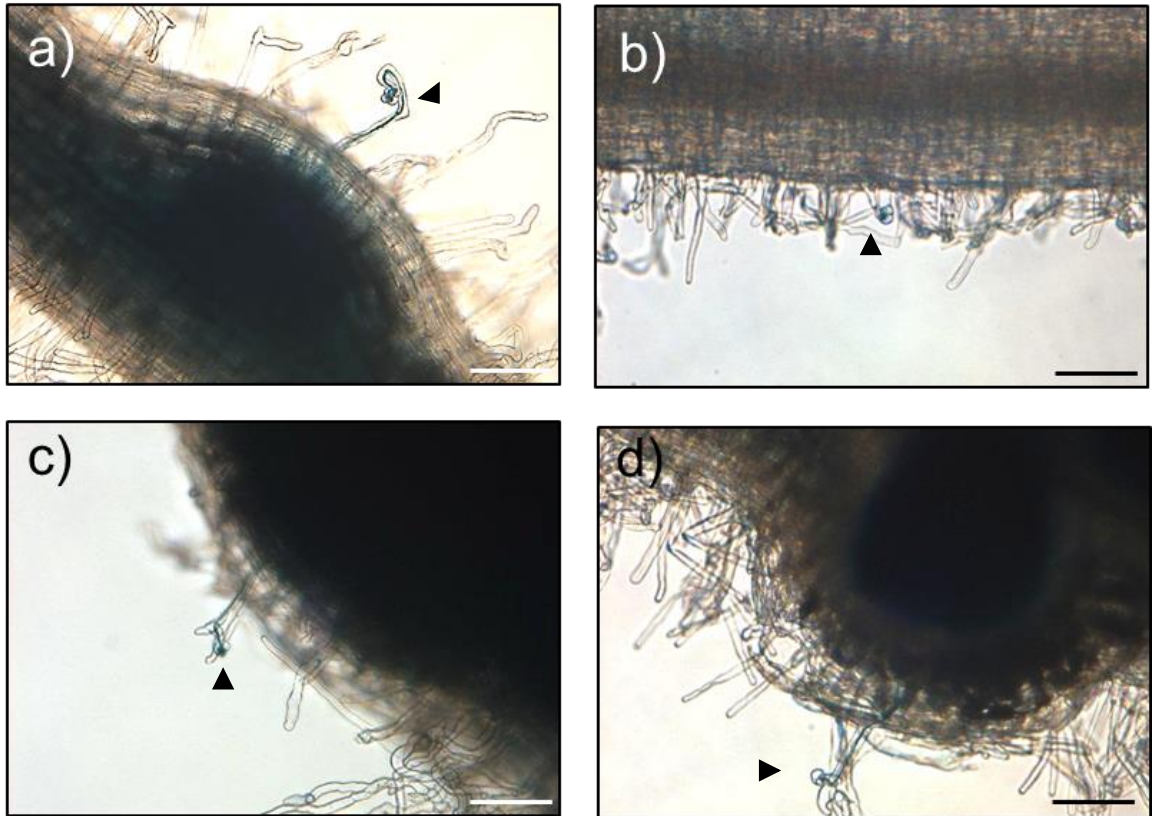


Figure 3.3.1.3. Differences between *rlck2* and WT (R108 and A17) infection threads. The infection threads (arrows) in *rlck2-1* mutant (a) are normal compared to WT (R108) (c), however the *rlck2-2* mutant (b) has shorter root hairs and deformed infections compared to their WT (A17) control (d). Very few threads at 6 dpi progressed to nodule primordia in the *rlck2-2* mutant. Infections were visualised by using *LacZ*-expressing *S. meliloti*. Scale bars in (a) and (c) are 100 μm , scale bars in (b) and (d) are 50 μm . Images taken at 6 dpi.

3.3.2 Nodule formation

rlck1-2 and *rlck2* mutants were tested for their ability to form nodules at 21 dpi with *S. meliloti* strain Sm1021 using R108 and A17 as controls. *rlck1-2* had significantly fewer nodules than WT (R108) ($p=0.038$) with a specific reduction in the number of pink nodules ($p=0.015$) (fig. 3.3.2.1a). *rlck2-1* had significantly more nodules than WT (R108) ($p=0.048$) with more white nodules ($p=0.044$). *rlck2-2* had significantly fewer nodules than WT (A17) ($p=6.11 \times 10^{-5}$) with significantly fewer pink nodules ($p=3.22 \times 10^{-6}$) (fig. 3.3.2.1b).

To more closely examine the symbiotic phenotype, mature pink nodules were sectioned. Nodule sections showed that in *rlck1-2* mutants the bacteria are able to be released into the cortical cells of the nodule. In younger nodules the infection threads within the infection zone (Zone 2) are clearly visible in both the *rlck1-2* mutants and in WT (R108) (fig. 3.3.2.2 a-d). However, as the nodule matures, this zone becomes diminished in the WT (R108) nodules but stays prominent in *rlck1-2* with ITs seeming to reach into zone I (fig. 3.3.2.2e-f). This, along with the hyper-infected phenotype of the *rlck1-2* mutant at the early stages of nodulation, suggests a role for *RLCK1* during infection.

Nodule sections of *rlck2* mutants show that the bacteria were able to be released into the cortical cells of the nodules. *rlck2-1* nodules look as WT (R108) (fig. 3.3.2.3a-d). At 28 dpi *rlck2-2* had only produced small nodules compared to WT (A17) but zones I, II and II-III were visible and normal in appearance (fig. 3.3.2.3e-f).

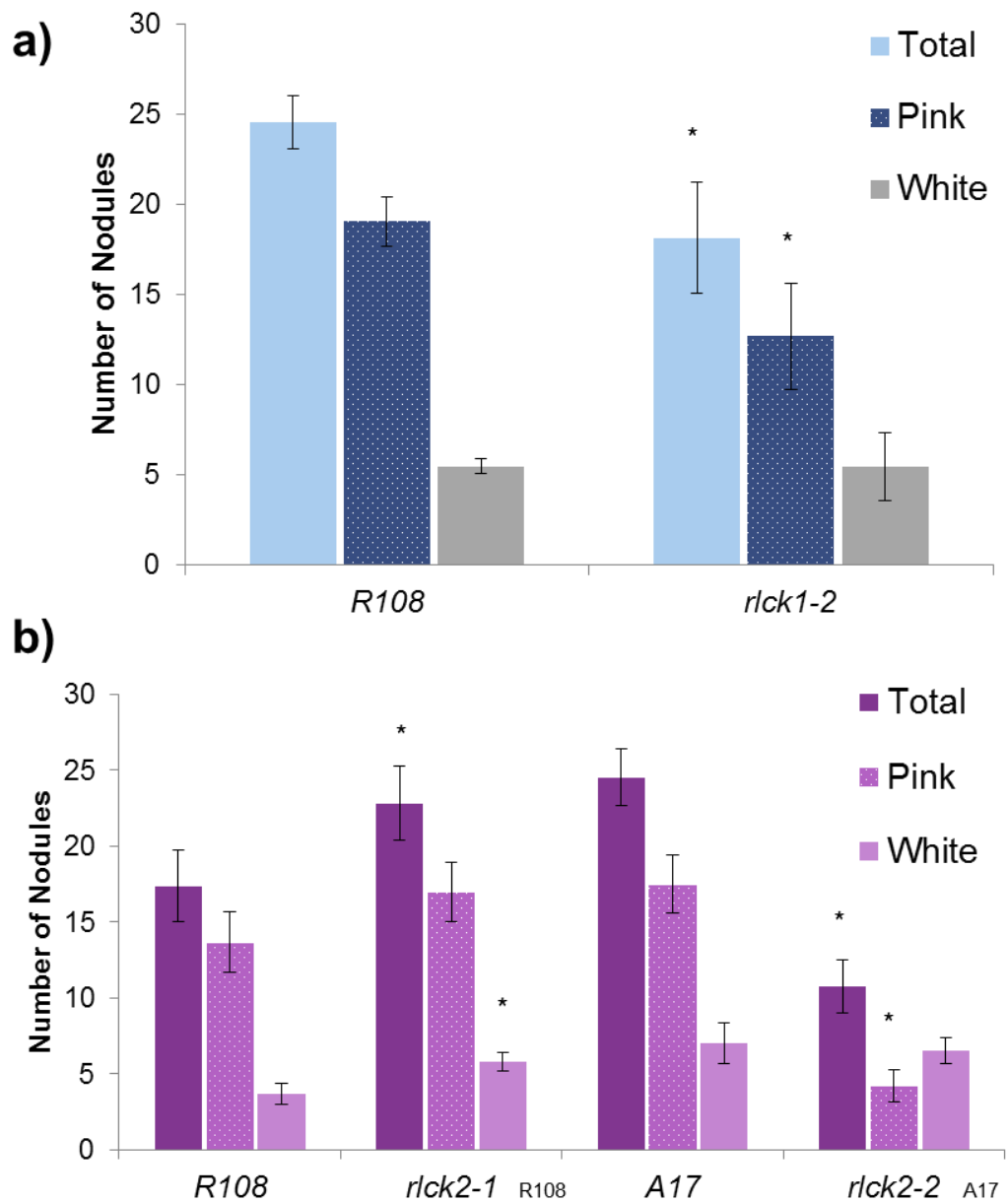


Figure 3.3.2.1. Nodulation in WT and *rick* mutants.

(a) Number of nodules for the *rick1* mutant alleles and WT (R108). The data are averages of 13 to 19 individual plants with error bars displaying the standard error. (b) Number of nodules for the *rick2* mutant alleles and respective control WT (R108 and A17). A 2-tailed t-test was used to compare the means of each allele to their corresponding control. The data are averages of 12 - 20 plants. Bars display standard error. * $p < 0.05$.

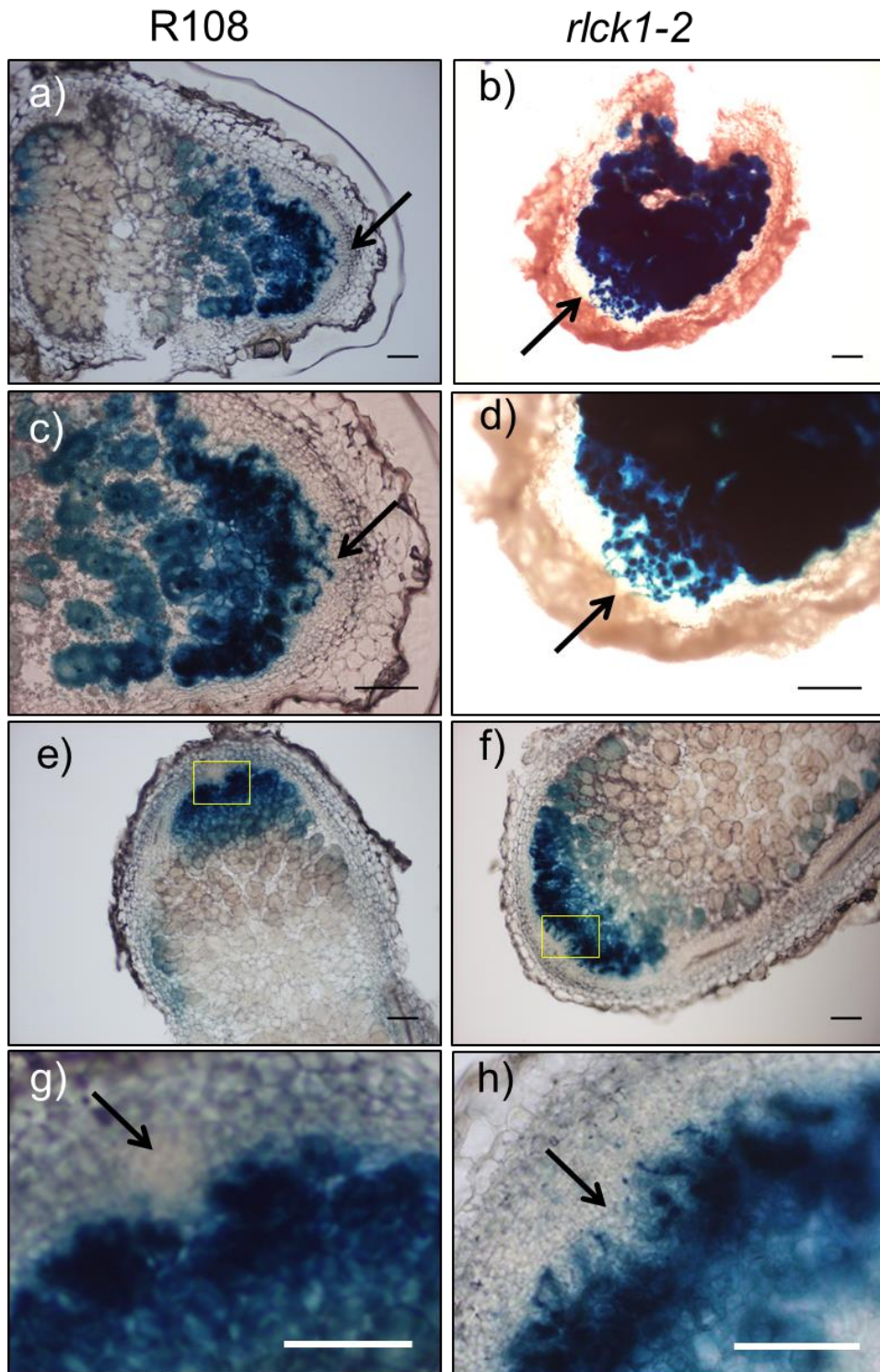


Figure 3.3.2.2. Nodule sections of *rlck1* mutants and R108 WT at different developmental stages.

In young nodules infection threads (arrows) can be seen in the apex of the nodule in both R108 WT (a and c) and in the *rlck1-2* mutant (b and d). However the infection threads can still be seen in mature *rlck1-2* mutant nodules (f) but not in the mature nodules of R108 WT (e). Images (g) and (h) are computationally magnified from images (e) and (f) respectively. Infections were visualised by using *LacZ*-expressing *S. meliloti*. Sections were taken at 28 dpi. 3 nodules sectioned per genotype. Scale bars are 100 μ m.

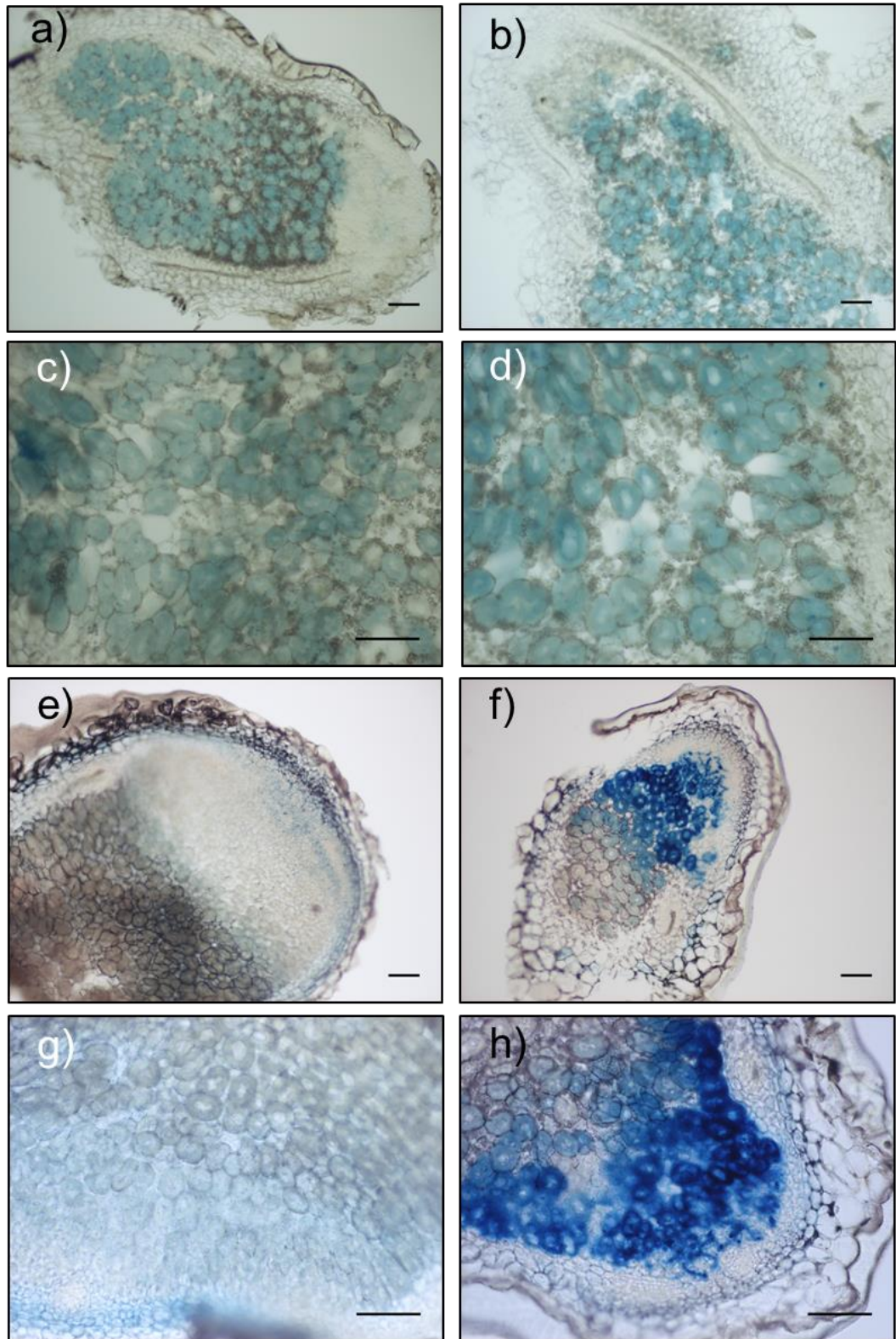


Figure 3.3.2.3 Nodule sections of *rick2* mutants and WT (R108 and A17).

rick2-1 nodules (b and d) appear normal compared to WT (R108) (a and c). *rick2-2* only produced small nodules (f and h) compared to WT (A17) (e and g) but these were colonised normally. Infections were visualised by using *LacZ*-expressing *S. meliloti* 1021. Sections were taken at 28 dpi. Scale bars are 100 μ m.

3.4 Mycorrhizal phenotyping of *rlck1* and *rlck2*

rlck1 and *rlck2* mutants were tested for their ability to be colonised by AMF *Rhizophagus irregularis* alongside WT R108 and A17. Colonisation was scored using the grid method (Giovannetti and Mosse, 1980) once WT colonisation was more than or equal to 50% (see materials and methods).

rlck1-2 was found to be reduced in mycorrhizal colonisation compared to WT (R108). *rlck1-2* mutants show a significant reduction in internal hyphae ($p=4.89 \times 10^{-5}$), vesicles ($p=5.12 \times 10^{-7}$) and arbuscules ($p=7.38 \times 10^{-7}$) (fig. 3.4.1a). Arbuscules in *rlck1-2* were small and did not fill the plant inner cortical cell as in WT (R108) (fig. 3.4.2).

rlck2-1 and *rlck2-2* were also reduced in mycorrhizal colonisation compared to their respective WT controls (R108 and A17). The *rlck2* mutants were significantly reduced in internal hyphae ($p=3.16 \times 10^{-8}$ and $p=0.006$, *rlck2-1* and *rlck2-2* respectively), vesicles ($p=1.07 \times 10^{-5}$ and $p=0.004$, *rlck2-1* and *rlck2-2* respectively) and arbuscules ($p=1.62 \times 10^{-7}$ and $p=0.009$, *rlck2-1* and *rlck2-2* respectively) (fig. 3.4.1b). Arbuscules in *rlck2-1* appear smaller and do not fill the plant inner cortical cells as in WT (R108). However, in *rlck2-2* arbuscules, although fewer in number, fill the plant inner cortical cell as seen in WT (A17) (fig. 3.4.3).

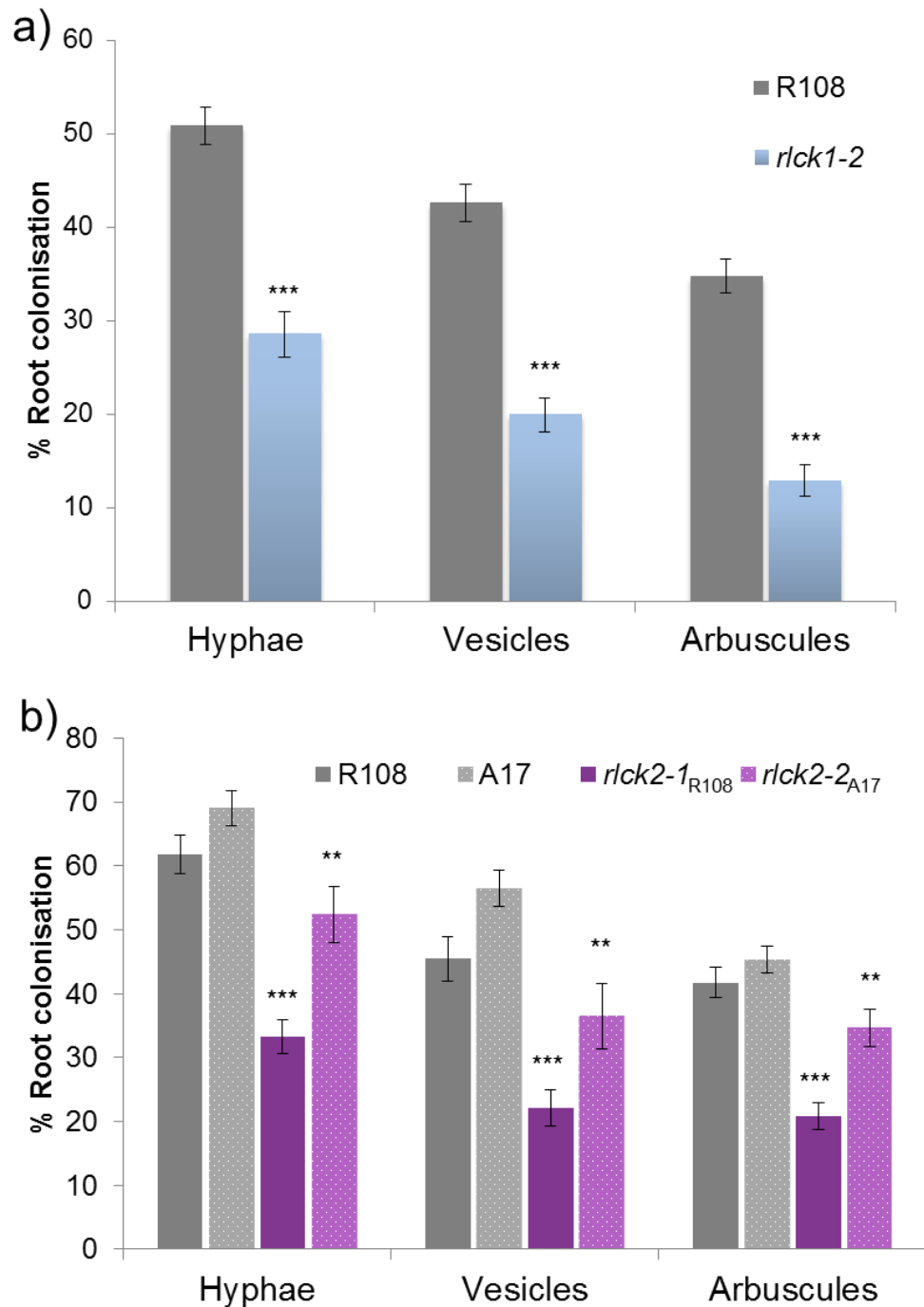


Figure 3.4.1. AMF (*R. irregularis*) colonisation is reduced in *rick* mutants.

(a) Percentage AMF colonisation for the *rick1* mutant alleles and WT (R108). The data are averages of 18 – 25 individual plants. (b) Percentage of AMF colonisation of the *rick2* alleles and WT (R108 and A17). The data are averages of 13- 25 plants. Plants were scored when WT (R108) plants reached $\geq 50\%$ colonisation (see materials and methods). Bars display standard error. A 2-tailed t-test was used to compare the means of each allele to their corresponding control. ** $p < 0.01$ *** $p < 0.001$

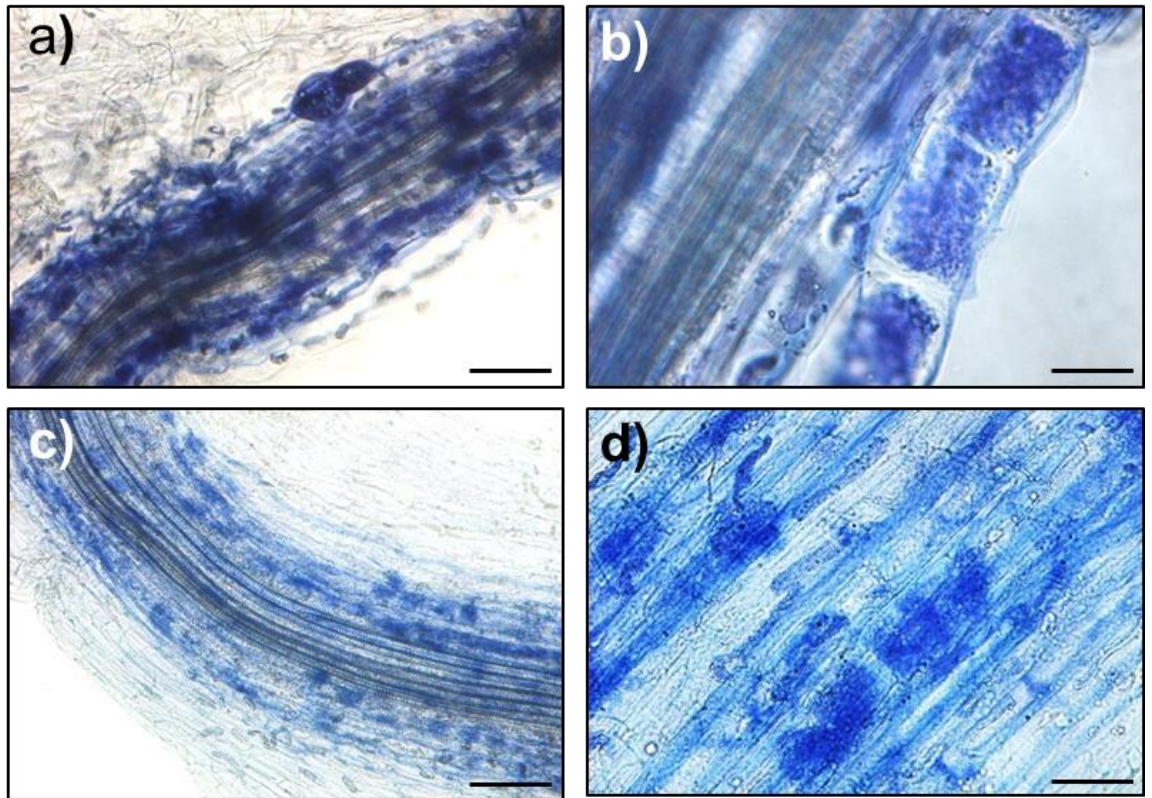


Figure 3.4.2. AMF colonisation phenotypes of *rlck1* mutants and WT (R108).

R108 (a, b) and *rlck1-2* (c, d) mutant roots colonised by *R. irregularis*. Arbuscules in *rlck1-2* were smaller, and did not fill the inner cortical cells (d). AMF is stained by ink.

Phenotypes were scored when WT (R108) was colonised >50 % by AMF. Scale bars on (a) and (c) are 100 μm . Scale bars on (b) and (d) are 25 μm .

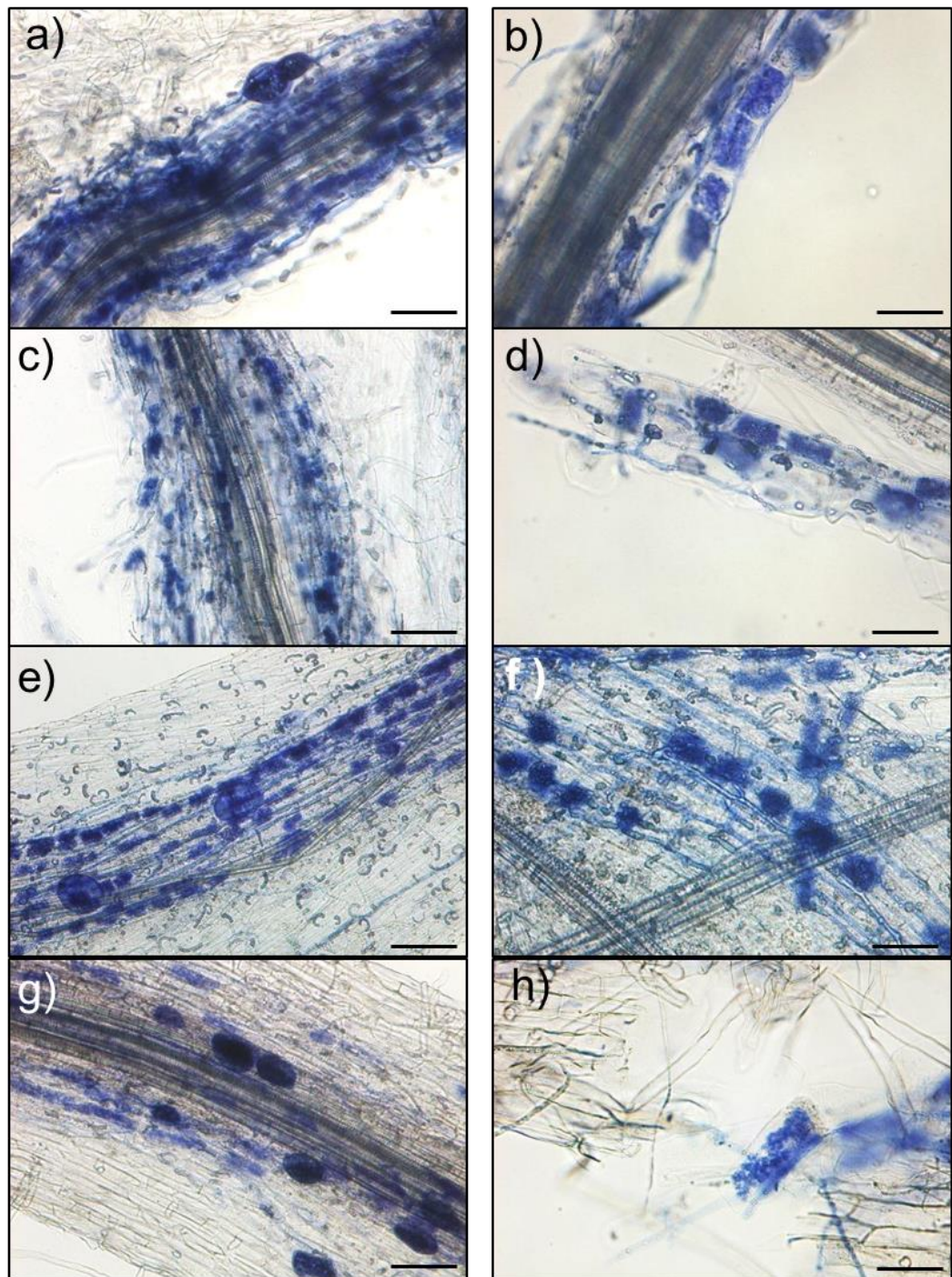


Figure 3.4.3. AMF colonisation phenotypes of *rlck2* mutants and WT plants.

(a,b) R108 and A17 (c,d) WT and (e,f) *rlck2-1* and (g,h) *rlck2-2* mutant roots colonised by *R. irregularis*. Arbuscules in *rlck2-1* did not fill the plant inner cortical cell as occurred in WT (R108). Arbuscules appeared normal in *rlck2-2* compared to WT (A17). AMF is stained by ink. Plants were scored when WT (R108 and A17) were colonised >50 % by AMF. Scale bars on (a), (c), (e) and (g) are 100 μm . Scale bars on (b), (d), (f) and (h) are 50 μm .

3.5 Expression of *RLCK1* and *RLCK2*

3.5.1 Expression of *RLCK1* and *RLCK2* by Microarray

The Medicago Gene Expression Atlas (MtGEA) was used to survey expression data for *RLCK1* and *RLCK2* under varying biological and chemical conditions. *RLCK1* expression is recorded via probe set Mtr.16214.1.S1_at (fig. 3.5.1.1). *RLCK1* expression is upregulated just 6 hours after inoculation with Nod Factors and AM “Myc Factors” S-LCOs or NS-LCOs (unpublished data). *RLCK1* expression is also high in young nodules (3, 4 and 6 dpi) and during AM infection. This upregulation at the early stages of both symbioses supports the *rlck1* phenotype seen during infection processes. Expression data acquired using laser capture of the AM colonised roots (Hogekamp *et al.*, 2011) shows that *RLCK1* expression is higher in the cortical cells adjacent to the arbusculated cortical cells than in the cells that contain arbuscules. These adjacent cells are potentially preparing for AM colonisation which fits with the infection related expression of *RLCK1* seen at earlier time-points. Unpublished microarray data show that *RLCK1* is upregulated in root hairs of rhizobially infected plant at 3 and 5 dpi, the former time point corresponding to microcolony formation and the latter to when the infection thread is progressing through the root hair (Murray Lab)(fig. 3.5.1.2). The microarray data also suggests that the expression of *RLCK1* in response to Nod Factor is dependent on *NFP*, *DMI1* and *DMI3*. *RLCK1* expression seems to be lower than WT in the transcription factor mutants *nsp1*, *nsp2*, *ern1* and *nin* at 6 hours post inoculation (hpi) with NF. At 24 hpi with NF *RLCK1* expression is dependant also on *NSP1* and *NSP2*, but not *ERN1* or *NIN* (Oldroyd Lab).

RLCK2 expression is recorded via probe set Mtr.24207.1.S1_at. *RLCK2* has a constitutive expression in root tissue and is upregulated in response to rhizobia or mycorrhization (fig. 3.5.1.3). *RLCK2* expression is upregulated in young nodules (3, 4 and 6 dpi) and during AM infection. Laser capture of the AM colonised roots (Hogekamp *et al.*, 2011) shows that *RLCK2* is expressed higher in the root cortical cells that contain arbuscules than other cortical cells. Unpublished microarray data (fig. 3.5.1.4) shows that *RLCK2* has some constitutive expression in root hairs and is upregulated at 3 and 5 dpi (Murray Lab). It also shows that *RLCK2* upregulation in response to NF is dependent on *NFP*, *DMI1*, *DMI3*, *NSP2*, *ERN1* and *NIN* (Oldroyd Lab). These differing expression profiles suggest the two RLCKs could have differing but overlapping roles, or be working synergistically, during symbiosis and that the regulation their expression is under different genetic control.

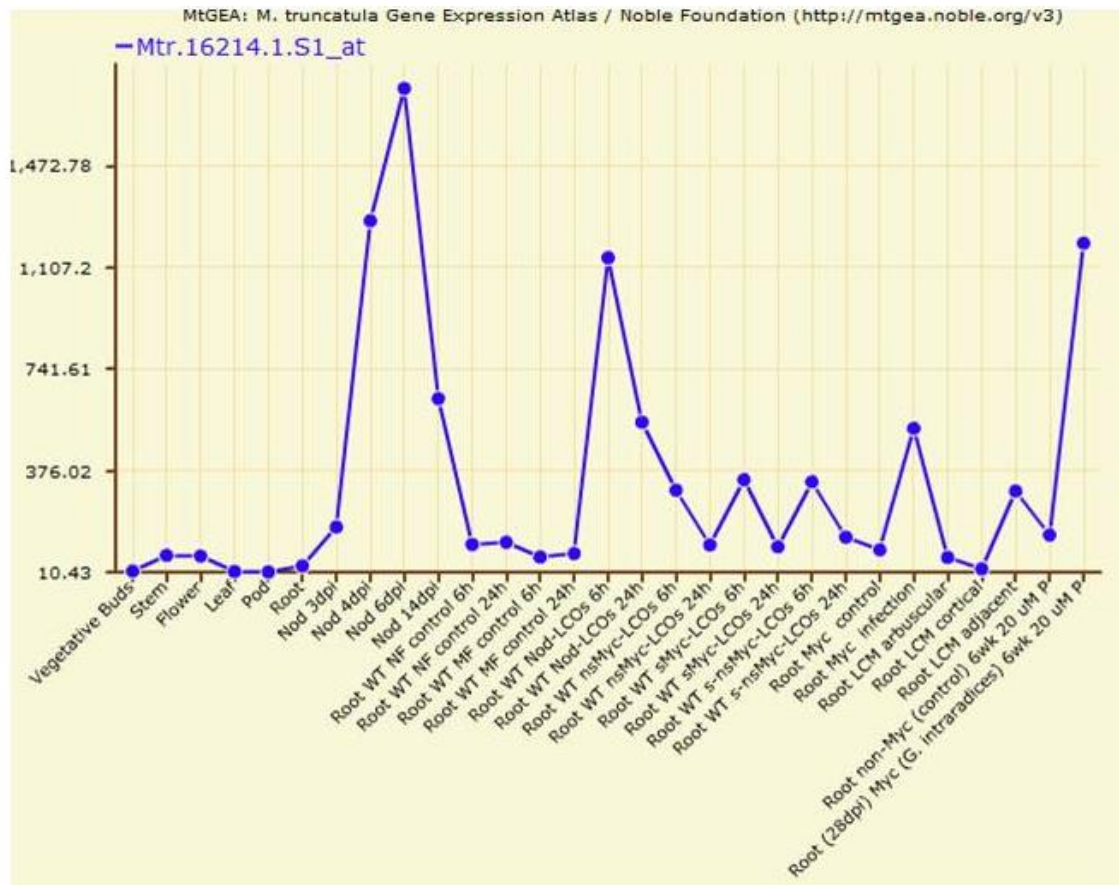


Figure 3.5.1.1. Medicago Gene Expression Atlas (MtGEA) data for *RLCK1*.

RLCK1 expression across a number of different experimental conditions. *RLCK1* is highly expressed during early stages of both symbioses – nodulation (4dpi) and mycorrhizal infection. *RLCK1* is also upregulated quickly after treatment with bacterial and mycorrhizal LCOs (NF and myc-LCOs). Laser capture dissection of AMF colonised roots (Root LCM) show that *RLCK1* expression is higher in plant inner cortical cells neighbouring arbusculated cells than the arbusculated cells.

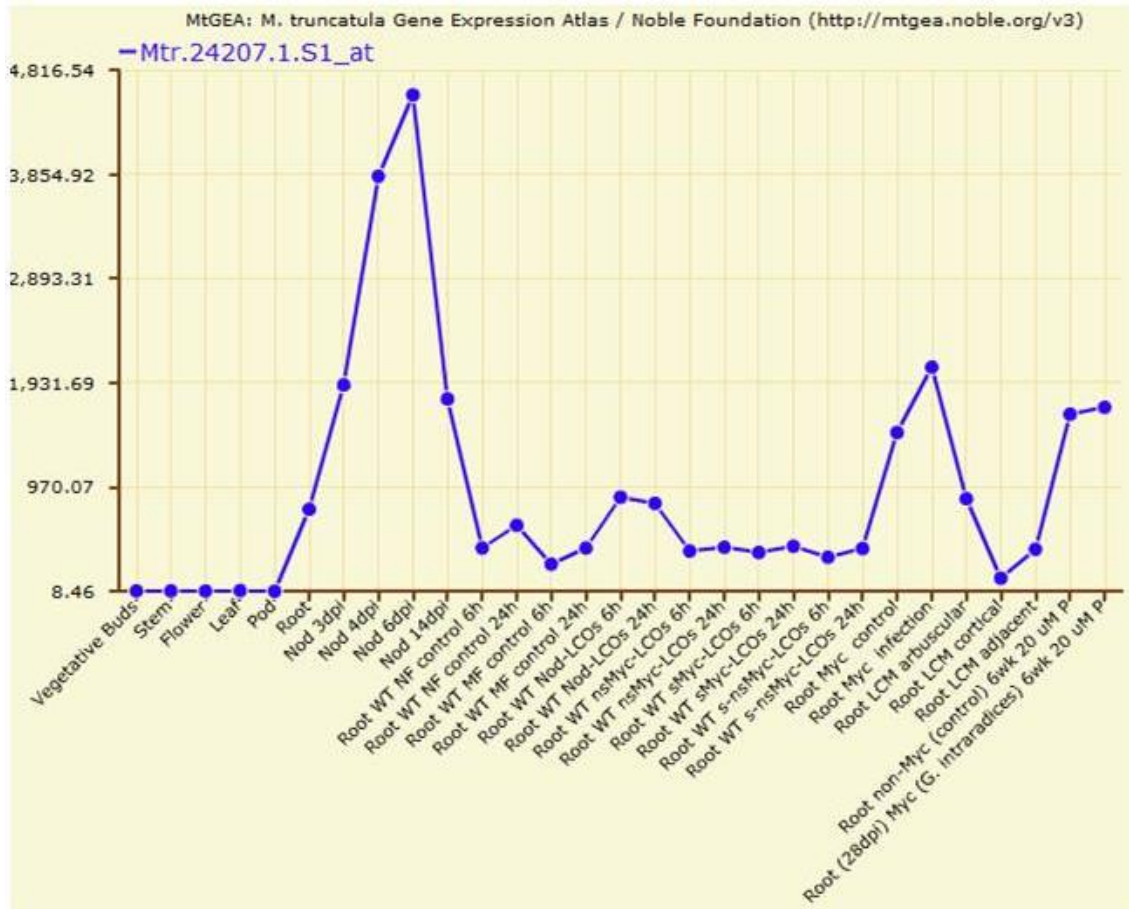


Figure 3.5.1.3 Medicago Gene Expression Atlas (MtGEA) data for *RLCK2*.

RLCK2 expression in a number of different tissues and experimental conditions. *RLCK2* is constitutively expressed in root tissue. Expression of *RLCK2* is strongly upregulated during both symbioses – nodulation and mycorrhization. *RLCK2* is also upregulated after treatment with bacterial LCOs (Nod factor) but not with mycorrhizal LCOs. Laser capture dissection of AMF colonised roots (Root LCM) show that *RLCK2* expression is higher in arbusculated plant inner cortical cells than neighbouring cells.



Figure 3.5.1.4. Unpublished *Medicago* Gene Expression Atlas data for *RLCK2*.

Affymetrix *Medicago* Gene Chip® data for *RLCK2* in symbiosis mutants and in response to various conditions. *RLCK2* is up regulated in root hairs during rhizobial infection. Early upregulation of *RLCK2* in response to NF is dependent on the symbiosis genes *NFP* and *DMI3*. *RLCK2* is not upregulated in response to *P. infestans*.

3.5.2 Symbiotically enhanced expression of *RLCK1* and *RLCK2*

The *MtRLCK1* promoter-GUS construct (pRLCK1:GUS) was obtained from Nicolas Pauly (*SPK1*) (Andrio *et al.*, 2013) and was transformed into *M. truncatula* R108 via *A. rhizogenes*. Roots were checked at 4, 7, 10, and 14 dpi with *LacZ*-expressing Sm1021. The GUS expression was visualised using X-GlcA staining and the bacteria were counterstained using Magenta-Gal. Expression was confirmed for *RLCK1* in infected root hairs, nodule primordia and in developing nodules as previously shown by Andrio *et al.* (2013). There was some non-symbiotic expression of *RLCK1* in the root tips and lateral root primordia (fig. 3.5.2.1). Roots were also checked at 5, 10, 15 and 20 dpi with *R. irregularis* (Chive inoculum). The GUS expression was visualised using X-GlcA staining and the AMF was visualised by WGA staining. *RLCK1* is expressed in the early stages of mycorrhizal infection with GUS expression visible in cells surrounding AMF penetration. *RLCK1* is expressed at later stages of mycorrhizal infection, with GUS visible in the plant inner cortical cells surrounding AMF progression through the root (fig. 3.5.2.2).

To compare the expression of *RLCK2* to *RLCK1* an *RLCK2* promoter-GUS (pRLCK2:GUS) construct was made by PCR amplifying 2.3kb of the promoter region and cloning via Gateway into vector pKGWFS7 (Karimi *et al.*, 2002). The construct was transformed into *M. truncatula* R108 via *A. rhizogenes*. Roots were checked at 4, 7, 10, and 14 dpi with *LacZ*-expressing Sm1021 and was visualised as described above. *RLCK2* was expressed throughout the root during the early stages of rhizobial symbiosis and at later stages in the developing nodule (fig. 3.5.2.3a-c). Roots were also checked at 5, 10, 15 and 20 dpi with *R. irregularis* (Chive inoculum) as described above. *RLCK2* was expressed throughout the root during the early stages of AM symbiosis and it was strongly expressed in the inner plant cortical cells that contain arbuscules (fig. 3.5.2.3e-f).

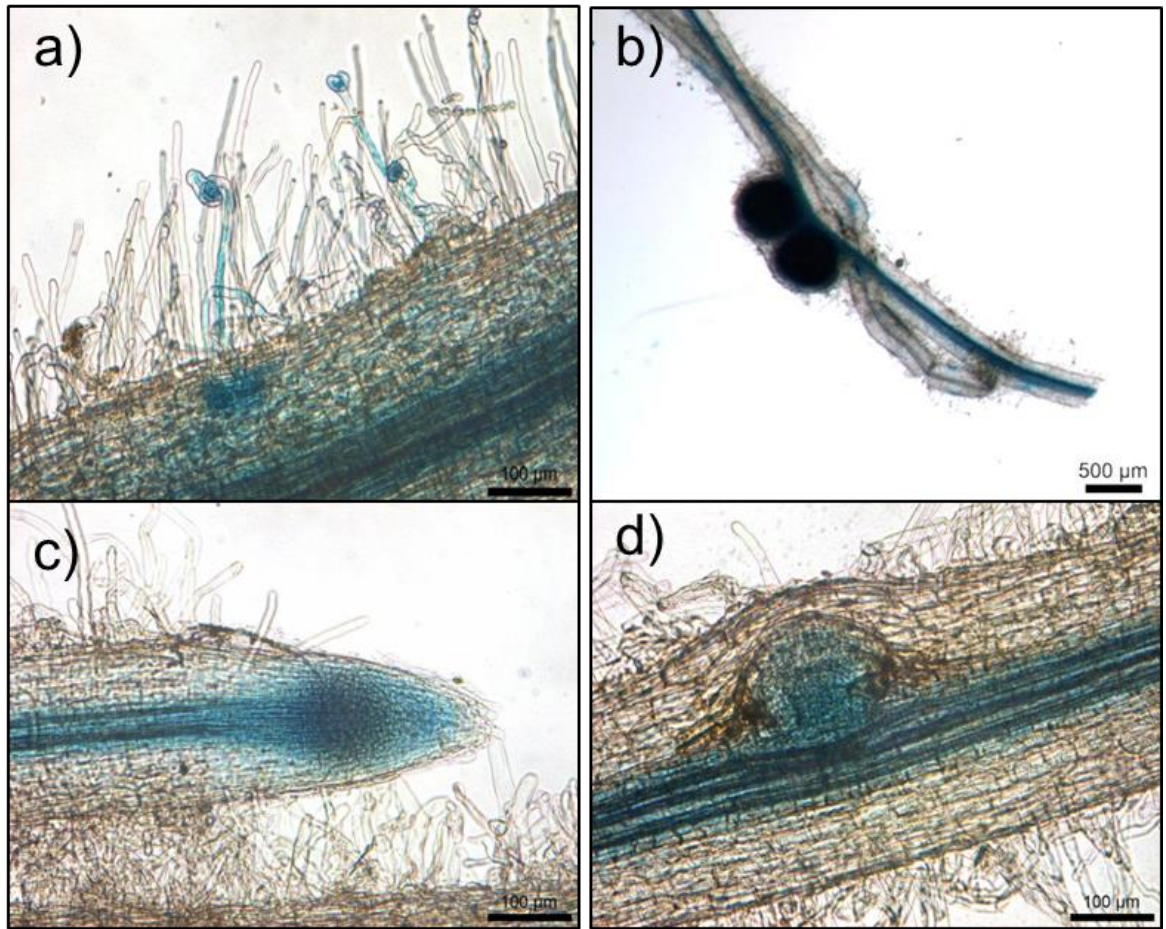


Figure 3.5.2.1. pMtRLCK1:GUS expression during rhizobial symbiosis.

The GUS activity (stained in blue) shows that *RLCK1* is expressed in infected root hairs and cortical cells (a), and in nodules (b) as well as in root tips (c) and lateral root primordia (d). Scale bars in (a), (c) and (d) are 100 μm and 500 μm in (b).

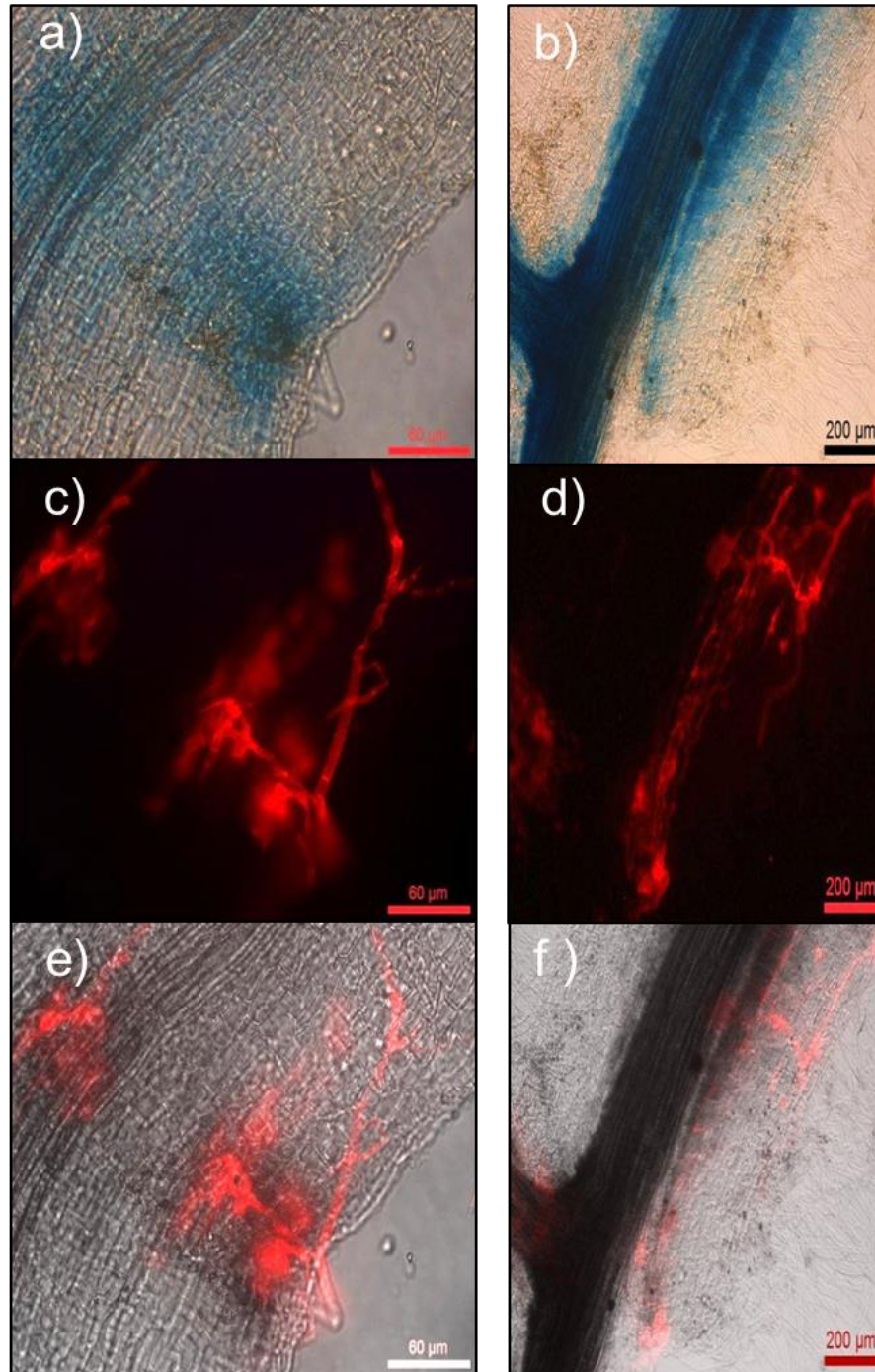


Figure 3.5.2.2. pRLCK1:GUS expression during mycorrhizal symbiosis.

GUS activity (stained blue) shows that *RLCK1* is expressed during the early stages of mycorrhizal infection (a), (c) and (e), and in cortical cells surrounding mycorrhizal progression through the root (b), (d) and (f). The AMF is stained in red with WGA, shown in red in images (c) to (f). Scale bars are 60 μm in (a), (c) and (e), and 200 μm in (b), (d) and (f).

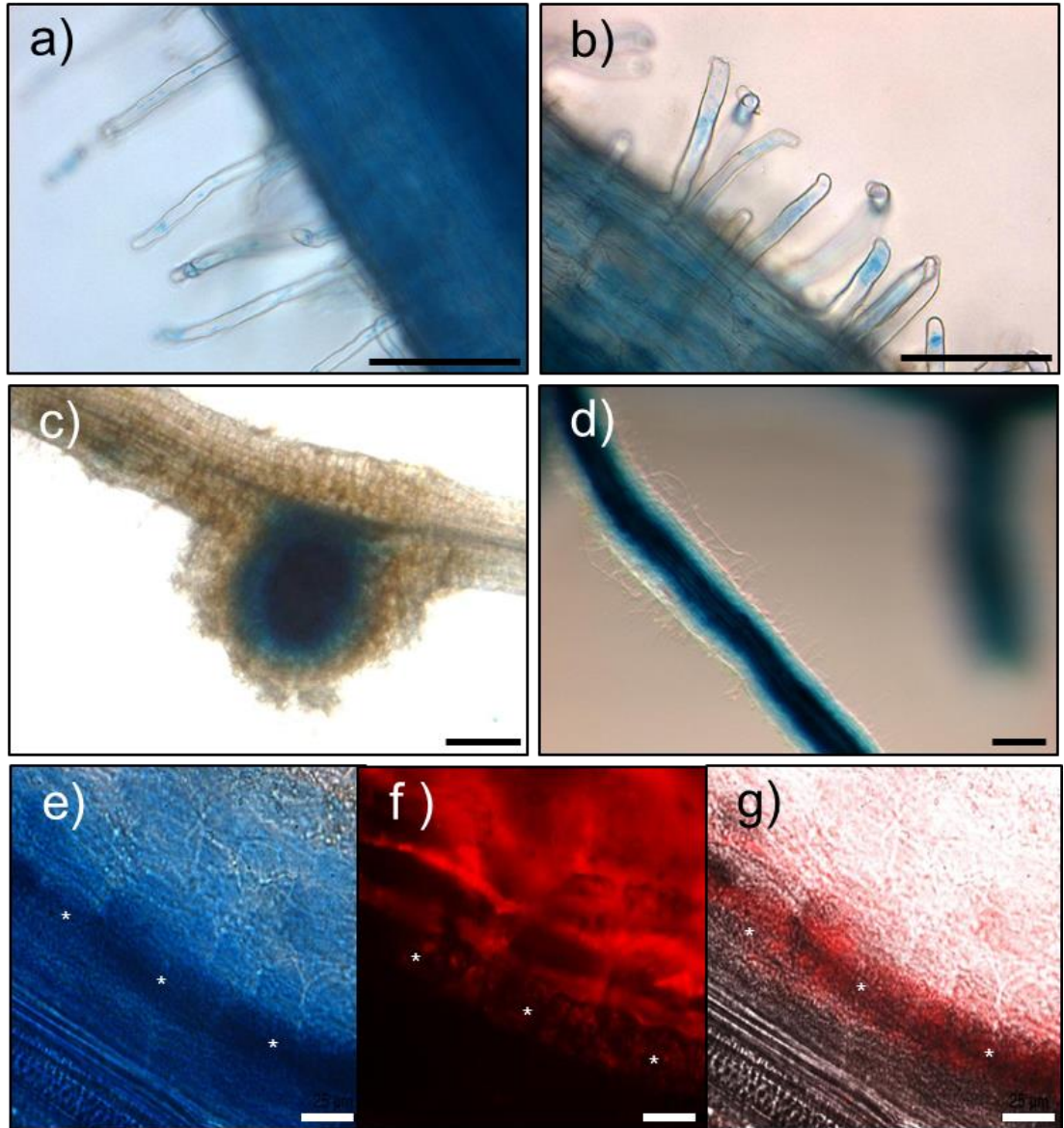


Figure 3.5.2.3. pRLCK2:GUS expression during rhizobial and mycorrhizal symbioses. The GUS expression (shown in blue) shows that *RLCK2* is expressed throughout the root during the early stages of rhizobial (4 dpi) (a) and (b) and mycorrhizal symbiosis (10 dpi) (d). During the later stages of rhizobial symbiosis *RLCK2* expression is can be seen in the nodule (14 dpi) (c). *RLCK2* expression remains in the cortical cells at later stages of mycorrhizal symbiosis and is higher in arbusculated cells (starred) (e) to (g). The AMF is stained with WGA, shown in red in images (f) and (g). Scale bars are 100 μm in (a) and (b), 200 μm in (c) and (d), and 25 μm in (e), (f) and (g).

3.6 Phylogenetic analysis of RLCK1 and RLCK2 proteins

It has been shown that legumes have undergone several Whole Genome Duplication (WGD) events (Cannon *et al.*, 2006; Young *et al.*, 2011); many of these gene duplicates have been retained, and some have been recruited into the legume-rhizobia symbiosis. The high homology between *RLCK1* and *RLCK2* could be due to the WGD in *M. truncatula* or it is possible that these two genes evolved much earlier in plant evolution. In order to determine the evolutionary history of *RLCK1* and *RLCK2* a phylogenetic analysis of *RLCK1* and *RLCK2* amino acid sequence was carried out identifying orthologues in a variety of different species across the plant kingdom (fig. 3.6.1).

RLCK1 and *RLCK2* have representatives in legumes (fig. 3.6.1 in blue) such as soybean and chickpea, and in monocots (fig. 3.6.1 in light brown) such as rice, switchgrass and maize known to symbiose with AMF. Interestingly orthologues are present in ancient species such as *Selaginella mollendorffii* (spikemoss) and *Physcomitrella patens* (moss), and the basal angiosperm *Amborella trichopoda*. It is also important to note that the non-symbiotic species *Arabidopsis thaliana* does not have orthologues of the RLCKs. The presence of both *RLCK1* and *RLCK2* in such diverse plant species suggests that *RLCK1* and *RLCK2* evolved before the WGD event in legumes. The fact that there seems to be at least one copy each of *RLCK1* and *RLCK2* in most species supports the phenotypic evidence that they are both required for properly functional symbiosis.

Figure 3.6.1. Phylogenetic tree for *RLCK1* and *RLCK2* proteins.

RLCK1 and *RLCK2* are closely related proteins but have their own distinct subclades across a wide variety of plants including Soybean (*Glycine max*), Rice (*Oryza sativa* and *Oryza indica*), Poplar (*Populus trichocarpa*), and *Amborella trichopoda*. The tree is rooted using the moss (*Physcomitrella patens*) orthologues. There are no *Arabidopsis* orthologues for either *RLCK1* or *RLCK2*. Legumes are coloured blue, monocots are coloured in light brown, and mosses are coloured in green. Figure over leaf.

3.7 Discussion

Evidence of RLCK1 and RLCK2 in ancient and basal land plants, such as mosses and *Amborella*, shows that these proteins evolved from an early gene duplication event. The persistence of these proteins in symbiotic plant species, and the lack of them in non-mycorrhizal plants such as *A. thaliana*, suggests that both RLCK1 and RLCK2 play an important role during plant-microbe symbiosis. Based upon available gene expression data, expression of *RLCK1* and *RLCK2* is increased during both rhizobial and AMF symbiosis and this increase in expression may be dependent upon NF perception and calcium spiking. *RLCK2* has some constitutive expression in the *Medicago* root which suggests *RLCK2* might have a role during root growth and that it has been recruited for symbiotic interactions. The constitutive expression *RLCK2* could also indicate that it is required for the very early stages of symbiosis and thus its expression may be required prior to signalling, an example of this is the Nod Factor receptors NFP and LYK3 (Amor *et al.*, 2003; Smit *et al.*, 2007).

Stable *Tnt1* insertion mutants for *rlck1* and *rlck2* were isolated and found to have a reduction in AMF colonisation. Both *rlck1-2* and *rlck2-1* alleles had smaller, misshapen arbuscules compared to WT R108. The smaller arbuscules were not evident on the EMS generated *rlck2-2* allele. The small arbuscules seen are similar to those seen on *Mtpt4* and Mt-ha1 (Javot *et al.*, 2007; Krajinski *et al.*, 2014; Wang *et al.*, 2014). It is unclear if this phenotype is due to stunted development of arbuscules or premature senescence. A time course looking at arbuscule development will be able to differentiate these two things.

The reduction in nodulation with the *rlck1-2* allele agrees with the effects reported for RNAi knockdown against *RLCK1* carried out by Andrio *et al.* (2013). *RLCK1* does appear to have a role in rhizobial infection with the *rlck1-2* mutants showing a hyper infected phenotype which is sometimes seen on mutants that have a reduced nodule number (Murray *et al.*, 2011). Promoter-GUS analysis showed *RLCK1* expression in infected root hairs which contributes to the evidence of a role for *RLCK1* during rhizobial infection.

The *rlck2-1* allele had an increased number of mature nodules compared to the WT (R108) control while in contrast the *rlck2-2* allele showed a decreased number of infection events and fewer mature nodules compared to the WT (A17) control. The insertion in the *rlck2-1* allele produces a cDNA that is missing 147bp from the middle of the sequence which encodes the RD domain, and results in a tract of missense amino acid sequence and a premature stop codon removing the majority of the kinase domain.

rlck2-2 originated from a mutant population generated by EMS mutagenesis (RevGen, UK). The seeds obtained were 5th generation after mutagenesis (M5) and by this time many mutations would be fixed through self-pollination. It seems likely that background mutations in *rlck2-2* are contributing to the severe nodulation phenotype. A backcross of the *rlck2-2* allele would reduce the number of background mutations and would help to clarify the *rlck2* phenotypes. The promoter-GUS analysis for *RLCK2* revealed expression in developing nodules, however the constitutive expression of *RLCK2* in the root makes it hard to distinguish any symbiotically induced increases of expression in the root hairs and during early stages of rhizobial infection. However, the symbiotic induction of *RLCK2* expression is clear from available microarray data.

The discrepancy between the different *rlck2* alleles makes it difficult to conclude about the role of this gene in the symbioses. Further alleles or complementation of the *rlck1* and *rlck2* mutants are needed to better define their roles in symbiosis, however this study has shown that they both have a positive role in mycorrhizal symbiosis.

Chapter 4: Double Knockdown of *RLCK1* and *RLCK2*

4.1 Introduction

Prokaryotes and eukaryotes contain many classes of RNAs with varying cellular functions, such as messenger RNAs (mRNA) and structural features within ribosomes (rRNAs). Eukaryotes contain a class of single-stranded small RNAs involved in endogenous gene silencing and post-transcriptional regulation of mRNA as well as protection from viral genomes by the destruction of viral RNA (Bazin *et al.*, 2012). These single-stranded small RNAs are referred to as silencing RNAs (sRNAs). Two classes of sRNAs are microRNA (miRNA) and short interfering RNA (siRNA) (Hannon, 2002; Molnar *et al.*, 2005; Ossowski *et al.*, 2008).

miRNAs are derived from longer RNA transcripts that contain imperfect complementary sequences that cause fold backs in the RNA. miRNA create the accumulation of a unique sRNA that tends to bind to one specific target sequence (Ossowski *et al.*, 2008). siRNAs are derived from long strands of RNA that contain perfectly complementary sequences separated by an intronic region. This creates a hairpin RNA (hpRNA) with a long region of double stranded RNA (dsRNA) (Chuang and Meyerowitz, 2000; Wesley *et al.*, 2001). siRNA generate several species of sRNA that can bind to many different sequences of mRNA. For both miRNA and siRNA the double stranded RNA is processed by a member of the DICER family of RNases that cut the dsRNA into short pieces of dsRNA between 20 and 30 bp long with 5' and 3' overhangs (Depicker and Van Montagu, 1997; Zamore *et al.*, 2000; Bernstein *et al.*, 2001; Elbashir *et al.*, 2001). The sRNAs act as part of the RNA-induced silencing complexes (RISCs) providing the target specificity for the Argonaute catalytic subunit (Hammond *et al.*, 2000; Bernstein *et al.*, 2001; Baumberger and Baulcombe, 2005). It has been shown that siRNA in plants can also cause transcriptional gene silencing (TGS) by interacting with matching DNA, and recruiting DNA- and histone-modifying proteins to put the locus into a silent chromatin state (Hamilton, 2002; Xie *et al.*, 2004).

Jackson *et al.* (2003) showed in mammalian cells that siRNAs could affect the transcripts with partially complementary sequences as well as the intended target. This is known as off-target silencing. It is thought to be due to the way that Dicer and Dicer-like proteins process the hairpin RNA transcripts, and the generation of multiple different sRNAs. It was also shown by Palatnik *et al.* (2003) that miRNAs in *Arabidopsis* could have up to 5 mismatches with a target sequence and still be able to cause degradation. Off-target degradation is useful if trying to knockdown homologues or gene families, but is something to be mindful of when designing specific silencing constructs. The

effectiveness of silencing constructs can vary greatly, the reason for which is not greatly understood, but could be due to positive feedback systems where transcription rates increase due to the reduced levels of mRNA.

The best way of studying genes that are potentially functionally redundant is to cross stable single mutants to produce a double mutant. However, this is not always possible for example if the genes are closely linked on a chromosome or in cases where the double mutant is inviable. As an alternative, methods such as RNA interference (RNAi) can be used to investigate the double mutant phenotype. Despite many attempts to cross *rlck1-2* and *rlck2-1*, in both directions, a viable seed was not produced. In this chapter I describe use of two different RNAi approaches to observe the nodulation phenotype of the *rlck1/rlck2* double mutant.

4.2 Strategy 1: RNAi double knockdown

In the first approach an RNAi construct was designed to target the *RLCK1* mRNA using 99 bp at the 3' end of the *RLCK1* CDS (fig.4.2.1) (see appendix I for construct map) was provided by Myriam Charpentier, John Innes Centre. It was made by TOPO® and Gateway® cloning of the fragment into a modified destination vector of pK7GW|WG2D(II) (Karimi *et al.*, 2002) in which the eGFP has been replaced with dsRED as a plant marker - the new backbone is called pK7GW|WG2D(II)R (Capoen *et al.*, 2011). This construct is named pK7GW|WG2D(II)R *RLCK1* RNAi.

WT (R108) roots were transformed with the RNAi construct pK7GW|WG2D(II)R *RLCK1* RNAi via *Agrobacterium rhizogenes*-mediated hairy root transformation (Boisson-Dernier *et al.*, 2001). The transformed roots were inoculated with Sm1021 and examined at 21 dpi. The knockdown roots showed a significant reduction in the number of nodules at 21 dpi ($p=0.019$) compared to the empty vector controls (fig. 4.2.2a). qRT-PCR was used to determine the efficiency of the knockdown of the *RLCK1* and *RLCK2* transcripts. The construct knocks down *RLCK1* by ~90% ($p=0.030$) compared to the empty vector control (fig. 4.2.2b). The construct also causes a reduction of *RLCK2* expression compared to the empty vector control ($p=0.13$) (fig. 4.2.2b), this could be due to off-target gene silencing as the *RLCK2* CDS has a 76% sequence homology to the *RLCK1* CDS at the nucleotide level.

CLUSTAL O(1.2.1) multiple sequence alignment

```

RLCK1  ---ATTGGCTTTGCCGGCATTGAAAGTGAGATATTTTGTGATGACCAGTTACCATTCT  57
RLCK2  CCGATATATTTTGGCT-TCITTCITGTAATCTAATTTTCCCATTCCTACTACTCA  59
      *  *  *  *  *  *  *  *  *  *  *  *  *  *  *  *  *  *  *  *  *  *

RLCK1  TTCTTTAAAA-----GAAAATATTTCAITGGAGACATG-ITCCTTAAA  100
RLCK2  CCTCCAAAAACTTCTTAATATTATCATCTATTTTCAATAGGAAATTAGATTCTAAAT  119
      ****                               *  *  *  *  *  *  *  *  *  *

RLCK1  GTTGTCTACACTTCAATATAACATAACATAACACATAGTAACTAGTACTAC--CA  158
RLCK2  ACCATCTCCAAGTGA---GITAGAGATTCTATCACAAGGAAATatgccccttgaatg  175
      *  *  *  *  *  *  *  *  *  *  *  *  *  *  *  *  *  *  *  *

RLCK1  ATTATGGGATCTTCCTTGAGTTGTTGTGGCTCAGAGAAGGTTGATGAAGTGCCAACATCA  218
RLCK2  tttatgtgttttctctctaatgaa--gagcaaagccataaacggaatggtgatgacaag  233
      ***** *  *  *  *  *  *  *  *  *  *  *  *  *  *  *  *

RLCK1  TATGGTGTAGCTAACAAITCTTGGAGAATTTTACATACAAGGAGTTGCATACAGCTACA  278
RLCK2  aaaaatattaggactatccatgggaagatacaccttgaagagttgcttcgtgcaaca  293
      *  *  *  *  *  *  *  *  *  *  *  *  *  *  *  *  *  *  *

RLCK1  AACGGGTCAGTGAIGATTATAAGCTTGGTGAAGGIGGGITGGGAGTGTCTATTGGGGA  338
RLCK2  aacaactttcatcaagataacaagattggagaagtgatttgaagtgatattgggggt  353
      ***  *  *  *  *  *  *  *  *  *  *  *  *  *  *  *  *  *  *  *

RLCK1  AGAACCAAGTATGGGCTACAGATAGCAGTGAAGAACTGAAAGCAATGAACCTCAAAGGCA  398
RLCK2  caacaagtaaaagcgctgagattgctgtgaagcggttgaagacaatgactgcaaaagca  413
      *  *  *  *  *  *  *  *  *  *  *  *  *  *  *  *  *  *  *

RLCK1  GAGATGGAATTTGCTGTAGAAGTGAAGTGTCTGGAAGGTTAGGCACAAAAATTTGTTA  458
RLCK2  gagatggaatttgcagttgaagtggaagtactaggaagggtaggcataagaatttgta  473
      ***** *  *  *  *  *  *  *  *  *  *  *  *  *  *  *  *  *

RLCK1  GGCTAAGGGGCTATTGTGTGGCGATGATCAAAGGCTTATTGCTATGATTACATGCCA  518
RLCK2  ggattgagggggttctatgcaggaggagatgaaaggtaattgtgatgattacatgtct  533
      **  *  *  *  *  *  *  *  *  *  *  *  *  *  *  *  *  *  *  *

RLCK1  AATCTAAGTCTGCTTCTCATCTCCATGGTCAATATGCTGGTGAAGTGAACCTCAACTGG  578
RLCK2  aatcatagcttgcctcactcatttacatggtcaactgcttcagattgtttacttgattgg  593
      **** *  *  *  *  *  *  *  *  *  *  *  *  *  *  *  *  *  *  *

RLCK1  CAAAAGAGAATGAGCATTGCAATGGCTCTGCTGAAGGCATTTTGTACTTGACCATGAG  638
RLCK2  cctagaagaatgagcataaacagttggtgcagctgaaggttagcgtactgacccatgag  653
      *  *  *  *  *  *  *  *  *  *  *  *  *  *  *  *  *  *  *  *

RLCK1  GTCACACCCACATCATTATAGAGACATCAAGGCAAGTAATGTTTGTCTGATTAGATG  698
RLCK2  gcaaatcctcacataattcatagagacataaaggcaagcaatgttctattagacacagaa  713
      *  *  *  *  *  *  *  *  *  *  *  *  *  *  *  *  *  *  *

RLCK1  TTTGTGCTCTAGTTGCTGATTTTGGTTTGGCAAAGCTAATACCAGAAGGAGTTAGTCAC  758
RLCK2  tttcaagccaaggtagctgattttggttttgcaaagctaataaccagcaggtgtaagccat  773
      ***  *  *  *  *  *  *  *  *  *  *  *  *  *  *  *  *  *  *

RLCK1  ATGACAACCAGGTTAAGGGTACCTTAGGATACTTAGCACCTGAGTATGCTATGTGGGGA  818
RLCK2  cttacaacaagggttaaaggcacacttggttatttggcaccagaatgctatgtggggt  833
      *  *  *  *  *  *  *  *  *  *  *  *  *  *  *  *  *  *  *

RLCK1  AAAGTTTCTGAAAGCTGTGATGCTATAGTTTGGAAATCTTCTATTAGAGCTAGTAACT  878
RLCK2  aaggtttctgagagttgtgatgtttatagctttggaatttgcctttggagattataagt  893
      **  *  *  *  *  *  *  *  *  *  *  *  *  *  *  *  *  *  *

RLCK1  GGTAGAAAGCCCATAGAGAAGTTACCTGGTGGGCTTAAGAGAACAATAACTGAATGGGCT  938
RLCK2  gccagaaccaattgaaaactacctggtggaataaaaaggacattgttcaatggggtc  953
      *  *  *  *  *  *  *  *  *  *  *  *  *  *  *  *  *  *  *

RLCK1  GAGCCTTTGATAACCAAAGGAGTTTGGGATATGGTTGATCCAAACTCAGAGGAAAC  998
RLCK2  acaccatattgtaaaaagggtgttttaaacatattgctgatccaaaattgaaaggggat  1013
      *  *  *  *  *  *  *  *  *  *  *  *  *  *  *  *  *  *  *

RLCK1  TTIGATGAAAATCAAGTTAAACGACAGTTAATGTAGCTGCTCTTGTGTGCAAAGTGAG  1058
RLCK2  tttgatttagagcaattgaaatcgtgattatgatagctgtgaggtgactgatagtagt  1073
      ***** *  *  *  *  *  *  *  *  *  *  *  *  *  *  *  *

```

Figure 4.2.1. Clustal Omega alignment of *RLCK1* and *RLCK2* CDS with 5' and 3' UTR. Continued over page.

```

RLCK1 TTTGATGAAAAATCAAGTTAAACAGACAGTTAATGTAGCTGCTCTTTGTGIGCAAAGTGAG 1058
RLCK2 tttgatttagagcaattgaaatctgtgattatgatagctgtgaggtgacctgatagtagt 1073
***** * * * * * * * * * * * * * * * * * * * * * * * * * * * * * * * *

RLCK1 CCTGAGAAACGACCAAACATGAAGCAAGTTGTTAGTCTTTTGAAGGACAAGAACCCTGAT 1118
RLCK2 cctgataaaaggccttagcatgatagaggtggtggaatggcttaaggatggtggtttcaaag 1133
***** * * * * * * * * * * * * * * * * * * * * * * * * * * * * * * * *

RLCK1 CAAGGGAAA-----GIGACTAAGATGAGAATTGATAGTGTCAAATATAAT--- 1163
RLCK2 agaaaaaaagagattccaatttgagtaacaataaggacatgatgaagaaaatgatgaa 1193
* * * * * * * * * * * * * * * * * * * * * * * * * * * * * * * * *

RLCK1 -----GATGAATTACTGGCAC-----TTGATCAAC-----CTAGT 1193
RLCK2 aactatgaagagtttgaacaatgcagtcacaacaatttgaaaataactaagtgacaatgat 1253
* * * * * * * * * * * * * * * * * * * * * * * * * * * * * * * * *

RLCK1 GATGATGATTATGATGGAACAGCAGCTATGGTGTITTTTAGTGCTATTGATGTCCAAAAG 1253
RLCK2 aggcgtccttcggataaggacacgacatctcttctgatccaatgctattatatactgcacac 1313
* * * * * * * * * * * * * * * * * * * * * * * * * * * * * * * * *

RLCK1 ATGAAAGATCCTTACAAGAAAATTGGCTAAATTTATGTAATGTAACCAACTTAAATGCTT 1313
RLCK2 gaaa-----ttgttgaaggacattcattttctgaaatgata-----tttatcataagg 1362
* * * * * * * * * * * * * * * * * * * * * * * * * * * * * * * * *

RLCK1 TGTATGTATTGGTAATTTATTCCATTTGGTAGTAGAACTATTTTGTAAIGACTAATAGG 1373
RLCK2 tgttgtatgttccctcc-----tttacttgtattatgaTATTTAGTGTCTGCTTGT 1413
***** * * * * * * * * * * * * * * * * * * * * * * * * * * * * * * * *

RLCK1 TTCATTC-----ATC----- 1383
RLCK2 TGAAATTTAAAATACATCTCTTATGTTTGAGAGAACTAAGATAAAAAATTTAGTATATT 1473
* * * * * * * * * * * * * * * * * * * * * * * * * * * * * * * * *

RLCK1 ----- 1383
RLCK2 TGTAGGTAICTTGTGGCCTT 1494

```

Figure 4.2.1. Clustal Omega alignment of *RLCK1* and *RLCK2* CDS with 5' and 3' UTR. *RLCK1* and *RLCK2* transcripts aligned using Clustal Omega. Estimated 5' UTR 161 bp upstream of start codon and 3' UTR 100 bp downstream of stop codon. pK7GW|WG2D(II)R *RLCK1* RNAi target region highlighted in blue. pK7GW|WG2D(II)R *RLCK2* RNAi target region highlighted in yellow. Asterisks signify matching alignment.

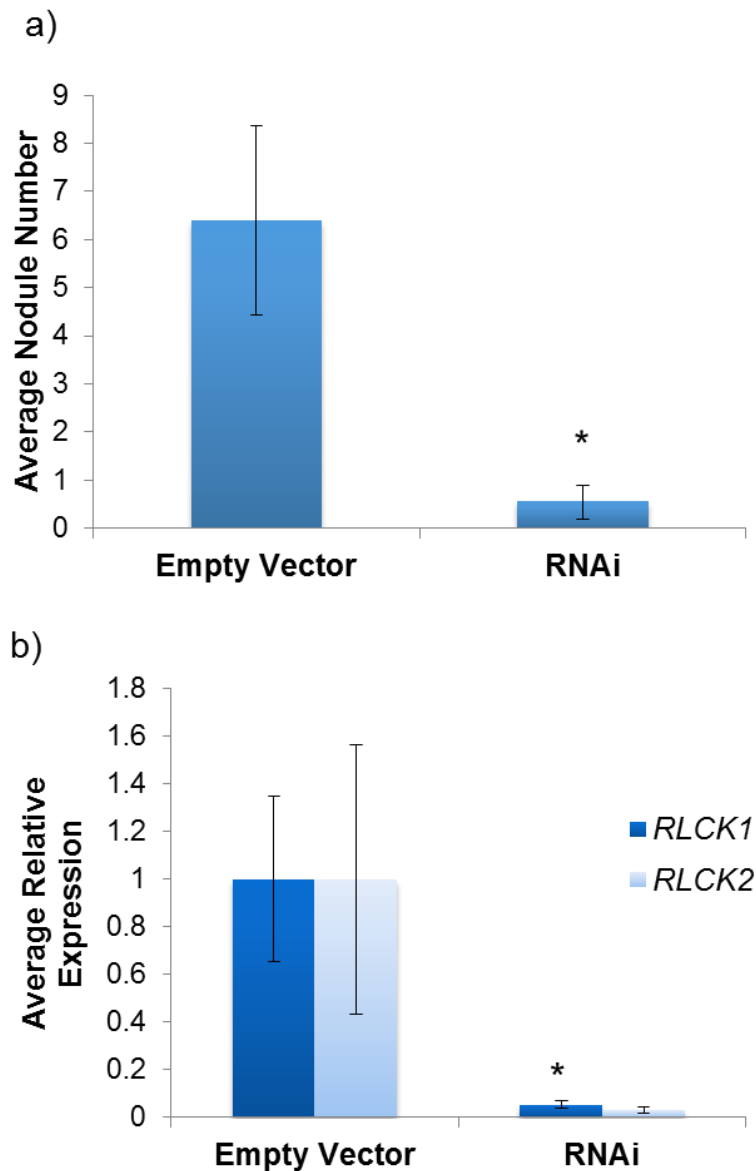


Figure 4.2.2. pK7GW|WG2D(II)R *RLCK1* RNAi nodule number and fold change of expression of *RLCK1* and *RLCK2* relative to empty vector controls.

(a) Knockdown plants show on average a significant reduction in the number of nodules compared to the empty vector control. Bars represent standard error. (b) *RLCK1* and *RLCK2* expression in the empty vector and *RLCK1* knockdown roots was analysed by qRT-PCR. Knockdown plants have a reduced expression of *RLCK1* and *RLCK2* by approximately 90%. Bars represent relative standard error. Averages are composed of 10 to 11 transformed roots. Data shown is representative of 2 experiments. A 2-tailed t-test was used to compare the means to the empty vector control * = $p < 0.05$

4.3 Strategy 2: *RLCK2* knockdown in the *RLCK1-2* mutant

In order to confirm if the phenotype seen with pK7GW|WG2D(II)R *RLCK1* RNAi was due to the *rlck1/rlck2* knockdown and not due to off-target silencing of an alternative gene, a new RNAi construct was made using a 161 bp region of the estimated 5' UTR of *RLCK2* immediately upstream of the start codon (fig. 4.2.1). This construct was designed to be more specific to *RLCK2* and named pK7GW|WG2D(II)R *RLCK2* RNAi (see appendix I for plasmid map). As a stable *Tnt1* mutant for *RLCK1* was available, construct pK7GW|WG2D(II)R *RLCK2* RNAi alongside an empty vector control, was transformed into WT (R108) and *rlck1-2* roots via *A. rhizogenes*-mediated transfer (Boisson-Dernier *et al.*, 2001). Plants were inoculated with Sm1021 and roots observed at 14 dpi.

rlck1-2 empty vector (EV *rlck1-2*) roots had significantly ($p=0.04$) fewer nodules than the R108 empty vector control (EV R108) (fig. 4.3.1a). This is consistent with the nodule phenotype seen previously for *rlck1-2* (fig.3.3.2.1). *RLCK2* knockdown roots (RNAi R108) resulted in a significant reduction in the number of nodules compared to EV R108 ($p=0.007$). Knockdown of *RLCK2* in *rlck1-2* roots (RNAi *rlck1-2*) have a significant reduction in nodule number compared to EV R108 ($p=3.57 \times 10^{-6}$), but also a further reduction in nodule number compared to EV *rlck1-2* ($p=0.002$) and RNAi R108 ($p=0.05$) (fig. 4.3.1a). The *RLCK2* specific RNAi construct significantly reduces the expression of *RLCK2* in both the R108 and *rlck1-2* backgrounds by an average of approximately 50% ($p=0.03$ for both) (fig. 4.3.1b).

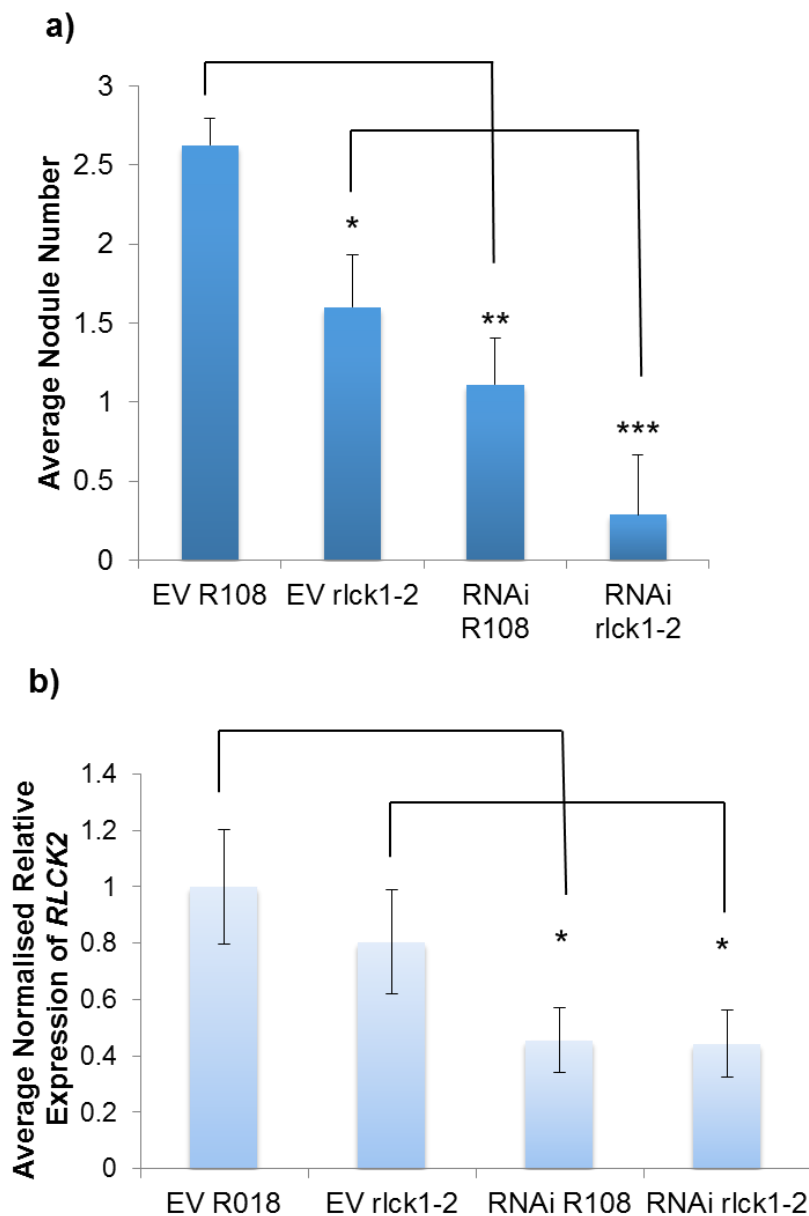


Figure 4.3.1. pK7GW|WG2D(II)*R RLCK2* RNAi nodule number and relative expression of *RLCK2* in *RLCK2*-specific knockdown roots.

(a) WT (*R108*) or *rlck1-2* roots transformed with empty vector (EV) or *RLCK2* RNAi knockdown (RNAi) constructs. Roots transformed with the *RLCK2* knockdown construct had a significantly reduced nodule number compared to their EV control. Nodulation scored at 14 dpi. Bars represent standard error. (b) *RLCK2* expression was analysed by qRT-PCR. *RLCK2* expression was significantly reduced in in the knockdown roots. Bars represent relative standard error. Averages are from of 7 to 14 transformed roots. Data shown is representative of 2 experiments. A 2-tailed t-test was used to compare the means to the *R108* empty vector control * $p < 0.05$, ** $p < 0.01$ *** $p < 0.001$

4.4 Discussion

A stable *rlck1/rlck2* double knockout mutant would be the best material to determine quantitative symbiotic phenotypes. In the absence of a stable double mutant, the effect of an *rlck1/rlck2* double mutant on rhizobial symbiosis was investigated using RNAi. pK7GW|WG2D(II)R RLCK1 RNAi creates a hairpin RNA that is identical in sequence to a region of the *RLCK1* mRNA and highly similar to *RLCK2* mRNA. pK7GW|WG2D(II)R RLCK1 RNAi was designed to work via PTGS to directly reduce the level of *RLCK1* transcript and to reduce the levels of *RLCK2* transcript by off-target gene silencing. The second construct pK7GW|WG2D(II)R RLCK2 RNAi was designed to be more specific to *RLCK2*, creating a hairpin RNA identical to the 5' UTR of *RLCK2* immediately upstream of the start codon.

Both RNAi constructs caused a reduction of *RLCK2* expression, however pK7GW|WG2D(II)R *RLCK2* RNAi is less effective in reducing *RLCK2* transcript levels than pK7GW|WG2D(II)R *RLCK1* RNAi; This could be due to the 5'UTR being AT rich and thus less efficient at binding the target transcript. When levels of *RLCK1* and *RLCK2* expression were simultaneously reduced, either by double knockdown or by selective targeting of *RLCK2* in the *rlck1* mutant, transformed roots showed a near complete reduction in the number of nodules.

The strong reduction in nodulation in the RNAi-mediated double knockdown roots supports the idea that *RLCK1* and *RLCK2* may have partially overlapping or synergistic functions during symbiotic interactions. *rlck1* and *rlck2* single mutants had relatively stronger phenotypes during AMF interactions than with rhizobial interactions, therefore it would be interesting to see how the double knockdown roots interact with AMF. I would expect that in the absence of *RLCK1* and *RLCK2* arbuscular mycorrhization would be massively reduced compared to WT and single mutants.

Chapter 5: Work towards identification of interacting partners of RLCK1 and RLCK2 Proteins

5.1 Introduction

In PAMP triggered immunity and brassinosteroid signalling cytoplasmic kinases have been shown to interact with RLKs at the plasma membrane and relay the signal through the cytoplasm to activate gene expression in the nucleus (Tang *et al.*, 2008; Zhang *et al.*, 2010a; Kim *et al.*, 2011; Shi *et al.*, 2013a; Shi *et al.*, 2013b; Wang *et al.*, 2013). As RLCK1 and RLCK2 are predicted to be cytoplasmic kinases and are expressed during both symbioses it is possible that they interact with the other kinases of the CSP such as NFP, LYK3, DMI2 or DMI3 or themselves (Stracke *et al.*, 2002; Lévy *et al.*, 2004; Mitra *et al.*, 2004). Potential interactions could be tested through yeast-2-hybrid assays and co-immunoprecipitation (Co-IP) experiments. In addition, fluorescent fusions of these proteins could be used for co-localization studies and to determine their subcellular localization. Towards accomplishing these goals a large suite of constructs were made using different epitope tags and fusions that could be used for localization, yeast-2-hybrid and Co-IP approach to find interacting partners. In order to make the large set of multigene constructs needed for Co-IP a more advanced cloning approach was taken using the new Golden Gate cloning system (Engler *et al.*, 2008; Engler *et al.*, 2009; Weber *et al.*, 2011).

Traditionally molecular cloning was a long process comprised of multiple steps, cutting and sticking DNA with restriction enzymes and ligases until the desired construct was complete. Many attempts have been made to streamline the process of molecular cloning and make DNA construction a standardised process. In 1996 Rebatchouk *et al.* published the NOMAD strategy where modules could be combined sequentially using the Styl restriction enzyme to form a composite module that can then be subcloned into alternate preconstructed expression vectors (Rebatchouk *et al.*, 1996). Knight (2003) proposed the BioBrick standard of assembly where each biological part (promoter, gene, tag etc.) is sequentially combined using restriction enzymes, such that when two or more pieces are joined there is still the same restriction sites on the ends as before making the basic and composite parts idempotent. The beauty of the BioBrick system was that any of the basic or composite parts could be joined to any other and an ever growing library of parts was available (Shetty *et al.*, 2008). The Gateway® cloning system by Invitrogen™ remains a popular cloning system, using recombination sites rather than restriction enzymes, to place fragments of interest into destination vectors in frame with tags or signals already present in the destination vector (Hartley *et al.*, 2000; Karimi *et al.*, 2002). This reduces the cloning process to 3 steps; amplification, BP reaction and LR reaction. The compatibility between entry and destination vectors means that the same cloned

fragment within an entry vector can be inserted into multiple different destination vectors reducing the time taken to create new constructs. However, there are limitations with all of these cloning systems. For NOMAD and BioBrick the limitations lie in only being able to assemble fragments in single sequential steps. In Gateway® the limits are the limited number of destination vectors available, the maximum size of the vector and the creation of unavoidable linker nucleotides at the recombination site.

The Golden Gate cloning system allows directional multi-fragment assembly in one reaction (Engler *et al.*, 2008; Engler *et al.*, 2009). Golden Gate cloning is based on Type IIS restriction enzymes which cleave outside of their recognition site. This allows the creation of many different cleavage sites and when the recognition sites are placed flanking a DNA fragment of interest the cleavage sites are removed from the ligated product. The design of the cleavage sites can be such that the pieces can be ligated without additional nucleotides or linkage sequences i.e. the restriction enzyme cut and ligation sequence can be the last base pair of the CDS sequence and the first 3 bases of a tag allowing for the seamless ligation of CDS to tag (Engler *et al.*, 2008; Engler *et al.*, 2009; Weber *et al.*, 2011).

The Golden Gate system works by having 3 levels of construction. Level 0 modules (L0) are the basic components, such as promoters, signal peptides, 5'UTRs Terminators, 3' Tags, and CDSs. These modules can be plasmid inserts, PCR amplicons or synthesised double stranded DNA. Each type of component would be flanked by the same cleavage sites and these sites would be compatible with the flanking module. For example, all promoter sequences would have a 5' overhang of GGAG and 3' overhang of TACT, all 5' UTR sequences have 5' overhangs of TACT and 3' overhangs of AATG, and so on. In this way any combination of basic modules from the L0 library can be used as long as the overhangs match up. The combined L0 constructs combine using the Type IIS restriction enzyme *Bsal* and a T4 DNA ligase to create a Level 1 (L1) module which is a complete transcriptional unit. Multiple L1 modules can then be combined using a different Type IIS restriction enzyme *BpiI* and a T4 DNA ligase to create multigene constructs. Up to 7 L1 modules can be combined into Level 2 (L2) constructs (Engler *et al.*, 2008; Engler *et al.*, 2009; Weber *et al.*, 2011). If an L2 construct is required with more than 7 transcriptional units, an additional reaction can be performed using the L2i destination vector which can then accommodate an extra 6 constructs (13 transcriptional units in total), as demonstrated by Weber *et al.* (2011).

In this chapter I have used both the Gateway® and Golden Gate systems to create a suite of destination vectors that can be used for subcellular localisation and biochemical analysis of RLCK1 and RLCK2 using a yeast 2-hybrid and Co-IP approach.

5.2 *In silico* analysis of RLCK1 and RLCK2 proteins

The 373 and 374 amino acid sequences of RLCK1 and RLCK2 were analysed for potential protein domains initially using InterProScan4 (Hunter *et al.*, 2012) and the ExPASy Bioinformatics Portal (Artimo *et al.*, 2012) (accessed in 2011) and then again later using InterProScan5 (Jones *et al.*, 2014) and the Calmodulin target database (<http://calcium.uhnres.utoronto.ca/ctdb/ctdb/home.html>) (accessed in 2014) .

Initial predictions suggested that RLCK1 and RLCK2 were predominantly kinase domain with an ATP binding site and an RD active site. A Concanavalin A-like lectin domain and a calmodulin binding domain at the N-terminal region of the protein before the RD active site were identified using the updated protein prediction software (table 5.2.1). No signal sequences or transmembrane domains are predicted suggesting cytoplasmic localisation. Therefore the full length proteins can be used in the yeast 2-hybrid system as they are suggested to be soluble proteins.

Domain	Amino acid position in RLCK1	Amino acid position in RLCK2
Concanavalin A-like Lectin domain	12-54	27-59
Calmodulin binding domain	55-119	60-124
ATP binding domain	48-71	53-75
RD active site	164-176	169-181
Kinase domain	23-313	31-329

Table 5.2.1. Positions of predicted protein domains in RLCK1 and RLCK2.

5.3 Preliminary Yeast 2-Hybrid Analysis

A preliminary yeast 2-hybrid experiment was conducted testing RLCK1 and RLCK2 for interactions with symbiosis pathway kinases DMI2 and DMI3, as well as with themselves and each other. Yeast 2-hybrid constructs were made for RLCK1 and RLCK2 by the TOPO® and Gateway® cloning systems into both bait (pGADT7) and prey (pGBKT7) vectors. DMI2 and DMI3 constructs were obtained from the lab construct library. Interactions with AD-T or BD-53 were used as negative controls and the AD-T/BD-53 interaction was used as a positive control. When grown on the selection plate only the positive control yeast grew (fig. 5.3.1). These preliminary results suggest that the RLCKs do not interact with these components of the Nod factor signalling pathway. This approach was not pursued further.

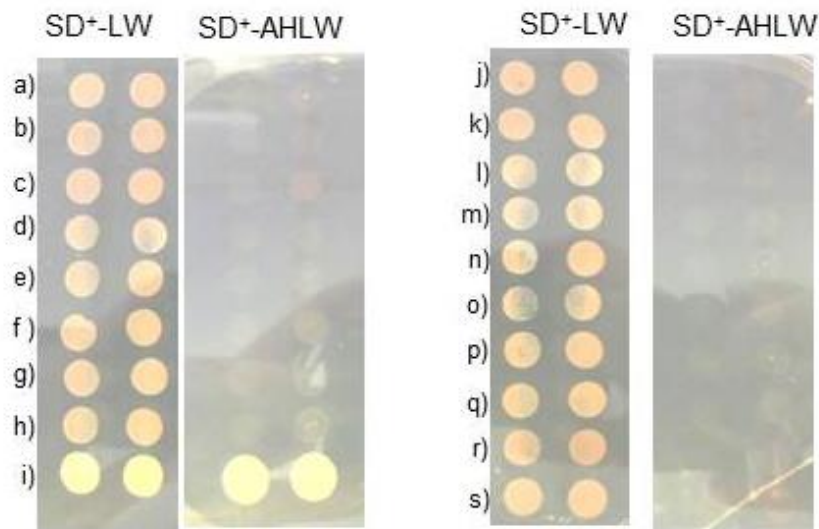


Figure 5.3.1. Yeast 2-Hybrid assay for RLCK1 and RLCK2 protein interactions.

RLCK1 and RLCK2 were tested for interactions with RLCK1, RLCK2, DMI2 and DMI3.

(a) AD-DMI2, BD-RLCK1, (b) AD-DMI2, BD-RLCK2, (c) AD-DMI2, BD-53, (d) AD-DMI3, BD-RLCK1, (e) AD-DMI3 BD-RLCK2, (f) AD-DMI3, BD-53, (g) AD-T, BD-RLCK1, (h) AD-T, BD-RLCK2, (i) AD-T, BD-53 (positive control), (j) AD-RLCK1, BD-RLCK1, (k) AD-RLCK1, BD-RLCK2, (l) AD-RLCK1, BD-DMI2, (m) AD-RLCK1, BD-DMI3, (n) AD-RLCK1, BD-53, (o) AD-RLCK2, BD-RLCK1, (p) AD-RLCK2, BD-RLCK2, (q) AD-RLCK2, BD-DMI2, (r) AD-RLCK2, BD-DMI3, (s) AD-RLCK2, BD-53.

5.4 Protein localisation

Protein localisation constructs were made by cloning the CDS of *RLCK1* and *RLCK2* fused to mCherry behind the Ubiquitin promoter. *RLCK1* and *RLCK2* were fused at the 5' end to mCherry through PCR and then cloned into vector pUB-GW-GFP (Maekawa *et al.*, 2008) by the Gateway® cloning system. This destination vector contains a constitutively expressed GFP to allow the easy identification of transgenic roots. To check that the fused proteins were expressed the constructs were infiltrated into *N. benthamiana* leaves. Leaf discs were taken at 1, 2 and 3 dpi and checked on a confocal microscope for protein localisation. No mCherry expression was seen. GFP expression was seen at 2 dpi which suggests that the constructs were transformed into *N. benthamiana*. The lack of mCherry fluorescence suggests that the constructs are not correctly expressing the fusion protein or that the fusion protein was being degraded. Due to uncertainty over the functionality of the constructs they were not transformed into *M. truncatula* roots.

5.5 Construction of Golden Gate constructs for future protein interaction studies

Using the Golden Gate cloning system constructs were made that can be used to look for interaction partners by Co-IP in *Medicago* roots or targeted interactions in *N. benthamiana* (table 5.5.1; more detail in appendix 1). Interactions of the RLCKs would help us elucidate a role for these proteins during symbiosis. *N. benthamiana* leaves were infiltrated with *A. tumefaciens* transformed with the constructs and leaf discs were taken at 1, 2 and 3 dpi. Proteins were detected using Western blots and α -myc or α -eGFP antibodies. Expected protein sizes are listed in table 5.5.2.

C-terminally myc tagged *RLCK1* and *RLCK2* were detectable at 2 and 3 dpi with most constructs with the exception of constructs EC67044 to EC67047. N-terminally tagged *RLCK1* was detectable at 1, 2 and 3 dpi for most constructs but myc-*RLCK2* was not very well expressed and was only detectable with the EC67035 construct at 1 and 3 dpi. Out of all the eGFP tagged proteins MtHMGR1-GFP was the easiest to detect via Western Blot and was expressed with all its respective constructs being detectable at 2 and 3 dpi. Otherwise MtDMI2-GFP was weakly detected at 2dpi with construct EC67022 (fig. 5.5.1).

Construct	Protein 1	Protein 2
EC67007	RLCK1-myc	-
EC67008	RLCK2-myc	-
EC67014	RLCK1-myc	MtNFP-eGFP
EC67015	RLCK1-myc	MtLYK3-eGFP
EC67016	RLCK1-myc	MtHMGR-eGFP
EC67017	RLCK1-myc	MtDMI2-eGFP
EC67018	RLCK1-myc	RLCK2-eGFP
EC67019	RLCK2-myc	MtNFP-eGFP
EC67020	RLCK2-myc	MtLYK3-eGFP
EC67021	RLCK2-myc	MtHMGR-eGFP
EC67022	RLCK2-myc	MtDMI2-eGFP
EC67034	myc-RLCK1	-
EC67035	myc-RLCK2	-
EC67038	myc-RLCK1	MtNFP-eGFP
EC67039	myc-RLCK1	MtLYK3-eGFP
EC67040	myc-RLCK1	MtHMGR-eGFP
EC67041	myc-RLCK1	MtDMI2-eGFP
EC67042	myc-RLCK1	RLCK2-eGFP
EC67043	myc-RLCK1	eGFP-RLCK2
EC67044	myc-RLCK2	MtNFP-eGFP
EC67045	myc-RLCK2	MtLYK3-eGFP
EC67046	myc-RLCK2	MtHMGR-eGFP
EC67047	myc-RLCK2	MtDMI2-eGFP

Table 5.5.1. A list of Golden Gate constructs and the proteins they express.

Protein	Size (kD)
RLCK1-myc	45.37
RLCK2-myc	45.75
myc-RLCK1	45.37
myc-RLCK2	45.75
MtNFP-eGFP	93.03
MtLYK3-eGFP	95.58
MtHMGR-eGFP	86.03
MtDMI2-eGFP	131.18
RLCK2-eGFP	68.99
eGFP-RLCK2	68.99
eGFP	26.9
myc	3.67

Table 5.5.2. Expected protein sizes for the proteins expressed by the Golden Gate constructs.

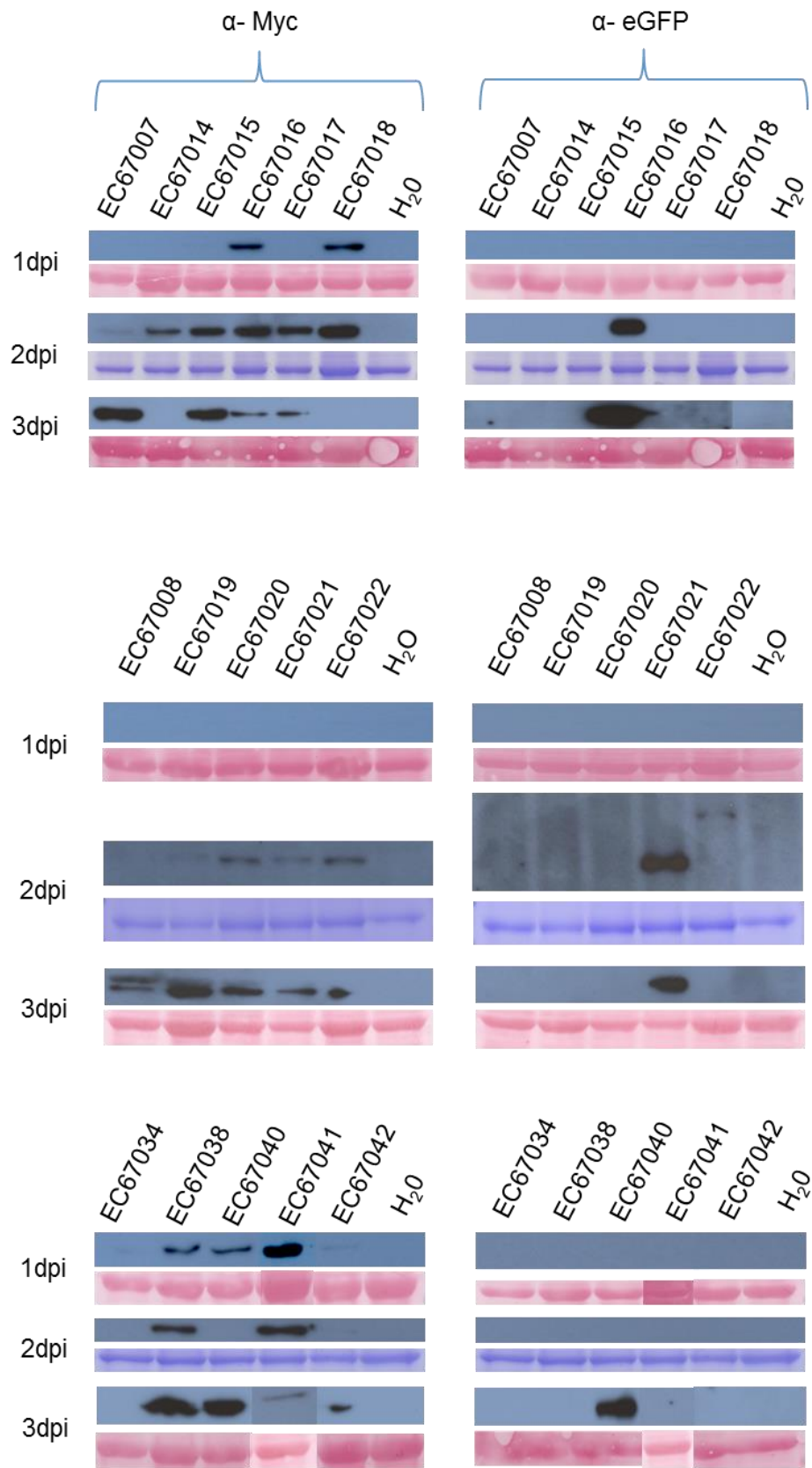


Figure 5.5.1. continued overleaf

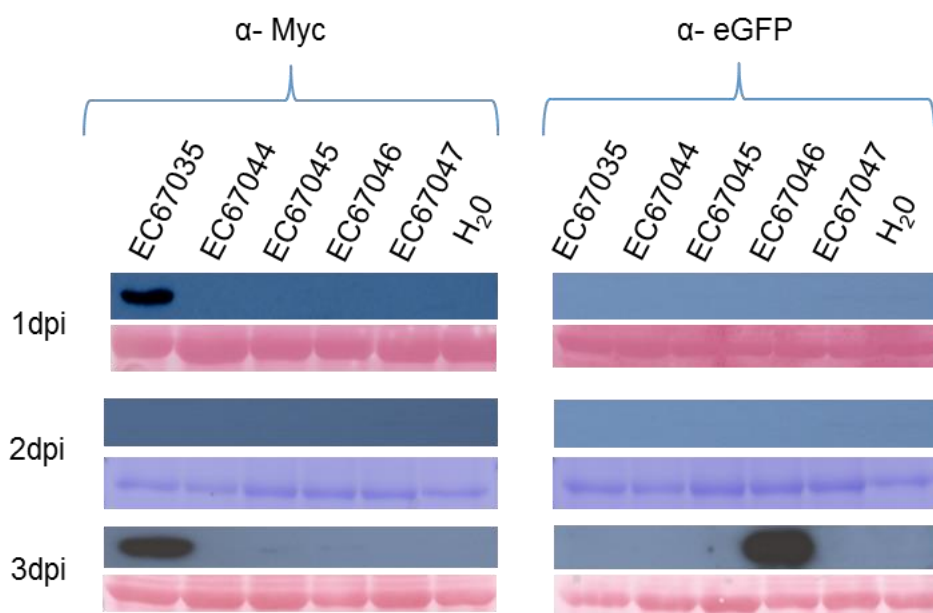


Figure 5.5.1. Expression of Proteins in *N. benthamiana* from the Golden Gate constructs. Expression of tagged proteins in *N. benthamiana* infiltrated with Golden Gate constructs using *A. tumefaciens* was checked at 1, 2 and 3 dpi by Western blot. RLCK1-myc and RLCK2-myc bands could be detected at 2 and 3 dpi (~45kD). myc-RLCK1 can be seen with some constructs at 1, 2 and 3 dpi. myc-RLCK2 could only be detected with one construct (EC67035) at 1 and 3 dpi. HMGR-GFP could be detected at 2 or 3 dpi (~86kD). DMI2-GFP was weakly detected at 2 dpi with construct EC67022 (~131.18kD). See table 5.4.1 for construct details and table 5.4.2 for protein sizes. Protein levels were checked using Coomassie (blue) or Ponceau (Red) staining; Rubisco bands shown beneath the western blot.

5.6 Discussion

An attempt was made to visualise protein localisation using mCherry tagged overexpressed RLCK1 and RLCK2. In preliminary experiments in *N. benthamiana* no mCherry fluorescence was seen in the leaf discs under the confocal microscope at 1, 2 or 3 dpi. A Western blot is needed to be sure that the proteins are being properly expressed. It may be that no mCherry was seen because expression was being suppressed in the *N. benthamiana* leaves. Co-infiltration with a silencing suppressor plasmid such as p19 would improve expression of the tagged proteins in *N. benthamiana* (Voinnet *et al.*, 2003). Ideally localisation of the RLCKs would be best performed in *M. truncatula* roots where these proteins are naturally expressed. Alternate constructs using the ubiquitin and the native promoters in combination with the genomic and CDS sequences could be used to maximise the construct expression *in Planta*. It would also be good to check the localisation of the RLCKs with and without rhizobia and AMF in *M. truncatula* roots as the localisation may be different upon interaction with symbiotic partners.

Based on the expression patterns of *RLCK1* and *RLCK2* and the symbiotic phenotypes observed, members of the Nod factor signalling pathway were chosen to be investigated as possible interacting partners. Yeast 2-hybrid constructs have been made for RLCK1 and RLCK2. The yeast 2-hybrid constructs described here can be used in the future with a yeast 2-hybrid library to screen for interacting partners. A western blot should be performed to check that the proteins were correctly expressed in yeast. Yeast 2-hybrid uses the soluble regions of proteins, so for transmembrane proteins such as MtNFP1 and MtLYK3 and MtDMI2 this may not be the best method to use for the receptor kinases as they may require the full length protein for activation, or activation by a ligand such as Nod Factor, before they are able to interact. For this reason interaction studies of PAMP RKs and RLKs such as FLS2 tend to be investigated using a Co-IP method in *N. benthamiana* leaves.

Several constructs have been made for expressing RLCK1 and RLCK2 tagged to a myc tag, at either N or C termini, on their own or in combination with GFP tagged components of the symbiosis pathway. Preliminary analysis showed that only a handful of these constructs have given clearly expressed tagged proteins of the correct size on the Western blots. The proteins which were detected by Western blot analysis were the RLCKs and MtHMGR1. The RLCK proteins are smaller and are predicted to be localised within the cytoplasm which would make them easier to extract from the plant material than the larger membrane bound proteins. Further testing is needed to optimize expression of these constructs. Once expression is confirmed, these constructs can be used for a targeted Co-IP to see if RLCK1 and RLCK2 interact with MtNFP, MtLYK3, MtHMGR1 or

MtDMI2 in *N. benthamiana*. They can also be transformed into *M. truncatula* roots by *A. rhizogenes*-mediated hairy root transformation to look for interacting partners *in planta* and to confirm any positive interactions observed in *N. benthamiana*.

Additionally in the analysis of *RLCK1* and *RLCK2* is to look at the protein functions and to discover interacting partners. *RLCK1* and *RLCK2* are predicted to contain a Concanavalin A lectin or lectin-like domain. Lectins have been shown to bind sugars and oligosaccharides. It would be worth testing these proteins with a carbohydrate-chip to attempt to determine their potential carbohydrate substrate(s) (Houseman and Mrksich, 2002; Park *et al.*, 2004).

Chapter 6: Identification of a mycorrhizal phenotype in *M. truncatula* *Tnt1* insertion line NF5270

6.1 Introduction

Alongside the main project of *RLCK1* and *RLCK2*, *Tnt1* insertion seeds were obtained from the Samuel Roberts Noble Foundation for a third predicted kinase, the gene Medtr7g116650. The protein was predicted to contain a transmembrane domain and a cytoplasmic kinase domain, but have no extracellular domain, and as such the gene was named *receptor-like cytoplasmic kinase 3* *RLCK3*. The MtGEA profile for *RLCK3* showed that it was upregulated during AMF colonisation and during nodule senescence, though interestingly not during nodule development (fig. 6.2.1) (Benedito *et al.*, 2008; He *et al.*, 2009; Hogekamp *et al.*, 2011; Czaja *et al.*, 2012; Gaude *et al.*, 2012; Seabra *et al.*, 2012). It was possible that *RLCK3* could provide insight to, and play a role in, the differentiation between rhizobial and mycorrhizal symbiosis.

6.2 Identification of the *RLCK3* mutant and Characterization of its Nodulation and Mycorrhizal Phenotypes

A gene of interest was selected based on the expression profile of probe set Mtr.20292.1.S1_at on the Medicago Gene Expression Atlas (MtGEA) (Benedito *et al.*, 2008; He *et al.*, 2009; Hogekamp *et al.*, 2011; Czaja *et al.*, 2012; Gaude *et al.*, 2012; Seabra *et al.*, 2012). The gene named as *RLCK3* (Medtr7g116650) is up-regulated in later stages in nodulation and in nodules treated with phosphinothricin (PPT), a glutamine synthetase inhibitor. It is also up-regulated during mycorrhizal infection by *R. irregularis* and in root inner cortical cells that contain arbuscules (fig. 6.2.1). To study this gene a *Tnt1* line NF5270 was identified that contained a *Tnt1* insertion in the second exon of *RLCK3* at 1238 bp. This allele was named *rlck3-1* (fig. 6.2.2 a). R1 generation seeds were obtained from the Samuel Roberts Noble Foundation and homozygote mutants for *rlck3-1* were identified by PCR using the gene specific primers #11 and #12 and primers #10 and #11 for *Tnt1* identification within *RLCK3* (fig. 6.2.2b and 7.2.2c). See Appendix 1 for primer details.

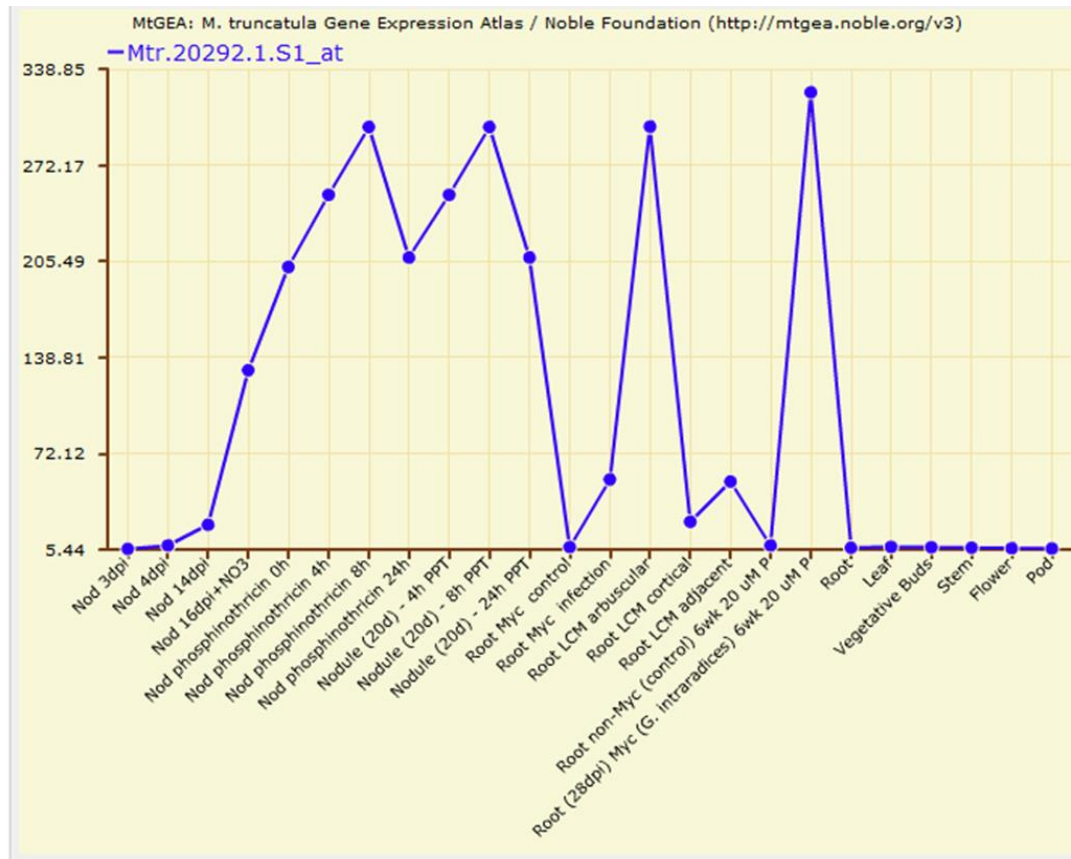


Figure 6.2.1. Medicago Gene Expression Atlas data for *RLCK3*.

The graph shows the expression level of *RLCK3* under a number of different experimental conditions. Expression of *RLCK3* is highly induced at later stages of nodulation and mycorrhization. *RLCK3* is specifically upregulated in arbusculated inner cortical cells during AMF colonisation and in nodules treated with a source nitrogen or a Glutamine synthetase (GS) inhibitor (Phosphinothricin (PPT)).

6.2.1 Preliminary Nodulation and Mycorrhizal phenotypes of *rlck3-1*

Two homozygous mutant sibling lines 9_NF5270 and 15_NF5270 were chosen for further study (fig 6.2.2). Preliminary nodulation and mycorrhizal phenotypes were examined in the progeny of these lines (fig. 6.2.3). Plants were inoculated with Sm1021 and examined at 21 dpi. Unexpectedly, line 15_NF5270 has significantly fewer nodules than WT (R108) ($p=0.002$) at 21 dpi, however only 5 plants were scored and so requires confirmation. Line 9_NF5270 was not significantly different from WT (R108) ($p=0.3$) (fig. 6.2.3a).

Plants were inoculated with the PlantWorks mycorrhizal inoculum and scored for percentage arbuscultation at 8 wpi. A few progeny for 9_NF5270 was checked whilst seeds for 9_NF5270 and 15_NF5270 were being bulked for further phenotypic analysis. *rlck3-1* line 9_NF5270 has significantly fewer arbuscules at 8wpi than WT (R108) ($p=3.43 \times 10^{-5}$) (fig. 6.2.3b).

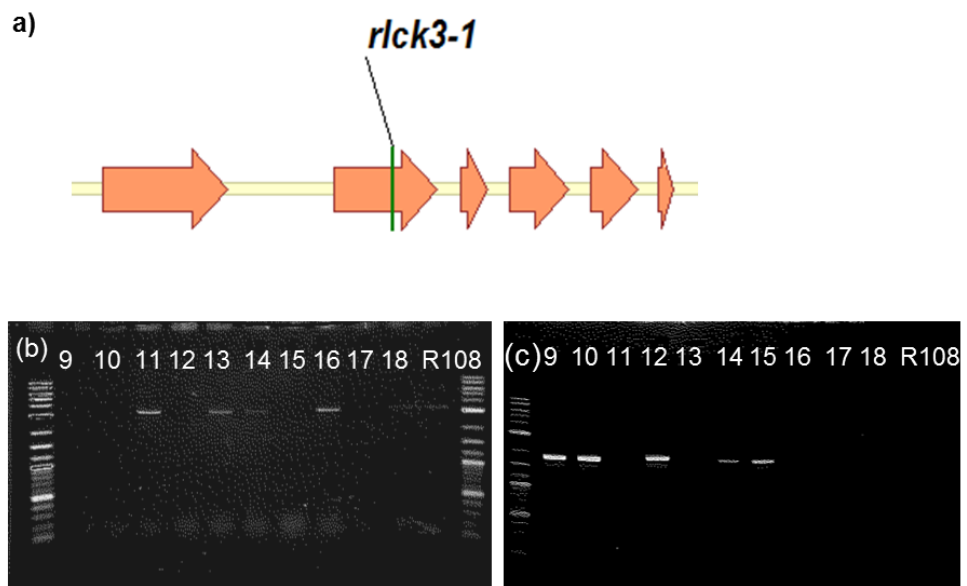


Figure 6.2.2. Identification of *RLCK3 Tnt1* insertion mutants in line NF5270.

(a) Gene structure for *RLCK3*. Arrows represent exons. The position of the *Tnt1* insertion is shown as *rlck3-1*. Gel electrophoresis image showing (b) WT *RLCK3* and (c) *Tnt1* insertions amplified by PCR using DNA from individual NF5270 R1 plants. WT (R108) DNA was used as a control. Plants number 9 and 15 were selected as homozygote mutants and plant number 14 was chosen as a heterozygote for further study.

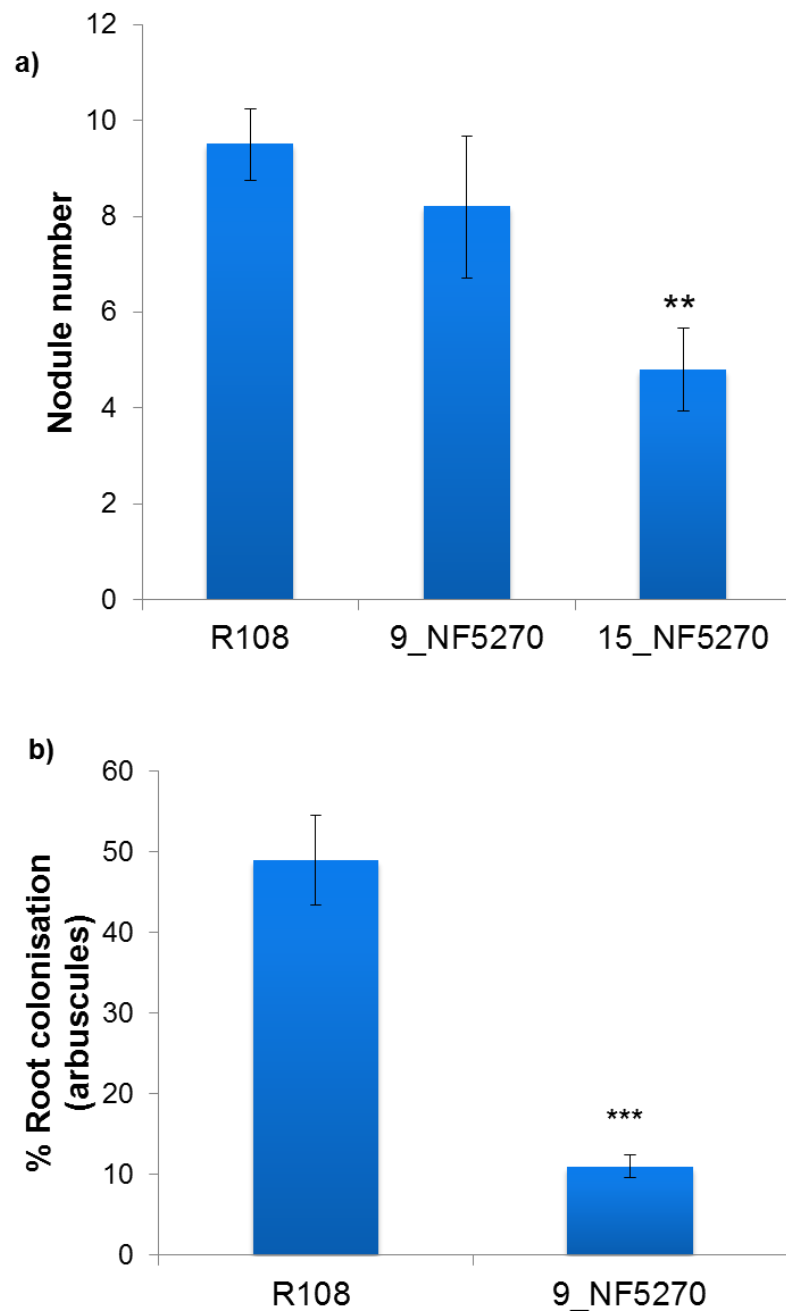


Figure 6.2.3. Preliminary nodulation and AMF colonisation phenotypes of *rlck3-1*

(a) The NF5270 *Tnt1* sibling line 15 has fewer nodules than line 9 and WT (R108). Data is an average of 5 - 10 plants. Plants were scored at 21 dpi. A 2-tailed t-test was used to compare the means of each line and the WT (R108) ($p < 0.01$). (b) Percentage of the root with arbuscules at 8 wpi with the PlantWorks inoculum. The 9_NF5270 line has significantly fewer arbuscules than WT (R108). Data is an average of 11 (R108) and 17 (NF5270) plants. A 2-tailed t-test was used to compare the means ($p < 0.001$). Bars are standard error.

6.2.2 Segregation population of *rlck3-1*

To test whether the mutation in *RLCK3* cosegregated with the mycorrhizal phenotype observed in 9_NF5270, progeny from an *rlck3-1* heterozygote sibling line 14 (14_NF5270) was used to generate a segregating population. The *rlck3/rlck3* plants were not significantly different from the *RLCK3/RLCK3* plants for levels of arbusculation in the root (Fig. 6.2.4).

These results strongly suggest that the symbiotic phenotypes observed in NF5270 were not due to the insertion in *RLCK3*, and instead resulted from alternative mutations arising in the original R0 NF5270 *Tnt1* insertion mutant line. It also indicates that the gene responsible for the mycorrhizal phenotype present in 9_NF5270, is not in the sibling line 14_NF5270 used to generate the segregating population for *rlck3-1*, and that the gene responsible for the mycorrhizal phenotype was segregating in the parental generation (R2). The unknown gene conferring the strong mycorrhizal phenotype was named *SCOOBY*.

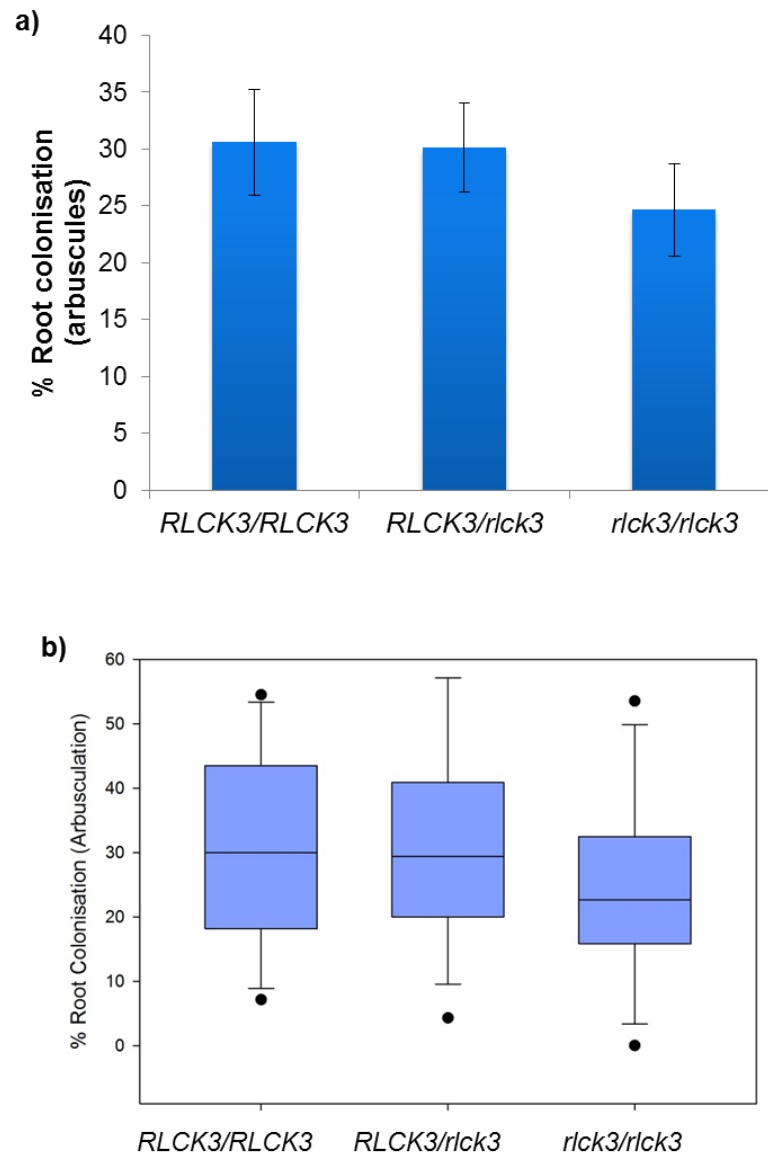


Figure 6.2.4. AMF colonisation of progeny for different genotypic classes from the 14_NF5270 segregating population for *rlck3-1*.

(a) Average percentage of arbusculation in the *rlck3-1* segregating population generated from plant 14_NF5270. Roots were scored at 3 wpi with the *Symplanta* inoculum (see materials and methods). The data are averages of 11, 20 and 12 plants respectively. The means were not significantly different from each other (2-tailed t-test, $p > 0.05$). The bars represent standard error. (b) A box plot to show the distribution of arbusculation in each *rlck3-1* genotype.

6.3 *scooby* mycorrhizal phenotype

A further investigation into the *scooby* mycorrhizal phenotype was carried out. Lines 9_NF5270 and 15_NF5270 were grown with AMF chive inoculum for 5 weeks, until the WT colonisation was $\geq 50\%$. Both the 9_NF5270 and 15_NF5270 line showed a reduced percentage of root that contained arbuscules, with a mean average of 7.2% and 5.2% respectively compared to WT (R108) mean average of 81.4% and 77.33% respectively. A 2-tailed t-test shows the colonization in both lines was significant ($P=1.08 \times 10^{-13}$ and $P=4.92 \times 10^{-16}$ for 15_NF5270 and 9_NF5270 respectively) (fig. 6.3.1). Microscopic examination of the *scooby* roots shows that as well as having a reduced number of arbuscules in the inner cortical cells, the arbuscules that were formed did not fill the cells and were misshapen (fig. 6.3.2). The AMF was able to penetrate the root, grow intracellular hyphae and form vesicles in the *scooby* mutant as in WT (R108).

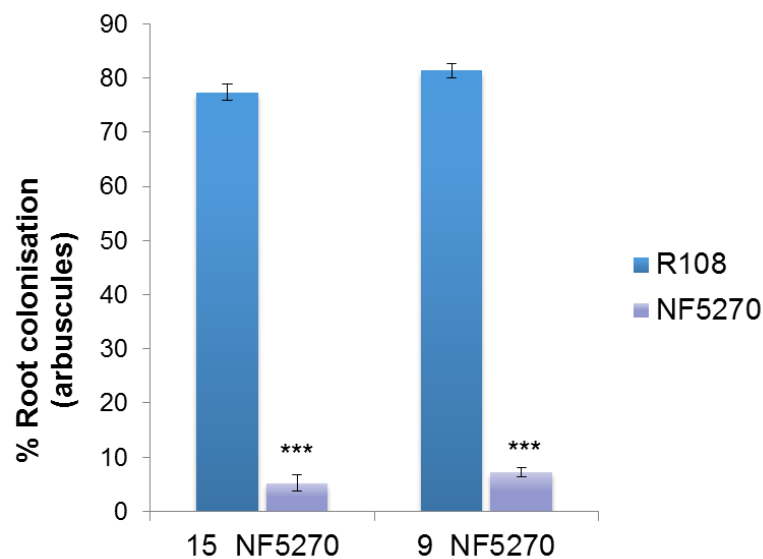


Figure 6.3.1. AMF colonisation of NF5270 *Tnt1* lines

(a) Percentage of the root with arbuscules with the chive inoculum when colonisation of WT (R108) is $>50\%$. Both 9_NF5270 and 15_NF5270 have significantly fewer arbuscules than WT (R108). Data is an average of 5 15_NF5270, 5 9_NF5270 and 9 and 10 WT (R108) plants respectively. A 2-tailed t-test was used to compare the means of the mutant to the WT (R108) control ($p < 0.001$).

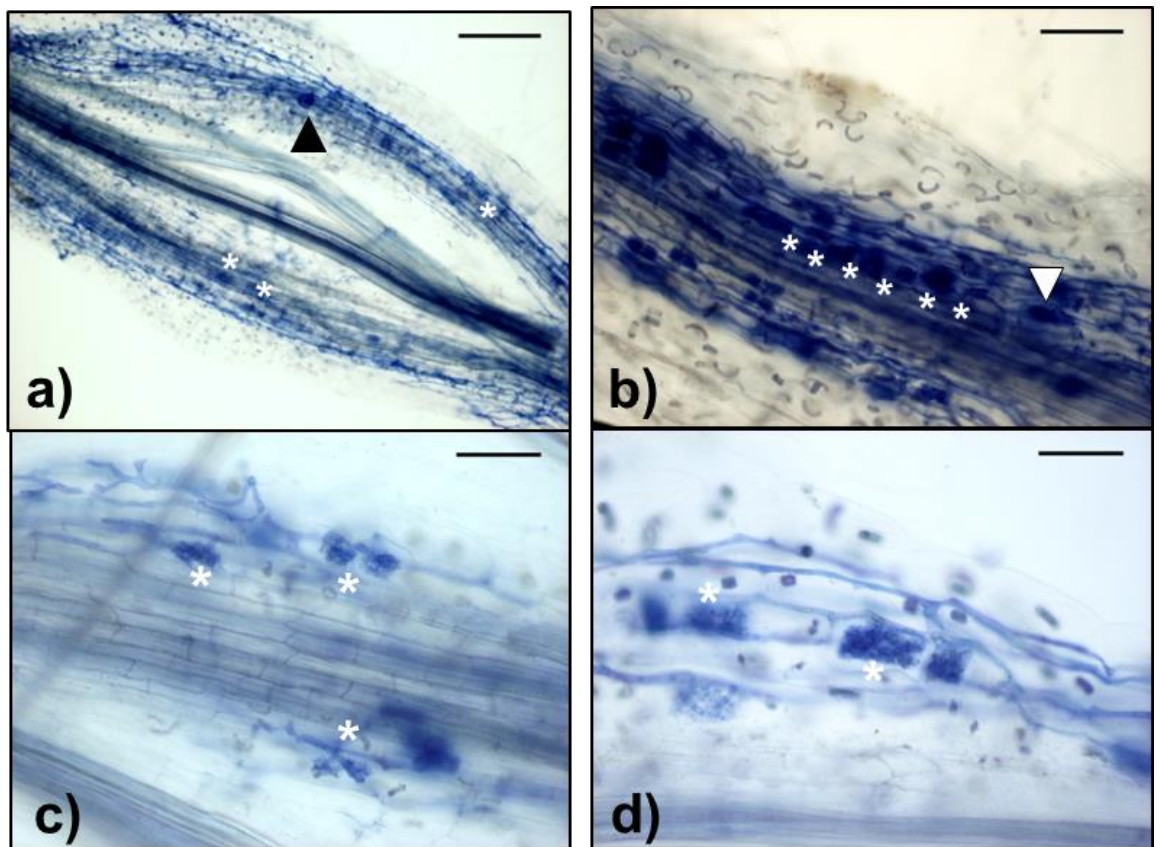


Figure 6.3.2. Mycorrhizal phenotypes of *scooby* and WT (R108).

Light microscope images of (a, c) *scooby* mutant and (b, d) WT (R108) roots colonised by *R. irregularis*. AMF hyphae are able penetrate and grow through the root cortex of NF5270 (a) and form vesicles (black arrowhead) as the WT (R108) (white arrowhead). Although the mutant can form structures resembling arbuscules (asterisks) they are much fewer in number and are misshapen compared to WT (R108) (b and d, starred). Images were taken at 5wpi. Scale bars are 200µm (a), 100µm (b) and 50µm (c and d).

6.4 Discussion

The regeneration of *M. truncatula* containing the *Tnt1* retrotransposon can cause many insertion mutations (Tadege *et al.*, 2008). When taking a reverse genetics approach, the phenotype seen in one of the *Tnt1* mutant lines may not necessarily be caused by the gene of interest but by a different background mutation. The Samuel Roberts Noble Foundation lists the mutant population by generating FSTs which show the genomic regions around the *Tnt1* insertion. However, due to the possible number of insertions and limitations to the approach not all FSTs in a regeneration line are identified.

In the case of the mutant line NF5270, it was selected based on a known FST for the gene *RLCK3* (Medtr7g116650), a predicted cytoplasmic kinase. Initial phenotyping in a sibling line homozygous for this gene showed a strong mycorrhizal phenotype. However a segregating population for *rlck3-1*, which was generated from a heterozygote sibling line (14_NF5270), showed that the mycorrhizal phenotype was not caused by the *rlck3* mutation. It also indicates that the mutation responsible for the mycorrhizal phenotype seen in 9_NF5270 and 15_NF5270 (*scooby*), was hemizygous at R0 and was segregating at R2 (fig. 6.4.1).

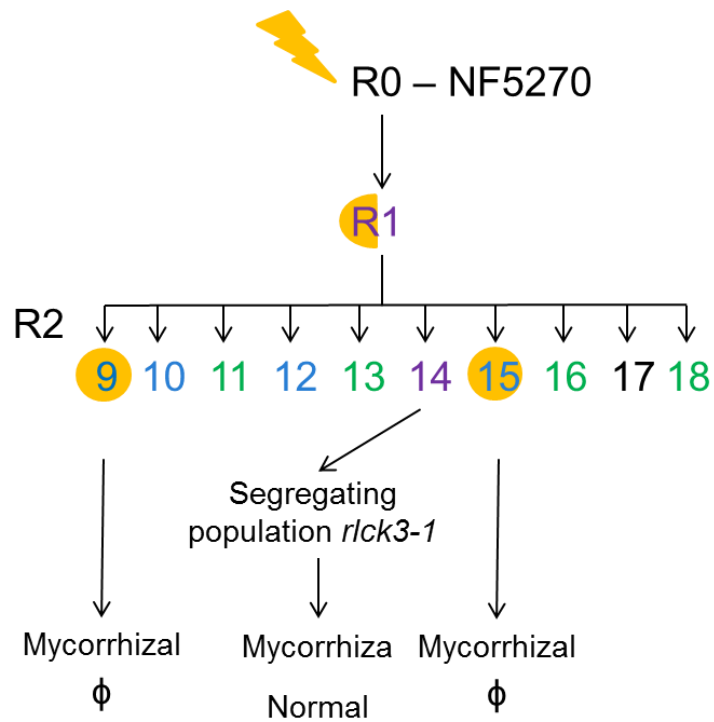


Figure 6.4.1. *Tnt1* insertion line NF5270

A diagram of the *Tnt1* insertion line NF520. Generation R0 are hemizygous for many *Tnt1* insertions. Seeds from generation R1 are obtained and generation R2 plants which were genotyped (fig 6.2.2) – green are WT, blue are homozygous mutants and purple are heterozygous for the *rlck3-1* *Tnt1* insertion. Another insertion mutation in the line responsible for reduced mycorrhization, symbolised by the yellow circles, is also segregating in the R2 population and is homozygous in plant 9 and 15 but WT in plant 14.

As the mycorrhizal phenotype, *scooby*, is strong in the two sibling lines 9_NF5270 and 15_NF5270, and is sustained over generations, it is worthy of further investigation. The gene, or genes, responsible for the phenotype can be investigated through genetic mapping and additional TAIL-PCR to look for more FSTs. Single base pair mutations, deletions and frame-shift mutations can also occur during the regeneration process. Whole genome sequencing such as Illumina sequencing, or transcriptome sequencing via RNA-seq could be used to identify these mutations.

Further characterisation of the *scooby* mycorrhizal phenotype should be carried out. A time-course following AMF colonisation of mutant roots overtime could help to establish at which stage the AMF is inhibited. Lack of arbuscultation could be caused by inhibition of the AMF at the epidermis or at a cortical level. Growth with nurse plants would establish if 9_NF5270 and 15_NF5270 are missing signalling molecules causing the *scooby* phenotype. Differential gene regulation and genetic markers could shed light on the function or position of *SCOOBY* relative to the symbiosis pathway.

SCOOBY may prove to be a mycorrhizal specific gene, of which there are only a few currently known for *M. truncatula* including a GRAS-type transcription factor (*RAM1*), a glycerol-3-phosphate acyltransferase (*RAM2*) an H⁺-ATPase (*Mt-HA1*), and a phosphate transporter (*MtPT4*) (Javot *et al.*, 2011; Gobbato *et al.*, 2012; Wang *et al.*, 2012; Krajinski *et al.*, 2014; Wang *et al.*, 2014). In *ram1* AMF is inhibited at the epidermal level (Gobbato *et al.*, 2012). In *ram2*, the AMF appears to be inhibited at the epidermal level through a lack of hyphopodia formation; however with increased AMF levels some arbuscules can be seen (Wang *et al.*, 2012). *mt-ha1* and *mtpt4* have similar phenotypes, allowing epidermal entry of AMF but have premature senescence of the arbuscules resulting in fewer arbuscules visible in the root cortex (Javot *et al.*, 2011; Wang *et al.*, 2014). To confirm that *SCOOBY* is not caused by *RAM2*, *Mt-HA1* or *MtPT4* these genes could be checked for *Tnt1* insertions by PCR. Alternatively complementation of the *scooby* phenotype could be checked by transformation of 9_NF5270 and 15_NF5270 root with WT *RAM2*, *Mt-HA1* or *MtPT4*.

Chapter 7: Discussion

Mutant studies have provided insight into many of the genetic components required for the establishment and maintenance of the plant-microbe symbioses. However, many of the genetic aspects of the plant-rhizobial and plant-mycorrhizal symbioses remain to be identified. It is as yet unknown how the signalling is transduced from the RLKs at the plasma membrane to the nucleus through the CSP, or how parallel signalling pathways help to modulate each symbiosis. It also remains unclear how the plant is able to establish the difference between friend and foe when both carry microbe-associated molecular patterns (MAMPs) that activate plant defence. The control of ROS levels during development and defence are tightly controlled, and whilst there is some evidence to suggest roles for ROS during symbiosis, it is not yet known how ROS levels are regulated during symbiosis. We are at an exciting time in the study of mycorrhizal symbiosis with the genome of *R. irregularis* being recently published (Tisserant *et al.*, 2013). This will provide the community with better tools to study this symbiosis in the future.

scooby is a novel mycorrhizal mutant in *M. truncatula*

The *scooby* mutant appears to be a novel mycorrhizal mutant in *M. truncatula*. *scooby* plants had fewer arbuscules (fig. 6.3.1) that appeared to be arrested between the birdsfoot stage and full arbuscule development. Arbuscules are smaller in *scooby* than WT (R108) and do not fully fill the cortical cell (fig. 6.3.2). However, the branches of the arbuscules are well defined and appear different than the early senescent arbuscules seen in *Mtpt4* or *Mt-ha1* (Javot *et al.*, 2007; Krajinski *et al.*, 2014; Wang *et al.*, 2014). AMF are able to penetrate the *scooby* roots as normal, which rules out *ram1* and *ram2* as these mutants are blocked at the epidermis, and *scooby* has a large amount of intraradical hyphae seen which is different to the phenotypes of *Mt-HA1* (Gobbato *et al.*, 2012; Wang *et al.*, 2012; Krajinski *et al.*, 2014; Wang *et al.*, 2014). Mutation or down regulation in the half-ABC transporters *STR* and *STR2* have been identified in *M. truncatula*, rice and *L. japonicus* (Zhang *et al.*, 2010b; Gutjahr *et al.*, 2012; Kojima *et al.*, 2014), however they have a lower total level of AMF colonisation compared to *scooby* despite similar stunted arbuscules in these mutants. Groth *et al.* (2013) recently described two mycorrhizal mutants in *L. japonicus*, SL0181-N mutant had two arbuscule phenotypes (type I and II). Type II arbuscules were severely stunted and appeared similar to the *scooby* phenotype. However segregation analysis revealed that the severe arbuscule stunting is likely to result from the combination of two distinct loci.

Further analysis of the mycorrhizal phenotype is needed to fully characterise the *scooby* mutant. A time-course following AMF colonisation of mutant roots over time could help to establish at which stage the AMF is inhibited. The phenotypes of some mycorrhizal mutants that are inhibited at the early stages of mycorrhization, such as *pre-mycorrhizal infection 1 (PMI1)* in tomato, are able to be rescued when grown alongside WT “nurse” plants in the presence of AMF (David-Schwartz *et al.*, 2001). In cases such as that of *Mtpt4* and *Mt-ha1*, nurse plants are unable to rescue the shrunken arbuscule phenotype, however the number of these type of arbuscules seen per root is increased (Javot *et al.*, 2007; Wang *et al.*, 2014); this is possibly due to the AMF being provided a source of carbon from the nurse plants and as such AMF growth is not inhibited as it would be with the *Mtpt4* and *Mt-ha1* mutants alone. Growth with nurse plants would establish if 9_NF5270 and 15_NF5270 are missing signalling molecules, such has been hypothesised for *pmi1* or are lacking in nutrient exchange as in *Mtpt4* or *Mt-ha*. Single base pair mutations, deletions and frame-shift mutations can also occur during the regeneration process and could be identified by whole genome sequencing, such as Illumina sequencing, or transcriptome sequencing via RNA-seq.

Two Receptor-like kinases required for nodulation and mycorrhization

RLCK2 is a novel symbiotic gene

RLCK2 encodes a putative receptor-like cytoplasmic kinase expressed constitutively in root tissue with up-regulation during symbiosis. *rlck2* mutants were significantly reduced in AMF colonisation (fig. 3.4.1) with smaller arbuscules that are similar in morphology to those seen in *M. truncatula* mutants *Mtpt4* and *Mt-ha1* (fig. 3.4.3) (Javot *et al.*, 2007; Wang *et al.*, 2014). *RLCK2* may have a nodulation phenotype, however due to disagreeing allelic phenotypes it is not clear if lack of *RLCK2* results in an increased (*rlck2-1*), or decreased (*rlck2-2*), nodule number compared to WT (fig. 3.3.2.1). On the other hand, due to the relative positions of the premature stop codons, it is more likely that *rlck2-1* is the stronger allele and thus it could be argued has the more reliable phenotype. The EMS mutagenesis method used to generate the *rlck2-2* allele is likely to have created mutations at many sites in the genome; one of these alternate mutations could be responsible for the nodulation phenotype. Complementation, backcrossing the two alleles or a third allele will be needed to confirm which the correct *rlck2* nodulation phenotype is.

RLCK1/SPK1 is required for correct mycorrhizal development as well as nodulation in *M. truncatula*

RLCK1/SPK1 has shown by Damiani *et al.* (2012) and Andrio *et al.* (2013) to be expressed during nodulation and upon ROS application. Andrio *et al.* (2013) showed via RNAi that a reduction of *RLCK1/SPK1* expression leads to a reduction in nodule number. Using a stable *Tnt1* insertion mutant, this study has confirmed that the absence of *RLCK1/SPK1* does lead to a reduction in the number of nodules. Additionally, the *rlck1/spk1* mutant had an increased number of infection events (fig. 3.3.1.1), with infection threads being misshaped compared to WT (R108) (fig. 3.3.1.2). This study also found that in mature nodules of the *rlck1/spk1* mutant, the infection threads that would normally be advancing only into the infection zone (Zone II) were advancing into the meristematic zone (Zone I) (fig. 3.3.2.2). There is a delicate balance between carbon provision and N acquisition which the plant controls by regulating the number of successful infections leading to nodule organogenesis. The fewer nodules on the *rlck1/spk1* plants may be a consequence of a feedback loop driven by the hyper-infection of root hairs and within Zone II of the nodule.

In addition to the nodulation phenotypes demonstrated, *rlck1/spk1* mutants had a significantly reduced level of colonisation by the AMF *R. irregularis* compared to WT (R108) (fig. 3.4.1). The arbuscules on *rlck1/spk1* were smaller and were similar in morphology to *Mtpt4* and *Mt-ha1* (Javot *et al.*, 2007; Wang *et al.*, 2014), suggesting that they may be senescing early. A time course checking the progression of the AMF through the root and the speed of the advancement of the mycorrhizal symbiosis is needed to determine if the arbuscules are stunted in growth or are prematurely senescing. This could be achieved by checking plant roots at earlier time points for the number of the arbuscules at each stage of development. If the mycorrhiza do not form mature arbuscules then this would suggest they are stunted before reaching maturity, however if mature arbuscules are seen at these early time points then this would suggest the arbuscules are collapsed and prematurely senescing.

RLCK1 and RLCK2 are partially redundant during symbiosis

RLCK1/SPK1 and *RLCK2* have overlapping expression patterns in the root which was visualised using promoter-GUS analysis. *RLCK2* was constitutively expressed in the root and was further upregulated upon symbiotic interactions (figs. 3.5.1.3, 3.5.1.4, and 3.5.2.3). Promoter-GUS analysis and MtGEA data shows that *RLCK1/SPK1* expression is more symbiosis specific than *RLCK2* with expression being highly upregulated upon

interaction with a symbiont or NF application (figs. 3.5.1.1, 3.5.1.2, and 3.5.2.1). *rlck1/spk1* and *rlck2* single mutants had very similar mycorrhizal phenotypes (fig. 3.4.1 to fig. 3.4.3). Knocking down *RLCK1/SPK1* and *RLCK2* by RNAi in *M. truncatula* roots results in a large reduction in the nodule number compared to the empty vector control (figs. 4.2.2 and 4.3.1).

Despite their high level of homology, orthologues of *RLCK1* and *RLCK2* are present in species across the plant kingdom, including ancient plant lineages such as moss and *Amborella*. Given the similarities of these two genes at both nucleotide and amino acid level, it is possible that *RLCK1* and *RLCK2* have partially redundant or synergistic roles during symbiotic development. In the single mutants, one *RLCK* may be able to partially compensate for the lack of the other. Considering the ubiquitous expression levels of *RLCK2* in the root, *RLCK2* could be required for a more general developmental process and is recruited during symbiosis whilst the expression and role of *RLCK1/SPK1* could be symbiosis specific. However, such a housekeeping role is contradicted by the loss of these genes in the *Brassicaceae*. It is also possible that *RLCK2* is required at the very early stages of symbiont perception, when a response is needed faster than there is time for new protein synthesis. An example of two genes being required partially redundantly whilst having overlapping yet different expression patterns is *ERN1* and *ERN2*, two gene encoding nodulation expressed transcription factors. *ERN1* and *ERN2* can independently activate symbiosis marker gene *ENOD11* (Andriankaja *et al.*, 2007; Cerri *et al.*, 2012) but the *ern1* single mutant is still able to form misshaped infection threads, and nodules which can be complemented by *ERN2* expressed under the *ERN1* promoter (Middleton *et al.*, 2007). Symbiotic gene *DMI3* has been shown to have different roles in cortical cells and epidermal cells when it's expression is driven via tissue specific promoters in a *dmi3* mutant (Rival *et al.*, 2012). It is possible that *RLCK1* and *RLCK2* have tissue specific roles during symbiosis.

Numerous attempts to cross pollinate *rlck1-2* and *rlck2-1* mutants have not produced any seed. It is possible that *RLCK1* and *RLCK2* also play redundant roles in seed development. Related to this, a rice gene belonging to the same subfamily as *RLCK1/2* (*RLCK-XV*) Os06g07070 has been shown to be upregulated in embryo and endosperm development (Gao and Xue, 2011). The *ram2* mycorrhizal mutant produces seeds with a dark seed coat that can be permeated by dyes (Wang *et al.*, 2012), demonstrating a link between the two developmental processes. Examples of mutants that are involved in both developmental and symbiotic processes are *sickle (skl)* an ethylene insensitive mutant named after the sickle shape of the hypocotyl, and *super numeric nodules (sunn)* a long-distance auxin transport mutant of *M. truncatula* that are

both hyper-nodulating and have root architecture phenotypes (Penmetsa and Cook, 1997; Prayitno *et al.*, 2006; van Noorden *et al.*, 2006). A review from Evangelisti *et al.* (2014) highlights the extensive cross-talk that exists between developmental processes and plant-microbe interactions.

Possible roles of *RLCK1/RLCK2* in symbiosis

RLCK1 and *RLCK2* are part of the RLCK-XV subfamily of the receptor-like cytoplasmic kinases. This subfamily does not have representatives in *A. thaliana* but is present in the model legumes *M. truncatula*, *L. japonicus* and *G. max*, as well as many species known to interact with AMF (e.g. rice and tomato). This suggests that this subfamily of RLCKs is required for symbiotic interactions. The RLCK-XV sub-family has not been widely studied. The subfamilies RLCK-V and RLCK-VI that display roles in PAMP and BR signalling, have led to these two subfamilies being relatively well studied. I am now going to discuss three possible roles for RLCKs in symbiotic interactions that are not necessarily exclusive: as part of NF signal transduction, as regulators helping to distinguish pathogen from symbiont, and as regulators of ROS mediated development.

Part of the NF signalling cascade

The PTI signalling pathway through FLS2 and the BR signalling pathway through BRI1 have been well studied. Both of these pathways recognise signalling molecules (flg22 and BR) at the cell surface through binding of the signal with RLK complexes. Both FLS2 and BRI1 associate with BAK1 and the RLCKs BIK1, BSKs, and CDG1 (Veronese *et al.*, 2006; Lu *et al.*, 2010; Zhang *et al.*, 2010a; Kim *et al.*, 2011; Sreeramulu *et al.*, 2013). Recognition of the signalling molecules causes phosphorylation of the RLCKs by the RLKs. The RLCKs then phosphorylate targets such as phosphatase BSU1 or the NADPH oxidase RbohD (Mora-García *et al.*, 2004; Li *et al.*, 2014). There is also some evidence that RLCKs BIK1 and BSKs are involved in the cross-talk between PTI and plant development (Lin *et al.*, 2013; Shi *et al.*, 2013a; Shi *et al.*, 2013b).

Currently it is not known in the CSP how the cell surface localised RLKs, NFP and LYK3, pass on the signal to the other RLK DMI2. It is also not known how the signal travels from the plasma membrane to the nucleus. There is some evidence showing the interaction of a MAP kinase with DMI2 (Chen *et al.*, 2012). MAP kinases, a class of RLCKs, are often involved in signal transduction during defence ultimately leading to gene expression (Nühse *et al.*, 2000; Asai *et al.*, 2002; Suarez-Rodriguez *et al.*, 2007; Zhang *et al.*, 2007). Using the PTI and BR signalling pathways as a guide, possible roles for the

RLCKs studied here could be the transactivation of the RLKs NFP and LYK3, and/or DMI2. Data from Antolín-Llovera *et al.* (2014) shows that *L. japonicus* SYMRK (MtDMI2) is able to interact with LjNFR5 (MtNFP) in *N. benthamiana* when the extracellular malectin-like domain (MLD) is cleaved (SYMRK- Δ MLD). SYMRK- Δ MLD is similar in structure to BAK1, which interacts with BRI1 and FLS2 to form receptor complexes in the BR and flagellin signalling pathways. However, the interaction between SYMRK- Δ MLD and NFR5 is able to occur without a ligand. The SYMRK- Δ MLD protein undergoes rapid endocytosis and degradation but low levels can still be detected *in planta* (Antolín-Llovera *et al.*, 2014). It is possible that the SYMRK- Δ MLD/NFR5 complex *in planta* binds to an RLCK similar to BIK1 or BSK1 which continues the signal transduction.

The proteins required for NF perception and fast responses to NF have a constitutive level of expression in the roots. Other genes, such as *Nodule inception (NIN)* are required for the early stages of symbiosis and are up regulated quickly upon NF perception (Schauser *et al.*, 1999). *RLCK2* has constitutive expression in *M. truncatula* roots and both *RLCK1/SPK1* and *RLCK2* are quickly up-regulated upon NF application. The tagged protein constructs made during this study (Chapter 5) can be used to test *RLCK1/SPK1* and *RLCK2* for interaction with the known CSP components to identify if *RLCK1/SPK1* and/or *RLCK2* could be the RLCKs involved in the signal transduction during symbiosis. The non-symbiotic expression of *RLCK2* is much higher than *RLCK1/SPK1*. This would suggest that if these proteins are involved in any initial signal transduction through the CSP that this would initially depend more on *RLCK2*, while *RLCK1/SPK1* may serve mainly to amplify the signal as the infection progresses. On the other hand, our results suggest that in the absence of *RLCK2*, *RLCK1* may still compensate and vice versa, suggesting that sufficient levels of *RLCK1* are present to support signalling through the CSP. The available transcriptomics data from mutants suggests that inductions of both genes are CCaMK, and therefore CSP, dependent, so successful signalling through the CSP in either single mutant would lead to induction of the remaining RLCK and fulfil most of the signalling role. This model could be tested by monitoring the onset of calcium oscillations (typically 10 minutes from time of NF application) in roots of the *rlck1*, *rlck2* and double knockdown roots and checking for delays in expression of early nodulation genes such as *ENOD11* and *NIN*.

Alternately the RLCKs may act in pathways that occur in parallel to the CSP that also require NF perception and enable the plant to accommodate the symbionts (Murray, 2011). For example, root hair growth/curling that follows rhizobial attachment in response to NF can still occur in *dmi2* and other downstream CSP mutants. Interestingly, root hair growth is associated with ROS production (Foreman *et al.*, 2003).

Differentiating between Pathogen and Symbiosis

Rhizobia and AMF, although symbiotic partners of plants, carry MAMPs that activate PTI such as flagellin and chitin. It has long been under discussion as to how plants are able to distinguish between friend and foe (Ausubel and Bisseling, 1999; Parniske, 2000; Kogel *et al.*, 2006; Paszkowski, 2006; Rey and Schornack, 2013). In both PTI and symbiosis there is an oxidative burst upon PAMP recognition (Alvarez *et al.*, 1998; Ramu *et al.*, 2002). In PTI the levels of ROS species, such as $\bullet\text{O}_2^-$ and H_2O_2 , stay high whereas in symbiosis there is a gradual decline of ROS levels (Shaw and Long, 2003). Studies have shown that PTI activated roots then treated with NF also show a decrease in ROS levels (Shaw and Long, 2003). ROS in PTI leads to the strengthening of cell walls through cross-linking and plays a central role in programmed cell death (Levine *et al.*, 1994). Contrastingly, ROS production induced by NF has been shown to be relatively short lived (Ramu *et al.*, 2002). ROS can also be found to be increased 12 hours after NF or rhizobial treatment of *Medicago* roots (Shaw and Long, 2003), which is likely to be due to the induction of developmental processes. Interestingly, *Medicago* roots inoculated with a mutant rhizobia strain that is unable to produce NFs, the ROS response of the plant is the same as that seen in PTI (Bueno *et al.*, 2001).

The defence pathways that are triggered by the MAMPs carried by rhizobia and AMF must be suppressed before the plant is able to accommodate a symbiotic partner. It takes 20 to 30 minutes after NF application until ROS levels in the root begin to decrease, suggesting that new proteins need to be synthesised first (Shaw and Long, 2003). RLCKs like BIK1 and the BSKs have been shown to act as cross-talk mediators between PTI and BR signalling (Lin *et al.*, 2013; Shi *et al.*, 2013a; Shi *et al.*, 2013b). It is possible that RLCKs play a similar function between PTI and symbiosis signalling. Andrio *et al.* (2013) showed that *RLCK1/SPK1* is upregulated upon H_2O_2 treatment and is expressed in nodule zones that also contain high levels of H_2O_2 . It is possible that *RLCK1/SPK1* and *RLCK2* play a role in the differentiation between pathogen and symbiont, possibly regulating ROS levels to enable infection by rhizobia and AMF. To test this hypothesis the response of *RLCK2* to ROS application should be investigated; it would be interesting to see if *RLCK2* responds similarly to *RLCK1/SPK1*. However, *RLCK2* was not identified by Andrio *et al.* (2013) in their microarray experiments.

RNAi knockdown *rlck1/rlck2* mutants produced almost no nodules (Chapter 4). This may be due to higher than normal ROS levels in the mutant than WT. ROS levels should be checked in the single mutants and in the double knockdown roots, this could be achieved through nitro blue tetrazolium (NBT) staining for $\bullet\text{O}_2^-$ or a ROS sensitive dye

such as HyPer probe for H₂O₂ could be used to track dynamic changes during infection (Belousov *et al.*, 2006).

The regulation of genes known to be induced during PTI should be checked in the *rlck1* and *rlck2* mutants and the *rlck1/rlck2* knockdown roots after treatment with a symbiont such as AMF and a pathogen such as *P. infestans*. Good candidates for this analysis are *PR4* (Medtr1g080800) and *PR5* (Medtr5g010635) which are pathogen-responsive genes which are repressed by NF and during infection by rhizobia, are initially induced and then repressed (Murray lab unpublished results).

Regulation of developmental processes by ROS

Data by Andrio *et al.* (2013) showing that *RLCK1/SPK1* is upregulated within one hour of H₂O₂ application to the root, may suggest a role for *RLCK1/SPK1* in the regulation of ROS during symbiosis promoting the correct development of symbiotic structures. Promoter-GUS analysis showed that *RLCK1/SPK1* expression was correlated with rhizobial entry through the infection thread, in nodule primordia and in Zones I and II of the nodule. *pRLCK2:GUS* expression shows that *RLCK2* is higher in arbusculated cortical cells. All of the regions that promoter-GUS expression was seen for both *RLCK1/SPK1* and *RLCK2* have been previously identified as being rich in ROS. Misregulation of ROS, which is finely controlled in many plant processes, could cause disruption to the development of plant-microbe symbioses.

During symbiosis the plant undergoes many different developmental processes which require changes in hormone and ROS levels. During rhizobial symbiosis root hair cells change the direction of growth to grow towards the source of NF (Esseling *et al.*, 2003). ROS production is required for apical growth of root hairs (Foreman *et al.*, 2003). It is believed that ROS generation drives a calcium influx into the tip of the root hair creating a calcium gradient (Foreman *et al.*, 2003). This calcium gradient is thought to give direction to tip growth by regulating exocytosis at the plasma membrane and actin reorganisation (Rato *et al.*, 2004; He *et al.*, 2006). Several ROS regulatory proteins such as NADPH oxidase, ROP GTPases and RopGEFs have been identified to be essential for correct root hair tip growth (Foreman *et al.*, 2003; Craddock *et al.*, 2012). This tip growth machinery is thought to be altered to enable the typical curling of the root hair around the rhizobia, which is supported by recent data from Shailles (2014) that showed a RopGAP mutants (*gap1*) with a decreased number of ITs, which were thicker than wildtype and sometimes ramified, and had abnormal root hair curling. The formation of the IT in the root hair during rhizobial infection could be thought of as an internally directed version of

polar tip growth (Oldroyd *et al.*, 2011). ROS has also been shown to be present in ITs (Santos *et al.*, 2001; Ramu *et al.*, 2002; Nanda *et al.*, 2010). ROS in this case could be acting in two roles. Firstly ROS is required for the cross-linking of cell wall material (Gapper and Dolan, 2006) and could make the IT structure more rigid, creating a clear route for the rhizobia. Secondly, it could act as another layer of defence whilst letting the rhizobia into the root; rhizobia that are mutant in catalase and superoxide dismutase genes, that convert ROS into H₂O and O₂, are unable to successfully traverse the infection threads (Santos *et al.*, 2000; Jamet *et al.*, 2003). Interestingly, the overexpression of the rhizobial catalase gene *KatB* also leads to compromised infection (Jamet *et al.*, 2007), which could be due to a lower level of ROS in the IT suggesting that a balance of ROS is needed for symbiotic infection. In the *rlck1/spk1* mutant the infection threads are misshaped; it is possible that this could be caused by lower levels of ROS present in the IT.

PIT and PPA formation are very similar developmental processes and the progression of the AMF through the root surrounded by a plant derived tube is much like the passage of rhizobia through ITs. It is possible that the regulation of ROS during mycorrhizal colonisation is as crucial for this process as for the correct development of the IT (Balestrini and Bonfante, 2014; Rich *et al.*, 2014). H₂O₂ has also been shown to accumulate in arbuscule cells (Fester and Hause, 2005). Again ROS could be involved in the hardening of cell wall material in the matrix surrounding the arbuscule, preventing the AMF from diverting from the plant determined route into the cell. Alternatively, ROS accumulation, and especially ROS transfer into the arbuscule, correlates with arbuscule senescence (Fester and Hause, 2005). In *rlck1/spk1* and *rlck2* mutants the arbuscules appear to be senescing early.

During rhizobial colonisation cortical cells must switch from their differentiated state and restart cell division to create the nodule, and in indeterminate nodules a meristem must be created to drive the growth of the nodule. ROS production has been seen in cortical cells after inoculation with *S. meliloti* (Peleg-Grossman *et al.*, 2007; Nanda *et al.*, 2010). ROS may be acting to strengthen the new cell walls after cell division. Alternatively, ROS gradients are seen in growing root tips with ROS levels being the highest at root meristems (Tsukagoshi *et al.*, 2010; Wells *et al.*, 2010); it is possible that there is a ROS gradient from the nodule meristem, as in root meristems, which determines the differentiation of the nodule cells. ROS have been found in Zone II, or infection zone, of the nodule (Andrio *et al.*, 2013). *RLCK1/SPK1* promoter-GUS analysis shows *RLCK1/SPK1* expression in Zone I and II of the nodule and could be contributing to the regulation of ROS in these zones.

The phenotypes seen in the *rlck1* mutant - early senescent arbuscules, a large number of infection events and the progress of ITs into Zone I of the nodule - suggest that in the absence of *RLCK1/SPK1* the plant is progressing through the symbiosis faster than it would in WT. It is possible that this faster progression is due to misregulation of ROS in these developmental processes.

Future Work

This study has provided some insight into the expression and requirement of *RLCK1/SPK1* and *RLCK2* during rhizobial and mycorrhizal symbioses. It has also created several expression constructs that can be used to identify interaction partners of *RLCK1/SPK1* and *RLCK2* in yeast and *in planta*. As the RNAi knock down *rlck1/rlck2* roots had a significant reduction in the number of nodules, the effect of the double knockdown should be investigated with AMF to help determine the role of these genes during symbiosis. Given that *RLCK1/SPK1* expression is induced by H₂O₂, the expression of *RLCK2* in response to ROS should be investigated in order to identify if this is a shared response of the two RLCKs. Also the levels of ROS in the *rlck* single mutants and the double knockdown roots should be investigated both with and without symbiotic interactions to see if they are part of the ROS regulatory machinery. Localisation of the *RLCK1/SPK1* and *RLCK2* proteins via fluorescent fusions would also help to define their role during symbiosis. These constructs can also be used to visualise co-localisation of the RLCK proteins with potential interaction partners. The recent suggestion from protein prediction software of a lectin-like domain and a putative calmodulin binding domain at the N-terminal end of the proteins would also be worthy of further investigation; this could be achieved via a carbohydrate chip to determine possible ligands, and an assay to confirm the calmodulin binding ability of the RLCKs with and without the presence of calcium – the existing expression constructs for the RLCKs could be used for this.

Conclusion

SCOOBY is a novel mycorrhizal mutant phenotype in *M. truncatula* with stunted arbuscule growth; further investigation could provide additional insight into the plant-mycorrhizal symbiosis. *RLCK1/SPK1* and *RLCK2* have a high nucleotide and amino acid similarity, and possibly have partially redundant or synergistic functions. Severe symbiotic defects are not evident in the single mutants and the full effect of *RLCK1/SPK1* and *RLCK2* mutations on symbiotic processes within the plant may only be evident in the absence of both proteins. This is supported by the extremely low nodule number on the double knockdown RNAi roots whilst the single mutants can still make nitrogen fixing nodules. They may be acting together, or redundantly, to control ROS during NF signalling,

potential PTI responses or symbiotic developmental processes such as nodule, IT or arbuscule formation.

Appendix I

Primers

Primer Number	Sequence	Description
1	ATGGGATCTTCCTTGAGTTG	<i>RLCK1</i> forward start codon
2	CACCATGGGATCTTCCTTGAGTTG	<i>RLCK1</i> forward with TOPO directional overhang (bold)
3	TTAGCCAATTTTCTTGTAAGG	<i>RLCK1</i> reverse with stop codon
4	ATGCCCTTGAAATGTTTATGTTG	<i>RLCK2</i> forward start codon
5	CACCATGCCCTTGAAATGTTTATGTTG	<i>RLCK2</i> forward with TOPO directional overhang (bold)
6	TCATCTCATTTCGCGCCTATC	<i>RLCK2</i> reverse with stop codon
7	GGGACAAGTTTGTACAAAAAAGCAGGCTTCGTGGAGTGAGTTGGCAAGC	<i>RLCK2</i> promoter forwards with attB recombination site (bold)
8	GGGACCACCTTTGTACAAGAAAGCTGGGTCATTTCTTTTGTGATAGAATCTCTAACTAAC	<i>RLCK2</i> promoter reverse with attB recombination site (bold)
9	TCCTTGTTGGATTGGTAGCC	<i>Tnt1</i> Forward
10	CAGTGAACGAGCAGAACCTGTG	<i>Tnt1</i> Reverse
11	ATGCCTTTTGGTGAATGTGGGG	<i>RLCK3</i> forward start condon
12	TCAGTTAGAGCTAGATGTTG	<i>RLCK3</i> reverse with stop codon
13	GGGACAAGTTTGTACAAAAAAGCAGGCTTCATGCCCTTGAAATGTTTATGTTG	<i>RLCK2</i> CDS with pDONR207 overhang (bold)
14	GGGACAAGTTTGTACAAAAAAGCAGGCTTCATGGGATCTTCCTTGAGTTGT	<i>RLCK1</i> CDS with pDONR207 overhang (bold)
15	AAGTGACAATGATAGGCGCAATGGTGAGCAAGGGCGAG	<i>RLCK2</i> CDS 3' with mCherry overhang (bold)
16	CTCGCCCTTGCTCACCATTGCGCCTATCATTGTCACCTT	mCherry 5' complementary with <i>RLCK2</i> 3' complementary overhang (bold)
17	GATGAAAGATCCTTACAAGAAAATTGGATGGTGAGCAAGGGCGAG	<i>RLCK1</i> CDS 3' with mCherry overhang (bold)
18	CTCGCCCTTGCTCACCATTCCAATTTCTTGTAAGGATCTTTCATC	mCherry 5' complementary with <i>RLCK1</i> 3' complementary overhang (bold)

Table A1. List of PCR primers for cloning or genotyping

Primer Number	Sequence	Description
19	CTTTGCTTGGTGCTGTTTAGATGG	<i>EF1 α</i> forward qPCR
20	ATTCCAAAGGCGGCTGCATA	<i>EF1 α</i> reverse qPCR
21	ACTGGCACTTGATCAACCTAGTGATG	<i>RLCK1</i> forwards qPCR
22	TTAGCCAATTTTCTTGTAAGGAT	<i>RLCK1</i> reverse qPCR
23	GTGGTGAATGGCTTAAGGA	<i>RLCK2</i> forward qPCR
24	TCATTTTGCGCCTATCATTG	<i>RLCK2</i> reverse qPCR
25	GCCGAAAACAGCTAGAAGA	<i>Ubiquitin</i> forward qPCR
26	GGAGACGGAGAACAAGGTGA	<i>Ubiquitin</i> reverse qPCR
27	GCTTTGCCACCTGTTGAAGT	<i>Tip41</i> forwards qPCR
28	AGCACCGCTTCCACAATAAG	<i>Tip41</i> reverse qPCR

Table A2. List of primers for qPCR

Primer Number	Sequence	Description
29	GTA AACGACGGCCAG	M13 forward
30	CAGGAAACAGCTATGAC	M13 reverse
31	TCGCGTTAACGCTAGCATGGATCTC	pDONR207 forward flanking insert region
32	GTAACACATCAGAGATTTTGAGACA C	pDONR207 reverse flanking insert region
33	GGAGTGAGTTGGGCAAGCTA	PromoterRLCK2 forward sequencing primer 1
34	AAGGGAATGTGGTCGTTCAAG	PromoterRLCK2 forward sequencing primer 2
35	TGAATACAACACTACAACAGTACAAAA GG	PromoterRLCK2 forward sequencing primer 3
36	TTAGGCCAAAAGCCCTCATT	PromoterRLCK2 forward sequencing primer 4
37	TTGTTAATTATTGTGTCACCGTCT	PromoterRLCK2 forward sequencing primer 5
38	TCATGCACCCATTAGATAGCA	PromoterRLCK2 reverse sequencing primer 1
39	CCGGAGCAAACATGCTCTTA	PromoterRLCK2 reverse sequencing primer 2
40	CGTTCTGAATTCAAGGCGTTA	PromoterRLCK2 reverse sequencing primer 3
41	CCATCAACAAAAGTTGATAGAGGTT	PromoterRLCK2 reverse sequencing primer 4
42	TGGAGGTGAGTGTAGAGTTGGA	PromoterRLCK2 reverse sequencing primer 5
43	TTGACCCTTATTTTCTCTCTCCTC	PromoterRLCK2 reverse sequencing primer 6
44	CATAACTCAGCACACCAGAG	pK7GW WG2D(II)R hairpin intron

Primer Number	Sequence	Description
45	TTCCCTTATCTGGGAACACTCAC	pK7GW WG2D(II)R T35S reverse
46	CGTTGTGGCTGTTGTAGTTGT	eGFP reverse
47	ACAAC TACAACAGCCACAACG	eGFP forwards
48	GTGAGTAGTTCCCAGATAAGGGAA	T35S forwards
49	AGACCAGAGTGTCGTGCTCC	35S (short) Promoter reverse
50	TCGTTCAAACATTTGGCAAT	TNOS forwards
51	GAGAAGCGATATGAACAAGAATTG	LjUB1 reverse
52	CCCGCCAATATATCCTGTC	Golden Gate 3
53	GCGGACGTTTTTAATGTA CTG	Golden Gate 4
54	ACCAGCAGGTGTAAGCCATC	TILLING 7569 forwards
55	TTAAGCCATTCCACCACCTC	TILLING 7569 reverse
56	TGCTATGTGGGGTAAGGTTTC	TILLING 7925 forwards
57	TTTTCTTCATCATGTCCCTTATTG	TILLING 7925 reverse
58	CAATTGCTAAACCGAAATCG	pUB-GW-GFP upstream of insert forward
59	TGGTGATGATCCGGTACCTAGGC	pUB-GW-GFP downstream of insert reverse
60	CGGTCTGGGTGCCCTCGTAG	mCherry internal reverse
61	AGACCACCTACAAGGCCAAGAAGC	mCherry internal forward

Table A3. List of sequencing primers

RNAi Plasmid Maps

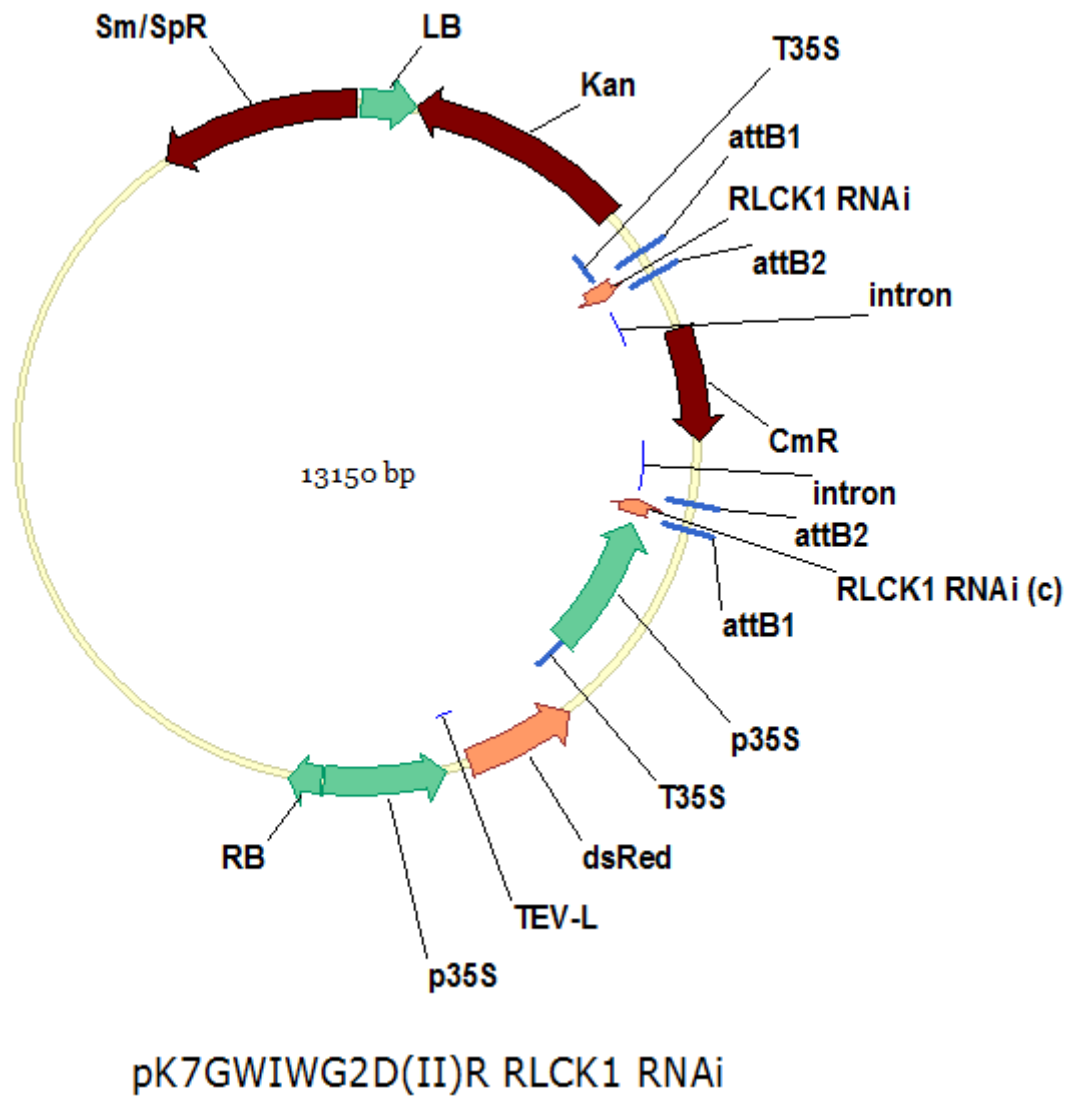
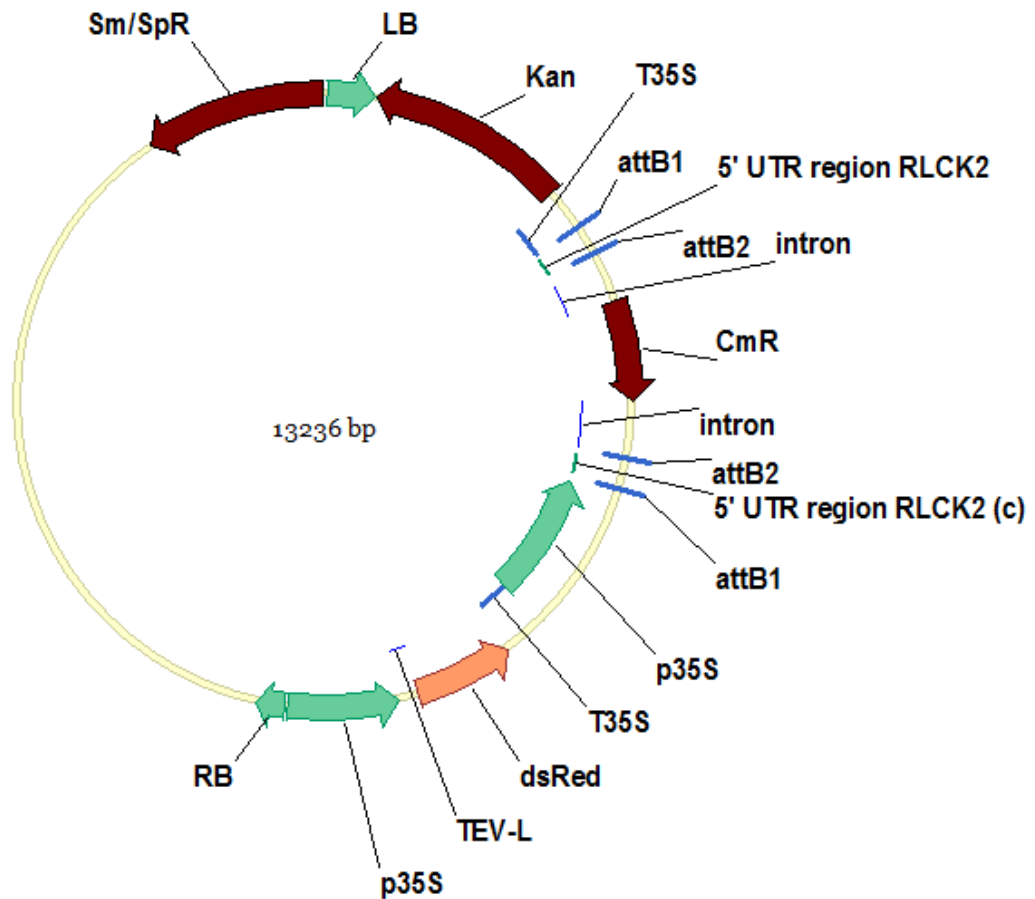


Figure A1. pK7GW|WG2D(II)R RLCK1 RNAi – RNAi vector designed on *RLCK1*.

The vector map for RNAi Construct 1 designed on a 99bp region of *RLCK1*. The vector was made by TOPO® and Gateway® cloning. Destination vector modified from pK7GW|WG2D(II).



pK7GWIWG2D(II)R RLCK2 RNAi

Figure A2. pK7GW|WG2D(II)R RLCK2 RNAi – RNAi vector designed on the 5' UTR region of *RLCK2*.

The vector map for RNAi Construct 2 designed on the 5' UTR region of *RLCK2*. The vector was made by TOPO® and Gateway® cloning. Destination vector modified from pK7GW|WG2D(II).

Golden Gate constructs

ENSA ID	ENSA Standard name
EC67001	pL0M-SC1-MtRLCK1-67001
EC67002	pL0M-SC1-MtRLCK2-67002
EC67003	pL0M-SC1-MtNFP-67003
EC67004	pL0M-SC1-MtLYK3-67004
EC67005	pL0M-SC1-MtHMGR-67005
EC67006	pL0M-SC1-MtDMI2-67006
EC67030	pL0M-C-MtRLCK1-67030
EC67031	pL0M-C-MtRLCK2-67031
EC67032	pL0M-PU-pMtRLCK1-67032
EC67033	pL0M-PU-pMtRLCK2-67033

Table A4. List of Level 0 Golden gate modules

ENSA ID	ENSA Standard name	Backbone
EC67007	pL1M-R1-p35S-MtRLCK1-3xMyc-T35S-67007	EC47802 pL1V-R1
EC67008	pL1M-R1-p35S-MtRLCK2-3xMyc-T35S-67008	EC47802 pL1V-R1
EC67009	pL1M-R2-pLjUBI1-MtNFP-eGFP-tNOS-67009	EC47811 pL1V-R2
EC67010	pL1M-R2-pLjUBI1-MtLYK3-eGFP-tNOS-67010	EC47811 pL1V-R2
EC67011	pL1M-R2-pLjUBI1-MtHMGR-eGFP-tNOS-67011	EC47811 pL1V-R2
EC67012	pL1M-R2-pLjUBI1-MtDMI2-eGFP-tNOS-67012	EC47811 pL1V-R2
EC67013	pL1M-R2-pLjUBI1-RLCK2-eGFP-tNOS-67013	EC47811 pL1V-R2
EC67034	pL1M-R1-p35S-3xMyc-MtRLCK1-T35S-67034	EC47802 pL1V-R1
EC67035	pL1M-R1-p35S-3xMyc-MtRLCK2-T35S-67035	EC47802 pL1V-R1
EC67036	pL1M-R2-pLjUBI1-eGFP-RLCK2-tNOS-67036	EC47811 pL1V-R2
EC67037	pL1M-R2-pLjUBI1-eGFP-RLCK1-tNOS-67037	EC47811 pL1V-R2

Table A5. List of Level 1 Golden Gate modules

ENSA ID	ENSA Standard name	Backbone vector
EC67014	pL2V-MtRLCK1-3xMyc-MtNFP-eGFP-67014	EC50505 pL2V-1
EC67015	pL2V-MtRLCK1-3xMyc-MtLYK3-eGFP-67015	EC50505 pL2V-1
EC67016	pL2V-MtRLCK1-3xMyc-MtHMGR-eGFP-67016	EC50505 pL2V-1
EC67017	pL2V-MtRLCK1-3xMyc-MtDMI2-eGFP-67017	EC50505 pL2V-1
EC67018	pL2V-MtRLCK1-3xMyc-MtRLCK2-eGFP-67018	EC50505 pL2V-1
EC67019	pL2V-MtRLCK2-3xMyc-MtNFP-eGFP-67019	EC50505 pL2V-1
EC67020	pL2V-MtRLCK2-3xMyc-MtLYK3-eGFP-67020	EC50505 pL2V-1
EC67021	pL2V-MtRLCK2-3xMyc-MtHMGR-eGFP-67021	EC50505 pL2V-1
EC67022	pL2V-MtRLCK2-3xMyc-MtDMI2-eGFP-67022	EC50505 pL2V-1
EC67038	pL2V-3xMyc-MtRLCK1-MtNFP-eGFP-67038	EC50505 pL2V-1
EC67039	pL2V-3xMyc-MtRLCK1-MtLYK3-eGFP-67039	EC50505 pL2V-1
EC67040	pL2V-3xMyc-MtRLCK1-MtHMGR-eGFP-67040	EC50505 pL2V-1
EC67041	pL2V-3xMyc-MtRLCK1-MtDMI2-eGFP-67041	EC50505 pL2V-1
EC67042	pL2V-3xMyc-MtRLCK1-MtRLCK2-eGFP-67042	EC50505 pL2V-1
EC67043	pL2V-3xMyc-MtRLCK1-eGFP-MtRLCK2-67043	EC50505 pL2V-1
EC67044	pL2V-3xMyc-MtRLCK2-MtNFP-eGFP-67044	EC50505 pL2V-1
EC67045	pL2V-3xMyc-MtRLCK2-MtLYK3-eGFP-67045	EC50505 pL2V-1
EC67046	pL2V-3xMyc-MtRLCK2-MtHMGR-eGFP-67046	EC50505 pL2V-1
EC67047	pL2V-3xMyc-MtRLCK2-MtDMI2-eGFP-67047	EC50505 pL2V-1

Table A6. List of Level 2 Golden Gate constructs

Golden Gate Plasmid Maps

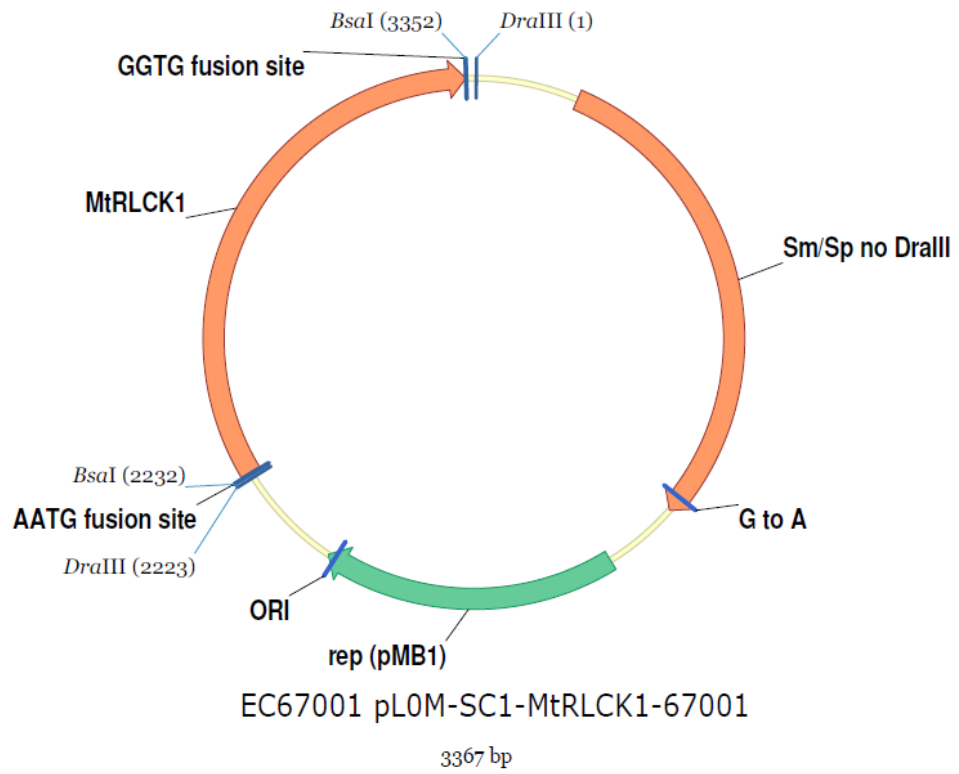


Figure A3. EC67001 plasmid map

Level 0 Golden Gate SC1 construct. Contains *RLCK1* CDS with no stop codon.

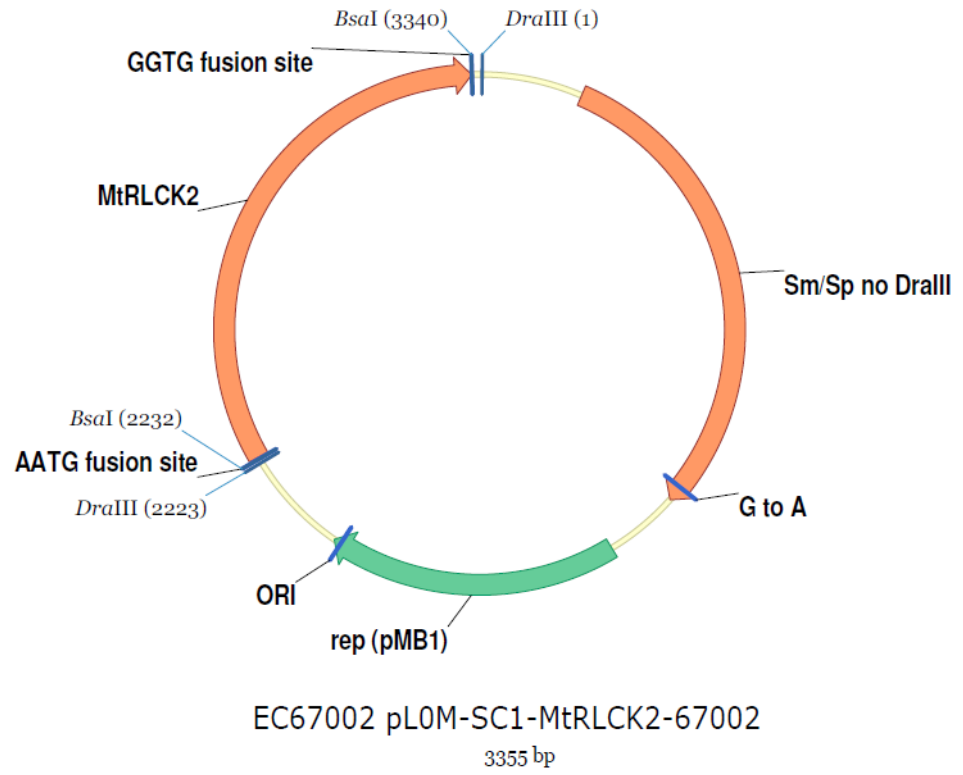


Figure A4. EC67002 plasmid map

Level 0 Golden Gate SC1 construct. Contains *RLCK2* CDS with no stop codon.

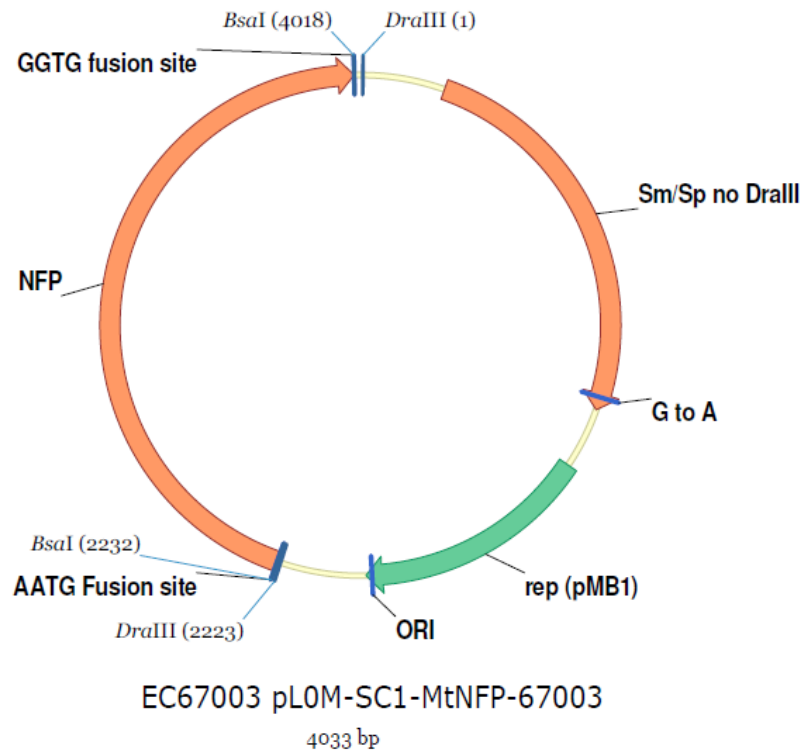


Figure A5. EC67003 plasmid map

Level 0 Golden Gate SC1 construct. Contains *MtNFP* CDS with no stop codon.

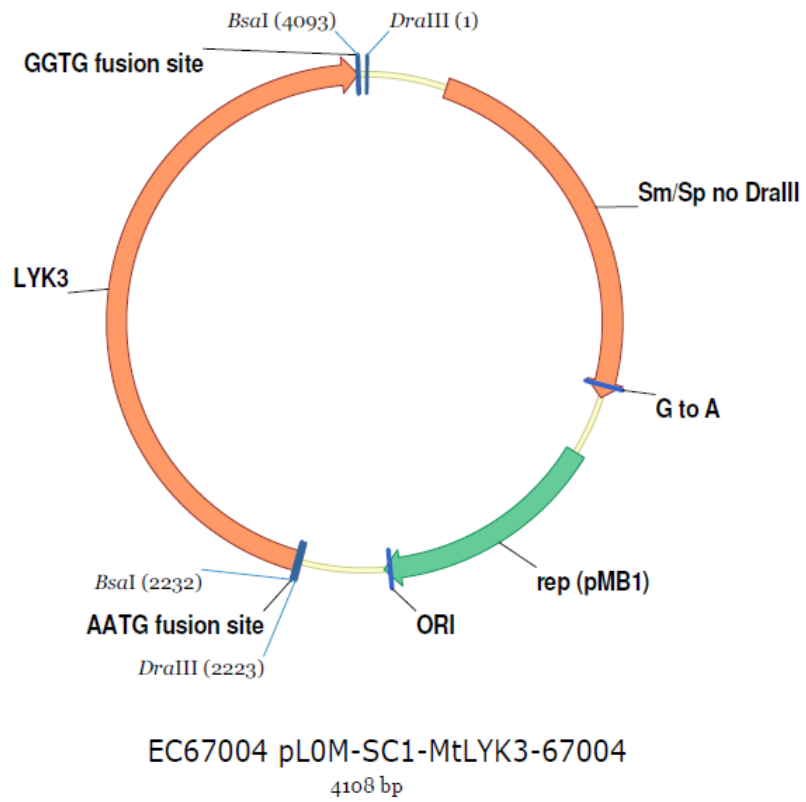


Figure A6. EC67004 plasmid map

Level 0 Golden Gate SC1 construct. Contains *MtLYK3* CDS with no stop codon.

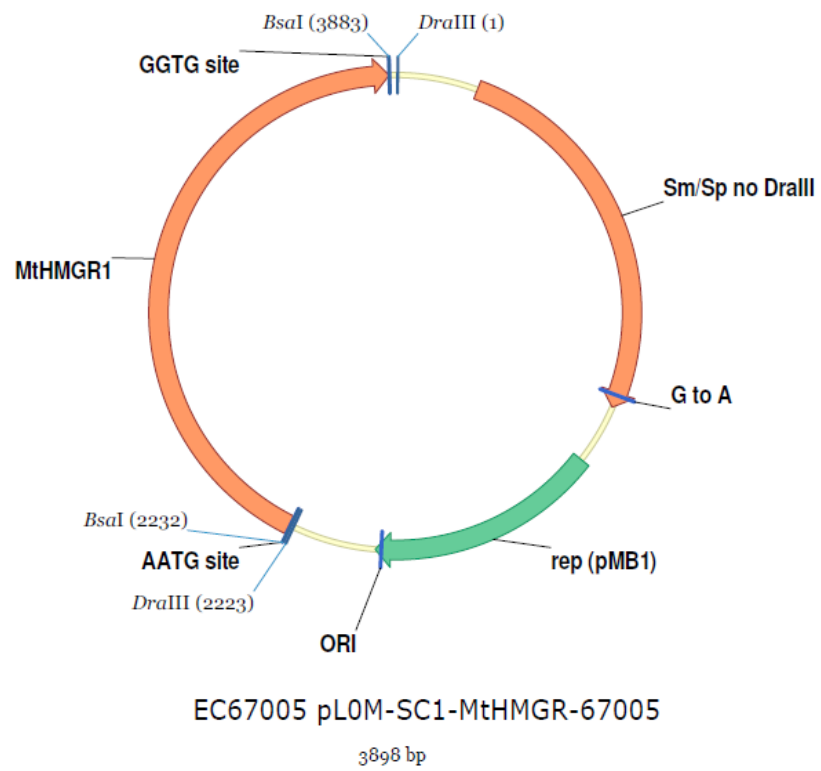


Figure A7. EC67005 plasmid map

Level 0 Golden Gate SC1 construct. Contains *MtHMGR1* CDS with no stop codon.

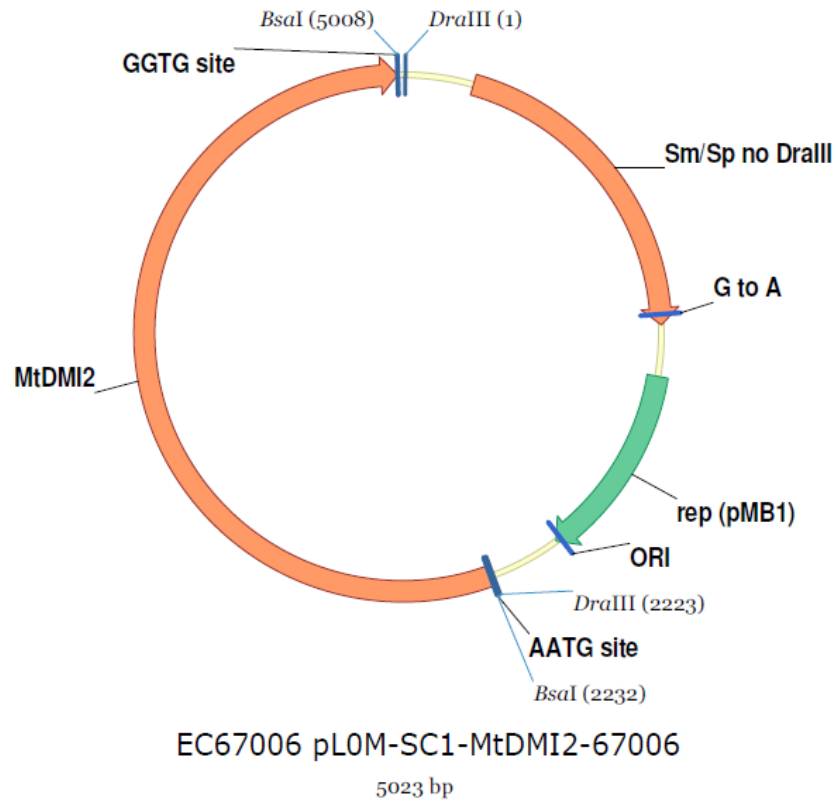
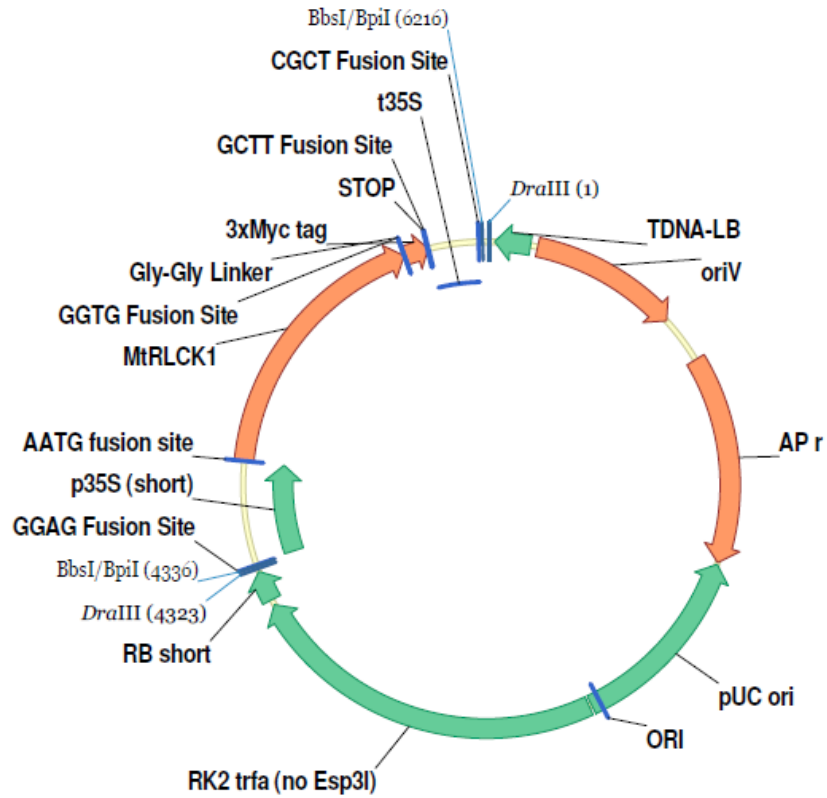


Figure A8. EC67006 plasmid map

Level 0 Golden Gate SC1 construct. Contains *MtDMI2* CDS with no stop codon.

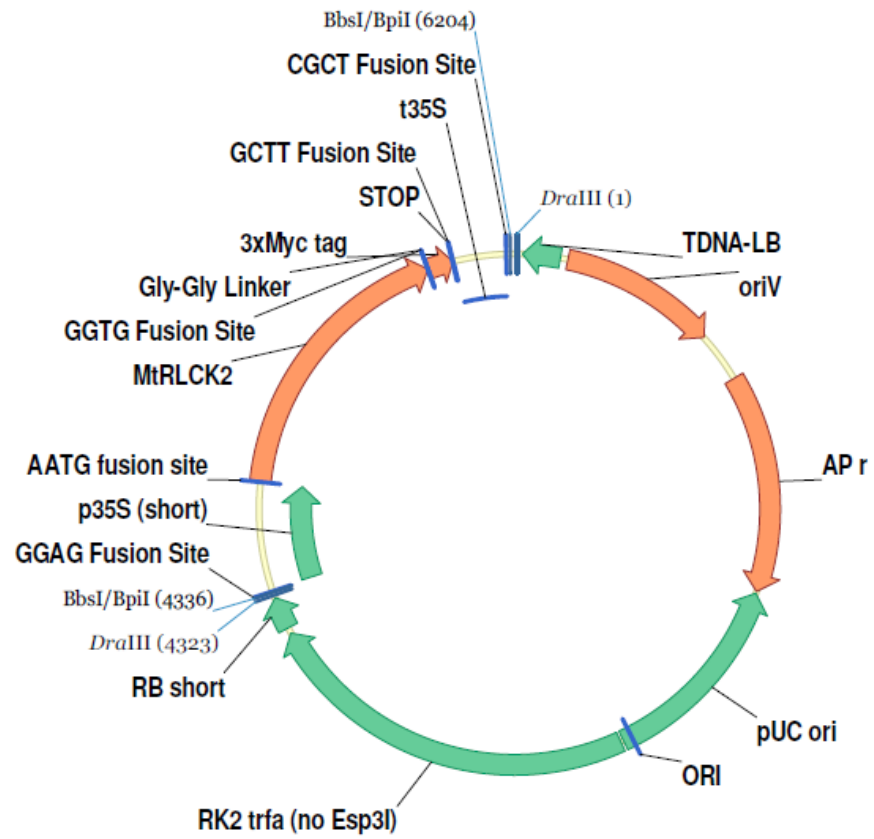


EC67007 pL1M-R1-p35S-MtRLCK1-3xMyc-T35S-67007

6232 bp

Figure A9. EC67007 plasmid map

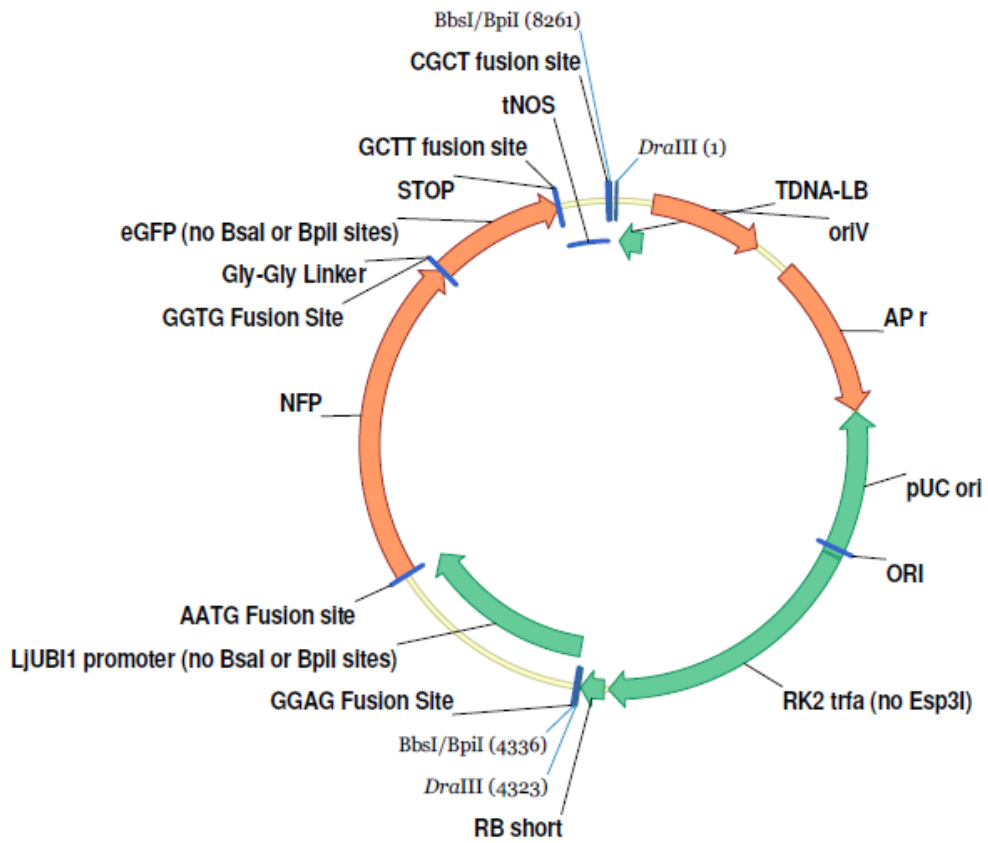
Level 1 module Golden Gate construct. 35S Promoter, *RLCK1* CDS, 3x myc c-terminal tag, 35S terminator. Compatible with position R1 of Golden Gate Level 2 constructs.



EC67008 pL1M-R1-p35S-MtRLCK2-3xMyc-T35S-67008
6220 bp

Figure A10. EC67008 plasmid map

Level 1 module Golden Gate construct. 35S Promoter, *RLCK2* CDS, 3x myc C-terminal tag, 35S terminator. Compatible with position R1 of Golden Gate Level 2 constructs.

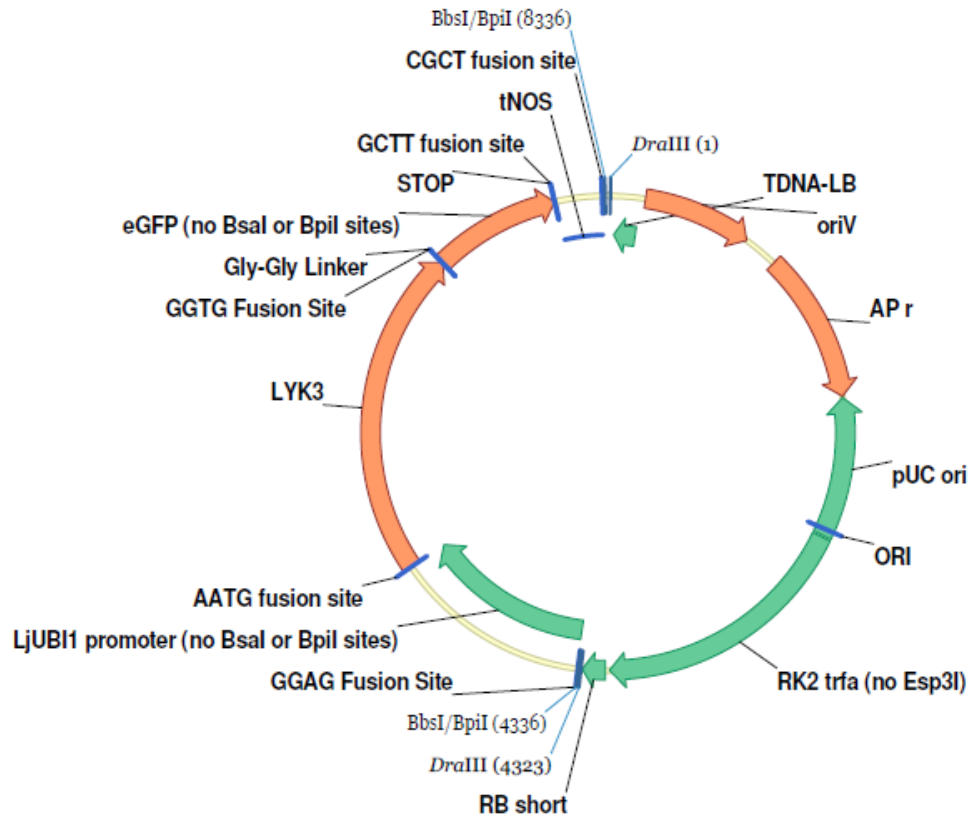


EC67009 pL1M-R2-pLjUBI1-MtNFP-eGFP-tNOS-67009

8277 bp

Figure A11. EC67009 plasmid map

Level 1 module Golden Gate construct. *L. japonicus Ubiquitin* Promoter, *MtNFP* CDS, C-terminal GFP tag, NOS terminator. Compatible with position R2 of Golden Gate Level 2 constructs.



EC67010 pL1M-R2-pLjUBI1-MtLYK3-eGFP-tNOS-67010
8352 bp

Figure A11. EC67009 plasmid map

Level 1 module Golden Gate construct. *L. japonicus Ubiquitin* Promoter, *MtNFP* CDS, C-terminal GFP tag, NOS terminator. Compatible with position R2 of Golden Gate Level 2 constructs.

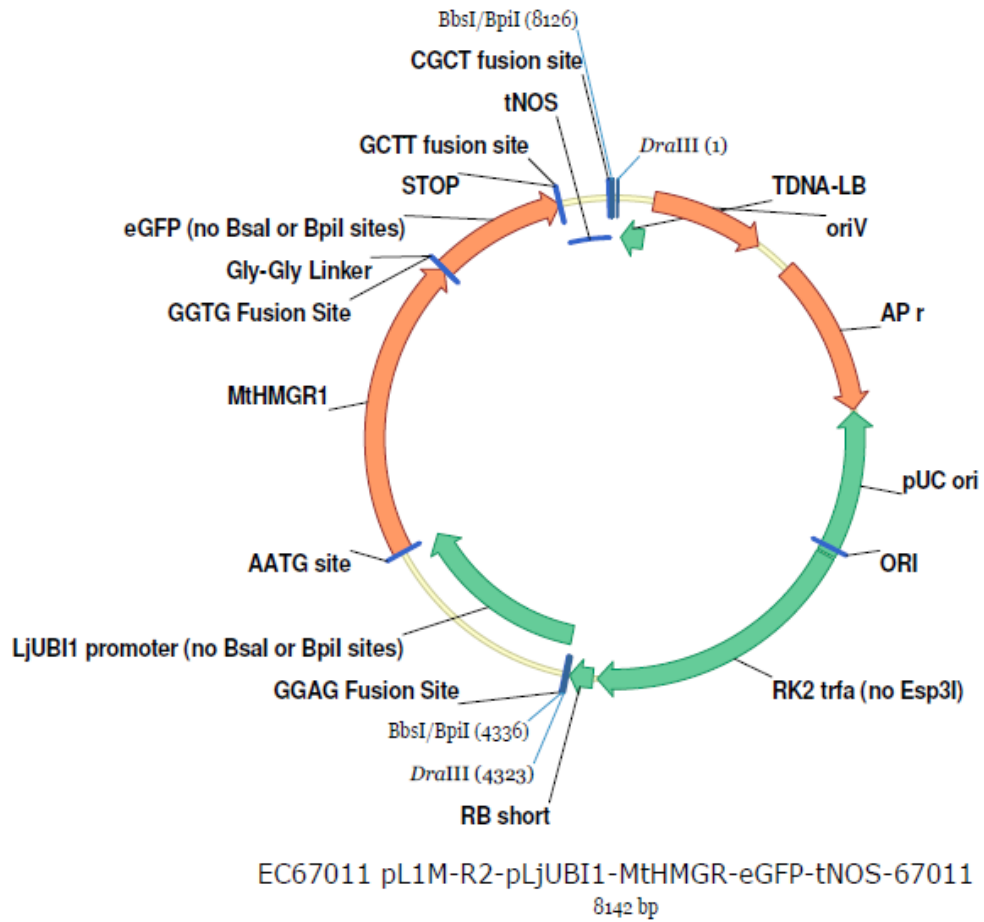


Figure A13. EC67011 plasmid map

Level 1 module Golden Gate construct. *L. japonicus Ubiquitin* Promoter, *MtHMGR1* CDS, C-terminal GFP tag, NOS terminator. Compatible with position R2 of Golden Gate Level 2 constructs.

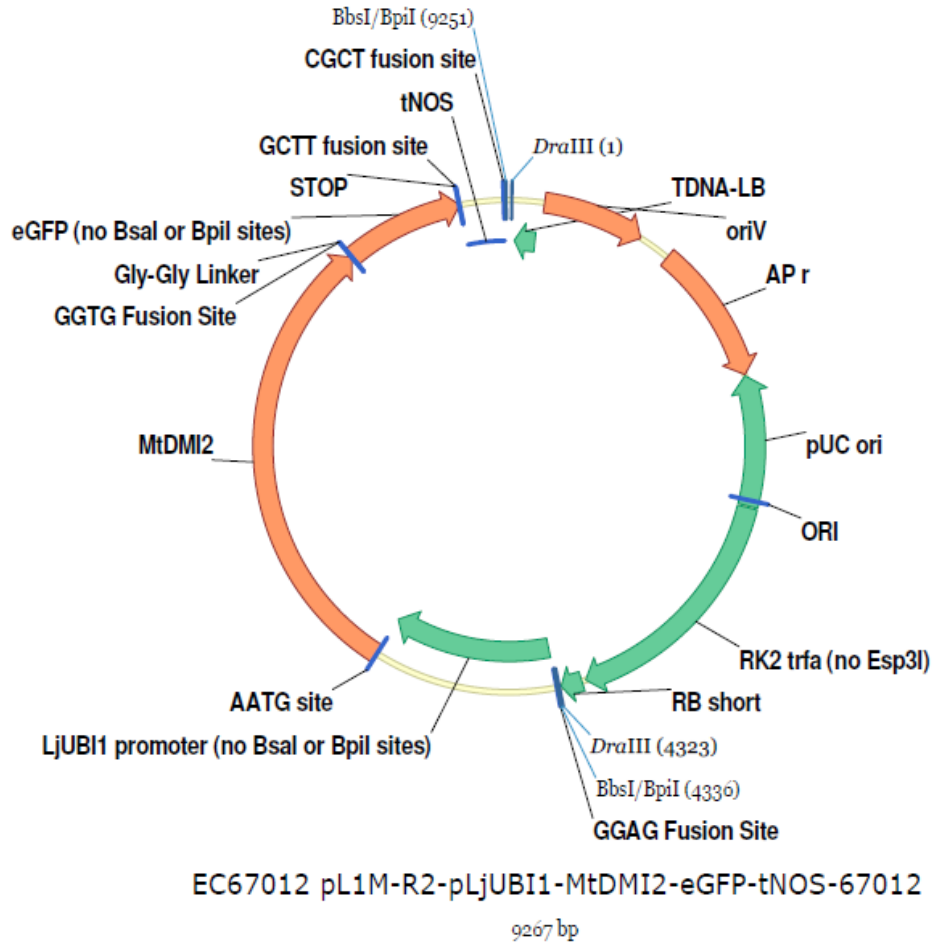


Figure A14. EC67012 plasmid map

Level 1 module Golden Gate construct. *L. japonicus Ubiquitin* Promoter, *MtDMI2* CDS, C-terminal GFP tag, NOS terminator. Compatible with position R2 of Golden Gate Level 2 constructs.

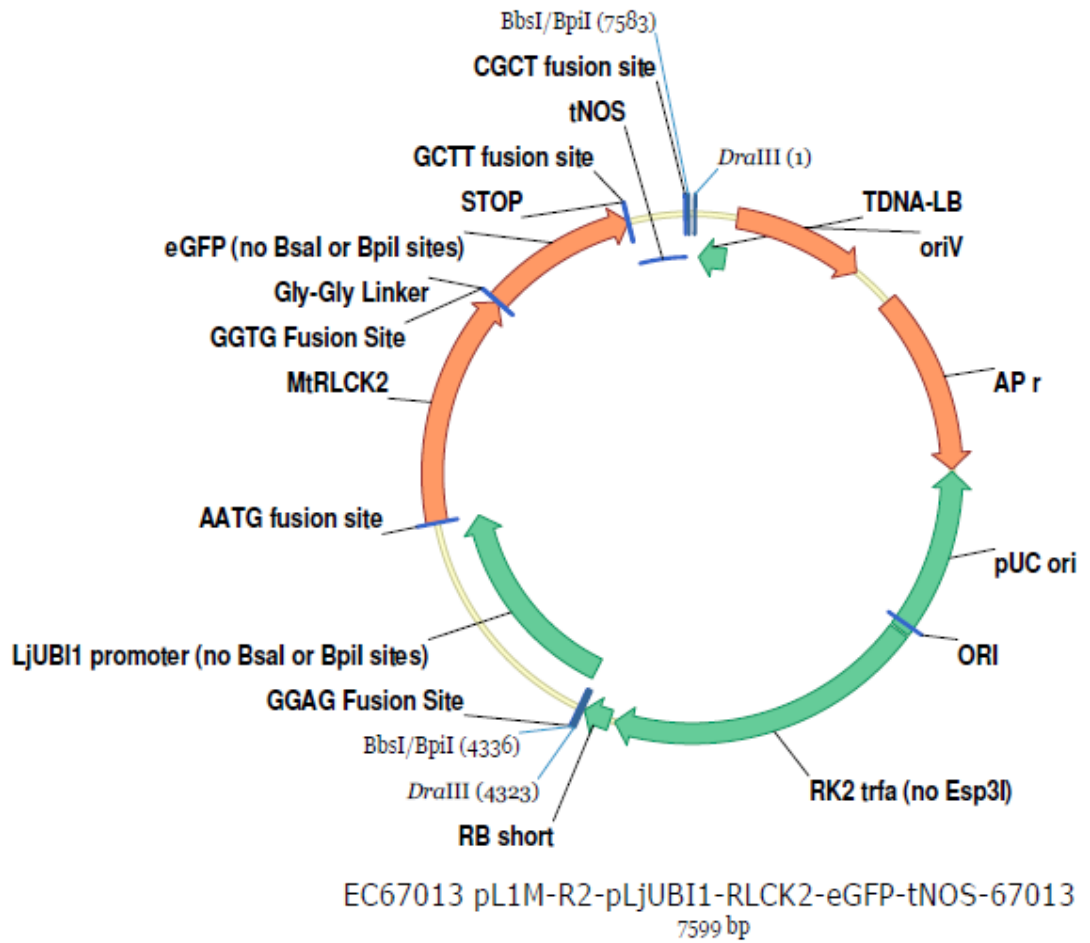


Figure A15. EC67013 plasmid map

Level 1 module Golden Gate construct. *L. japonicus Ubiquitin* Promoter, *MtRLCK2* CDS, C-terminal GFP tag, NOS terminator. Compatible with position R2 of Golden Gate Level 2 constructs.

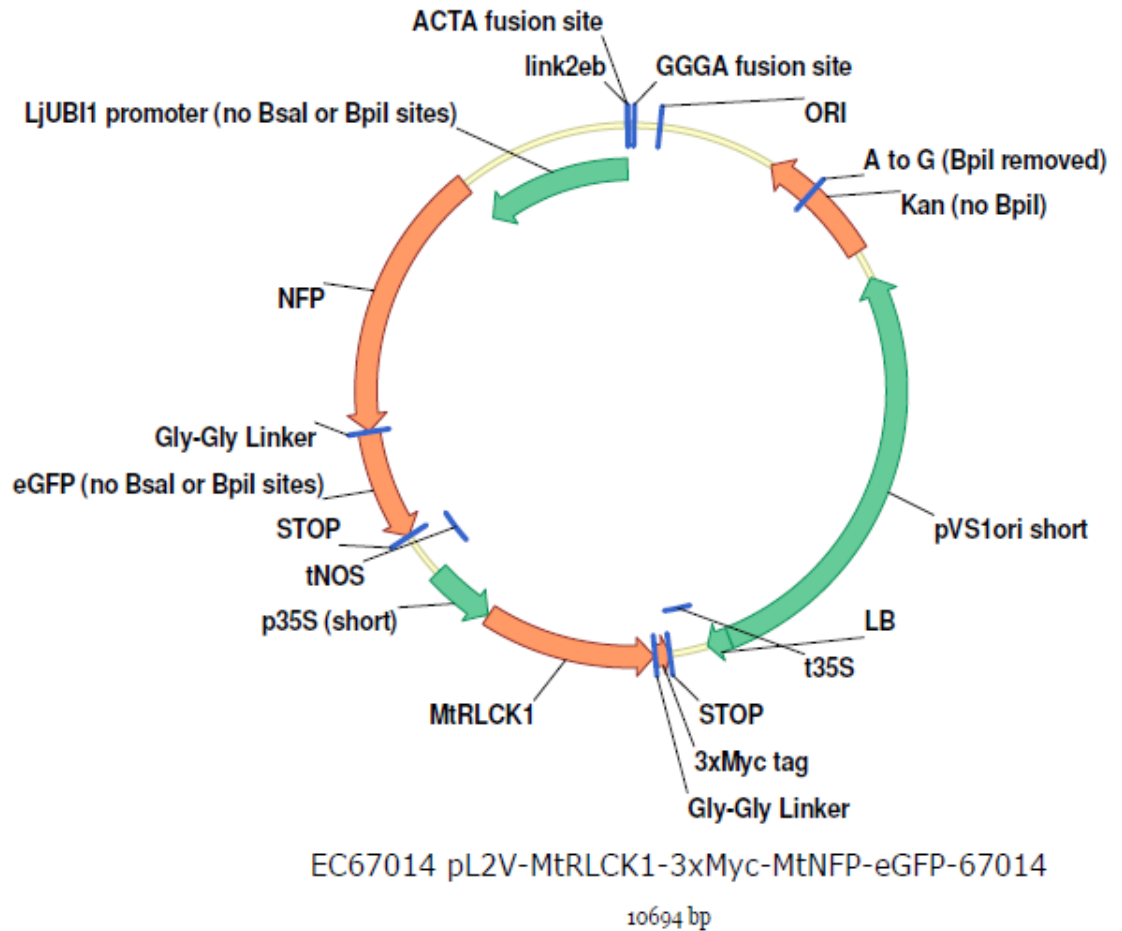


Figure A16. EC67014 plasmid map

Level 2 Golden Gate vector. In position R1: 35S Promoter, *RLCK1* CDS, 3x myc c-terminal tag, 35S terminator. In position R2: *L. japonicus Ubiquitin* Promoter, *MtNFP* CDS, C-terminal GFP tag, NOS terminator. Endlinker 2 in position F3.

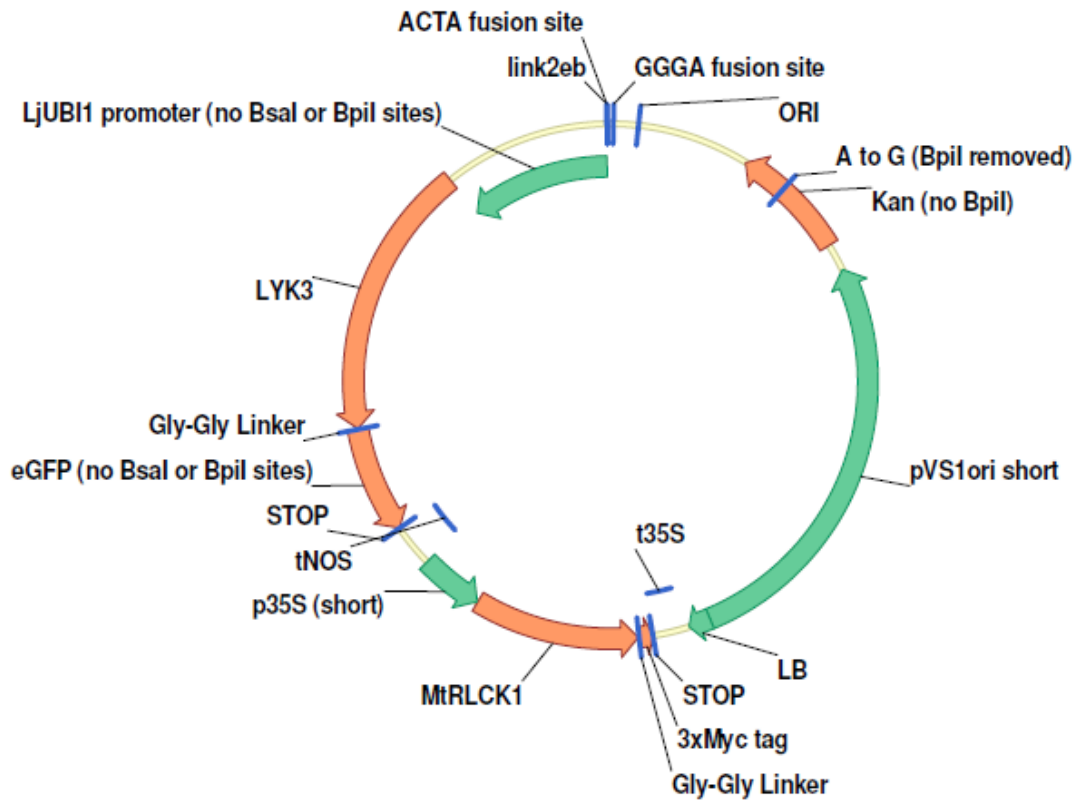
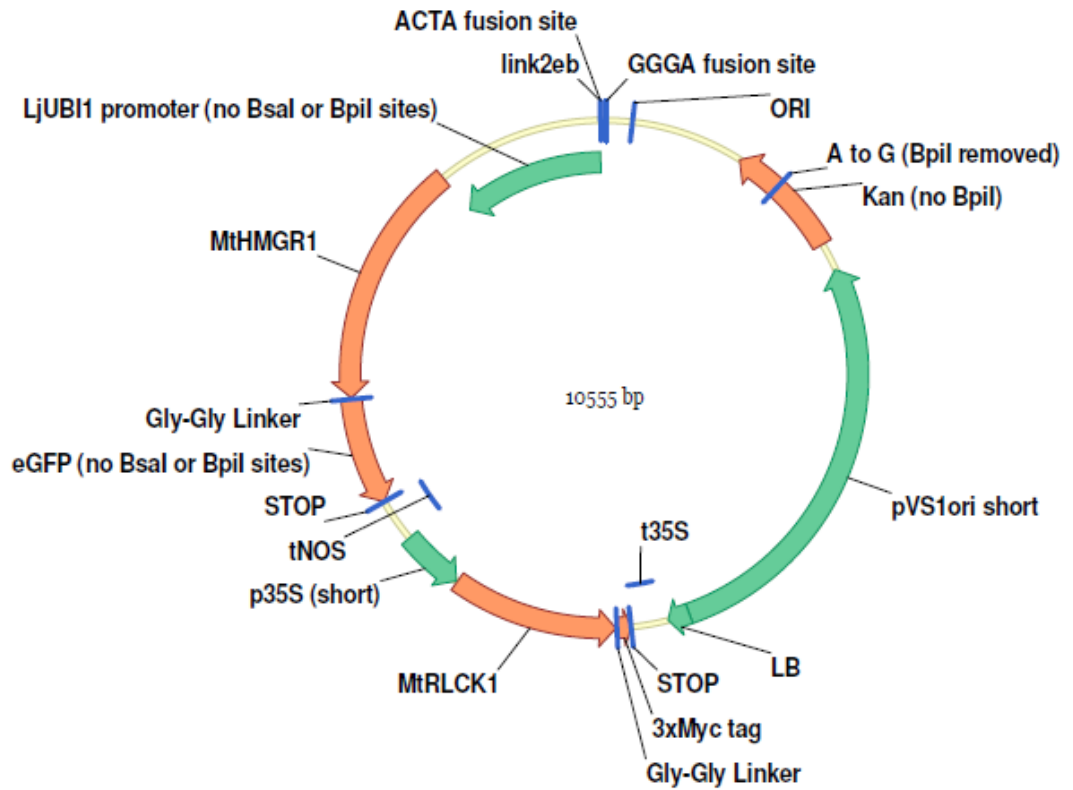


Figure A17. EC67015 plasmid map

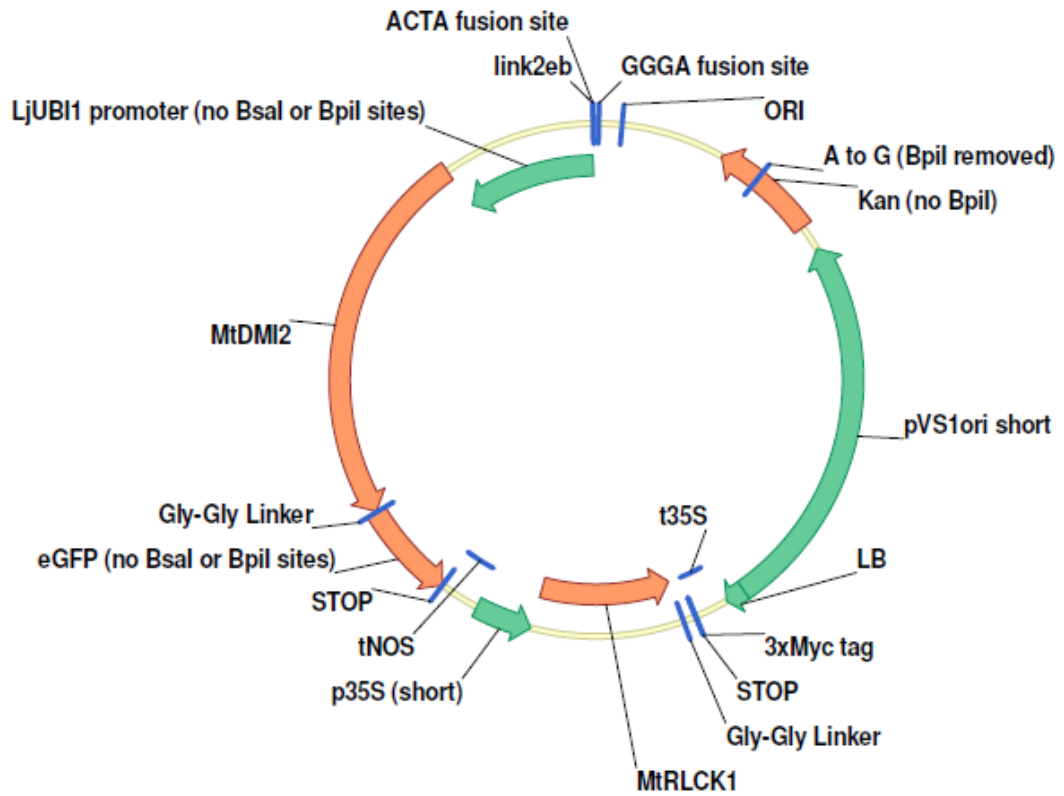
Level 2 Golden Gate vector. In position R1: 35S Promoter, *RLCK1* CDS, 3x myc c-terminal tag, 35S terminator. In position R2: *L. japonicus Ubiquitin* Promoter, *MtLYK3* CDS, C-terminal GFP tag, NOS terminator. Endlinker 2 in position F3.



EC67016 pL2V-MtRLCK1-3xMyc-MtHMGR1-eGFP-67016

Figure A18. EC67016 plasmid map

Level 2 Golden Gate vector. In position R1: 35S Promoter, *RLCK1* CDS, 3x myc c-terminal tag, 35S terminator. In position R2: *L. japonicus Ubiquitin* Promoter, *MtHMGR1* CDS, C-terminal GFP tag, NOS terminator. Endlinker 2 in position F3.



EC67017 pL2V-MtRLCK1-3xMyc-MtDMI2-eGFP-67017
11680 bp

Figure A19. EC67017 plasmid map

Level 2 Golden Gate vector. In position R1: 35S Promoter, *RLCK1* CDS, 3x myc c-terminal tag, 35S terminator. In position R2: *L. japonicus Ubiquitin* Promoter, *MtDMI2* CDS, C-terminal GFP tag, NOS terminator. Endlinker 2 in position F3.

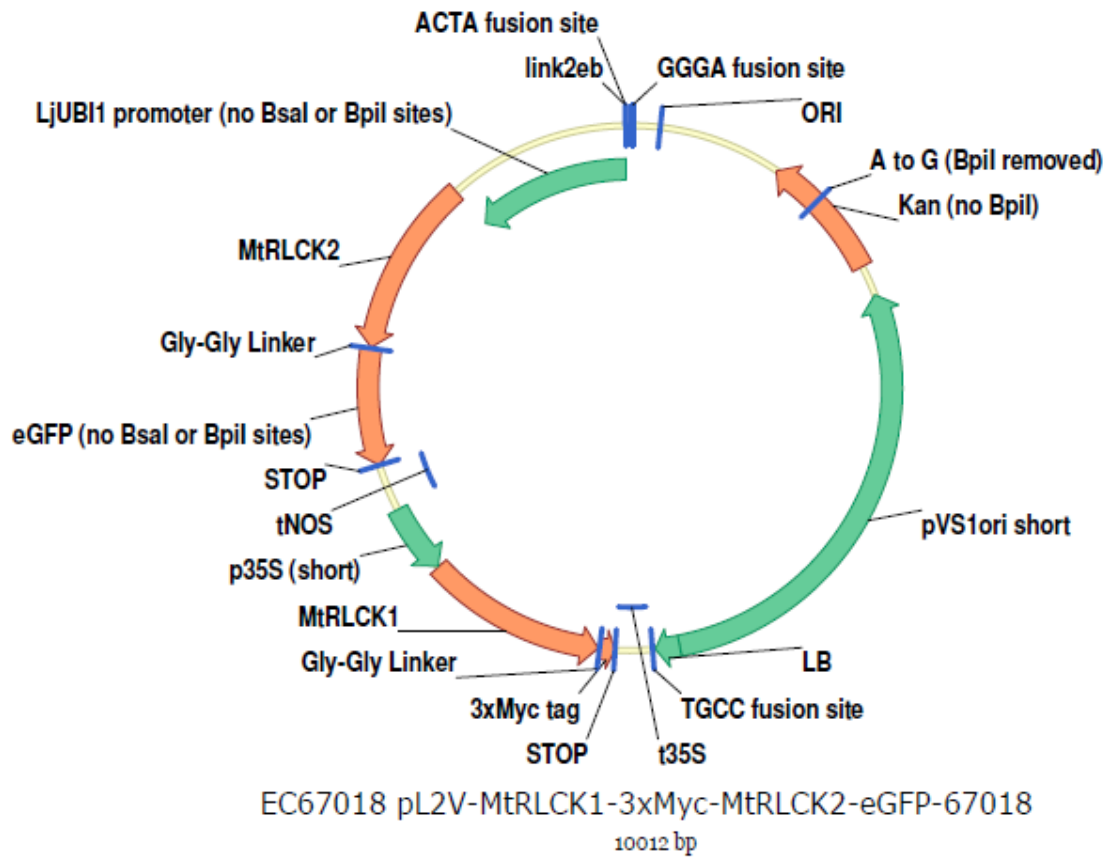


Figure A20. EC67018 plasmid map

Level 2 Golden Gate vector. In position R1: 35S Promoter, *RLCK1* CDS, 3x myc c-terminal tag, 35S terminator. In position R2: *L. japonicus Ubiquitin* Promoter, *RLCK2* CDS, C-terminal GFP tag, NOS terminator. Endlinker 2 in position F3.

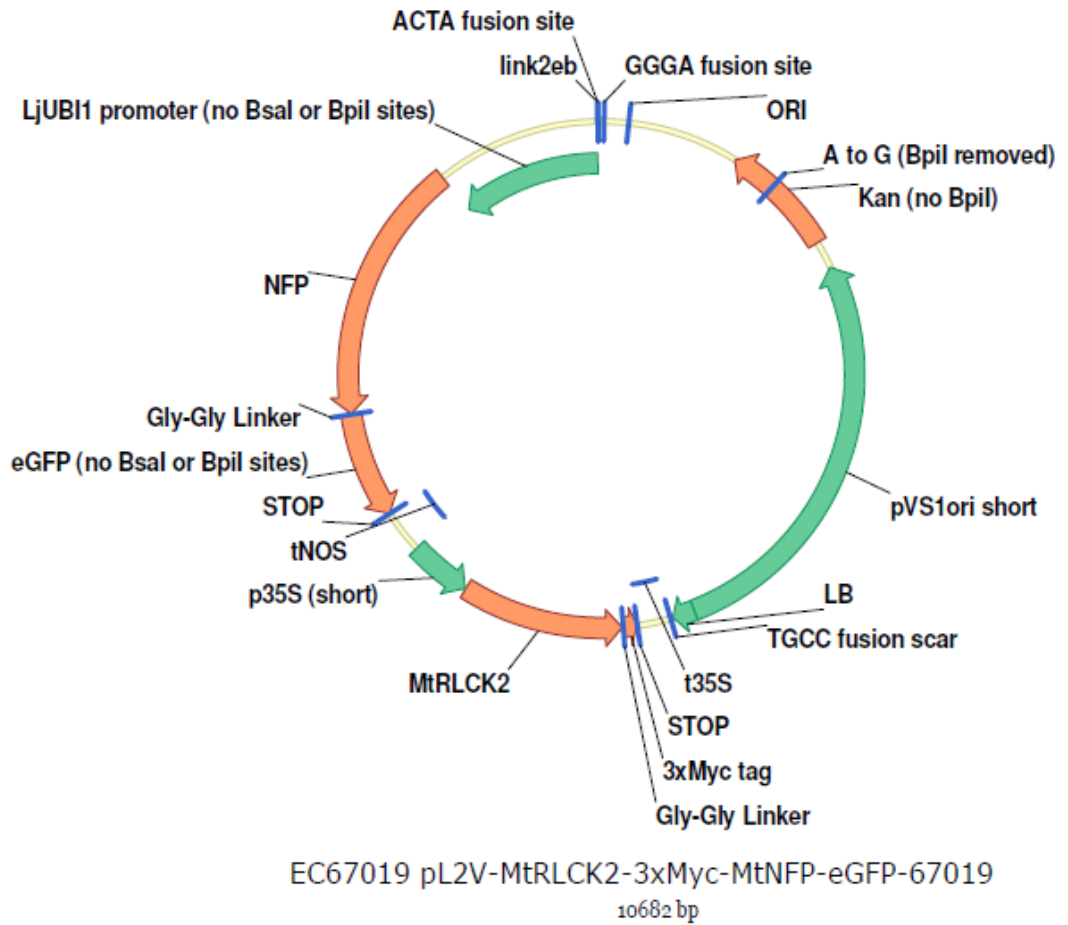


Figure A21. EC67019 plasmid map

Level 2 Golden Gate vector. In position R1: 35S Promoter, *RLCK2* CDS, 3x myc c-terminal tag, 35S terminator. In position R2: *L. japonicus Ubiquitin* Promoter, *MtNFP* CDS, C-terminal GFP tag, NOS terminator. Endlinker 2 in position F3.

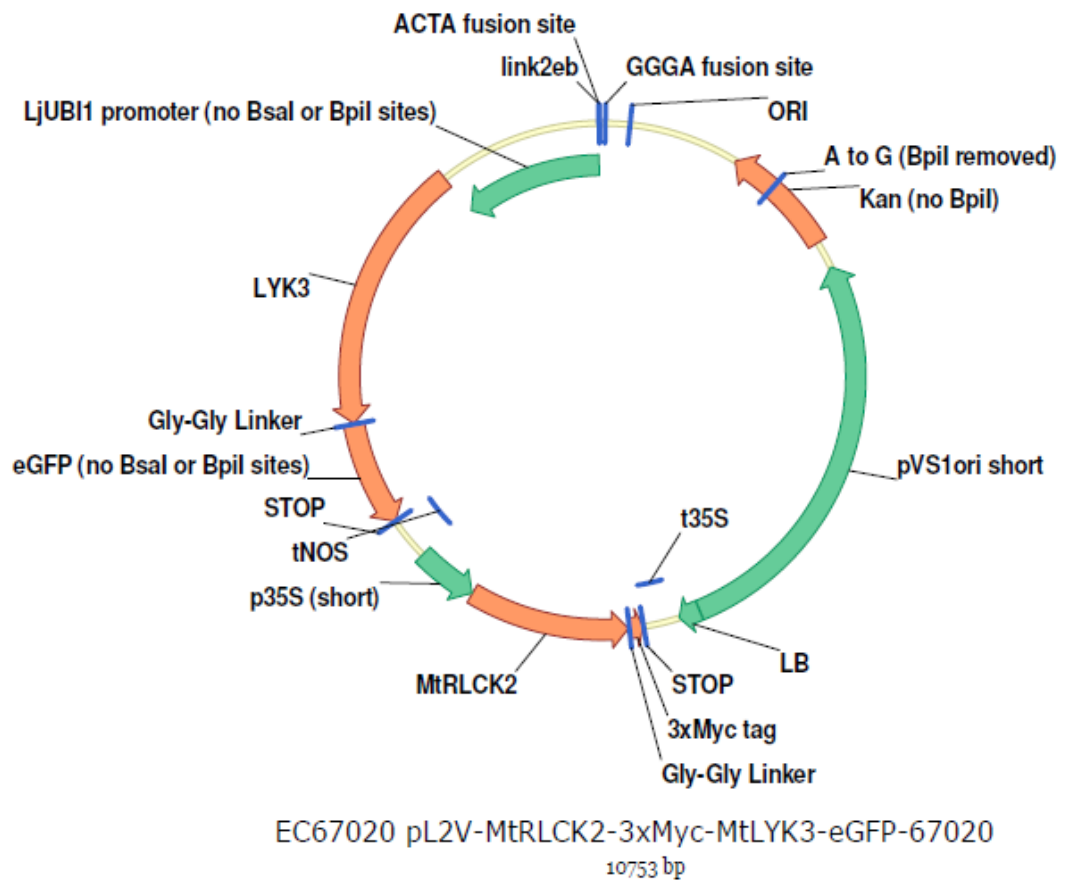


Figure A22. EC67020 plasmid map

Level 2 Golden Gate vector. In position R1: 35S Promoter, *RLCK2* CDS, 3x myc c-terminal tag, 35S terminator. In position R2: *L. japonicus Ubiquitin* Promoter, *MtLYK3* CDS, C-terminal GFP tag, NOS terminator. Endlinker 2 in position F3.

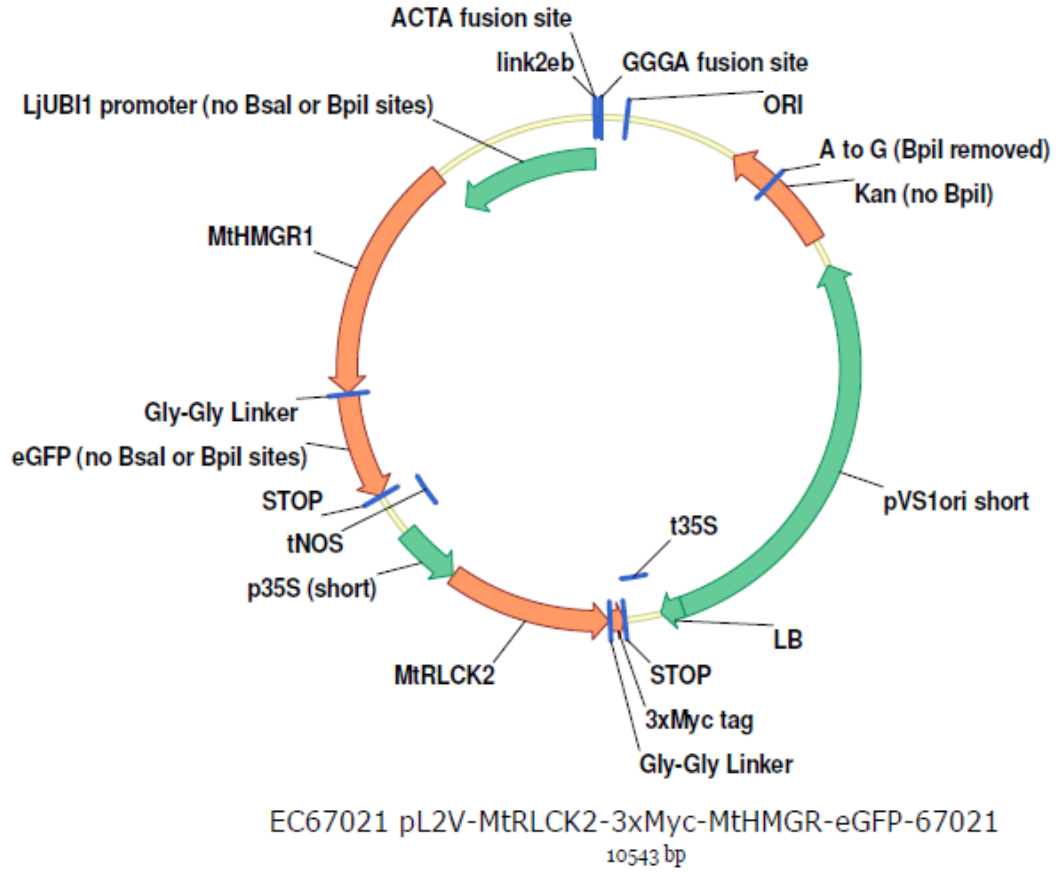


Figure A23. EC67021 plasmid map

Level 2 Golden Gate vector. In position R1: 35S Promoter, *RLCK2* CDS, 3x myc c-terminal tag, 35S terminator. In position R2: *L. japonicus Ubiquitin* Promoter, *MtHMGR1* CDS, C-terminal GFP tag, NOS terminator. Endlinker 2 in position F3.

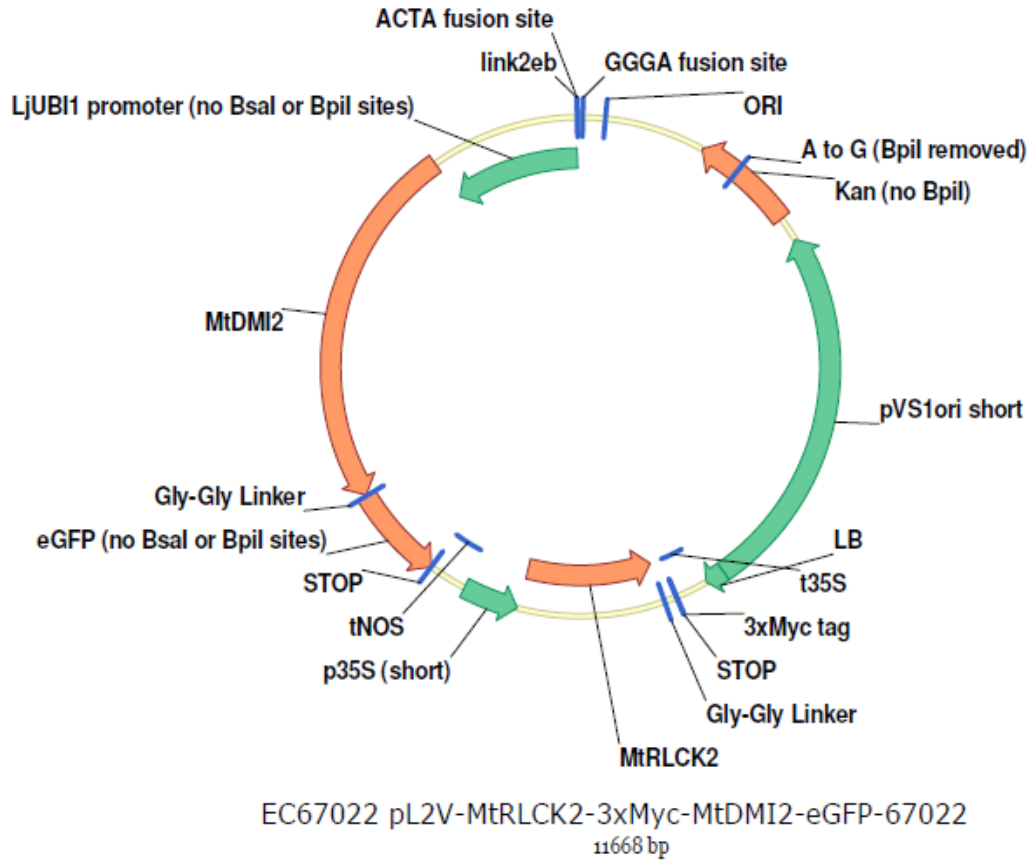


Figure A23. EC67021 plasmid map

Level 2 Golden Gate vector. In position R1: 35S Promoter, *RLCK2* CDS, 3x myc c-terminal tag, 35S terminator. In position R2: *L. japonicus Ubiquitin* Promoter, *MtHMGR1* CDS, C-terminal GFP tag, NOS terminator. Endlinker 2 in position F3.

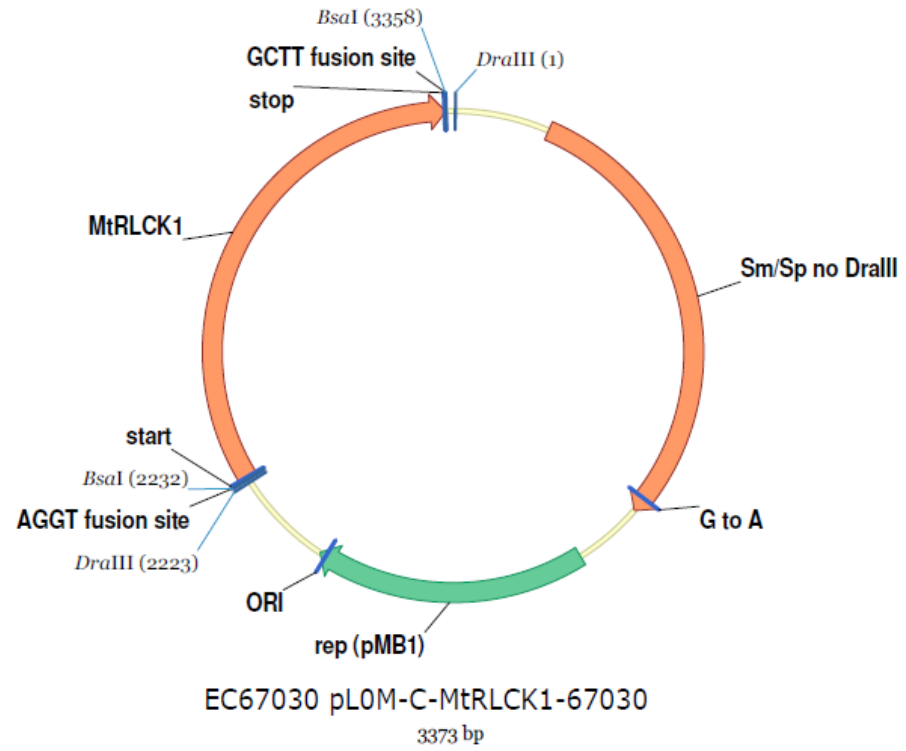


Figure A25. EC67030 plasmid map

Level 0 Golden Gate C construct. Contains *RLCK1* CDS with a stop codon.

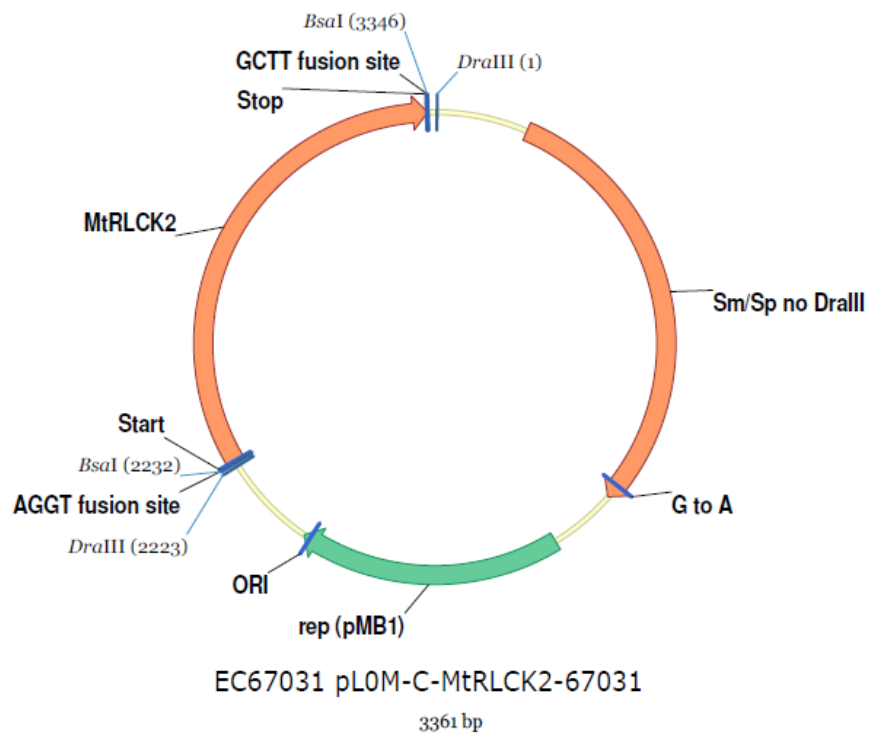


Figure A26. EC67031 plasmid map

Level 0 Golden Gate C construct. Contains *RLCK2* CDS with a stop codon.

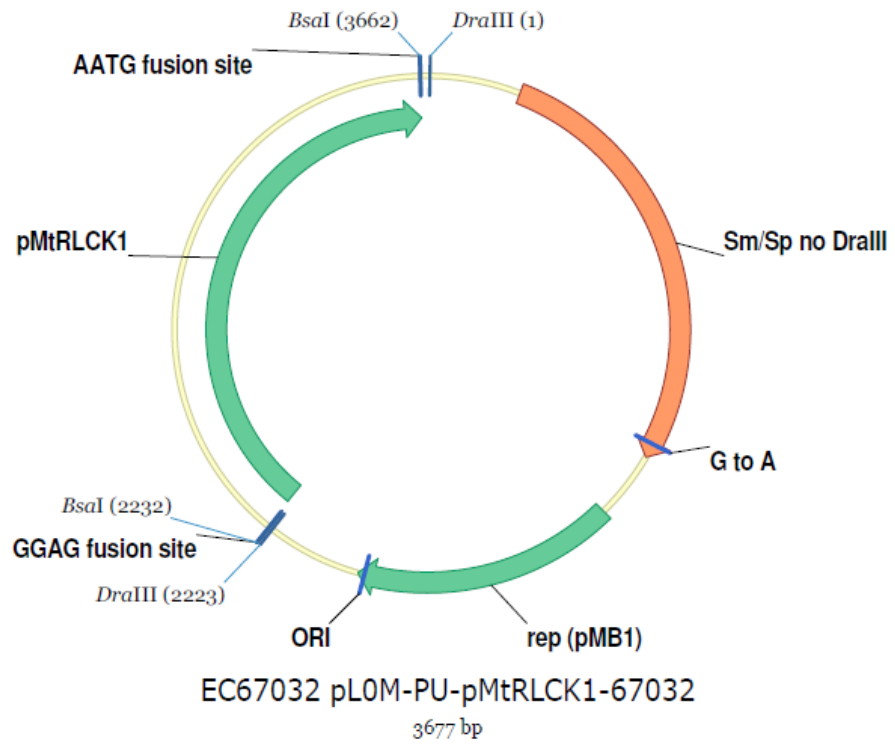


Figure A27. EC67032 plasmid map

Level 0 Golden Gate PU construct. Contains *RLCK1* promoter region.

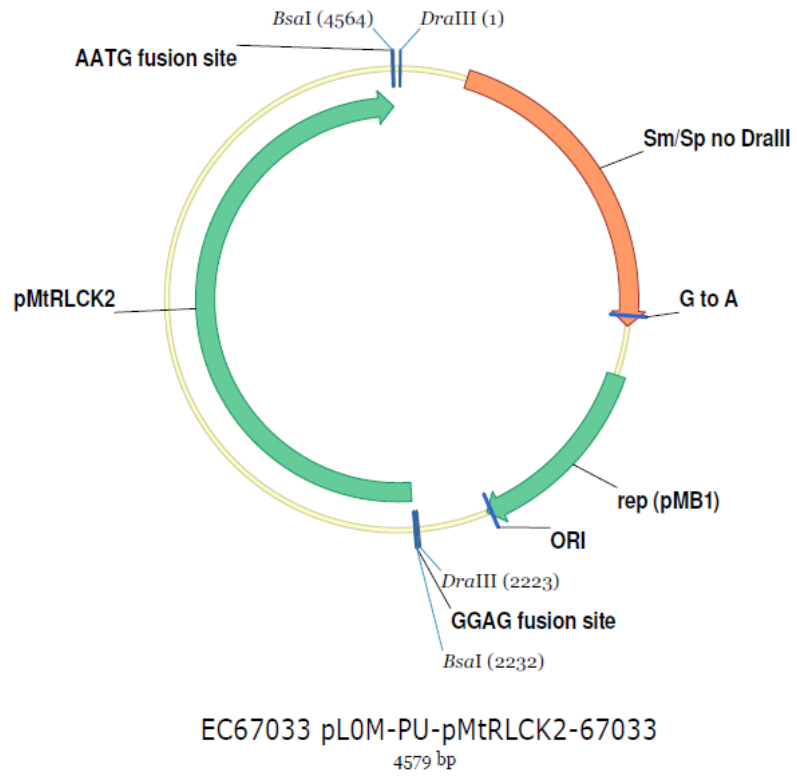
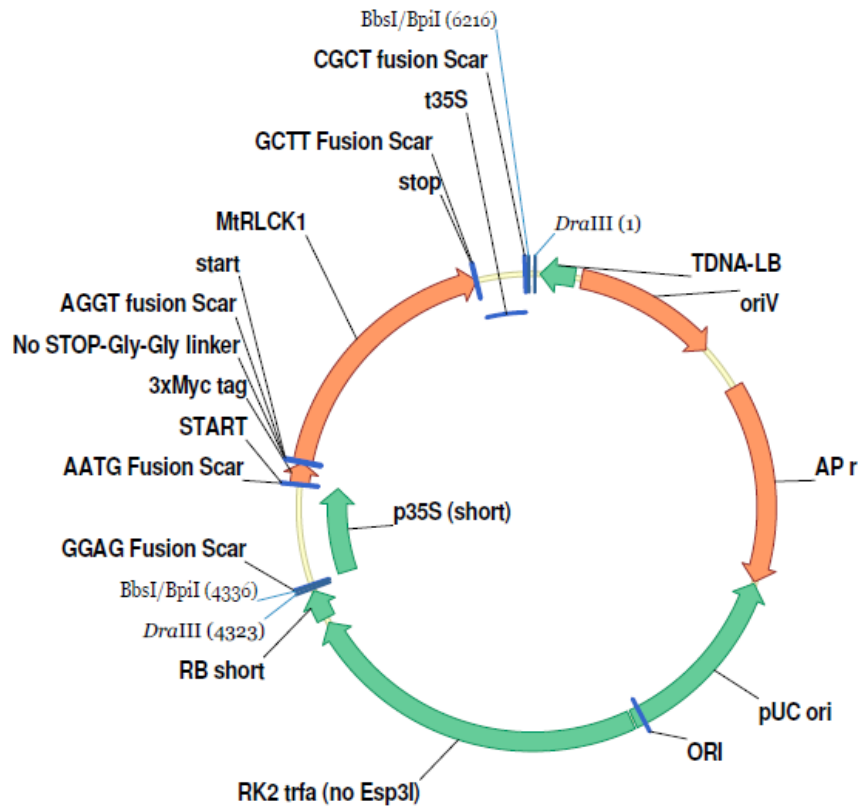


Figure A28. EC67033 plasmid map

Level 0 Golden Gate PU construct. Contains *RLCK2* promoter region.

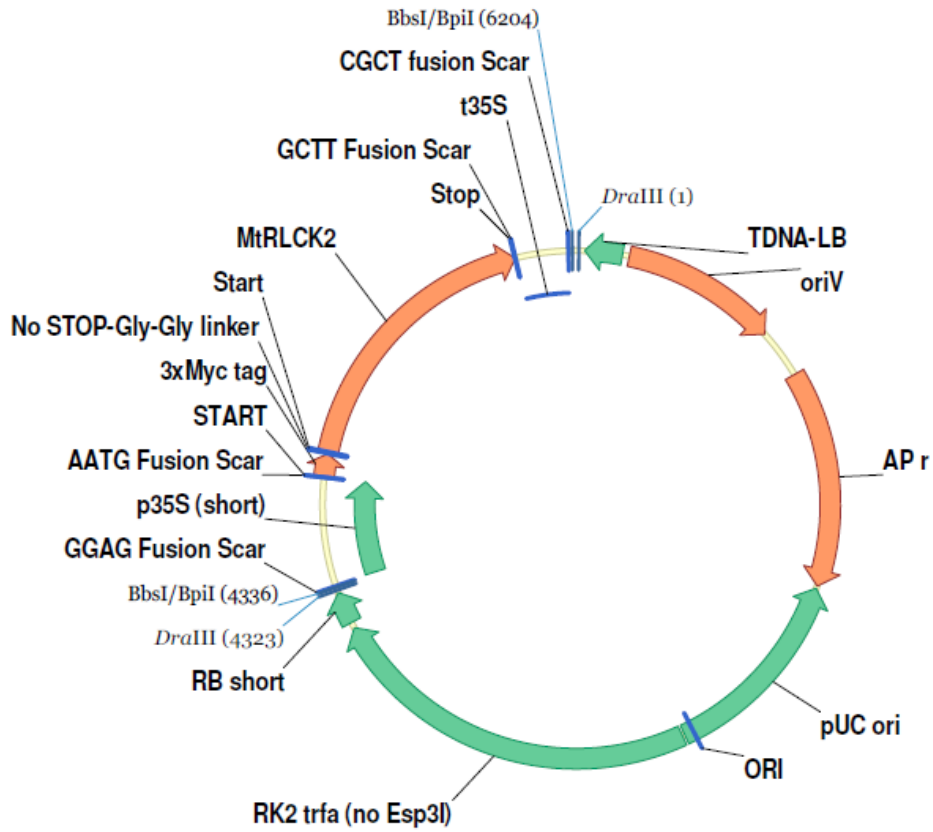


EC67034 pL1M-R1-p35S-3xMyc-MtRLCK1-T35S-67034

6232 bp

Figure A29. EC67034 plasmid map

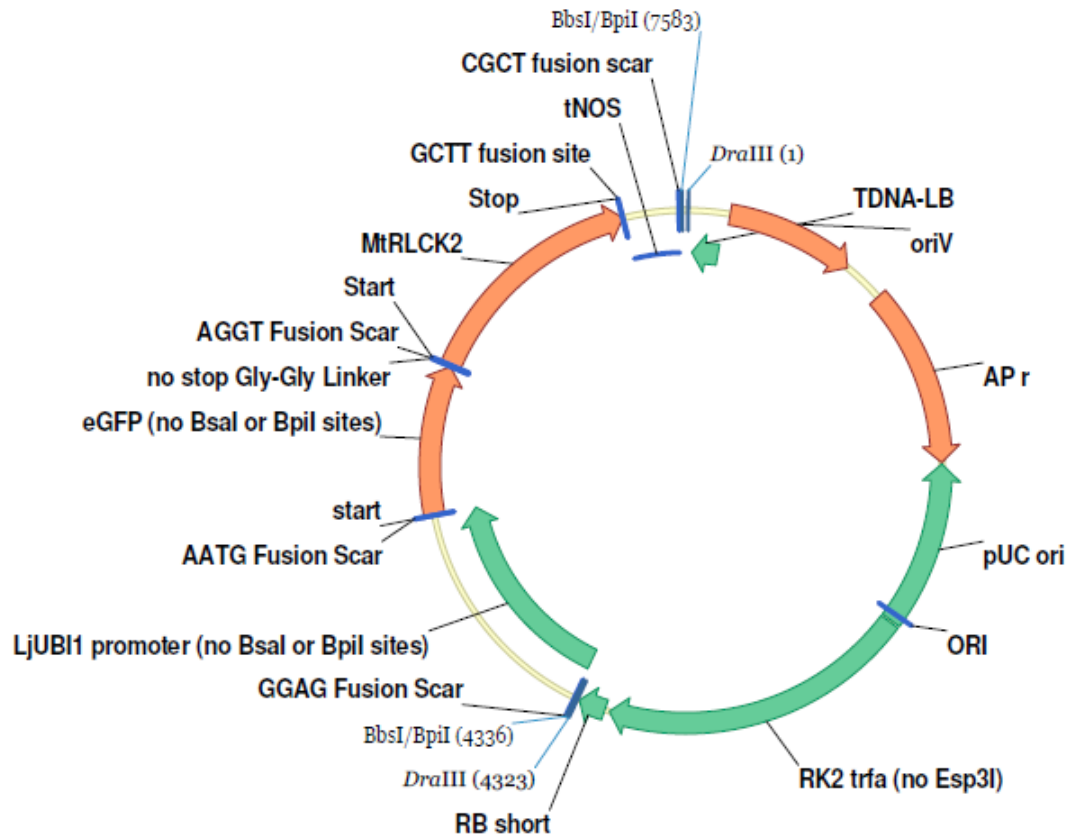
Level 1 module Golden Gate construct. 35S Promoter, 3x myc N-terminal tag *RLCK1* CDS, 35S terminator. Compatible with position R1 of Golden Gate Level 2 constructs.



EC67035 pL1M-R1-p35S-3xMyc-MtRLCK2-T35S-67035
6220 bp

Figure A30. EC67035 plasmid map

Level 1 module Golden Gate construct. 35S Promoter, 3x myc N-terminal tag *RLCK2* CDS, 35S terminator. Compatible with position R1 of Golden Gate Level 2 constructs.



EC67036 pL1M-R2-pLjUBI1-eGFP-RLCK2-tNOS-67036
7599 bp

Figure A31. EC67036 plasmid map

Level 1 module Golden Gate construct. *L. japonicus Ubiquitin* Promoter, N-terminal GFP tag *RLCK2* CDS, NOS terminator. Compatible with position R2 of Golden Gate Level 2 constructs.

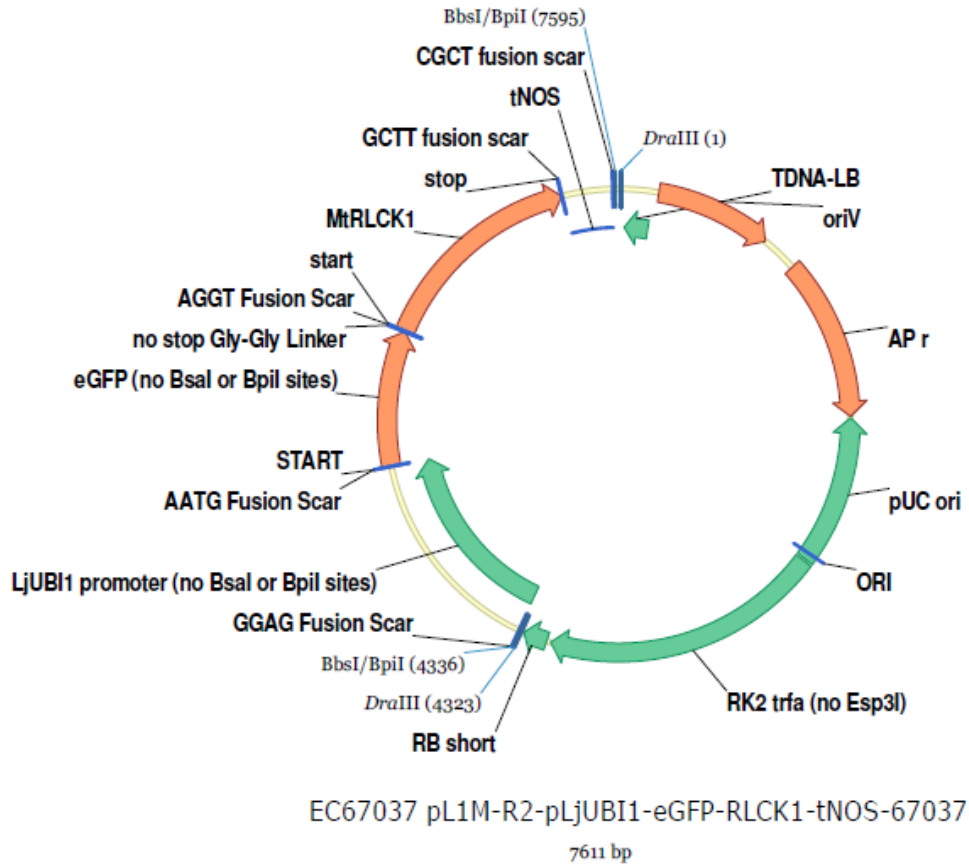


Figure A32. EC67037 plasmid map

Level 1 module Golden Gate construct. *L. japonicus Ubiquitin* Promoter, N-terminal GFP tag *RLCK1* CDS, NOS terminator. Compatible with position R2 of Golden Gate Level 2 constructs.

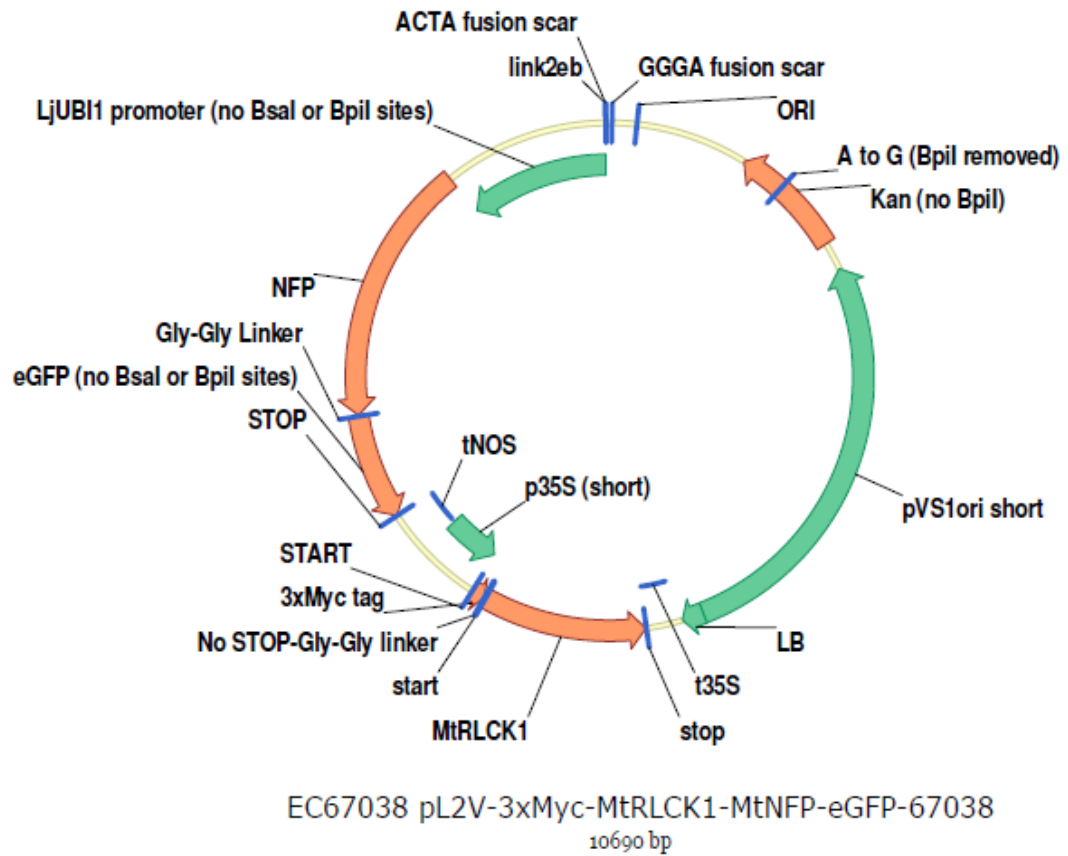


Figure A33. EC67038 plasmid map

Level 2 Golden Gate vector. In position R1: 35S Promoter, 3x myc N-terminal tag *RLCK1* CDS, 35S terminator. In position R2: *L. japonicus Ubiquitin* Promoter, *MtNFP* CDS, C-terminal GFP tag, NOS terminator. Endlinker 2 in position F3.

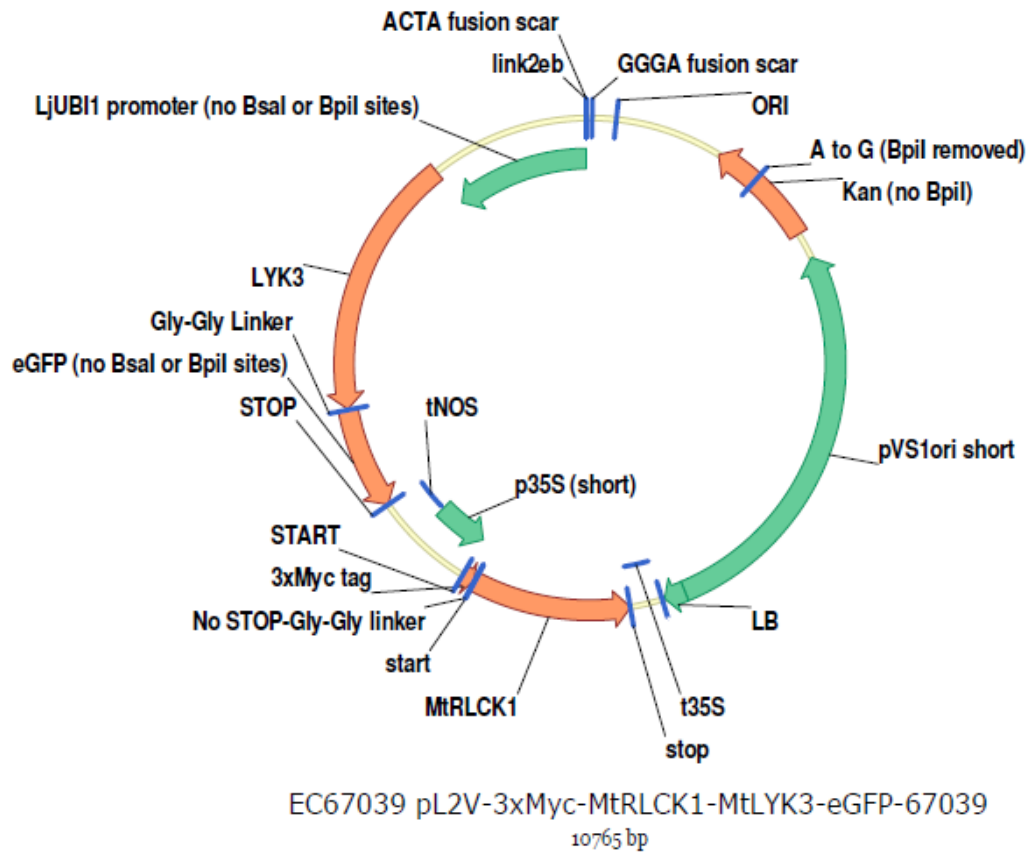


Figure A34. EC67039 plasmid map

Level 2 Golden Gate vector. In position R1: 35S Promoter, 3x myc N-terminal tag *RLCK1* CDS, 35S terminator. In position R2: *L. japonicus Ubiquitin* Promoter, *MtLYK3* CDS, C-terminal GFP tag, NOS terminator. Endlinker 2 in position F3.

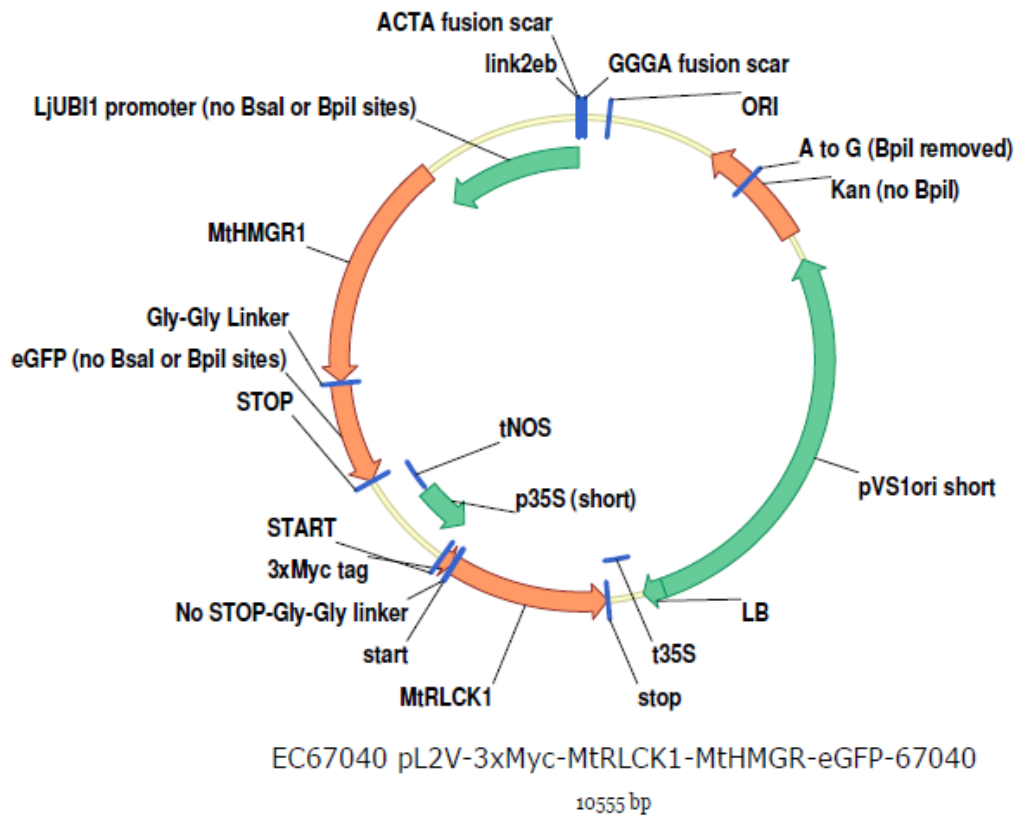


Figure A35. EC67040 plasmid map

Level 2 Golden Gate vector. In position R1: 35S Promoter, 3x myc N-terminal tag *RLCK1* CDS, 35S terminator. In position R2: *L. japonicus Ubiquitin* Promoter, *MtHMGR2* CDS, C-terminal GFP tag, NOS terminator. Endlinker 2 in position F3.

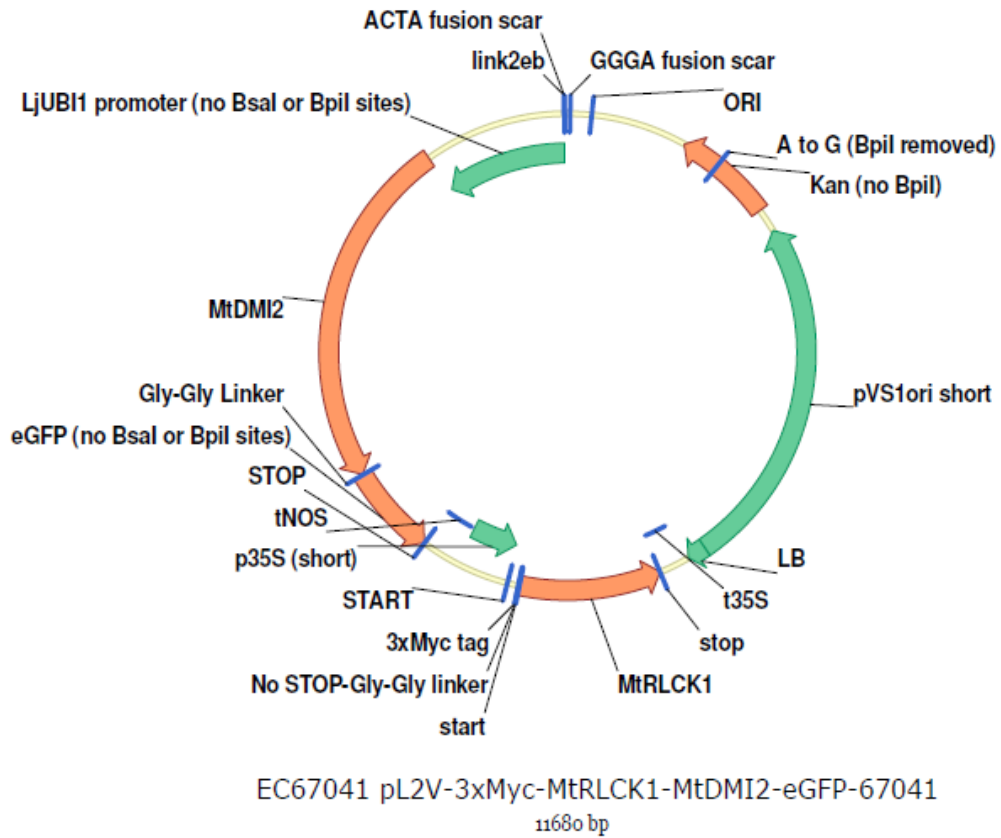


Figure A36. EC67041 plasmid map

Level 2 Golden Gate vector. In position R1: 35S Promoter, 3x myc N-terminal tag *RLCK1* CDS, 35S terminator. In position R2: *L. japonicus Ubiquitin* Promoter, *MtDMI2* CDS, C-terminal GFP tag, NOS terminator. Endlinker 2 in position F3.

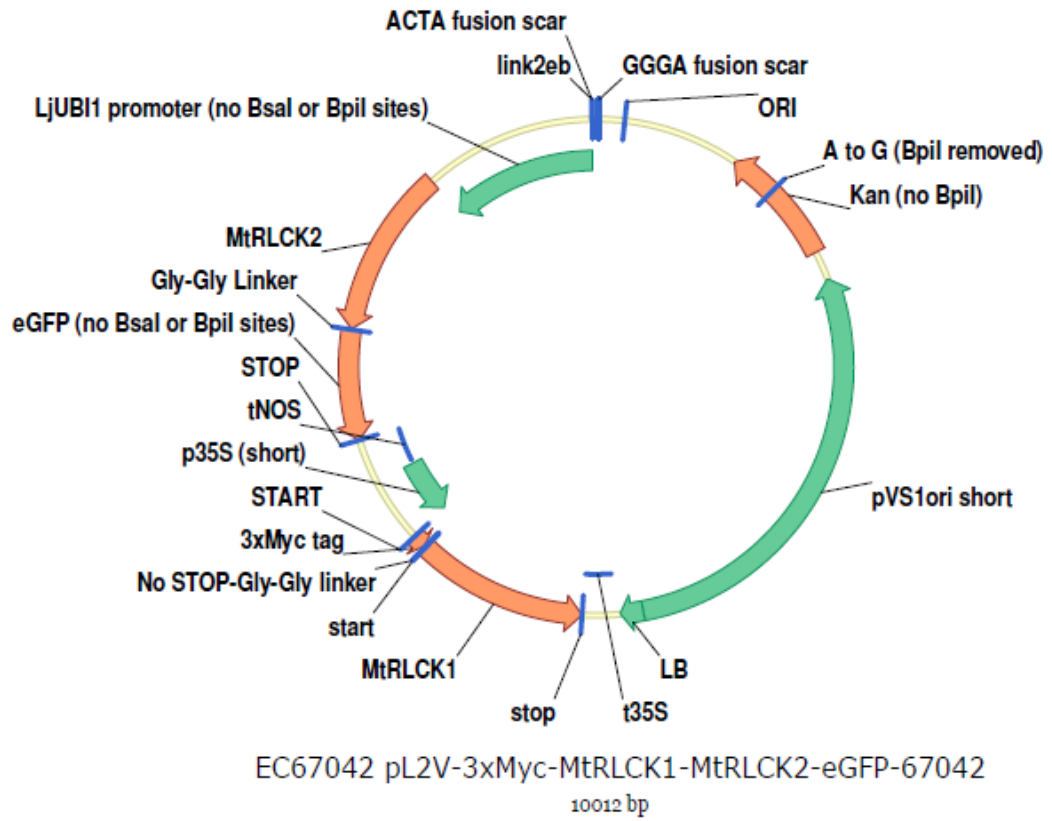


Figure A37. EC67042 plasmid map

Level 2 Golden Gate vector. In position R1: 35S Promoter, 3x myc N-terminal tag *RLCK1* CDS, 35S terminator. In position R2: *L. japonicus Ubiquitin* Promoter, *RLCK2* CDS, C-terminal GFP tag, NOS terminator. Endlinker 2 in position F3.

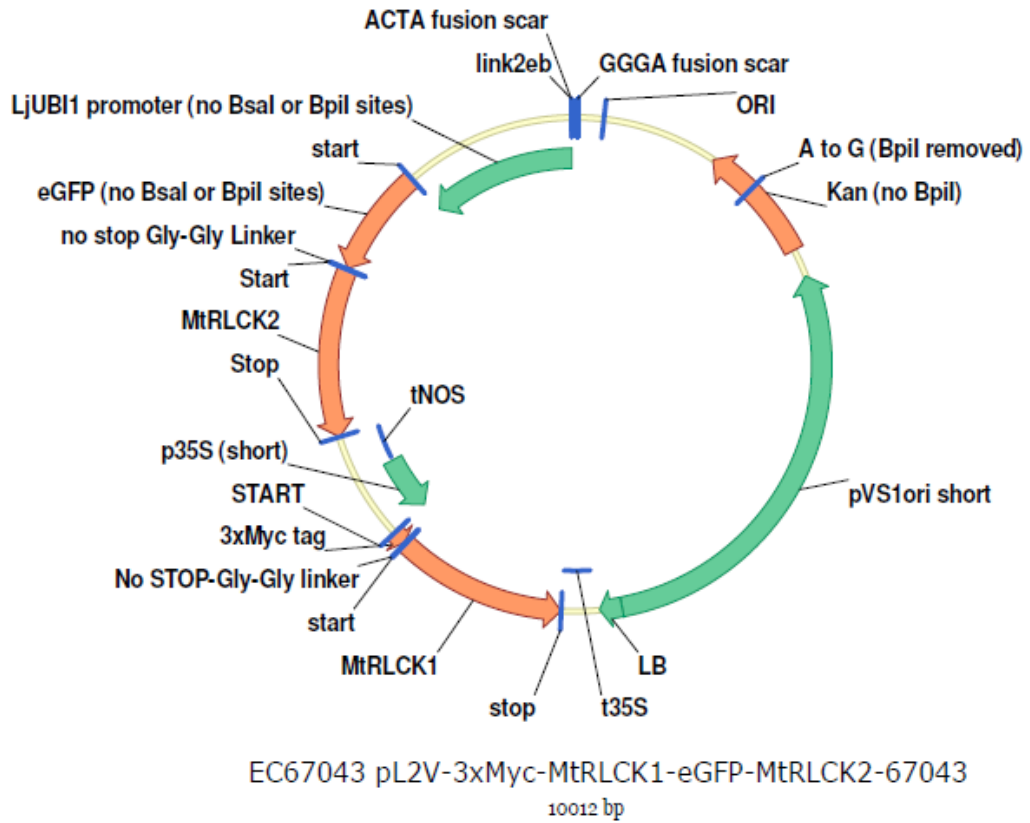


Figure A38. EC67043 plasmid map

Level 2 Golden Gate vector. In position R1: 35S Promoter, 3x myc N-terminal tag *RLCK2* CDS, 35S terminator. In position R2: *L. japonicus Ubiquitin* Promoter, N-terminal GFP tag, *RLCK2* CDS, NOS terminator. Endlinker 2 in position F3.

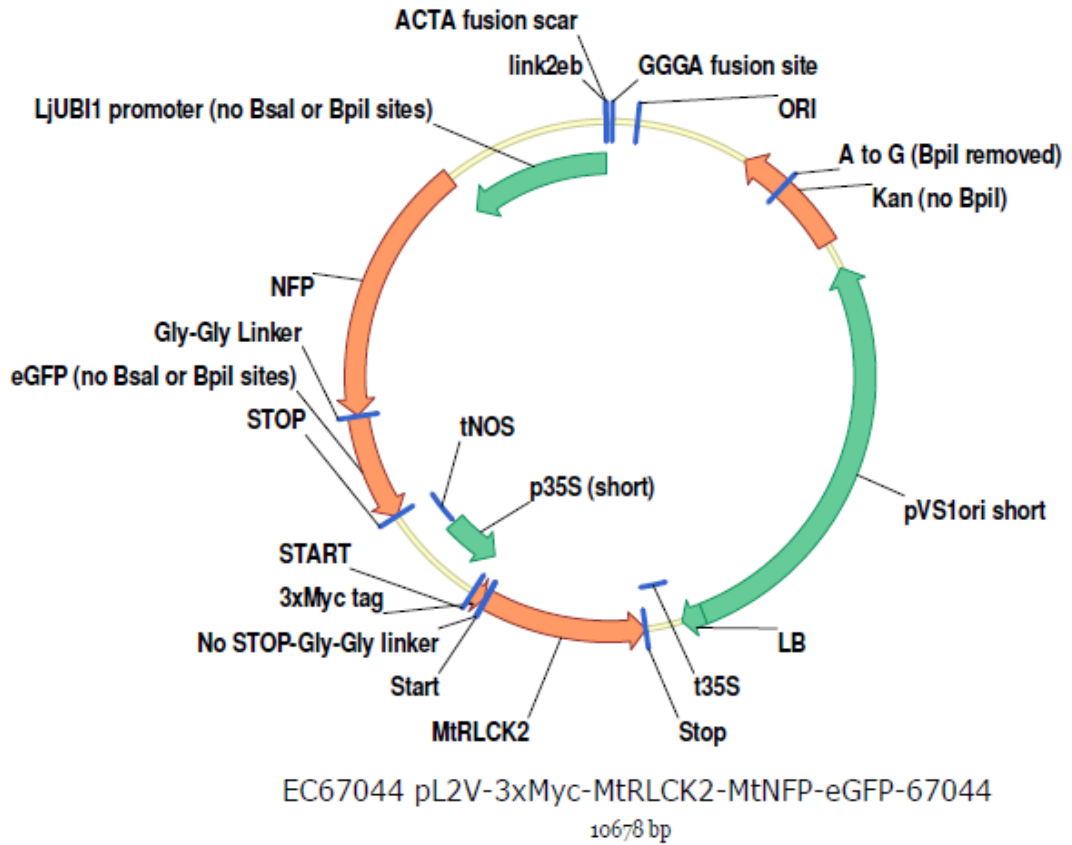


Figure A39. EC67044 plasmid map

Level 2 Golden Gate vector. In position R1: 35S Promoter, 3x myc N-terminal tag *RLCK2* CDS, 35S terminator. In position R2: *L. japonicus Ubiquitin* Promoter, *MtNFP* CDS, C-terminal GFP tag, NOS terminator. Endlinker 2 in position F3.

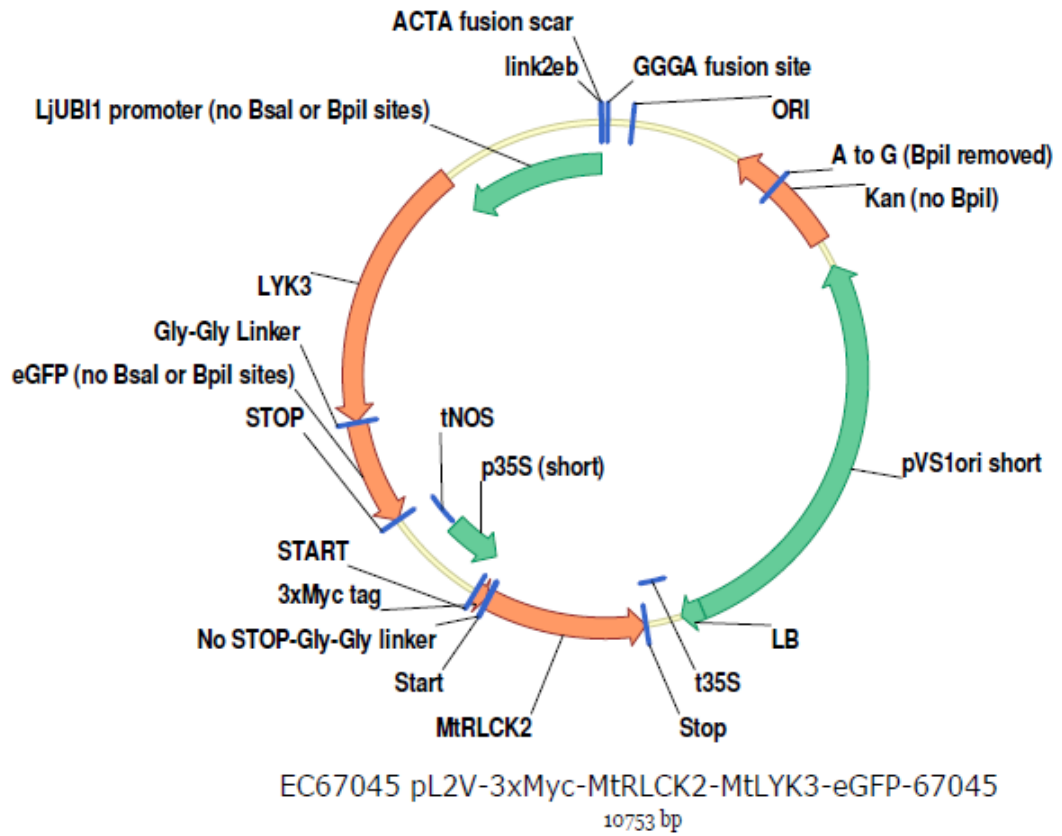


Figure A40. EC67045 plasmid map

Level 2 Golden Gate vector. In position R1: 35S Promoter, 3x myc N-terminal tag *RLCK2* CDS, 35S terminator. In position R2: *L. japonicus Ubiquitin* Promoter, *MtLYK3* CDS, C-terminal GFP tag, NOS terminator. Endlinker 2 in position F3.

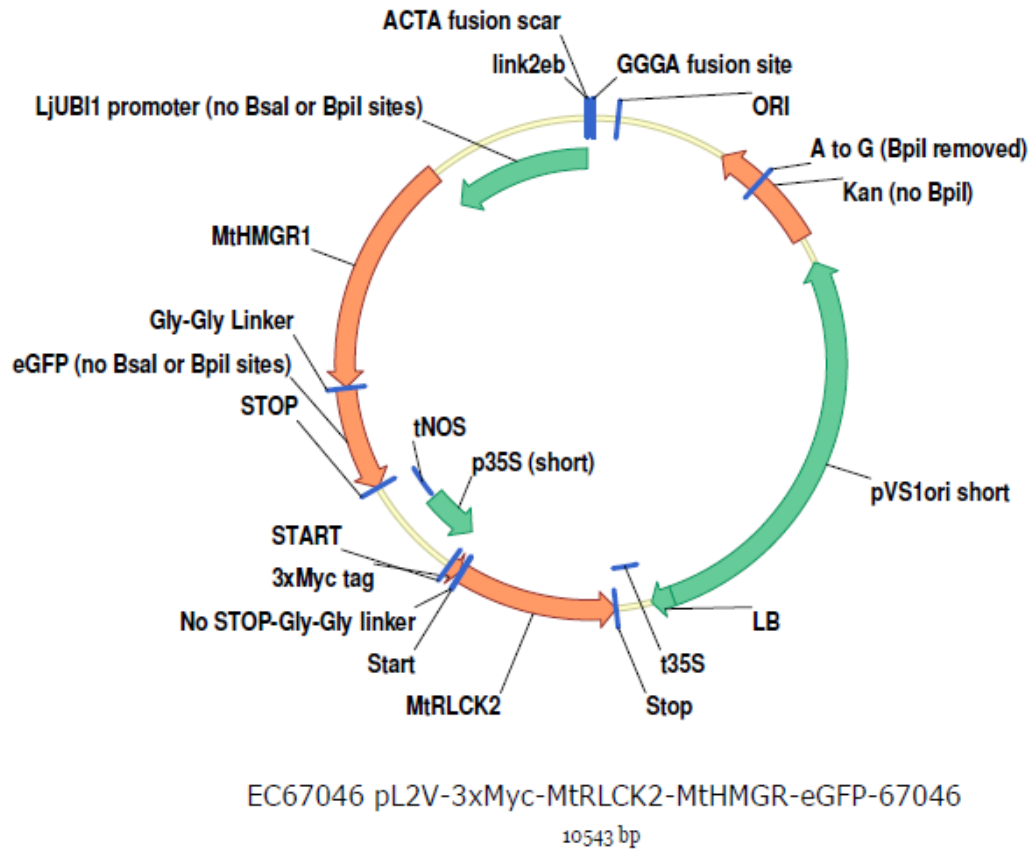


Figure A41. EC67046 plasmid map

Level 2 Golden Gate vector. In position R1: 35S Promoter, 3x myc N-terminal tag *RLCK2* CDS, 35S terminator. In position R2: *L. japonicus Ubiquitin* Promoter, *MtHMGR1* CDS, C-terminal GFP tag, NOS terminator. Endlinker 2 in position F3.

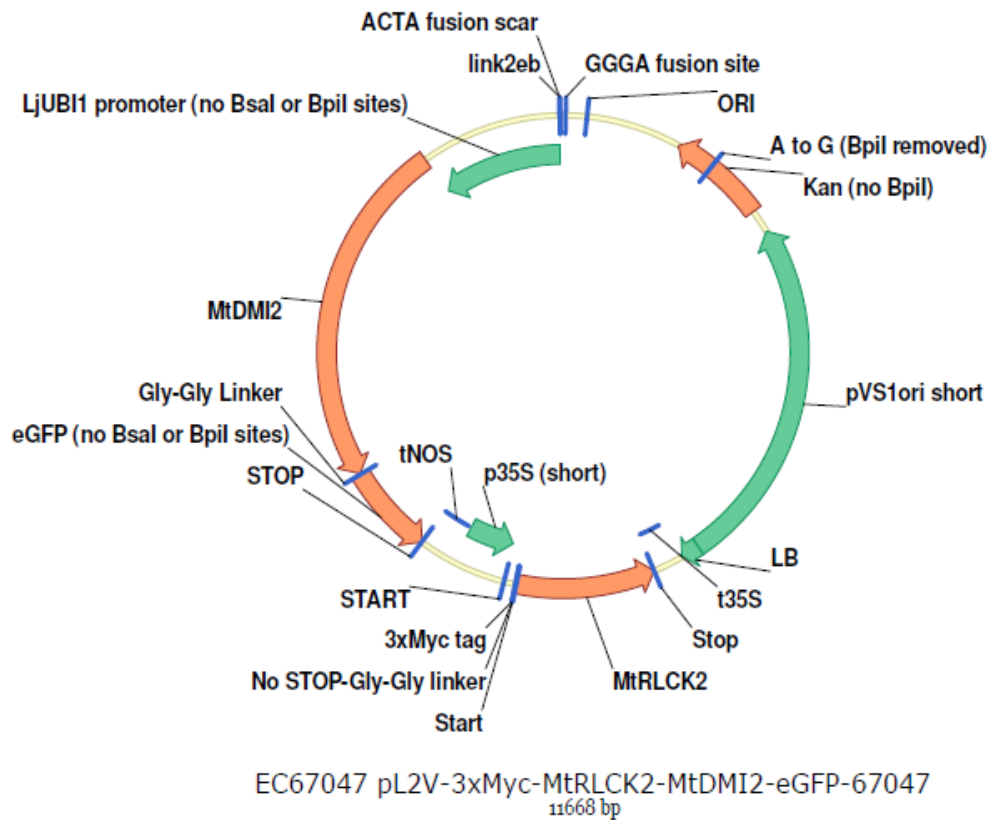


Figure A42. EC67047 plasmid map

Level 2 Golden Gate vector. In position R1: 35S Promoter, 3x myc N-terminal tag *RLCK2* CDS, 35S terminator. In position R2: *L. japonicus Ubiquitin* Promoter, *MtDMI2* CDS, C-terminal GFP tag, NOS terminator. Endlinker 2 in position F3.

References

- ALBERTS, B. J., A.; LEWIS, J.; RAFF, M.; ROBERTS, K.; WALTER, P. 2002. *Molecular Biology of the Cell*, New York, Garland Science.
- ALBRECHT, C., BOUTROT, F., SEGONZAC, C., SCHWESSINGER, B., GIMENEZ-IBANEZ, S., CHINCHILLA, D., RATHJEN, J. P., DE VRIES, S. C. & ZIPFEL, C. 2012. Brassinosteroids inhibit pathogen-associated molecular pattern-triggered immune signaling independent of the receptor kinase BAK1. *Proceedings of the National Academy of Sciences*, 109, 303-308.
- ALVAREZ, M. A. E., PENNELL, R. I., MEIJER, P.-J., ISHIKAWA, A., DIXON, R. A. & LAMB, C. 1998. Reactive Oxygen Intermediates Mediate a Systemic Signal Network in the Establishment of Plant Immunity. *Cell*, 92, 773-784.
- AMOR, B. B., SHAW, S. L., OLDROYD, G. E. D., MAILLET, F., PENMETSA, R. V., COOK, D., LONG, S. R., DÉNARIÉ, J. & GOUGH, C. 2003. The NFP locus of *Medicago truncatula* controls an early step of Nod factor signal transduction upstream of a rapid calcium flux and root hair deformation. *The Plant Journal*, 34, 495-506.
- ANDRIANKAJA, A., BOISSON-DERNIER, A., FRANCES, L., SAUVIAC, L., JAUNEAU, A., BARKER, D. G. & DE CARVALHO-NIEBEL, F. 2007. AP2-ERF Transcription Factors Mediate Nod Factor-Dependent *Mt ENOD11* Activation in Root Hairs via a Novel *cis*-Regulatory Motif. *The Plant Cell Online*, 19, 2866-2885.
- ANDRIO, E., MARINO, D., MARMEYS, A., DE SEGONZAC, M. D., DAMIANI, I., GENRE, A., HUGUET, S., FRENO, P., PUPPO, A. & PAULY, N. 2013. Hydrogen peroxide-regulated genes in the *Medicago truncatula*-*Sinorhizobium meliloti* symbiosis. *New Phytologist*, 198, 179-189.
- ANÉ, J.-M., KISS, G. B., RIELY, B. K., PENMETSA, R. V., OLDROYD, G. E. D., AYAX, C., LÉVY, J., DEBELLÉ, F., BAEK, J.-M., KALO, P., ROSENBERG, C., ROE, B. A., LONG, S. R., DÉNARIÉ, J. & COOK, D. R. 2004. *Medicago truncatula DMI1* Required for Bacterial and Fungal Symbioses in Legumes. *Science*, 303, 1364-1367.
- ANTOLÍN-LLOVERA, M., RIED, MARTINA K. & PARNISKE, M. 2014. Cleavage of the SYMBIOSIS RECEPTOR-LIKE KINASE Ectodomain Promotes Complex Formation with Nod Factor Receptor 5. *Current Biology*, 24, 422-427.
- APPLEBY, C. A. 1984. Leghemoglobin and *Rhizobium* Respiration. *Annual Review of Plant Physiology*, 35, 443-78.
- ARRIGHI, J.-F., BARRE, A., BEN AMOR, B., BERSOULT, A., SORIANO, L. C., MIRABELLA, R., DE CARVALHO-NIEBEL, F., JOURNET, E.-P., GHÉRARDI, M., HUGUET, T., GEURTS, R., DÉNARIÉ, J., ROUGÉ, P. & GOUGH, C. 2006. The *Medicago truncatula* Lysine Motif-Receptor-Like Kinase Gene Family Includes *NFP* and New Nodule-Expressed Genes. *Plant Physiology*, 142, 265-279.
- ARTIMO, P., JONNALAGEDDA, M., ARNOLD, K., BARATIN, D., CSARDI, G., DE CASTRO, E., DUVAUD, S., FLEGEL, V., FORTIER, A., GASTEIGER, E., GROSDIDIER, A., HERNANDEZ, C., IOANNIDIS, V., KUZNETSOV, D., LIECHTI, R., MORETTI, S., MOSTAGUIR, K., REDASCHI, N., ROSSIER, G., XENARIOS, I. & STOCKINGER, H. 2012. ExpASY: SIB bioinformatics resource portal. *Nucleic Acids Research*.
- ASAI, T., TENA, G., PLOTNIKOVA, J., WILLMANN, M. R., CHIU, W.-L., GOMEZ-GOMEZ, L., BOLLER, T., AUSUBEL, F. M. & SHEEN, J. 2002. MAP kinase signalling cascade in *Arabidopsis* innate immunity. *Nature*, 415, 977-983.
- AUSUBEL, F. & BISSELING, T. 1999. Biotic interactions pathogenesis and symbiosis: Two sides of the same coin that should be united by a common web-accessible database: Editorial overview. *Current Opinion in Plant Biology*, 2, 265-267.
- BALESTRINI, R. & BONFANTE, P. 2014. Cell wall remodeling in mycorrhizal symbiosis: a way towards biotrophism. *Frontiers in Plant Science*, 5.

- BAUER, Z., GÓMEZ-GÓMEZ, L., BOLLER, T. & FELIX, G. 2001. Sensitivity of Different Ecotypes and Mutants of *Arabidopsis thaliana* toward the Bacterial Elicitor Flagellin Correlates with the Presence of Receptor-binding Sites. *Journal of Biological Chemistry*, 276, 45669-45676.
- BAUMBERGER, N. & BAULCOMBE, D. C. 2005. Arabidopsis ARGONAUTE1 is an RNA Slicer that selectively recruits microRNAs and short interfering RNAs. *Proceedings of the National Academy of Sciences*, 102, 11928-33.
- BAZIN, J., BUSTOS-SANMAMED, P., HARTMANN, C., LELANDAIS-BRIÈRE, C. & CRESPI, M. 2012. Complexity of miRNA-dependent regulation in root symbiosis. *Philosophical Transactions of the Royal Society B: Biological Sciences*, 367, 1570-1579.
- BECHTOLD, N. & PELLETIER, G. 1998. In planta *Agrobacterium*-mediated transformation of adult *Arabidopsis thaliana* plants by vacuum infiltration. *Methods in Molecular Biology*, 82, 259-66.
- BELOUSOV, V. V., FRADKOV, A. F., LUKYANOV, K. A., STAROVEROV, D. B., SHAKHBAZOV, K. S., TERSKIKH, A. V. & LUKYANOV, S. 2006. Genetically encoded fluorescent indicator for intracellular hydrogen peroxide. *Nat Meth*, 3, 281-286.
- BENEDITO, V. A., TORRES-JEREZ, I., MURRAY, J. D., ANDRIANKAJA, A., ALLEN, S., KAKAR, K., WANDREY, M., VERDIER, J., ZUBER, H., OTT, T., MOREAU, S., NIEBEL, A., FRICKEY, T., WEILLER, G., HE, J., DAI, X., ZHAO, P. X., TANG, Y. & UDVARDI, M. K. 2008. A gene expression atlas of the model legume *Medicago truncatula*. *The Plant Journal*, 55, 504-513.
- BERNSTEIN, E., CAUDY, A. A., HAMMOND, S. M. & HANNON, G. J. 2001. Role for a bidentate ribonuclease in the initiation step of RNA interference. *Nature*, 409, 363-6.
- BESSERER, A., PUECH-PAGES, V., KIEFER, P., GOMEZ-ROLDAN, V., JAUNEAU, A., ROY, S., PORTAIS, J. C., ROUX, C., BECARD, G. & SEJALON-DELMAS, N. 2006. Strigolactones stimulate arbuscular mycorrhizal fungi by activating mitochondria. *Plos Biology*, 4, 1239-1247.
- BETHKE, G., UNTHAN, T., UHRIG, J. F., PÖSCHL, Y., GUST, A. A., SCHEEL, D. & LEE, J. 2009. Flg22 regulates the release of an ethylene response factor substrate from MAP kinase 6 in *Arabidopsis thaliana* via ethylene signaling. *Proceedings of the National Academy of Sciences*, 106, 8067-8072.
- BHAT, R. A., MIKLIS, M., SCHMELZER, E., SCHULZE-LEFERT, P. & PANSTRUGA, R. 2005. Recruitment and interaction dynamics of plant penetration resistance components in a plasma membrane microdomain. *Proceedings of the National Academy of Sciences of the United States of America*, 102, 3135-3140.
- BLUME, B., NÜRNBERGER, T., NASS, N. & SCHEEL, D. 2000. Receptor-Mediated Increase in Cytoplasmic Free Calcium Required for Activation of Pathogen Defense in Parsley. *The Plant Cell Online*, 12, 1425-1440.
- BOISSON-DERNIER, A., CHABAUD, M., GARCIA, F., BÉCARD, G., ROSENBERG, C. & BARKER, D. G. 2001. *Agrobacterium* rhizogenes-Transformed Roots of *Medicago truncatula* for the Study of Nitrogen-Fixing and Endomycorrhizal Symbiotic Associations. *Molecular Plant-Microbe Interactions*, 14, 695-700.
- BREWIN, N. J. 1998. Tissue and cell invasion by *Rhizobium*: the structure and development of infection threads and symbiosomes. In: SPAINK, H. P., KONDOROSI, A., AND HOOYKAAS, P. J. J (ed.) *The Rhizobiaceae*. Kluwer Academic Publishers, Dordrecht, The Netherlands.
- BUENO, P., SOTO, M. J., RODRÍGUEZ-ROSALES, M. P., SANJUAN, J., OLIVARES, J. & DONAIRE, J. P. 2001. Time-course of lipoxygenase, antioxidant enzyme activities and H₂O₂ accumulation during the early stages of *Rhizobium*-legume symbiosis. *New Phytologist*, 152, 91-96.
- CAI, R., LEWIS, J., YAN, S., LIU, H., CLARKE, C. R., CAMPANILE, F., ALMEIDA, N. F., STUDHOLME, D. J., LINDEBERG, M., SCHNEIDER, D., ZACCARDELLI, M.,

- SETUBAL, J. C., MORALES-LIZCANO, N. P., BERNAL, A., COAKER, G., BAKER, C., BENDER, C. L., LEMAN, S. & VINATZER, B. A. 2011. The Plant Pathogen *Pseudomonas syringae* pv. *tomato* is Genetically Monomorphic and under Strong Selection to Evade Tomato Immunity. *PLoS Pathogens*, 7, e1002130.
- CANNON, S. B., STERCK, L., ROMBAUTS, S., SATO, S., CHEUNG, F., GOUZY, J., WANG, X., MUDGE, J., VASDEWANI, J., SCHIEX, T., SPANNAGL, M., MONAGHAN, E., NICHOLSON, C., HUMPHRAY, S. J., SCHOOF, H., MAYER, K. F. X., ROGERS, J., QUÉTIER, F., OLDROYD, G. E., DEBELLÉ, F., COOK, D. R., RETZEL, E. F., ROE, B. A., TOWN, C. D., TABATA, S., VAN DE PEER, Y. & YOUNG, N. D. 2006. Legume genome evolution viewed through the *Medicago truncatula* and *Lotus japonicus* genomes. *Proceedings of the National Academy of Sciences*, 103, 14959-14964.
- CAPOEN, W., SUN, J., WYSHAM, D., OTEGUI, M. S., VENKATESHWARAN, M., HIRSCH, S., MIWA, H., DOWNIE, J. A., MORRIS, R. J., ANÉ, J.-M. & OLDROYD, G. E. D. 2011. Nuclear membranes control symbiotic calcium signaling of legumes. *Proceedings of the National Academy of Sciences*.
- CATOIRA, R., GALERA, C., DE BILLY, F., PENMETS, R. V., JOURNET, E.-P., MAILLET, F., ROSENBERG, C., COOK, D., GOUGH, C. & DÉNARIÉ, J. 2000. Four Genes of *Medicago truncatula* Controlling Components of a Nod Factor Transduction Pathway. *The Plant Cell Online*, 12, 1647-1665.
- CERRI, M. R., FRANCES, L., LALOUM, T., AURIAC, M.-C., NIEBEL, A., OLDROYD, G. E. D., BARKER, D. G., FOURNIER, J. & DE CARVALHO-NIEBEL, F. 2012. *Medicago truncatula* ERN Transcription Factors: Regulatory Interplay with NSP1/NSP2 GRAS Factors and Expression Dynamics throughout Rhizobial Infection. *Plant Physiology*, 160, 2155-2172.
- CHARPENTIER, M., BREDEMEIER, R., WANNER, G., TAKEDA, N., SCHLEIFF, E. & PARNISKE, M. 2008. *Lotus japonicus* CASTOR and POLLUX Are Ion Channels Essential for Perinuclear Calcium Spiking in Legume Root Endosymbiosis. *Plant Cell*, 20, 3467-3479.
- CHEN, T., ZHU, H., KE, D., CAI, K., WANG, C., GOU, H., HONG, Z. & ZHANG, Z. 2012. A MAP Kinase Kinase Interacts with SymRK and Regulates Nodule Organogenesis in *Lotus japonicus*. *The Plant Cell Online*, 24, 823-838.
- CHENG, X., WEN, J., TADEGE, M., RATET, P. & MYSORE, K. S. 2011. Reverse Genetics in *Medicago truncatula* Using *Tnt1* Insertion Mutants. In: PEREIRA, A. (ed.) *Plant Reverse Genetics: Methods and Protocols*. Humana Press Inc.
- CHINCHILLA, D., ZIPFEL, C., ROBATZEK, S., KEMMERLING, B., NURNBERGER, T., JONES, J. D. G., FELIX, G. & BOLLER, T. 2007. A flagellin-induced complex of the receptor FLS2 and BAK1 initiates plant defence. *Nature*, 448, 497-500.
- CHUANG, C.-F. & MEYEROWITZ, E. M. 2000. Specific and heritable genetic interference by double-stranded RNA in *Arabidopsis thaliana*. *Proceedings of the National Academy of Sciences*, 97, 4985-4990.
- CLARK, S. E., WILLIAMS, R. W. & MEYEROWITZ, E. M. 1997. The *CLAVATA1* Gene Encodes a Putative Receptor Kinase That Controls Shoot and Floral Meristem Size in *Arabidopsis*. *Cell*, 89, 575-585.
- CRADDOCK, C., LAVAGI, I. & YANG, Z. 2012. New insights into Rho signaling from plant ROP/Rac GTPases. *Trends in Cell Biology*, 22, 492-501.
- CZAJA, L. F., HOGEKAMP, C., LAMM, P., MAILLET, F., MARTINEZ, E. A., SAMAIN, E., DENARIE, J., KUSTER, H. & HOHNJEC, N. 2012. Transcriptional responses toward diffusible signals from symbiotic microbes reveal *MtNFP*- and *MtDMI3*-dependent reprogramming of host gene expression by arbuscular mycorrhizal fungal lipochitooligosaccharides. *Plant Physiology*, 159, 1671-85.
- D'ERFURTH, I., COSSON, V., ESCHSTRUTH, A., LUCAS, H., KONDOROSI, A. & RATET, P. 2003. Efficient transposition of the *Tnt1* tobacco retrotransposon in the model legume *Medicago truncatula*. *The Plant Journal*, 34, 95-106.

- DAMIANI, I., BALDACCI-CRESP, F., HOPKINS, J., ANDRIO, E., BALZERGUE, S., LECOMTE, P., PUPPO, A., ABAD, P., FAVERY, B. & HEROUART, D. 2012. Plant genes involved in harbouring symbiotic rhizobia or pathogenic nematodes. *New Phytologist*, 194, 511-522.
- DANIEL GIETZ, R. & WOODS, R. A. 2002. Transformation of yeast by lithium acetate/single-stranded carrier DNA/polyethylene glycol method. In: CHRISTINE, G. & GERALD, R. F. (eds.) *Methods in Enzymology*. Academic Press.
- DANIEL, R. & GUEST, D. 2005. Defence responses induced by potassium phosphonate in *Phytophthora palmivora*-challenged *Arabidopsis thaliana*. *Physiological and Molecular Plant Pathology*, 67, 194-201.
- DAVID-SCHWARTZ, R., BADANI, H., SMADAR, W., LEVY, A. A., GALILI, G. & KAPULNIK, Y. 2001. Identification of a novel genetically controlled step in mycorrhizal colonization: plant resistance to infection by fungal spores but not extra-radical hyphae. *The Plant Journal*, 27, 561-569.
- DEMCHENKO, K., WINZER, T., STOUGAARD, J., PARNISKE, M. & PAWLOWSKI, K. 2004. Distinct roles of *Lotus japonicus* SYMRK and SYM15 in root colonization and arbuscule formation. *New Phytologist*, 163, 381-392.
- DENARIE, J., DEBELLE, F. & PROME, J. C. 1996. Rhizobium lipo-chitooligosaccharide nodulation factors: Signaling molecules mediating recognition and morphogenesis. *Annual Review of Biochemistry*, 65, 503-535.
- DEPICKER, A. & VAN MONTAGU, M. 1997. Post-transcriptional gene silencing in plants. *Current Opinion in Cell Biology*, 9, 373-382.
- DEVERS, E., TEPLY, J., REINERT, A., GAUDE, N. & KRAJINSKI, F. 2013. An endogenous artificial microRNA system for unraveling the function of root endosymbioses related genes in *Medicago truncatula*. *BMC Plant Biology*, 13, 82.
- EHRHARDT, D. W., WAIS, R. & LONG, S. R. 1996. Calcium Spiking in Plant Root Hairs Responding to Rhizobium Nodulation Signals. *Cell*, 85, 673-681.
- ELBASHIR, S. M., HARBORTH, J., LENDECKEL, W., YALCIN, A., WEBER, K. & TUSCHL, T. 2001. Duplexes of 21-nucleotide RNAs mediate RNA interference in cultured mammalian cells. *Nature*, 411, 494-8.
- ENDRE, G., KERESZT, A., KEVEI, Z., MIHACEA, S., KALO, P. & KISS, G. B. 2002. A receptor kinase gene regulating symbiotic nodule development. *Nature*, 417, 962-966.
- ENGLER, C., GRUETZNER, R., KANDZIA, R. & MARILLONNET, S. 2009. Golden gate shuffling: a one-pot DNA shuffling method based on type IIs restriction enzymes. *PLoS One*, 4, e5553.
- ENGLER, C., KANDZIA, R. & MARILLONNET, S. 2008. A one pot, one step, precision cloning method with high throughput capability. *PLoS One*, 3, e3647.
- ESSELING, J. J., LHUISSIER, F. G. P. & EMONS, A. M. C. 2003. Nod Factor-Induced Root Hair Curling: Continuous Polar Growth towards the Point of Nod Factor Application. *Plant Physiology*, 132, 1982-1988.
- EVANGELISTI, E., REY, T. & SCHORNACK, S. 2014. Cross-interference of plant development and plant-microbe interactions. *Current Opinion in Plant Biology*, 20, 118-126.
- FEDDERMANN, N., DUVVURU MUNI, R. R., ZEIER, T., STUURMAN, J., ERCOLIN, F., SCHORDERET, M. & REINHARDT, D. 2010. The PAM1 gene of petunia, required for intracellular accommodation and morphogenesis of arbuscular mycorrhizal fungi, encodes a homologue of VAPYRIN. *The Plant Journal*, 64, 470-481.
- FELIX, G., DURAN, J. D., VOLKO, S. & BOLLER, T. 1999. Plants have a sensitive perception system for the most conserved domain of bacterial flagellin. *The Plant Journal*, 18, 265-276.
- FESTER, T. & HAUSE, G. 2005. Accumulation of reactive oxygen species in arbuscular mycorrhizal roots. *Mycorrhiza*, 15, 373-379.

- FIRMIN, J. L., WILSON, K. E., ROSSEN, L. & JOHNSTON, A. W. B. 1986. Flavonoid activation of nodulation genes in *Rhizobium* reversed by other compounds present in plants. *Nature*, 324, 90-92.
- FOREMAN, J., DEMIDCHIK, V., BOTHWELL, J. H. F., MYLONA, P., MIEDEMA, H., TORRES, M. A., LINSTED, P., COSTA, S., BROWNLEE, C., JONES, J. D. G., DAVIES, J. M. & DOLAN, L. 2003. Reactive oxygen species produced by NADPH oxidase regulate plant cell growth. *Nature*, 422, 442-446.
- FOUCHER, F. & KONDOROSI, E. 2000. Cell cycle regulation in the course of nodule organogenesis in *Medicago*. *Plant Molecular Biology*, 43, 773-786.
- FOURNIER, J., TIMMERS, A. C. J., SIEBERER, B. J., JAUNEAU, A., CHABAUD, M. & BARKER, D. G. 2008. Mechanism of Infection Thread Elongation in Root Hairs of *Medicago truncatula* and Dynamic Interplay with Associated Rhizobial Colonization. *Plant Physiology*, 148, 1985-1995.
- FREYTAG, S., ARABATZIS, N., HAHLBROCK, K. & SCHMELZER, E. 1994. Reversible cytoplasmic rearrangements precede wall apposition, hypersensitive cell death and defense-related gene activation in potato/*Phytophthora infestans* interactions. *Planta*, 194, 123-135.
- GAMPALA, S. S., KIM, T.-W., HE, J.-X., TANG, W., DENG, Z., BAI, M.-Y., GUAN, S., LALONDE, S., SUN, Y., GENDRON, J. M., CHEN, H., SHIBAGAKI, N., FERL, R. J., EHRHARDT, D., CHONG, K., BURLINGAME, A. L. & WANG, Z.-Y. 2007. An Essential Role for 14-3-3 Proteins in Brassinosteroid Signal Transduction in *Arabidopsis*. *Developmental Cell*, 13, 177-189.
- GAO, L.-L. & XUE, H.-W. 2011. Global Analysis of Expression Profiles of Rice Receptor-Like Kinase Genes. *Molecular Plant*.
- GAPPER, C. & DOLAN, L. 2006. Control of Plant Development by Reactive Oxygen Species. *Plant Physiology*, 141, 341-345.
- GAUDE, N., BORTFELD, S., DUENSING, N., LOHSE, M. & KRAJINSKI, F. 2012. Arbuscule-containing and non-colonized cortical cells of mycorrhizal roots undergo extensive and specific reprogramming during arbuscular mycorrhizal development. *The Plant Journal*, 69, 510-28.
- GENRE, A., CHABAUD, M., BALZERGUE, C., PUECH-PAGÈS, V., NOVERO, M., REY, T., FOURNIER, J., ROCHANGE, S., BÉCARD, G., BONFANTE, P. & BARKER, D. G. 2013. Short-chain chitin oligomers from arbuscular mycorrhizal fungi trigger nuclear Ca²⁺ spiking in *Medicago truncatula* roots and their production is enhanced by strigolactone. *New Phytologist*, 198, 190-202.
- GENRE, A., CHABAUD, M., TIMMERS, T., BONFANTE, P. & BARKER, D. G. 2005. Arbuscular mycorrhizal fungi elicit a novel intracellular apparatus in *Medicago truncatula* root epidermal cells before infection. *Plant Cell*, 17, 3489-3499.
- GEURTS, R. & BISSELING, T. 2002. Rhizobium Nod Factor Perception and Signalling. *The Plant Cell Online*, 14, S239-S249.
- GIOVANNETTI, M. & MOSSE, B. 1980. Evaluation of techniques for measuring vesicular arbuscular mycorrhizal infection in roots. *New Phytologist*, 84, 489-500.
- GLEASON, C., CHAUDHURI, S., YANG, T., MUNOZ, A., POOVAIAH, B. W. & OLDROYD, G. E. D. 2006. Nodulation independent of rhizobia induced by a calcium-activated kinase lacking autoinhibition. *Nature*, 441, 1149-1152.
- GOBBATO, E., MARSH, JOHN F., VERNIÉ, T., WANG, E., MAILLET, F., KIM, J., MILLER, J. B., SUN, J., BANO, S. A., RATET, P., MYSORE, KIRANKUMAR S., DÉNARIÉ, J., SCHULTZE, M. & OLDROYD, GILES E. D. 2012. A GRAS-Type Transcription Factor with a Specific Function in Mycorrhizal Signaling. *Current Biology*, 22, 2236-2241.
- GÓMEZ-GÓMEZ, L. & BOLLER, T. 2000. FLS2: An LRR Receptor-like Kinase Involved in the Perception of the Bacterial Elicitor Flagellin in *Arabidopsis*. *Molecular Cell*, 5, 1003-1011.
- GOMEZ, S. K., JAVOT, H., DEEWATTHANAWONG, P., TORRES-JEREZ, I., TANG, Y., BLANCAFLOR, E., UDVARDI, M. & HARRISON, M. 2009. *Medicago truncatula*

- and *Glomus intraradices* gene expression in cortical cells harboring arbuscules in the arbuscular mycorrhizal symbiosis. *BMC Plant Biology*, 9, 10.
- GRANDBASTIEN, M. A., SPIELMANN, A. & CABOCHE, M. 1989. *Tnt1*, a mobile retroviral-like transposable element of tobacco isolated by plant cell genetics. *Nature*, 337, 376-80.
- GREBE, T. W. & STOCK, J. B. 1999. The histidine protein kinase superfamily. *Advances in Microbial Physiology*, 41, 139-227.
- GROTH, M., KOSUTA, S., GUTJAHR, C., HAAGE, K., HARDEL, S. L., SCHAUB, M., BRACHMANN, A., SATO, S., TABATA, S., FINDLAY, K., WANG, T. L. & PARNISKE, M. 2013. Two *Lotus japonicus* symbiosis mutants impaired at distinct steps of arbuscule development. *The Plant Journal*, 75, 117-129.
- GROTH, M., TAKEDA, N., PERRY, J., UCHIDA, H., DRAXL, S., BRACHMANN, A., SATO, S., TABATA, S., KAWAGUCHI, M., WANG, T. L. & PARNISKE, M. 2010. *NENA*, a *Lotus japonicus* Homolog of *Sec13*, Is Required for Rhizodermal Infection by Arbuscular Mycorrhiza Fungi and Rhizobia but Dispensable for Cortical Endosymbiotic Development. *Plant Cell*, 22, 2509-2526.
- GUEST, D. I. 1984. Modification of defense responses in tobacco and capsicum following treatment with Fosetyl-AI [Aluminium tris (o-ethyl phosphonate)]. *Physiological Plant Pathology*, 25, 125-134.
- GUEST, D. I. 1986. Evidence from light microscopy of living tissues that Fosetyl-AI modifies the defence response in tobacco seedlings following inoculation by *Phytophthora nicotianae* var *nicotianae*. *Physiological and Molecular Plant Pathology*, 29, 251-261.
- GUTJAHR, C. & PARNISKE, M. 2013. Cell and Developmental Biology of Arbuscular Mycorrhiza Symbiosis. *Annual Review of Cell and Developmental Biology*, 29, 593-617.
- GUTJAHR, C. & PASZKOWSKI, U. 2013. Multiple control levels of root system remodeling in arbuscular mycorrhizal symbiosis. *Frontiers in Plant Science*, 4, 204.
- GUTJAHR, C., RADOVANOVIC, D., GEOFFROY, J., ZHANG, Q., SIEGLER, H., CHIAPELLO, M., CASIERI, L., AN, K., AN, G., GUIDERDONI, E., KUMAR, C. S., SUNDARESAN, V., HARRISON, M. J. & PASZKOWSKI, U. 2012. The half-size ABC transporters STR1 and STR2 are indispensable for mycorrhizal arbuscule formation in rice. *The Plant Journal*, 69, 906-920.
- HAMILTON, A. V. O. C. L. B. D. 2002. Two classes of short interfering RNA in RNA silencing. *The EMBO Journal*, 21, 4671-4679.
- HAMMOND, S. M., BERNSTEIN, E., BEACH, D. & HANNON, G. J. 2000. An RNA-directed nuclease mediates post-transcriptional gene silencing in *Drosophila* cells. *Nature*, 404, 293-6.
- HANEY, C. H. & LONG, S. R. 2010. Plant flotillins are required for infection by nitrogen-fixing bacteria. *Proceedings of the National Academy of Sciences*, 107, 478-483.
- HANNON, G. J. 2002. RNA interference. *Nature*, 418, 244-251.
- HARRISON, M. J. 2005. Signaling in the arbuscular mycorrhizal symbiosis. *Annual Review of Microbiology*, 59, 19-42.
- HARTLEY, J. L., TEMPLE, G. F. & BRASCH, M. A. 2000. DNA cloning using in vitro site-specific recombination. *Genome Res*, 10, 1788-95.
- HE, J.-X., GENDRON, J. M., SUN, Y., GAMPALA, S. S. L., GENDRON, N., SUN, C. Q. & WANG, Z.-Y. 2005. BZR1 Is a Transcriptional Repressor with Dual Roles in Brassinosteroid Homeostasis and Growth Responses. *Science*, 307, 1634-1638.
- HE, J.-X., GENDRON, J. M., YANG, Y., LI, J. & WANG, Z.-Y. 2002. The GSK3-like kinase BIN2 phosphorylates and destabilizes BZR1, a positive regulator of the brassinosteroid signaling pathway in *Arabidopsis*. *Proceedings of the National Academy of Sciences*, 99, 10185-10190.
- HE, J., BENEDITO, V., WANG, M., MURRAY, J., ZHAO, P., TANG, Y. & UDVARDI, M. 2009. The *Medicago truncatula* gene expression atlas web server. *BMC Bioinformatics*, 10, 441.

- HE, X., LIU, Y.-M., WANG, W. & LI, Y. 2006. Distribution of G-actin is Related to Root Hair Growth of Wheat. *Annals of Botany*, 98, 49-55.
- HEATH, M. C., NIMICHUK, Z. L. & XU, H. 1997. Plant nuclear migrations as indicators of critical interactions between resistant or susceptible cowpea epidermal cells and invasion hyphae of the cowpea rust fungus. *New Phytologist*, 135, 689-700.
- HECKMANN, A. B., LOMBARDO, F., MIWA, H., PERRY, J. A., BUNNEWELL, S., PARNISKE, M., WANG, T. L. & DOWNIE, J. A. 2006. *Lotus japonicus* Nodulation Requires Two GRAS Domain Regulators, One of Which Is Functionally Conserved in a Non-Legume. *Plant Physiology*, 142, 1739-1750.
- HELLEMANS, J., MORTIER, G., DE PAEPE, A., SPELEMAN, F. & VANDESOMPELE, J. 2007. qBase relative quantification framework and software for management and automated analysis of real-time quantitative PCR data. *Genome Biology*, 8, 1-14.
- HIRSCH, S., KIM, J., MUÑOZ, A., HECKMANN, A. B., DOWNIE, J. A. & OLDROYD, G. E. D. 2009. GRAS Proteins Form a DNA Binding Complex to Induce Gene Expression during Nodulation Signaling in *Medicago truncatula*. *The Plant Cell Online*, 21, 545-557.
- HOGKAMP, C., ARNDT, D., PEREIRA, P. A., BECKER, J. D., HOHNJEC, N. & KUSTER, H. 2011. Laser microdissection unravels cell-type-specific transcription in arbuscular mycorrhizal roots, including CAAT-box transcription factor gene expression correlating with fungal contact and spread. *Plant Physiology*, 157, 2023-43.
- HORVÁTH, B., YEUN, L. H., DOMONKOS, Á., HALÁSZ, G., GOBBATO, E., AYAYDIN, F., MIRÓ, K., HIRSCH, S., SUN, J., TADEGE, M., RATET, P., MYSORE, K. S., ANÉ, J.-M., OLDROYD, G. E. D. & KALÓ, P. 2011. *Medicago truncatula* IPD3 Is a Member of the Common Symbiotic Signaling Pathway Required for Rhizobial and Mycorrhizal Symbioses. *Molecular Plant-Microbe Interactions*, 24, 1345-1358.
- HOUSEMAN, B. T. & MRKSICH, M. 2002. Carbohydrate Arrays for the Evaluation of Protein Binding and Enzymatic Modification. *Chemistry & Biology*, 9, 443-454.
- HUNTER, S., JONES, P., MITCHELL, A., APWEILER, R., ATTWOOD, T. K., BATEMAN, A., BERNARD, T., BINNS, D., BORK, P., BURGE, S., DE CASTRO, E., COGILL, P., CORBETT, M., DAS, U., DAUGHERTY, L., DUQUENNE, L., FINN, R. D., FRASER, M., GOUGH, J., HAFT, D., HULO, N., KAHN, D., KELLY, E., LETUNIC, I., LONSDALE, D., LOPEZ, R., MADERA, M., MASLEN, J., MCANULLA, C., MCDOWALL, J., MCMENAMIN, C., MI, H., MUTOWO-MUELLENET, P., MULDER, N., NATALE, D., ORENGO, C., PESSEAT, S., PUNTA, M., QUINN, A. F., RIVOIRE, C., SANGRADOR-VEGAS, A., SELENGUT, J. D., SIGRIST, C. J. A., SCHEREMETJEW, M., TATE, J., THIMMAJANARTHANAN, M., THOMAS, P. D., WU, C. H., YEATS, C. & YONG, S.-Y. 2012. InterPro in 2011: new developments in the family and domain prediction database. *Nucleic Acids Research*, 40, D306-D312.
- IMAIZUMI-ANRAKU, H., TAKEDA, N., CHARPENTIER, M., PERRY, J., MIWA, H., UMEHARA, Y., KOUCHI, H., MURAKAMI, Y., MULDER, L., VICKERS, K., PIKE, J., ALLAN DOWNIE, J., WANG, T., SATO, S., ASAMIZU, E., TABATA, S., YOSHIKAWA, M., MUROOKA, Y., WU, G.-J., KAWAGUCHI, M., KAWASAKI, S., PARNISKE, M. & HAYASHI, M. 2005. Plastid proteins crucial for symbiotic fungal and bacterial entry into plant roots. *Nature*, 433, 527-531.
- JACKSON, A. L., BARTZ, S. R., SCHELTER, J., KOBAYASHI, S. V., BURCHARD, J., MAO, M., LI, B., CAVET, G. & LINSLEY, P. S. 2003. Expression profiling reveals off-target gene regulation by RNAi. *Nature Biotechnology*, 21, 635-7.
- JAMET, A., MANDON, K., PUPPO, A. & HÉROUART, D. 2007. H₂O₂ Is Required for Optimal Establishment of the *Medicago sativa*/*Sinorhizobium meliloti* Symbiosis. *Journal of Bacteriology*, 189, 8741-8745.
- JAMET, A., SIGAUD, S., VAN DE SYPE, G., PUPPO, A. & HÉROUART, D. 2003. Expression of the Bacterial Catalase Genes During *Sinorhizobium meliloti*-

- Medicago sativa* Symbiosis and Their Crucial Role During the Infection Process. *Molecular Plant-Microbe Interactions*, 16, 217-225.
- JAVOT, H., PENMETS, R. V., BREUILLIN, F., BHATTARAI, K. K., NOAR, R. D., GOMEZ, S. K., ZHANG, Q., COOK, D. R. & HARRISON, M. J. 2011. *Medicago truncatula* *mtpt4* mutants reveal a role for nitrogen in the regulation of arbuscule degeneration in arbuscular mycorrhizal symbiosis. *The Plant Journal*, 68, 954-965.
- JAVOT, H., PENMETS, R. V., TERZAGHI, N., COOK, D. R. & HARRISON, M. J. 2007. A *Medicago truncatula* phosphate transporter indispensable for the arbuscular mycorrhizal symbiosis. *Proceedings of the National Academy of Sciences*, 104, 1720-1725.
- JAYARAMAN, D. R., BRENDAN K; FORSHEY, KARI L; HE, HENGBIN; ROSE, CHRIS; GRIMSRUD, PAUL; COON, JOSHUA J; COOK, DOUGLAS R; ANE, JEAN-MICHEL 2011. Regulation of symbiotic HMGR1 by receptor-like kinases. *Plant Biology 2011*. Minneapolis, Minnesota.
- JONES, J. D. G. & DANGL, J. L. 2006. The plant immune system. *Nature*, 444, 323-329.
- JONES, P., BINNS, D., CHANG, H.-Y., FRASER, M., LI, W., MCANULLA, C., MCWILLIAM, H., MASLEN, J., MITCHELL, A., NUKA, G., PESSEAT, S., QUINN, A. F., SANGRADOR-VEGAS, A., SCHEREMETJEW, M., YONG, S.-Y., LOPEZ, R. & HUNTER, S. 2014. InterProScan 5: genome-scale protein function classification. *Bioinformatics*.
- JONES, V. A. S. & DOLAN, L. 2012. The evolution of root hairs and rhizoids. *Annals of Botany*.
- JUNG, K.-H., CAO, P., SEO, Y.-S., DARDICK, C. & RONALD, P. C. 2010. The Rice Kinase Phylogenomics Database: a guide for systematic analysis of the rice kinase super-family. *Trends in plant science*, 15, 595-599.
- KALÓ, P., GLEASON, C., EDWARDS, A., MARSH, J., MITRA, R. M., HIRSCH, S., JAKAB, J., SIMS, S., LONG, S. R., ROGERS, J., KISS, G. B., DOWNIE, J. A. & OLDROYD, G. E. D. 2005. Nodulation Signaling in Legumes Requires NSP2, a Member of the GRAS Family of Transcriptional Regulators. *Science*, 308, 1786-1789.
- KANAMORI, N., MADSEN, L. H., RADUTOIU, S., FRANDESCU, M., QUISTGAARD, E. M. H., MIWA, H., DOWNIE, J. A., JAMES, E. K., FELLE, H. H., HAANING, L. L., JENSEN, T. H., SATO, S., NAKAMURA, Y., TABATA, S., SANDAL, N. & STOUGAARD, J. 2006. A nucleoporin is required for induction of Ca²⁺ spiking in legume nodule development and essential for rhizobial and fungal symbiosis. *Proceedings of the National Academy of Sciences of the United States of America*, 103, 359-364.
- KARIMI, M., INZÉ, D. & DEPICKER, A. 2002. GATEWAY™ vectors for Agrobacterium-mediated plant transformation. *Trends in Plant Science*, 7, 193-195.
- KEVEI, Z., LOUGNON, G., MERGAERT, P., HORVÁTH, G. V., KERESZT, A., JAYARAMAN, D., ZAMAN, N., MARCEL, F., REGULSKI, K., KISS, G. B., KONDOROSI, A., ENDRE, G., KONDOROSI, E. & ANÉ, J.-M. 2007. 3-Hydroxy-3-Methylglutaryl Coenzyme A Reductase1 Interacts with NORK and Is Crucial for Nodulation in *Medicago truncatula*. *The Plant Cell Online*, 19, 3974-3989.
- KIERS, E. T., DUHAMEL, M., BEESETTY, Y., MENSAH, J. A., FRANKEN, O., VERBRUGGEN, E., FELLBAUM, C. R., KOWALCHUK, G. A., HART, M. M., BAGO, A., PALMER, T. M., WEST, S. A., VANDENKOORNHUYSE, P., JANS, J. & BÜCKING, H. 2011. Reciprocal Rewards Stabilize Cooperation in the Mycorrhizal Symbiosis. *Science*, 333, 880-882.
- KIM, T.-W. & WANG, Z.-Y. 2010. Brassinosteroid Signal Transduction from Receptor Kinases to Transcription Factors. *Annual Review of Plant Biology*, 61, 681-704.
- KIM, T. W., GUAN, S., BURLINGAME, A. L. & WANG, Z. Y. 2011. The CDG1 kinase mediates brassinosteroid signal transduction from BRI1 receptor kinase to BSU1 phosphatase and GSK3-like kinase BIN2. *Molecular Cell*, 43, 561-71.

- KIM, T. W., GUAN, S., SUN, Y., DENG, Z., TANG, W., SHANG, J. X., SUN, Y., BURLINGAME, A. L. & WANG, Z. Y. 2009. Brassinosteroid signal transduction from cell-surface receptor kinases to nuclear transcription factors. *Nature Cell Biology*, 11, 1254-60.
- KISTNER, C. & PARNISKE, M. 2002. Evolution of signal transduction in intracellular symbiosis. *Trends in Plant Science*, 7, 511-518.
- KNIGHT, T. 2003. *Idempotent Vector Design for Standard Assembly of Biobricks* [Online]. MIT Artificial Intelligence Laboratory; MIT Synthetic Biology Working Group. Available: <http://hdl.handle.net/1721.1/21168> 2014].
- KOBAE, Y. & HATA, S. 2010. Dynamics of Periarbuscular Membranes Visualized with a Fluorescent Phosphate Transporter in Arbuscular Mycorrhizal Roots of Rice. *Plant and Cell Physiology*, 51, 341-353.
- KOGEL, K.-H., FRANKEN, P. & HÜCKELHOVEN, R. 2006. Endophyte or parasite – what decides? *Current Opinion in Plant Biology*, 9, 358-363.
- KOJIMA, T., SAITO, K., OBA, H., YOSHIDA, Y., TERASAWA, J., UMEHARA, Y., SUGANUMA, N., KAWAGUCHI, M. & OHTOMO, R. 2014. Isolation and Phenotypic Characterization of *Lotus japonicus* Mutants Specifically Defective in Arbuscular Mycorrhizal Formation. *Plant and Cell Physiology*, 55, 928-941.
- KRAJINSKI, F., COURTY, P.-E., SIEH, D., FRANKEN, P., ZHANG, H., BUCHER, M., GERLACH, N., KRYVORUCHKO, I., ZOELLER, D., UDVARDI, M. & HAUSE, B. 2014. The H⁺-ATPase HA1 of *Medicago truncatula* Is Essential for Phosphate Transport and Plant Growth during Arbuscular Mycorrhizal Symbiosis. *The Plant Cell Online*, 26, 1808-1817.
- KUPPUSAMY, K. T., ENDRE, G., PRABHU, R., PENMETS, R. V., VEERESHINGAM, H., COOK, D. R., DICKSTEIN, R. & VANDENBOSCH, K. A. 2004. *LIN*, a *Medicago truncatula* Gene Required for Nodule Differentiation and Persistence of Rhizobial Infections. *Plant Physiology*, 136, 3682-3691.
- LALUK, K., LUO, H., CHAI, M., DHAWAN, R., LAI, Z. & MENGISTE, T. 2011. Biochemical and Genetic Requirements for Function of the Immune Response Regulator BOTRYTIS-INDUCED KINASE1 in Plant Growth, Ethylene Signaling, and PAMP-Triggered Immunity in Arabidopsis. *The Plant Cell Online*, 23, 2831-2849.
- LECOURIEUX, D., MAZARS, C., PAULY, N., RANJEVA, R. & PUGIN, A. 2002. Analysis and Effects of Cytosolic Free Calcium Increases in Response to Elicitors in *Nicotiana plumbaginifolia* Cells. *The Plant Cell Online*, 14, 2627-2641.
- LEFEBVRE, B., TIMMERS, T., MBENGUE, M., MOREAU, S., HERVÉ, C., TÓTH, K., BITTENCOURT-SILVESTRE, J., KLAUS, D., DESLANDES, L., GODIARD, L., MURRAY, J. D., UDVARDI, M. K., RAFFAELE, S., MONGRAND, S., CULLIMORE, J., GAMAS, P., NIEBEL, A. & OTT, T. 2010. A remorin protein interacts with symbiotic receptors and regulates bacterial infection. *Proceedings of the National Academy of Sciences*, 107, 2343-2348.
- LEVINE, A., TENHAKEN, R., DIXON, R. & LAMB, C. 1994. H₂O₂ from the oxidative burst orchestrates the plant hypersensitive disease resistance response. *Cell*, 79, 583-593.
- LÉVY, J., BRES, C., GEURTS, R., CHALHOUB, B., KULIKOVA, O., DUC, G., JOURNET, E.-P., ANÉ, J.-M., LAUBER, E., BISSELING, T., DÉNARIÉ, J., ROSENBERG, C. & DEBELLÉ, F. 2004. A Putative Ca²⁺ and Calmodulin-Dependent Protein Kinase Required for Bacterial and Fungal Symbioses. *Science*, 303, 1361-1364.
- LI, J., NAM, K. H., VAFEADOS, D. & CHORY, J. 2001. *BIN2*, a New Brassinosteroid-Insensitive Locus in *Arabidopsis*. *Plant Physiology*, 127, 14-22.
- LI, J., WEN, J., LEASE, K. A., DOKE, J. T., TAX, F. E. & WALKER, J. C. 2002. BAK1, an *Arabidopsis* LRR Receptor-like Protein Kinase, Interacts with BRI1 and Modulates Brassinosteroid Signaling. *Cell*, 110, 213-222.
- LI, L., LI, M., YU, L., ZHOU, Z., LIANG, X., LIU, Z., CAI, G., GAO, L., ZHANG, X., WANG, Y., CHEN, S. & ZHOU, J.-M. 2014. The FLS2-Associated Kinase BIK1 Directly

- Phosphorylates the NADPH Oxidase RbohD to Control Plant Immunity. *Cell Host & Microbe*, 15, 329-338.
- LIMPENS, E., FRANKEN, C., SMIT, P., WILLEMSE, J., BISSELING, T. & GEURTS, R. 2003. LysM Domain Receptor Kinases Regulating Rhizobial Nod Factor-Induced Infection. *Science*, 302, 630-633.
- LIN, W., LU, D., GAO, X., JIANG, S., MA, X., WANG, Z., MENGISTE, T., HE, P. & SHAN, L. 2013. Inverse modulation of plant immune and brassinosteroid signaling pathways by the receptor-like cytoplasmic kinase BIK1. *Proceedings of the National Academy of Sciences*, 110, 12114-12119.
- LIU, W., KOHLEN, W., LILLO, A., OP DEN CAMP, R., IVANOV, S., HARTOG, M., LIMPENS, E., JAMIL, M., SMACZNIAK, C., KAUFMANN, K., YANG, W.-C., HOOIVELD, G. J. E. J., CHARNIKHOVA, T., BOUWMEESTER, H. J., BISSELING, T. & GEURTS, R. 2011. Strigolactone Biosynthesis in *Medicago truncatula* and Rice Requires the Symbiotic GRAS-Type Transcription Factors NSP1 and NSP2. *The Plant Cell Online*, 23, 3853-3865.
- LU, D., WU, S., GAO, X., ZHANG, Y., SHAN, L. & HE, P. 2010. A receptor-like cytoplasmic kinase, BIK1, associates with a flagellin receptor complex to initiate plant innate immunity. *Proceedings of the National Academy of Sciences*, 107, 496-501.
- MADSEN, E. B., MADSEN, L. H., RADUTOIU, S., OLBRYT, M., RAKWALSKA, M., SZCZYGLOWSKI, K., SATO, S., KANEKO, T., TABATA, S., SANDAL, N. & STOUGAARD, J. 2003. A receptor kinase gene of the LysM type is involved in legume perception of rhizobial signals. *Nature*, 425, 637-640.
- MAEKAWA, T., KUSAKABE, M., SHIMODA, Y., SATO, S., TABATA, S., MUROOKA, Y. & HAYASHI, M. 2008. Polyubiquitin Promoter-Based Binary Vectors for Overexpression and Gene Silencing in *Lotus japonicus*. *Molecular Plant-Microbe Interactions*, 21, 375-382.
- MAILLET, F., POINSOT, V., ANDRE, O., PUECH-PAGES, V., HAOUY, A., GUEUNIER, M., CROMER, L., GIRAUDET, D., FORMEY, D., NIEBEL, A., MARTINEZ, E. A., DRIGUEZ, H., BECARD, G. & DENARIE, J. 2011. Fungal lipochitooligosaccharide symbiotic signals in arbuscular mycorrhiza. *Nature*, 469, 58-U1501.
- MBENGUE, M., CAMUT, S., DE CARVALHO-NIEBEL, F., DESLANDES, L., FROIDURE, S., KLAUS-HEISEN, D., MOREAU, S., RIVAS, S., TIMMERS, T., HERVÉ, C., CULLIMORE, J. & LEFEBVRE, B. 2010. The *Medicago truncatula* E3 Ubiquitin Ligase PUB1 Interacts with the LYK3 Symbiotic Receptor and Negatively Regulates Infection and Nodulation. *The Plant Cell Online*, 22, 3474-3488.
- MERGAERT, P., UCHIUMI, T., ALUNNI, B., EVANNO, G., CHERON, A., CATRICE, O., MAUSSET, A.-E., BARLOY-HUBLER, F., GALIBERT, F., KONDOROSI, A. & KONDOROSI, E. 2006. Eukaryotic control on bacterial cell cycle and differentiation in the *Rhizobium*-legume symbiosis. *Proceedings of the National Academy of Sciences of the United States of America*, 103, 5230-5235.
- MESSINESE, E., MUN, J. H., YEUN, L. H., JAYARAMAN, D., ROUGE, P., BARRE, A., LOUGNON, G., SCHORNACK, S., BONO, J. J., COOK, D. R. & ANE, J. M. 2007. A novel nuclear protein interacts with the symbiotic DMI3 calcium- and calmodulin-dependent protein kinase of *Medicago truncatula*. *Molecular Plant-Microbe Interactions*, 20, 912-921.
- MIDDLETON, P. H., JAKAB, J., PENMETSIA, R. V., STARKER, C. G., DOLL, J., KALÓ, P., PRABHU, R., MARSH, J. F., MITRA, R. M., KERESZT, A., DUDAS, B., VANDENBOSCH, K., LONG, S. R., COOK, D. R., KISS, G. B. & OLDROYD, G. E. D. 2007. An ERF Transcription Factor in *Medicago truncatula* That Is Essential for Nod Factor Signal Transduction. *The Plant Cell Online*, 19, 1221-1234.
- MILLER, J. B., PRATAP, A., MIYAHARA, A., ZHOU, L., BORNEMANN, S., MORRIS, R. J. & OLDROYD, G. E. D. 2013. Calcium/Calmodulin-Dependent Protein Kinase Is Negatively and Positively Regulated by Calcium, Providing a Mechanism for Decoding Calcium Responses during Symbiosis Signaling. *The Plant Cell Online*.

- MITRA, R. M., GLEASON, C. A., EDWARDS, A., HADFIELD, J., DOWNIE, J. A., OLDROYD, G. E. D. & LONG, S. R. 2004. A Ca²⁺/calmodulin-dependent protein kinase required for symbiotic nodule development: Gene identification by transcript-based cloning. *Proceedings of the National Academy of Sciences of the United States of America*, 101, 4701-4705.
- MIWA, H., SUN, J., OLDROYD, G. E. D. & DOWNIE, J. A. 2006. Analysis of nod-factor-induced calcium signaling in root hairs of symbiotically defective mutants of *Lotus japonicus*. *Molecular Plant-Microbe Interactions*, 19, 914-923.
- MOLNAR, A., CSORBA, T., LAKATOS, L., VARALLYAY, E., LACOMME, C. & BURGYN, J. 2005. Plant virus-derived small interfering RNAs originate predominantly from highly structured single-stranded viral RNAs. *Journal of Virology*, 79, 7812-8.
- MORA-GARCÍA, S., VERT, G., YIN, Y., CAÑO-DELGADO, A., CHEONG, H. & CHORY, J. 2004. Nuclear protein phosphatases with Kelch-repeat domains modulate the response to brassinosteroids in *Arabidopsis*. *Genes & Development*, 18, 448-460.
- MURRAY, J. D. 2011. Invasion by Invitation: Rhizobial Infection in Legumes. *Molecular Plant-Microbe Interactions*, 24, 631-639.
- MURRAY, J. D., MUNI, R. R. D., TORRES-JEREZ, I., TANG, Y., ALLEN, S., ANDRIANKAJA, M., LI, G., LAXMI, A., CHENG, X., WEN, J., VAUGHAN, D., SCHULTZE, M., SUN, J., CHARPENTIER, M., OLDROYD, G., TADEGE, M., RATET, P., MYSORE, K. S., CHEN, R. & UDVARDI, M. K. 2011. *Vapyrin*, a gene essential for intracellular progression of arbuscular mycorrhizal symbiosis, is also essential for infection by rhizobia in the nodule symbiosis of *Medicago truncatula*. *The Plant Journal*, 65, 244-252.
- MUTO, H., YABE, N., ASAMI, T., HASUNUMA, K. & YAMAMOTO, K. T. 2004. Overexpression of *Constitutive Differential Growth 1* Gene, Which Encodes a RLCKVII-Subfamily Protein Kinase, Causes Abnormal Differential and Elongation Growth after Organ Differentiation in *Arabidopsis*. *Plant Physiology*, 136, 3124-3133.
- NAM, K. H. & LI, J. 2002. BRI1/BAK1, a Receptor Kinase Pair Mediating Brassinosteroid Signaling. *Cell*, 110, 203-212.
- NANDA, A. K., ANDRIO, E., MARINO, D., PAULY, N. & DUNAND, C. 2010. Reactive Oxygen Species during Plant-microorganism Early Interactions. *Journal of Integrative Plant Biology*, 52, 195-204.
- NIWA, S., KAWAGUCHI, M., IMAIZUMI-ANRAKU, H., CHECHETKA, S. A., ISHIZAKA, M., IKUTA, A. & KOUCHI, H. 2001. Responses of a Model Legume *Lotus japonicus* to Lipochitin Oligosaccharide Nodulation Factors Purified from *Mesorhizobium loti* JRL501. *Molecular Plant-Microbe Interactions*, 14, 848-856.
- NÜHSE, T. S., BOTTRILL, A. R., JONES, A. M. E. & PECK, S. C. 2007. Quantitative phosphoproteomic analysis of plasma membrane proteins reveals regulatory mechanisms of plant innate immune responses. *The Plant Journal*, 51, 931-940.
- NÜHSE, T. S., PECK, S. C., HIRT, H. & BOLLER, T. 2000. Microbial Elicitors Induce Activation and Dual Phosphorylation of the *Arabidopsis thaliana* MAPK 6. *Journal of Biological Chemistry*, 275, 7521-7526.
- OLÁH, B., BRIÈRE, C., BÉCARD, G., DÉNARIÉ, J. & GOUGH, C. 2005. Nod factors and a diffusible factor from arbuscular mycorrhizal fungi stimulate lateral root formation in *Medicago truncatula* via the DMI1/DMI2 signalling pathway. *The Plant Journal*, 44, 195-207.
- OLDROYD, G. E. D. & DOWNIE, J. A. 2008. Coordinating Nodule Morphogenesis with Rhizobial Infection in Legumes. *Annual Review of Plant Biology*, 59, 519-546.
- OLDROYD, G. E. D. & LONG, S. R. 2003. Identification and Characterization of *Nodulation-Signaling Pathway 2*, a Gene of *Medicago truncatula* Involved in Nod Factor Signaling. *Plant Physiology*, 131, 1027-1032.
- OLDROYD, G. E. D., MURRAY, J. D., POOLE, P. S. & DOWNIE, J. A. 2011. The Rules of Engagement in the Legume-Rhizobial Symbiosis. *In*: BASSLER, B. L., LICHTEN,

- M. & SCHUPBACH, G. (eds.) *Annual Review Genetics, Vol 45*. Palo Alto: Annual Reviews.
- OP DEN CAMP, R., STRENG, A., DE MITA, S., CAO, Q., POLONE, E., LIU, W., AMMIRAJU, J. S. S., KUDRNA, D., WING, R., UNTERGASSER, A., BISSELING, T. & GEURTS, R. 2011. LysM-Type Mycorrhizal Receptor Recruited for Rhizobium Symbiosis in Nonlegume *Parasponia*. *Science*, 331, 909-912.
- OPALSKI, K. S., SCHULTHEISS, H., KOGEL, K.-H. & HÜCKELHOVEN, R. 2005. The receptor-like MLO protein and the RAC/ROP family G-protein RACB modulate actin reorganization in barley attacked by the biotrophic powdery mildew fungus *Blumeria graminis f.sp. hordei*. *The Plant Journal*, 41, 291-303.
- OSSOWSKI, S., SCHWAB, R. & WEIGEL, D. 2008. Gene silencing in plants using artificial microRNAs and other small RNAs. *Plant Journal*, 53, 674-90.
- PALATNIK, J. F., ALLEN, E., WU, X., SCHOMMER, C., SCHWAB, R., CARRINGTON, J. C. & WEIGEL, D. 2003. Control of leaf morphogenesis by microRNAs. *Nature*, 425, 257-263.
- PARK, S., LEE, M.-R., PYO, S.-J. & SHIN, I. 2004. Carbohydrate Chips for Studying High-Throughput Carbohydrate-Protein Interactions. *Journal of the American Chemical Society*, 126, 4812-4819.
- PARNISKE, M. 2000. Intracellular accommodation of microbes by plants: a common developmental program for symbiosis and disease? *Current Opinion in Plant Biology*, 3, 320-328.
- PARNISKE, M. 2008. Arbuscular mycorrhiza: the mother of plant root endosymbioses. *Nature Review Microbiology*, 6, 763-775.
- PASZKOWSKI, U. 2006. Mutualism and parasitism: the yin and yang of plant symbioses. *Current Opinion in Plant Biology*, 9, 364-370.
- PAULY, N., PUCCIARIELLO, C., MANDON, K., INNOCENTI, G., JAMET, A., BAUDOIN, E., HÉROUART, D., FREND, P. & PUPPO, A. 2006. Reactive oxygen and nitrogen species and glutathione: key players in the legume-Rhizobium symbiosis. *Journal of Experimental Botany*, 57, 1769-1776.
- PECK, M. C., FISHER, R. F. & LONG, S. R. 2006. Diverse flavonoids stimulate NodD1 binding to *nod* gene promoters in *Sinorhizobium meliloti*. *Journal of Bacteriology*, 188, 5417-27.
- PELEG-GROSSMAN, S., MELAMED-BOOK, N. & LEVINE, A. 2012. ROS production during symbiotic infection suppresses pathogenesis-related gene expression. *Plant Signaling & Behavior*, 7, 409-415.
- PELEG-GROSSMAN, S., VOLPIN, H. & LEVINE, A. 2007. Root hair curling and Rhizobium infection in *Medicago truncatula* are mediated by phosphatidylinositol-regulated endocytosis and reactive oxygen species. *Journal of Experimental Botany*, 58, 1637-1649.
- PENNETSA, R. V. & COOK, D. R. 1997. A Legume Ethylene-Insensitive Mutant Hyperinfected by Its Rhizobial Symbiont. *Science*, 275, 527-530.
- PETERSON, R. L., MASSICOTTE, H. B. & MELVILLE, L. H. 2004. *Myorrhiza: Anatomy and Cell Biology*, CABI Publishing.
- PETUTSCHNIG, E. K., JONES, A. M. E., SERAZETDINOVA, L., LIPKA, U. & LIPKA, V. 2010. The Lysin Motif Receptor-like Kinase (LysM-RLK) CERK1 Is a Major Chitin-binding Protein in *Arabidopsis thaliana* and Subject to Chitin-induced Phosphorylation. *Journal of Biological Chemistry*, 285, 28902-28911.
- PRAYITNO, J., ROLFE, B. G. & MATHESIU, U. 2006. The Ethylene-Insensitive *sickle* Mutant of *Medicago truncatula* Shows Altered Auxin Transport Regulation during Nodulation. *Plant Physiology*, 142, 168-180.
- PUMPLIN, N., MONDO, S. J., TOPP, S., STARKER, C. G., GANTT, J. S. & HARRISON, M. J. 2010. *Medicago truncatula* Vapyrin is a novel protein required for arbuscular mycorrhizal symbiosis. *The Plant Journal*, 61, 482-494.
- RADUTOIU, S., MADSEN, L. H., MADSEN, E. B., FELLE, H. H., UMEHARA, Y., GRONLUND, M., SATO, S., NAKAMURA, Y., TABATA, S., SANDAL, N. &

- STOUGAARD, J. 2003. Plant recognition of symbiotic bacteria requires two LysM receptor-like kinases. *Nature*, 425, 585-592.
- RADUTOIU, S., MADSEN, L. H., MADSEN, E. B., JURKIEWICZ, A., FUKAI, E., QUISTGAARD, E. M. H., ALBREKTSEN, A. S., JAMES, E. K., THIRUP, S. & STOUGAARD, J. 2007. LysM domains mediate lipochitin-oligosaccharide recognition and Nfr genes extend the symbiotic host range. *EMBO J*, 26, 3923-3935.
- RAMU, S. K., PENG, H.-M. & COOK, D. R. 2002. Nod Factor Induction of Reactive Oxygen Species Production Is Correlated with Expression of the Early Nodulin Gene *rip1* in *Medicago truncatula*. *Molecular Plant-Microbe Interactions*, 15, 522-528.
- RATO, C., MONTEIRO, D., HEPLER, P. K. & MALHÓ, R. 2004. Calmodulin activity and cAMP signalling modulate growth and apical secretion in pollen tubes. *The Plant Journal*, 38, 887-897.
- REBATCHOUK, D., DARASELIA, N. & NARITA, J. O. 1996. NOMAD: a versatile strategy for in vitro DNA manipulation applied to promoter analysis and vector design. *Proc Natl Acad Sci U S A*, 93, 10891-6.
- RECH, S. S., HEIDT, S. & REQUENA, N. 2013. A tandem Kunitz protease inhibitor (KPI106)–serine carboxypeptidase (*SCP1*) controls mycorrhiza establishment and arbuscule development in *Medicago truncatula*. *The Plant Journal*, 75, 711-725.
- REDDY D. M. R, S., SCHORDERET, M., FELLER, U. & REINHARDT, D. 2007. A petunia mutant affected in intracellular accommodation and morphogenesis of arbuscular mycorrhizal fungi. *The Plant Journal*, 51, 739-750.
- REDMOND, J. W., BATLEY, M., DJORDJEVIC, M. A., INNES, R. W., KUEMPEL, P. L. & ROLFE, B. G. 1986. Flavones induce expression of nodulation genes in *Rhizobium*. *Nature*, 323, 632-635.
- REMY, W., TAYLOR, T. N., HASS, H. & KERP, H. 1994. Four hundred-million-year-old vesicular arbuscular mycorrhizae. *Proceedings of the National Academy of Sciences*, 91, 11841-11843.
- REY, T., NARS, A., BONHOMME, M., BOTTIN, A., HUGUET, S., BALZERGUE, S., JARDINAUD, M.-F., BONO, J.-J., CULLIMORE, J., DUMAS, B., GOUGH, C. & JACQUET, C. 2013. NFP, a LysM protein controlling Nod factor perception, also intervenes in *Medicago truncatula* resistance to pathogens. *New Phytologist*, 198, 875-886.
- REY, T. & SCHORNACK, S. 2013. Interactions of beneficial and detrimental root-colonizing filamentous microbes with plant hosts. *Genome Biology*, 14, 1-6.
- RICH, M. K., SCHORDERET, M. & REINHARDT, D. 2014. The role of the cell wall compartment in mutualistic symbioses of plants. *Frontiers in Plant Science*, 5.
- RIVAL, P., DE BILLY, F., BONO, J.-J., GOUGH, C., ROSENBERG, C. & BENSMIHEN, S. 2012. Epidermal and cortical roles of NFP and DMI3 in coordinating early steps of nodulation in *Medicago truncatula*. *Development*, 139, 3383-3391.
- ROBATZEK, S., BITTEL, P., CHINCHILLA, D., KÖCHNER, P., FELIX, G., SHIU, S.-H. & BOLLER, T. 2007. Molecular identification and characterization of the tomato flagellin receptor LeFLS2, an orthologue of *Arabidopsis* FLS2 exhibiting characteristically different perception specificities. *Plant Molecular Biology*, 64, 539-547.
- ROUX, M., SCHWESSINGER, B., ALBRECHT, C., CHINCHILLA, D., JONES, A., HOLTON, N., MALINOVSKY, F. G., TÖR, M., DE VRIES, S. & ZIPFEL, C. 2011. The *Arabidopsis* Leucine-Rich Repeat Receptor–Like Kinases BAK1/SERK3 and BKK1/SERK4 Are Required for Innate Immunity to Hemibiotrophic and Biotrophic Pathogens. *The Plant Cell Online*, 23, 2440-2455.
- RUIZ-LOZANO, J. M., GIANINAZZI, S. & GIANINAZZI-PEARSON, V. 1999. Genes involved in resistance to powdery mildew in barley differentially modulate root colonization by the mycorrhizal fungus *Glomus mosseae*. *Mycorrhiza*, 9, 237-240.

- RUSSINOVA, E., BORST, J.-W., KWAAITAAL, M., CAÑO-DELGADO, A., YIN, Y., CHORY, J. & DE VRIES, S. C. 2004. Heterodimerization and Endocytosis of *Arabidopsis* Brassinosteroid Receptors BRI1 and AtSERK3 (BAK1). *The Plant Cell Online*, 16, 3216-3229.
- SAITO, K., YOSHIKAWA, M., YANO, K., MIWA, H., UCHIDA, H., ASAMIZU, E., SATO, S., TABATA, S., IMAIZUMI-ANRAKU, H., UMEHARA, Y., KOUCHI, H., MUROOKA, Y., SZCZYGLOWSKI, K., DOWNIE, J. A., PARNISKE, M., HAYASHI, M. & KAWAGUCHI, M. 2007. NUCLEOPORIN85 is required for calcium spiking, fungal and bacterial symbioses, and seed production in *Lotus japonicus*. *Plant Cell*, 19, 610-624.
- SANTOS, R., HÉROUART, D., PUPPO, A. & TOUATI, D. 2000. Critical protective role of bacterial superoxide dismutase in *Rhizobium*-legume symbiosis. *Molecular Microbiology*, 38, 750-759.
- SANTOS, R., HÉROUART, D., SIGAUD, S., TOUATI, D. & PUPPO, A. 2001. Oxidative Burst in Alfalfa-*Sinorhizobium meliloti* Symbiotic Interaction. *Molecular Plant-Microbe Interactions*, 14, 86-89.
- SCHAUSER, L., ROUSSIS, A., STILLER, J. & STOUGAARD, J. 1999. A plant regulator controlling development of symbiotic root nodules. *Nature*, 402, 191-195.
- SCHULZE, B., MENTZEL, T., JEHL, A. K., MUELLER, K., BEELER, S., BOLLER, T., FELIX, G. & CHINCHILLA, D. 2010. Rapid Heteromerization and Phosphorylation of Ligand-activated Plant Transmembrane Receptors and Their Associated Kinase BAK1. *Journal of Biological Chemistry*, 285, 9444-9451.
- SCHWESSINGER, B. & RONALD, P. C. 2012. Plant Innate Immunity: Perception of Conserved Microbial Signatures. *Annual Review of Plant Biology*, 63, 451-482.
- SCHWESSINGER, B., ROUX, M., KADOTA, Y., NTOUKAKIS, V., SKLENAR, J., JONES, A. & ZIPFEL, C. 2011. Phosphorylation-Dependent Differential Regulation of Plant Growth, Cell Death, and Innate Immunity by the Regulatory Receptor-Like Kinase BAK1. *PLoS Genetics*, 7, e1002046.
- SEABRA, A. R., PEREIRA, P. A., BECKER, J. D. & CARVALHO, H. G. 2012. Inhibition of glutamine synthetase by phosphinothricin leads to transcriptome reprogramming in root nodules of *Medicago truncatula*. *Molecular Plant Microbe Interactions*, 25, 976-92.
- SHAILES, S. 2014. *Regulation of Calcium Influx and Reactive Oxygen Species Production During Infection of Legumes by Rhizobia*. Doctor of Philosophy, University of East Anglia.
- SHAW, S. L. & LONG, S. R. 2003. Nod Factor Inhibition of Reactive Oxygen Efflux in a Host Legume. *Plant Physiology*, 132, 2196-2204.
- SHETTY, R. P., ENDY, D. & KNIGHT, T. F., JR. 2008. Engineering BioBrick vectors from BioBrick parts. *Journal of Biological Engineering*, 2, 5.
- SHI, H., SHEN, Q., QI, Y., YAN, H., NIE, H., CHEN, Y., ZHAO, T., KATAGIRI, F. & TANG, D. 2013a. BR-SIGNALING KINASE1 physically associates with FLAGELLIN SENSING2 and regulates plant innate immunity in *Arabidopsis*. *Plant Cell*, 25, 1143-57.
- SHI, H., YAN, H., LI, J. & TANG, D. 2013b. BSK1, a receptor-like cytoplasmic kinase, involved in both BR signaling and innate immunity in *Arabidopsis*. *Plant Signalling and Behaviour*, 8.
- SHIMIZU, T., NAKANO, T., TAKAMIZAWA, D., DESAKI, Y., ISHII-MINAMI, N., NISHIZAWA, Y., MINAMI, E., OKADA, K., YAMANE, H., KAKU, H. & SHIBUYA, N. 2010. Two LysM receptor molecules, CEBiP and OsCERK1, cooperatively regulate chitin elicitor signaling in rice. *The Plant Journal*, 64, 204-214.
- SHIU, S.-H. & BLEECKER, A. B. 2001a. Plant receptor-like kinase gene family: diversity, function, and signaling. *Science STKE*, 2001, re22.
- SHIU, S.-H. & BLEECKER, A. B. 2001b. Receptor-like kinases from *Arabidopsis* form a monophyletic gene family related to animal receptor kinases. *Proceedings of the National Academy of Sciences*, 98, 10763-10768.

- SHIU, S.-H. & BLEECKER, A. B. 2003. Expansion of the receptor-like kinase/Pelle gene family and receptor-like proteins in *Arabidopsis*. *Plant Physiology*, 132, 530-543.
- SHIU, S.-H., KARLOWSKI, W. M., PAN, R., TZENG, Y.-H., MAYER, K. F. X. & LI, W.-H. 2004. Comparative Analysis of the Receptor-Like Kinase Family in *Arabidopsis* and Rice. *The Plant Cell Online*, 16, 1220-1234.
- SIEBERER, B. J., CHABAUD, M., TIMMERS, A. C., MONIN, A., FOURNIER, J. & BARKER, D. G. 2009. A Nuclear-Targeted Cameleon Demonstrates Intracellular Ca²⁺ Spiking in *Medicago truncatula* Root Hairs in Response to Rhizobial Nodulation Factors. *Plant Physiology*, 151, 1197-1206.
- SINGH, S., KATZER, K., LAMBERT, J., CERRI, M. & PARNISKE, M. 2014. CYCLOPS, A DNA-Binding Transcriptional Activator, Orchestrates Symbiotic Root Nodule Development. *Cell Host & Microbe*, 15, 139-152.
- SMIT, P., LIMPENS, E., GEURTS, R., FEDOROVA, E., DOLGIKH, E., GOUGH, C. & BISSELING, T. 2007. *Medicago* LYK3, an entry receptor in rhizobial nodulation factor signaling. *Plant Physiology*, 145, 183-191.
- SMIT, P., RAEDTS, J., PORTYANKO, V., DEBELLE, F., GOUGH, C., BISSELING, T. & GEURTS, R. 2005. NSP1 of the GRAS protein family is essential for rhizobial Nod factor-induced transcription. *Science*, 308, 1789-1791.
- SPRENT, J. I. 2001. *Nodulation in Legumes*, The Cromwell Press Ltd.
- SREERAMULU, S., MOSTIZKY, Y., SUNITHA, S., SHANI, E., NAHUM, H., SALOMON, D., HAYUN, L. B., GRUETTER, C., RAUH, D., ORI, N. & SESSA, G. 2013. BSKs are partially redundant positive regulators of brassinosteroid signaling in *Arabidopsis*. *Plant J*, 74, 905-19.
- STARKER, C. G., PARRA-COLMENARES, A. L., SMITH, L., MITRA, R. M. & LONG, S. R. 2006. Nitrogen Fixation Mutants of *Medicago truncatula* Fail to Support Plant and Bacterial Symbiotic Gene Expression. *Plant Physiology*, 140, 671-680.
- STONE, J. M. & WALKER, J. C. 1995. Plant Protein Kinase Families and Signal Transduction. *Plant Physiology*, 108, 451-457.
- STRACKE, S., KISTNER, C., YOSHIDA, S., MULDER, L., SATO, S., KANEKO, T., TABATA, S., SANDAL, N., STOUGAARD, J., SZCZYGLOWSKI, K. & PARNISKE, M. 2002. A plant receptor-like kinase required for both bacterial and fungal symbiosis. *Nature*, 417, 959-962.
- SUAREZ-RODRIGUEZ, M. C., ADAMS-PHILLIPS, L., LIU, Y., WANG, H., SU, S.-H., JESTER, P. J., ZHANG, S., BENT, A. F. & KRYSAN, P. J. 2007. MEKK1 Is Required for flg22-Induced MPK4 Activation in *Arabidopsis* Plants. *Plant Physiology*, 143, 661-669.
- TADEGE, M., RATET, P. & MYSORE, K. S. 2005. Insertional mutagenesis: a Swiss Army knife for functional genomics of *Medicago truncatula*. *Trends in Plant Science*, 10, 229-235.
- TADEGE, M., WEN, J., HE, J., TU, H., KWAK, Y., ESCHSTRUTH, A., CAYREL, A., ENDRE, G., ZHAO, P. X., CHABAUD, M., RATET, P. & MYSORE, K. S. 2008. Large-scale insertional mutagenesis using the *Tnt1* retrotransposon in the model legume *Medicago truncatula*. *The Plant Journal*, 54, 335-347.
- TAIZ, L. & ZEIGER, E. 1998. Mineral Nutrition. *Plant Physiology*. Second ed.
- TAKAI, R., ISOGAI, A., TAKAYAMA, S. & CHE, F.-S. 2008. Analysis of Flagellin Perception Mediated by flg22 Receptor *OsFLS2* in Rice. *Molecular Plant-Microbe Interactions*, 21, 1635-1642.
- TAKEDA, N., MAEKAWA, T. & HAYASHI, M. 2012. Nuclear-Localized and Deregulated Calcium- and Calmodulin-Dependent Protein Kinase Activates Rhizobial and Mycorrhizal Responses in *Lotus japonicus*. *The Plant Cell Online*, 24, 810-822.
- TANAKA, A., CHRISTENSEN, M. J., TAKEMOTO, D., PARK, P. & SCOTT, B. 2006. Reactive Oxygen Species Play a Role in Regulating a Fungus-Perennial Ryegrass Mutualistic Interaction. *The Plant Cell Online*, 18, 1052-1066.

- TANG, W., KIM, T.-W., OSES-PRIETO, J. A., SUN, Y., DENG, Z., ZHU, S., WANG, R., BURLINGAME, A. L. & WANG, Z.-Y. 2008. BSKs mediate signal transduction from the receptor kinase BRI1 in *Arabidopsis*. *Science*, 321, 557-560.
- TIMMERS, A. C., AURIAC, M. C. & TRUCHET, G. 1999. Refined analysis of early symbiotic steps of the *Rhizobium-Medicago* interaction in relationship with microtubular cytoskeleton rearrangements. *Development*, 126, 3617-3628.
- TIMMERS, A. C. J., SOUPÈNE, E., AURIAC, M.-C., DE BILLY, F., VASSE, J., BOISTARD, P. & TRUCHET, G. 2000. Saprophytic Intracellular Rhizobia in Alfalfa Nodules. *Molecular Plant-Microbe Interactions*, 13, 1204-1213.
- TIRICHINE, L., SANDAL, N., MADSEN, L. H., RADUTOIU, S., ALBREKTSEN, A. S., SATO, S., ASAMIZU, E., TABATA, S. & STOUGAARD, J. 2007. A Gain-of-Function Mutation in a Cytokinin Receptor Triggers Spontaneous Root Nodule Organogenesis. *Science*, 315, 104-107.
- TISSERANT, E., MALBREIL, M., KUO, A., KOHLER, A., SYMEONIDI, A., BALESTRINI, R., CHARRON, P., DUENSING, N., FREI DIT FREY, N., GIANINAZZI-PEARSON, V., GILBERT, L. B., HANDA, Y., HERR, J. R., HIJRI, M., KOUL, R., KAWAGUCHI, M., KRAJINSKI, F., LAMMERS, P. J., MASCLAUX, F. G., MURAT, C., MORIN, E., NDIKUMANA, S., PAGNI, M., PETITPIERRE, D., REQUENA, N., ROSIKIEWICZ, P., RILEY, R., SAITO, K., SAN CLEMENTE, H., SHAPIRO, H., VAN TUINEN, D., BÉCARD, G., BONFANTE, P., PASZKOWSKI, U., SHACHAR-HILL, Y. Y., TUSKAN, G. A., YOUNG, J. P. W., SANDERS, I. R., HENRISSAT, B., RENSING, S. A., GRIGORIEV, I. V., CORRADI, N., ROUX, C. & MARTIN, F. 2013. Genome of an arbuscular mycorrhizal fungus provides insight into the oldest plant symbiosis. *Proceedings of the National Academy of Sciences*, 110, 20117-20122.
- TÓTH, K., STRATIL, T. F., MADSEN, E. B., YE, J., POPP, C., ANTOLÍN-LLOVERA, M., GROSSMANN, C., JENSEN, O. N., SCHÜßLER, A., PARNISKE, M. & OTT, T. 2012. Functional Domain Analysis of the Remorin Protein LjSYMREM1 in *Lotus japonicus*. *PLoS ONE*, 7, e30817.
- TSUKAGOSHI, H., BUSCH, W. & BENFEY, P. N. 2010. Transcriptional Regulation of ROS Controls Transition from Proliferation to Differentiation in the Root. *Cell*, 143, 606-616.
- UDVARDI, M. K. & DAY, D. A. 1997. Metabolite transport across symbiotic membranes of legume nodules. *Annual Review of Plant Physiology and Plant Molecular Biology*, 48, 493-523.
- VAN BRUSSEL, A. A. N., BAKHUIZEN, R., VAN SPRONSEN, P. C., SPAINK, H. P., TAK, T., LUGTENBERG, B. J. J. & KIJNE, J. W. 1992. Induction of Pre-infection thread structures in the leguminous host plant by mitogenic lipo-oligosaccharides of *Rhizobium*. *Science*, 257, 70-72.
- VAN NOORDEN, G. E., ROSS, J. J., REID, J. B., ROLFE, B. G. & MATHESIUS, U. 2006. Defective Long-Distance Auxin Transport Regulation in the *Medicago truncatula* *super numeric nodules* Mutant. *Plant Physiology*, 140, 1494-1506.
- VASSE, J., DE BILLY, F., CAMUT, S. & TRUCHET, G. 1990. Correlation between ultrastructural differentiation of bacteroids and nitrogen fixation in alfalfa nodules. *Journal of Bacteriology*, 172, 4295-4306.
- VERONESE, P., NAKAGAMI, H., BLUHM, B., ABUQAMAR, S., CHEN, X., SALMERON, J., DIETRICH, R. A., HIRT, H. & MENGISTE, T. 2006. The Membrane-Anchored BOTRYTIS-INDUCED KINASE1 Plays Distinct Roles in *Arabidopsis* Resistance to Necrotrophic and Biotrophic Pathogens. *The Plant Cell Online*, 18, 257-273.
- VERT, G. & CHORY, J. 2006. Downstream nuclear events in brassinosteroid signalling. *Nature*, 441, 96-100.
- VIJ, S., GIRI, J., DANSANA, P. K., KAPOOR, S. & TYAGI, A. K. 2008. The Receptor-Like Cytoplasmic Kinase (OsRLCK) Gene Family in Rice: Organization, Phylogenetic Relationship, and Expression during Development and Stress. *Molecular Plant*, 1, 732-750.

- VOINNET, O., RIVAS, S., MESTRE, P. & BAULCOMBE, D. 2003. An enhanced transient expression system in plants based on suppression of gene silencing by the p19 protein of tomato bushy stunt virus. *The Plant Journal*, 33, 949-956.
- WAADT, R., SCHMIDT, L. K., LOHSE, M., HASHIMOTO, K., BOCK, R. & KUDLA, J. 2008. Multicolor bimolecular fluorescence complementation reveals simultaneous formation of alternative CBL/CIPK complexes in planta. *The Plant Journal*, 56, 505-516.
- WAIS, R. J., GALERA, C., OLDROYD, G., CATOIRA, R., PENNETSA, R. V., COOK, D., GOUGH, C., DÉNARIÉ, J. & LONG, S. R. 2000. Genetic analysis of calcium spiking responses in nodulation mutants of *Medicago truncatula*. *Proceedings of the National Academy of Sciences*, 97, 13407-13412.
- WALKER, J. C. 1994. Structure and function of the receptor-like protein-kinases of higher-plants. *Plant Molecular Biology*, 26, 1599-1609.
- WALKER, J. C. & ZHANG, R. 1990. Relationship of a putative receptor protein kinase from maize to the S-locus glycoproteins of Brassica. *Nature*, 345, 743-746.
- WANG, C., SHANG, J. X., CHEN, Q. X., OSES-PRIETO, J. A., BAI, M. Y., YANG, Y., YUAN, M., ZHANG, Y. L., MU, C. C., DENG, Z., WEI, C. Q., BURLINGAME, A. L., WANG, Z. Y. & SUN, Y. 2013. Identification of *BZR1*-interacting proteins as potential components of the brassinosteroid signaling pathway in *Arabidopsis* through tandem affinity purification. *Molecular Cell Proteomics*, 12, 3653-65.
- WANG, E., SCHORNACK, S., MARSH, J. F., GOBBATO, E., SCHWESSINGER, B., EASTMOND, P., SCHULTZE, M., KAMOUN, S. & OLDROYD, G. E. 2012. A common signaling process that promotes mycorrhizal and oomycete colonization of plants. *Current Biology*, 22, 2242-6.
- WANG, E., YU, N., BANO, S. A., LIU, C., MILLER, A. J., COUSINS, D., ZHANG, X., RATET, P., TADEGE, M., MYSORE, K. S., DOWNIE, J. A., MURRAY, J. D., OLDROYD, G. E. D. & SCHULTZE, M. 2014. A H⁺-ATPase That Energizes Nutrient Uptake during Mycorrhizal Symbioses in Rice and *Medicago truncatula*. *The Plant Cell Online*, 26, 1818-1830.
- WANG, H., YANG, C., ZHANG, C., WANG, N., LU, D., WANG, J., ZHANG, S., WANG, Z.-X., MA, H. & WANG, X. 2011. Dual Role of BKI1 and 14-3-3 s in Brassinosteroid Signaling to Link Receptor with Transcription Factors. *Developmental Cell*, 21, 825-834.
- WANG, X. & CHORY, J. 2006. Brassinosteroids Regulate Dissociation of BKI1, a Negative Regulator of BRI1 Signaling, from the Plasma Membrane. *Science*, 313, 1118-1122.
- WANG, X., GOSHE, M. B., SODERBLUM, E. J., PHINNEY, B. S., KUCHAR, J. A., LI, J., ASAMI, T., YOSHIDA, S., HUBER, S. C. & CLOUSE, S. D. 2005a. Identification and Functional Analysis of in Vivo Phosphorylation Sites of the *Arabidopsis* BRASSINOSTEROID-INSENSITIVE1 Receptor Kinase. *The Plant Cell Online*, 17, 1685-1703.
- WANG, X., KOTA, U., HE, K., BLACKBURN, K., LI, J., GOSHE, M. B., HUBER, S. C. & CLOUSE, S. D. 2008. Sequential Transphosphorylation of the BRI1/BAK1 Receptor Kinase Complex Impacts Early Events in Brassinosteroid Signaling. *Developmental Cell*, 15, 220-235.
- WANG, X., LI, X., MEISENHEDER, J., HUNTER, T., YOSHIDA, S., ASAMI, T. & CHORY, J. 2005b. Autoregulation and Homodimerization Are Involved in the Activation of the Plant Steroid Receptor BRI1. *Developmental Cell*, 8, 855-865.
- WEBER, E., ENGLER, C., GRUETZNER, R., WERNER, S. & MARILLONNET, S. 2011. A Modular Cloning System for Standardized Assembly of Multigene Constructs. *PLoS ONE*, 6, e16765.
- WEERASINGHE, R. R., BIRD, D. M. & ALLEN, N. S. 2005. Root-knot nematodes and bacterial Nod factors elicit common signal transduction events in *Lotus japonicus*. *Proceedings of the National Academy of Sciences of the United States of America*, 102, 3147-3152.

- WELLS, D. M., WILSON, M. H. & BENNETT, M. J. 2010. Feeling UPBEAT about Growth: Linking ROS Gradients and Cell Proliferation. *Developmental Cell*, 19, 644-646.
- WESLEY, S. V., HELLIWELL, C. A., SMITH, N. A., WANG, M. B., ROUSE, D. T., LIU, Q., GOODING, P. S., SINGH, S. P., ABBOTT, D., STOUTJESDIJK, P. A., ROBINSON, S. P., GLEAVE, A. P., GREEN, A. G. & WATERHOUSE, P. M. 2001. Construct design for efficient, effective and high-throughput gene silencing in plants. *Plant Journal*, 27, 581-90.
- XIE, Z., JOHANSEN, L. K., GUSTAFSON, A. M., KASSCHAU, K. D., LELLIS, A. D., ZILBERMAN, D., JACOBSEN, S. E. & CARRINGTON, J. C. 2004. Genetic and Functional Diversification of Small RNA Pathways in Plants. *PLoS Biology*, 2, e104.
- YANG, S.-Y., GRØNLUND, M., JAKOBSEN, I., GROTEMEYER, M. S., RENTSCH, D., MIYAO, A., HIROCHIKA, H., KUMAR, C. S., SUNDARESAN, V., SALAMIN, N., CATAUSAN, S., MATTES, N., HEUER, S. & PASZKOWSKI, U. 2012. Nonredundant Regulation of Rice Arbuscular Mycorrhizal Symbiosis by Two Members of the *PHOSPHATE TRANSPORTER1* Gene Family. *The Plant Cell Online*, 24, 4236-4251.
- YIN, Y., VAFEADOS, D., TAO, Y., YOSHIDA, S., ASAMI, T. & CHORY, J. 2005. A New Class of Transcription Factors Mediates Brassinosteroid-Regulated Gene Expression in *Arabidopsis*. *Cell*, 120, 249-259.
- YIN, Y., WANG, Z.-Y., MORA-GARCIA, S., LI, J., YOSHIDA, S., ASAMI, T. & CHORY, J. 2002. BES1 Accumulates in the Nucleus in Response to Brassinosteroids to Regulate Gene Expression and Promote Stem Elongation. *Cell*, 109, 181-191.
- YOUNG, N. D., DEBELLE, F., OLDROYD, G. E. D., GEURTS, R., CANNON, S. B., UDVARDI, M. K., BENEDITO, V. A., MAYER, K. F. X., GOUZY, J., SCHOOF, H., VAN DE PEER, Y., PROOST, S., COOK, D. R., MEYERS, B. C., SPANNAGL, M., CHEUNG, F., DE MITA, S., KRISHNAKUMAR, V., GUNDLACH, H., ZHOU, S., MUDGE, J., BHARTI, A. K., MURRAY, J. D., NAOUMKINA, M. A., ROSEN, B., SILVERSTEIN, K. A. T., TANG, H., ROMBAUTS, S., ZHAO, P. X., ZHOU, P., BARBE, V., BARDOU, P., BECHNER, M., BELLEC, A., BERGER, A., BERGES, H., BIDWELL, S., BISSELING, T., CHOISNE, N., COULOUX, A., DENNY, R., DESHPANDE, S., DAI, X., DOYLE, J. J., DUDEZ, A.-M., FARMER, A. D., FOUTEAU, S., FRANKEN, C., GIBELIN, C., GISH, J., GOLDSTEIN, S., GONZALEZ, A. J., GREEN, P. J., HALLAB, A., HARTOG, M., HUA, A., HUMPHRAY, S. J., JEONG, D.-H., JING, Y., JOCKER, A., KENTON, S. M., KIM, D.-J., KLEE, K., LAI, H., LANG, C., LIN, S., MACMIL, S. L., MAGDELENAT, G., MATTHEWS, L., MCCORRISON, J., MONAGHAN, E. L., MUN, J.-H., NAJAR, F. Z., NICHOLSON, C., NOIROT, C., O'BLENESS, M., PAULE, C. R., POULAIN, J., PRION, F., QIN, B., QU, C., RETZEL, E. F., RIDDLE, C., SALLET, E., SAMAIN, S., SAMSON, N., SANDERS, I., SAURAT, O., SCARPELLI, C., SCHIEX, T., SEGURENS, B., SEVERIN, A. J., SHERRIER, D. J., SHI, R., SIMS, S., SINGER, S. R., SINHAROY, S., STERCK, L., VIOLLET, A., WANG, B.-B., et al. 2011. The *Medicago* genome provides insight into the evolution of rhizobial symbioses. *Nature*, 480, 520-524.
- ZAMORE, P. D., TUSCHL, T., SHARP, P. A. & BARTEL, D. P. 2000. RNAi: double-stranded RNA directs the ATP-dependent cleavage of mRNA at 21 to 23 nucleotide intervals. *Cell*, 101, 25-33.
- ZHANG, J., LI, W., XIANG, T., LIU, Z., LALUK, K., DING, X., ZOU, Y., GAO, M., ZHANG, X., CHEN, S., MENGISTE, T., ZHANG, Y. & ZHOU, J. M. 2010a. Receptor-like cytoplasmic kinases integrate signaling from multiple plant immune receptors and are targeted by a *Pseudomonas syringae* effector. *Cell Host Microbe*, 7, 290-301.
- ZHANG, J., SHAO, F., LI, Y., CUI, H., CHEN, L., LI, H., ZOU, Y., LONG, C., LAN, L., CHAI, J., CHEN, S., TANG, X. & ZHOU, J.-M. 2007. A *Pseudomonas syringae* Effector Inactivates MAPKs to Suppress PAMP-Induced Immunity in Plants. *Cell Host & Microbe*, 1, 175-185.

- ZHANG, Q., BLAYLOCK, L. A. & HARRISON, M. J. 2010b. Two *Medicago truncatula* Half-ABC Transporters Are Essential for Arbuscule Development in Arbuscular Mycorrhizal Symbiosis. *The Plant Cell Online*, 22, 1483-1497.
- ZIPFEL, C., ROBATZEK, S., NAVARRO, L., OAKELEY, E. J., JONES, J. D. G., FELIX, G. & BOLLER, T. 2004. Bacterial disease resistance in *Arabidopsis* through flagellin perception. *Nature*, 428, 764-767.